GEOLOGICAL SURVEY OF CANADA
BULLETIN 552

MAPPING, GEOPHYSICS, AND GROUNDWATER MODELLING IN AQUIFER DELINEATION, FRASER LOWLAND AND DELTA, BRITISH COLUMBIA

Edited by
B.D. Ricketts

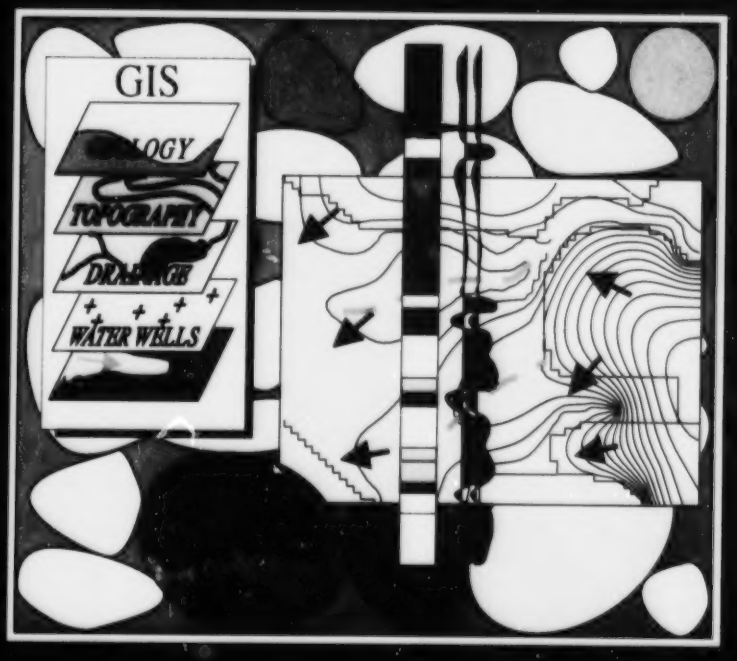

2000

Natural Resources Canada
Ressources naturelles Canada

Canada

GEOLOGICAL SURVEY OF CANADA
BULLETIN 552

MAPPING, GEOPHYSICS, AND GROUNDWATER MODELLING IN AQUIFER DELINEATION, FRASER LOWLAND AND DELTA, BRITISH COLUMBIA

Edited by
B.D. Ricketts

2000

Catalogue No. M42-552E
ISBN 0-660-18191-6

Available in Canada from
Geological Survey of Canada offices:

601 Booth Street
Ottawa, Ontario K1A 0E8

3303-33rd Street N.W.
Calgary, Alberta T2L 2A7

101-605 Robson Street
Vancouver, B.C. V6B 5J3

A deposit copy of this publication is also available for reference
in selected public libraries across Canada

Price subject to change without notice

Cover illustration

Hydrogeology is an interdisciplinary undertaking, exemplified in the Fraser Lowland Hydrogeology Project by links among sedimentary geology and geochemistry at both the grain/pore scale and aquifer scale, geophysical experiments and boreholes that allow us a glimpse of what lies below the Earth's suface, and digital mapping tools that provide the framework for data management and for evaluating fluid flow.

Editor's address

B.D. Ricketts
Department of Earth Sciences
University of Waikato
Private Bag 3105
Hamilton
New Zealand

Original manuscript submitted: 1998-09
Final version approved for publication: 1999-12

CONTENTS

Introduction

Brian D. Ricketts[1]

Ricketts, B.D., 2000: Introduction; in *Mapping, Geophysics, and Groundwater Modelling in Aquifer Delineation, Fraser Lowland and Delta, British Columbia, (ed.) B.D. Ricketts; Geological Survey of Canada, Bulletin 552, p. 1–3.*

The Fraser Lowland Hydrogeology Project in southwestern British Columbia was one of two hydrogeology-groundwater pilot projects launched by the Geological Survey of Canada in 1993. The second was the Oak Ridges Moraine Project north of Toronto. The principal aims of the Fraser Lowland Project were to 1) develop a groundwater-hydrogeology database, suitable for management at all levels of government and for scientific research; 2) choose an area to serve as template for development of a database and subsurface aquifer-aquitard mapping protocols, for the purpose of constructing stratigraphic cross-sections and overlaying geophysical profiles, using a geographic information system; 3) test the efficacy of different geophysical techniques, such as high-resolution seismic reflection, ground-penetrating radar, electromagnetism, and cone penetrometry, to provide new methods for defining hydrostratigraphic architecture and groundwater quality; and 4) undertake preliminary groundwater modelling by utilizing the new database and aquifer maps, and integrating the geophysical results.

The rationale for the project was based on several important socio-economic and scientific considerations, which were established in partnership with federal, provincial, and local government agencies, universities, and the geotechnical industry. Groundwater constitutes a potable water supply for approximately 600 000 people throughout British Columbia. The demand for potable water is growing rapidly, particularly in municipalities like Abbotsford, which registered a population increase of 32% (to about 87 000 people) between 1986 and 1991. Existing water resources for communities like this need protection, and new sources of surface and groundwater must be found. Groundwater, particularly in shallow

Le projet d'hydrogéologie des basses terres du Fraser, dans le sud-ouest de la Colombie-Britannique, était un de deux projets pilotes portant sur l'hydrogéologie et l'eau souterraine qu'a lancé la Commission géologique du Canada en 1993. Le deuxième était le Projet de la Moraine d'Oak Ridges, au nord de Toronto. Les objectifs principaux du projet d'hydrogéologie des basses terres du Fraser étaient 1) d'élaborer une base de données portant sur l'eau souterraine et l'hydrogéologie qui pourrait être utilisée par les gestionnaires, à tous les paliers de gouvernement, ainsi que pour la recherche scientifique; 2) de sélectionner une région qui servirait de modèle pour l'assemblage d'une base de données et l'élaboration de protocoles de cartographie des aquifères et des aquitards qui seront utilisés pour préparer des coupes stratigraphiques et superposer des profils géophysiques, au moyen d'un système d'information géographique; 3) de vérifier l'efficacité de diverses techniques géophysiques, comme la sismique réflexion à haute résolution, le géoradar, les levés électromagnétiques et les mesures au pénétromètre à cône, afin de trouver des nouvelles méthodes pour définir l'architecture hydrostratigraphique et la qualité de l'eau souterraine; et 4) d'effectuer une modélisation préliminaire de l'eau souterraine en utilisant la nouvelle base de données et les nouvelles cartes des aquifères et en intégrant les résultats des études géophysiques.

La raison d'être du projet était basée sur des considérations scientifiques et socio-économiques importantes qui ont été établies en partenariat par des organismes gouvernementaux fédéraux, provinciaux et locaux, par des universités et par l'industrie de la géotechnique. L'eau souterraine constitue la source d'eau potable pour environ 600 000 résidents de la Colombie-Britannique. La demande d'eau potable s'accroît rapidement, surtout dans des municipalités telles qu'Abbotsford, dont la population s'est accrue de 32 p.100 pour atteindre environ 87 000 personnes entre 1986 et 1991. Il faut protéger les ressources en eaux existantes de ces collectivités et trouver de nouvelles sources d'approvisionnement en eau de surface et en eau souterraine. L'eau souterraine, surtout celle des

[1] Department of Earth Sciences, University of Waikato, Private Bag 3105, Hamilton, New Zealand

unconfined aquifers, is commonly at risk of contamination from a variety of land-use practices. For example, dissolved nitrate in groundwater, derived from point and non-point sources, is a significant problem in several parts of the Fraser lowland where recorded concentrations commonly exceed (by up to eight times) federal and provincial government drinking-water guidelines. Pesticides are also being detected in an increasing number of wells. Excessive groundwater withdrawal can result in lowered water tables, and even ground subsidence due to irreversible compaction of aquifer materials. Lowering of regional water tables in the major unconfined aquifers of the Fraser lowland (e.g. Abbotsford–Sumas, Brookswood, and Aldergrove aquifers) because of increased demand does not seem to be a problem at this time. However, the effects of groundwater withdrawal from deeper, confined aquifers in the Fraser lowland is generally unknown.

Management of groundwater resources, risk assessment, and exploration for new sources depend on sound scientific and technical knowledge, including information on aquifer extent and geometry, the type and location of natural recharge and discharge areas, hydraulic parameters such as groundwater flow rates and directions, and groundwater-sediment chemistry. Factors such as groundwater mining (i.e. excess water withdrawal compared to recharge in confined aquifers), saltwater intrusion, and contaminant plume migration can be properly assessed only if the regional hydrogeological architecture of aquifers and aquitards is understood.

This bulletin contains six papers that provide details for each component of the project. The database structure is outlined by Makepeace and Ricketts, with emphasis on the digital methods developed for mapping of aquifers and aquitards using a geographic information system. Detailed subsurface mapping in south Surrey–Langley, the area chosen as the database structure template, has identified more than 30 confined aquifers in that area alone. The lateral extent and volume of each aquifer were calculated, thus providing a basis for comparing resource potential with demand. The maps also provide the means for estimating recharge rates for the confined aquifers, by using simulated velocities for the aquifer and aquitard sediment types.

Few geophysical studies in the Fraser lowland have been specifically targeted at groundwater. In this project, different geophysical methods were evaluated with respect to groundwater exploration and definition of the hydrostratigraphic architecture. A variety of geological settings, extending throughout the lower Fraser River valley, are represented by the sites chosen for shallow, high-resolution seismic-reflection (Pullan et al.) and electromagnetic surveys (Best and Todd).

aquifères libres peu profonds, est menacée de contamination par toute une gamme d'utilisations du territoire. Par exemple, les nitrates dissous dans l'eau souterraine, qu'ils proviennent de sources ponctuelles ou étendues, constituent un problème important à plusieurs endroits dans les basses terres du Fraser où on peut souvent mesurer des concentrations de nitrates qui dépassent (jusqu'à huit fois) les normes fédérales et provinciales de potabilité de l'eau. On trouve aussi des pesticides dans un nombre croissant de puits. Le pompage excessif d'eau souterraine peut abaisser la nappe phréatique et même causer un affaissement du sol par suite de la compaction irréversible des matériaux de l'aquifère. Il ne semble pas que l'abaissement de la nappe phréatique dans les principaux aquifères libres des basses terres du Fraser (p. ex. les aquifères d'Abbotsford–Sumas, de Brookswood et d'Aldergrove), causé par l'accroissement de la demande, entraîne des problèmes importants pour le moment. Toutefois, l'effet des prélèvements d'eau dans les aquifères captifs plus profonds des basses terres du Fraser demeure généralement inconnu.

La gestion des ressources en eau souterraine, l'évaluation du risque et la recherche de nouvelles sources d'approvisionnement reposent sur de solides connaissances scientifiques et techniques, y compris de l'information sur l'étendue et la géométrie des aquifères, le type et l'emplacement des aires naturelles d'alimentation et d'émergence, les paramètres hydrauliques comme les débits et les directions ainsi que la chimie de l'interaction de l'eau souterraine avec les sédiments. Des facteurs comme la surexploitation de l'eau souterraine (c.-à-d. les taux de prélèvement dépassent les taux d'alimentation des aquifères captifs), les invasions d'eau salée et la migration des panaches de contaminants ne peuvent être évalués correctement que si on comprend l'architecture hydrogéologique régionale des aquifères et des aquitards.

Le présent bulletin comprend six articles traitant des particularités de chaque composante du projet. Makepeace et Ricketts (ce volume) présentent les grandes lignes de la structure de la base de données en mettant l'accent sur les méthodes numériques mises au point pour la cartographie des aquifères et des aquitards au moyen d'un système d'information géographique. Lors de la cartographie détaillée de la subsurface dans la partie sud de la région de Surrey–Langley, région choisie comme modèle, on a reconnu plus de 30 aquifères captifs dans cette seule région. On a calculé la superficie et le volume de chaque aquifère, ce qui a fourni une base pour comparer les ressources potentielles et la demande. Les cartes permettent également d'estimer les taux d'alimentation des aquifères captifs, en utilisant des vitesses simulées pour les types de sédiments des aquifères et des aquitards.

Dans les basses terres du Fraser, on a réalisé très peu d'études géophysiques axées sur l'eau souterraine. Dans le cadre de ce projet, on a évalué diverses méthodes géophysiques quant à leur utilité pour l'exploration des eaux souterraines et la définition de l'architecture hydrostratigraphique. Les sites retenus pour les levés de sismique réflexion à faible profondeur et à haute résolution (Pullan et al., ce volume) et les levés électromagnétiques (Best et Todd, ce volume) représentent toute un gamme de cadres géologiques dans l'ensemble de la vallée du bas Fraser.

Ground-penetrating radar surveys concentrated on site-specific problems of the Brookswood aquifer, providing detailed pictures of its internal architecture (Rea and Knight). Rea and Knight also outline research aimed at quantifying radar reflections with respect to water tables and electrical conductivities (the latter complementing the electromagnetic studies). Roberts and co-workers used ground-penetrating radar to identify critical hydrostratigraphic relationships on the western margin of Brookswood aquifer, in particular the northwestern seepage face and the stratigraphic onlap onto the White Rock upland.

The final paper in the bulletin outlines preliminary two- and three-dimensional groundwater flow models for the Fraser River delta and the Brookswood aquifer (Ricketts).

A significant result of the geophysical surveys is the potential for discovering new aquifers. The electromagnetic results, in conjunction with ground-penetrating radar, provide clues regarding aquifer quality: higher conductivity layers may indicate relatively high clay content or brackish groundwater. For example, resistivity values of a silty sand unit underlying the northern and central Brookswood aquifer indicate a potential confined aquifer. Predicting the occurrence of confined aquifers is possible using seismic reflections in a layered succession. For example, channel structures and ancient beach and foreshore deposits not penetrated by existing water wells have been identified in the seismic-reflection profile along 8th Avenue in southeast Surrey.

Groundwater, as a sustainable resource, is of considerable importance to the social and economic well-being of Canada. The results of this project provide a sound scientific and technical basis from which to continue research and development of groundwater, not only in the Fraser lowland, but also on a global scale. Deceptively simple questions, such as "Where can clean groundwater be found?" and "Where has a particular contaminant gone?" cannot be answered without this kind of knowledge. To this extent, the Fraser Lowland Hydrogeology Project has developed digital methods of aquifer mapping and has successfully experimented with a variety of geophysical exploration methods for obtaining new data on groundwater and aquifers.

Les levés au géoradar se sont penchés sur des problèmes propres à l'aquifère de Brookswood et ont fourni des images détaillées de son architecture interne (Rea et Knight, ce volume). Rea et Knight ont aussi décrit les grandes lignes de la recherche sur la quantification des réflexions radar en fonction des nappes phréatiques et des conductivités électriques (ce dernier aspect complète les études électromagnétiques). Roberts et ses collègues (ce volume) ont utilisé le géoradar pour déterminer les relations hydrostratigraphiques critiques sur la marge occidentale de l'aquifère de Brookswood, surtout en ce qui concerne la zone de suintement située au nord-ouest ainsi que le biseau d'aggradation sur les hautes terres de White Rock.

Le dernier article du bulletin présente des modèles bi- et tridimensionnels préliminaires de l'écoulement de la nappe d'eau souterraine pour le delta du Fraser et pour l'aquifère de Brookswood (Ricketts, ce volume).

La possibilité de découvrir de nouveaux aquifères est un résultat important des levés géophysiques. Pris ensemble, les résultats des levés électromagnétiques et des levés au géoradar fournissent des indices sur la qualité des aquifères : des couches à conductivité élevée peuvent indiquer un contenu en argile relativement élevé ou la présence d'eau souterraine saumâtre. Par exemple, les valeurs de la résistivité pour une unité de sable silteux sous les parties nord et centrale de l'aquifère de Brookswood indiquent la présence d'un aquifère captif potentiel. Il est possible de prévoir la présence d'aquifères captifs dans une séquence stratifiée en utilisant les réflexions sismiques. Par exemple, dans le profil de sismique réflexion le long de la 8e Avenue dans le sud-ouest de Surrey, on a reconnu des structures de chenaux et d'anciens dépôts de plages et de bas de plage qui ne sont pénétrées par aucun puits d'eau.

En tant que ressource renouvelable, l'eau souterraine est d'une grande importance pour le bien-être social et économique du Canada. Les résultats de ce projet nous fournissent des fondements scientifiques et techniques solides pour la poursuite des travaux de recherche et de développement sur l'eau souterraine, non seulement dans les basses terres du Fraser, mais aussi à une échelle globale. On ne peut pas répondre à des questions comme «Où peut-on trouver de l'eau souterraine propre?» et «Où se trouve un contaminant donné?» sans des informations comme celles obtenues dans le cadre de ce projet. À cet égard, le projet d'hydrogéologie des basses terres du Fraser a permis la mise au point de méthodes numériques de cartographie des aquifères et des expériences concluantes sur l'acquisition de nouvelles données sur l'eau souterraine et sur les aquifères avec toute une gamme de méthodes d'exploration géophysique.

Overview of the Fraser Lowland Hydrogeology Project

Brian D. Ricketts[1]

Ricketts, B.D., 2000: Overview of the Fraser Lowland Hydrogeology Project; in *Mapping, Geophysics, and Groundwater Modelling in Aquifer Delineation, Fraser Lowland and Delta, British Columbia, (ed.) B.D. Ricketts; Geological Survey of Canada, Bulletin 552, p. 5–15.*

Abstract: The Fraser Lowland Hydrogeology Project (1993–1996) is outlined. A groundwater database has been created that is suitable for scientific research and resource management. With the aid of a geographic information system, the database was used to develop methods for subsurface aquifer mapping, construction of hydrostratigraphic cross-sections and three-dimensional models, and overlaying of geophysical profiles. A major component of the project was the testing of different geophysical methods (high-resolution seismic reflection, ground-penetrating radar, electromagnetism, cone penetrometry), to determine their usefulness for defining hydrostratigraphic architecture and groundwater quality. Although each method measures different properties of the Earth, they were found to complement one another with respect to depth of penetration and resolution. The groundwater database, aquifer maps, and results from the geophysical surveys were used in preliminary groundwater-flow models.

Résumé : On présente le projet d'hydrogéologie des basses terres du Fraser (1993–1996). On a créé une base de données sur l'eau souterraine qui peut servir pour la gestion de la ressource et les recherches scientifiques. On a utilisé la base de données avec un système d'information géographique afin de mettre au point des méthodes pour la cartographie des aquifères, pour l'élaboration de coupes transversales hydrostratigraphiques et de modèles tridimensionnels et pour la superposition de profils géophysiques. Une composante majeure du projet consistait à mettre à l'essai diverses méthodes géophysiques (sismique réflexion à haute résolution, géoradar, levés électromagnétiques, mesures au pénétromètre à cône) afin d'en déterminer l'utilité pour la définition de l'architecture hydrostratigraphique et la détermination de la qualité de l'eau souterraine. Bien que chaque méthode permette de mesurer des propriétés différentes, on a constaté qu'elles étaient complémentaires quant à la profondeur de pénétration et la résolution. On a utilisé la base de données sur l'eau souterraine, les cartes d'aquifères et les résultats des levés géophysiques dans des modèles préliminaires de l'écoulement de la nappe d'eau souterraine.

[1] Department of Earth Sciences, University of Waikato, Private Bag 3105, Hamilton, New Zealand

PROJECT RATIONALE

In April 1993, after an absence of nearly 20 years from groundwater research, the Geological Survey of Canada (GSC) initiated a program to delineate and characterize the hydrogeology, geophysics, and geochemistry of major aquifers that serve rapidly growing population centres in Canada. Two projects were launched to begin the program: the Oak Ridges Moraine Project north of Toronto, and the Fraser Lowland Hydrogeology Project in southwestern British Columbia. The principal aims of the Fraser Lowland Project were to (Fig. 1; Ricketts and Jackson, 1994):

1. develop a groundwater-hydrogeology database, suitable for management at all levels of government and for scientific research (Woodsworth and Ricketts, 1994);
2. choose an area to serve as template for development of a database and subsurface aquifer-aquitard mapping protocols, and for constructing stratigraphic cross-sections and overlaying geophysical profiles, using a geographic information system (GIS);
3. test the efficacy of different geophysical methods in the Fraser lowland (high-resolution seismic reflection, ground-penetrating radar, electromagnetism, cone penetrometry), in order to provide new methods for defining hydrostratigraphic architecture and groundwater quality; and
4. undertake preliminary groundwater modelling, by utilizing the new database and aquifer maps, and integrating the geophysical results.

Groundwater constitutes about 25% of potable water supplies in Canada; in British Columbia, some 600 000 people throughout the province depend on groundwater. The increasing demand for potable water in a rapidly growing region like Greater Vancouver requires rational planning by all levels of government. For example, Matsqui and Abbotsford (approximately 87 000 people in 1991), communities that rely heavily on groundwater, registered a population increase of 32% between 1986 and 1991 (unpub. data, Matsqui Economic Development Office, 1994). Existing water resources for communities such as these need protection, and new sources of surface and groundwater must be found. Groundwater, although commonly ignored or forgotten by much of the population, has distinct advantages over

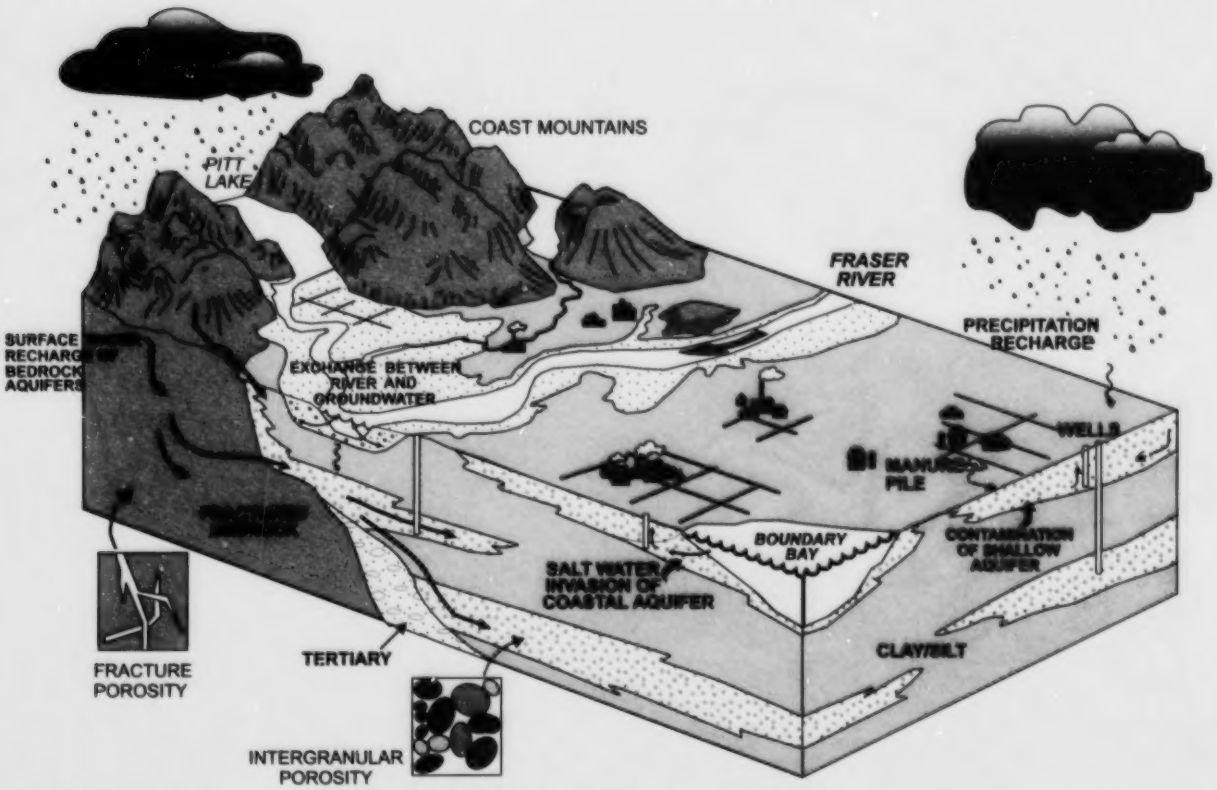

Figure 1. *Schematic diagram of the geological, geomorphic, and hydrostratigraphic setting for groundwater in the Fraser lowland and Fraser River delta, showing generalized groundwater sources and flow paths, and potential contaminant sources. View is approximately northeast, from Boundary Bay–Strait of Georgia.*

surface water supplies because of its inherently uniform quality and generally lower susceptibility to contamination. Groundwater is not directly infected by micro-organisms such as *Giardia* and *Cryptosporidium* cysts, which are becoming increasingly widespread in British Columbia surface waters (Bryck, 1991). Groundwater plays a significant role in global politics. For example, the fate of Canadian groundwater, and surface water for that matter, is ambiguous under the Canada–United States Free Trade Agreement. Contentious groundwater issues have already arisen, as in the nitrate-contaminated Abbotsford–Sumas aquifer that is recharged in southern British Columbia but extends into Watcom County, Washington.

Lowering of regional water tables in the major unconfined aquifers (e.g. Abbotsford–Sumas, Brookswood, Aldergrove), as a result of increased demand, does not seem to be a problem at this time, because groundwater discharge and withdrawal are compensated by recharge; however, the effects of groundwater withdrawal from deeper, confined aquifers in the Fraser lowland is generally unknown. Lessons can be learned from several major aquifers in the United States, where withdrawal of groundwater has greatly exceeded natural recharge. Head declines measuring several tens of metres have been recorded in California's Central Valley, the unconfined High Plains aquifer system in the south-central United States, and the Floridan aquifer system (Bush and Johnston, 1988; Weeks et al., 1988; Bertoldi et al., 1991). In addition to the resulting supply problems, land subsidence has occurred, exceeding 8 m in parts of the San Joaquin Valley. Subsidence of this kind results from irreversible compaction, which permanently damages the aquifer.

Groundwater requires careful management to remain a viable and renewable resource. The protection of existing groundwater water resources, and the exploration for and utilization of new sources, depend on sound scientific and technical knowledge for providing information on aquifer extent and geometry, the type and location of recharge areas, hydraulic parameters such as groundwater flow rates and directions, and groundwater-sediment chemistry. Factors such as groundwater mining (i.e. excess water withdrawal), salt-water intrusion, and contaminant plume migration (Fig. 1) can be properly assessed only if the regional hydrogeological architecture of aquifers and aquitards is understood. More sophisticated understanding of groundwater flow will improve the ability to identify contaminant flow paths, thereby reducing the cost of remediation programs.

GEOLOGICAL FRAMEWORK

The Fraser lowland is the region of low relief traversed by the Fraser River and sandwiched between the rugged Coast Mountains and Georgia Strait. It marks the southwestern limit of the Fraser River drainage basin, a basin which covers about one-third of British Columbia. The geological underpinning of the Fraser lowland and Fraser River delta consists of three, fundamentally different, tectonostratigraphic units (Fig. 1):

1. A band of Cretaceous and older plutonic rocks, with subordinate metasedimentary and metavolcanic rocks, constitutes the Coast Belt (Roddick, 1965, 1990; Gabrielse et al., 1991; Monger and Journeay, 1994). Permeabilities in these rocks are extremely low, and groundwater derived from this terrain flows through complex fracture systems. Fracture-derived groundwater, locally elevated in base metals such as copper and arsenic, can potentially affect groundwater compositions in overlying sedimentary deposits.

2. Upper Cretaceous (Nanaimo Group) and Tertiary (Paleocene to Pliocene) formations of sandstone, conglomerate, and mudstone, exposed locally in Stanley Park (Vancouver), along the north shore of the Fraser River, and on Sumas and Vedder mountains, are part of a panel of sedimentary rocks, more than 3 km thick, that dips south in a broad syncline beneath Vancouver, the Fraser lowland, and the Fraser River delta (Mustard and Rouse, 1994). Intergranular porosity (probably averaging 15% or less; e.g. Gordy (1988)) and fracture porosity exist. However permeabilities are low, approximately 8×10^{-15} m^2 (8 millidarcies; corresponding to hydraulic conductivities of 8×10^{-6} cm/s) from drill stem tests (DSTs) in a Conoco–Dynamic Oil well south of Langley (J. Britton, pers. comm., 1996). The same DSTs further indicated some overpressuring of groundwater at depths of 900 m and more, so it is possible that some of this water could seep into the overlying Quaternary deposits.

3. The contact between the Paleogene–Neogene succession and the Quaternary deposits is a profound unconformity, manifested as a high-relief erosion surface (*see* Hamilton and Ricketts, 1994; Britton et al., 1995; Ricketts, 2000). The unconformity is exposed well above sea level (e.g. along the north shore of the Fraser River) and plunges to depths of 700 m or more below sea level beneath the Fraser River delta and lowland. Closely spaced, deep, seismic-reflection profiles on the Fraser River delta enabled detailed reconstruction of this surface. Subsurface paleoslopes are as high as 10° near Sumas Mountain and in the Point Roberts area. Some paleovalleys on the sub-Pleistocene surface trend north-northeast and appear to be extensions of modern valleys in the Coast Mountains north of the Fraser River (e.g. Indian Arm, Pitt Lake, Stave Lake), suggesting that the larger, modern drainage patterns are at least as old as early Pleistocene.

Most of the groundwater issues dealt with in the Fraser Lowlands Hydrogeology Project, and indeed most of the groundwater utilized in the greater Vancouver region, originate in the Quaternary succession. Our understanding of Quaternary lithostratigraphy has evolved over many years through mapping of surficial deposits (Armstrong, 1980a, b; Armstrong and Hicock, 1980a, b), and stratigraphic studies (Halstead, 1960; Clague, 1976, 1991; Armstrong and Clague, 1977; Clague and Luternauer, 1982). The principal lithostratigraphic units, and periods of glaciation and nonglaciation, are summarized in Figure 2. Extension of this lithostratigraphic scheme into the subsurface is difficult, partly because of the remarkable complexity of the glacial

stratigraphy and partly because of a paucity of datable materials; however, progress on a local scale has been made using information from deep test wells (Halstead, 1957, 1959, 1961, 1978; H. Liebscher, pers. comm., 1997). The most comprehensive summaries, to date, of subsurface stratigraphy have been compiled by Armstrong (1984) and Halstead (1986). The stratigraphic complexity has resulted from interactions between sedimentation and erosion during advance and retreat of the ice sheets, the concomitant retreat and advance of the seas, and the isostatic effects of ice loading (subsidence) and unloading (uplift or rebound). Therefore, there are many units of sufficiently high porosity and hydraulic conductivity to qualify as aquifers, particularly those that accumulated in close proximity to ice. Mapping has identified more than 200 aquifers in the region (Liebscher et al., 1992); the plethora of aquifers is confirmed in this project (Makepeace and Ricketts, 2000), where more than 30 have been identified in southeast Surrey–southwest Langley alone.

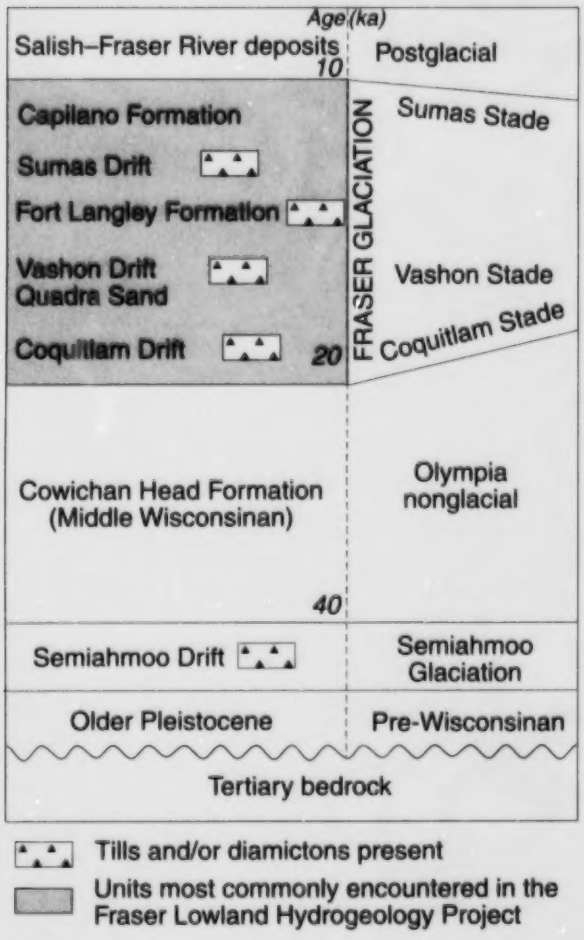

Figure 2. *Summary of lithostratigraphy and glaciation for the Fraser lowland* (modified from *Armstrong, 1981; Clague, 1991).*

The stratigraphic units most commonly referred to in this project accumulated during the Late Wisconsinan Fraser Glaciation (Fig. 2), although early Pleistocene and possible late Neogene deposits (Clague, 1991) occur deeper within the succession. In fact, most of the Fraser lowland is underlain by the Capilano Formation, Fort Langley Formation, and Sumas Drift of the latest Winconsinan, and the Fraser River delta is underlain by postglacial deposits, including modern delta and fluvial sediments. Vashon Drift and older units underlie upland areas around Vancouver, Surrey, White Rock, and Tsawwassen, and are exposed in cliffs and bluffs (e.g. Quadra Sand; Clague (1977)).

Aquifers that figure most prominently in the Fraser lowland, in terms of groundwater demand, are the unconfined Abbotsford–Sumas, Brookswood (Langley), and Aldergrove aquifers, consisting of glaciofluvial, delta, and ice-contact Sumas Drift deposits. They are also the most susceptible to contamination because of the mixture of urban, agricultural, and industrial land-use practices. Summaries of the sedimentology and stratigraphy of these, plus aquifers in other formations, can be found in Armstrong (1981, 1984), Halstead (1986), Kreye and Wei (1994), Ricketts and Jackson (1994), Ricketts and Liebscher (1994), and Ricketts (2000).

RECENT GROUNDWATER ISSUES

Several instances of point-source and more widespread contamination of British Columbia groundwater have come to light in recent years, highlighting the need for improved scientific knowledge and rational groundwater management. Perhaps the most pressing issue concerns nitrate in unconfined aquifers. Nitrate contamination is becoming increasingly common throughout southern British Columbia (e.g. Grand Forks; Wei et al. (1993)), but is especially significant in the Abbotsford–Sumas and Brookswood aquifers. Instances of nitrate-nitrogen levels exceeding the guidelines for Canadian drinking water (i.e. >10 mg/L; McNeely et al. (1979), Canadian Council of Resource and Envrionment Ministers (1987)) are increasing. Analytical data compiled in the 1980s showed concentrations up to 20 mg/L in parts of the Abbotsford–Sumas aquifer (Dakin, 1991). Levels increased in the early 1990s to 30 mg/L (Liebscher et al., 1992) and, in a later comprehensive study of observation wells, locally exceeded 70 mg/L; 25% of wells studied in the Brookswood aquifer contained nitrate-nitrogen greater than 10.0 mg/L (Carmichael et al., 1995). Nitrate in groundwater, other than that originating in the atmosphere, derives primarily from manure and septic effluent; however, the main culprit seems to be manure, stockpiled or spread as crop fertilizer (Dakin, 1991; Liebscher et al., 1992). Supporting evidence for this assertion is found in studies of oxygen and nitrogen stable isotopes in groundwater (Wassenaar, 1994).

Pesticides are being detected more frequently in shallow groundwater, although this trend is due, in part, to changing sampling practices and detection limits (Liebscher et al., 1992; Carmichael et al., 1995). Pesticide levels are usually below the limits set by the water-quality guidelines. Nevertheless, the fact that these compounds are present at all is

Table 1. Summary of characteristics of hydrostratigraphic units, based on the scheme of Halstead (1986). Additional data *from* Liebscher et al. (1992).

Unit	Lithology	Thickness	Origin	Extent	Dissolved solids	pH	Aquifer type
A	Clay, stoney clay, silty clay, minor silt and sand, shells, (e.g. Fort Langley and Capilano formations)	<30 m	Fallout from ice entering the sea	Near surface over most of the region	<120 mg/L	6.0–8.0	Aquitard or isolated aquifers
B	Stoney clay, shells (e.g. Fort Langley and Capilano formations)	<90 m	Glaciomarine	Langley upland and Serpentine valley			Aquitard
C	Sand and gravel, minor clay (e.g. Sumas Formation)	40 m	Glaciofluvial, deltaic	Near surface in Langley and Abbotsford	<120 mg/L to 300 mg/L beneath tills	6.5–8.5	Unconfined aquifer
D	Diamicton	<90 m	Ice-contact moraines	Discontinuous	<500 mg/L		Many small confined aquifers
E	Sand, silty clay predating Fraser Glaciation		Mixed marine estuarine, fluvial	Usually at depths >90 m	750-6000 mg/L		Aquifers and aquitards
F	Tertiary and Cretaceous bedrock			Substrate to Quaternary, exposed in peripheral areas			Mostly fracture porosity

cause for concern. Dense non-aqueous phase liquid (DNAPL) contamination appears to be relatively minor in British Columbia. Creosote, for example, is a potential problem near old timber mill and storage sites. Of greater notoriety is the train derailment near Fort Langley on February 15, 1986, where tankers of ethylene dichloride and sodium hydroxide ruptured and spilled (Carmichael et al., 1995). The DNAPL rapidly sank through the local aquifer (Fraser River sediments) and its present whereabouts is uncertain. Air-sparging over the spill site continues. The sodium hydroxide, a highly soluble and toxic alkali, also dispersed without obvious long-term effects on the river or local groundwater. Use of light non-aqueous phase liquids (LNAPLs) is widespread (e.g. gasoline and solvents such as chloroform), and they have been detected in vulnerable, shallow aquifers including Brookswood (Carmichael et al., 1995). Elsewhere in southern British Columbia, gasoline spills at Grand Forks have forced the closure of at least one municipal well.

The above list of real and potential groundwater contaminants is not intended to be exhaustive (greater detail is provided in the documents cited); however, the list does illustrate the need for reliable geological and hydrogeological information, in the event that cleanup or other remedial action is required. Simple questions such as "Where has the contaminant gone?" or "How long will it take for the contaminant to reach a point of discharge (production wells, rivers)?" cannot be answered without this knowledge. To this extent, the Fraser Lowland Hydrogeology Project tries not just to provide maps of aquifers, but also to examine new methods of aquifer mapping and characterization.

Previous aquifer classification schemes

The most comprehensive analysis of hydrostratigraphy in the Fraser lowland region, and certainly the one most often cited in other groundwater studies, is that of Halstead (1986). Hydrostratigraphic units (Table 1) were defined on the basis of lithology, permeability and porosity, and subordinate factors such as origin (marine, fluvial), stratigraphic position, and, to some extent, aquifer type (e.g. water-table aquifers). These units are different from formal lithostratigraphic units (Fig. 2), which are defined primarily on the basis of mappability and degree of homogeneity. Halstead's scheme is useful from a regional perspective, although detailed mapping in the south Surrey–Langley area reveals some ambiguities. His unit C, for example, corresponds to the easily mapped, unconfined Sumas Drift aquifers. However, other hydrostratigraphic units, such as A and B, correspond to the more heterogenous Fort Langley and Capilano formations and not specifically to aquifers within these formations. For example, several aquifers mapped in this project are confined by finer grained Fort Langley–Capilano deposits, and some of these confined aquifers appear very similar in general sedimentological characteristics and map extent to the unconfined unit C aquifers.

An aquifer classification scheme has been designed for groundwater management by Kreye and Wei (1994). Aquifers are ranked according to two principal criteria: the level of demand with respect to productivity, and the vulnerability of the aquifer to contamination from surface sources (Table 2). In general, unconfined aquifers are the most vulnerable and, in the Fraser lowland, the most utilized: the

Table 2. Aquifer management classification scheme (*from* Kreye and Wei, 1994).

Development class		
I	II	III
Heavy demand	Moderate demand	Light demand

Vulnerability class		
A	B	C
High vulnerability	Moderate vulnerability	Low vulnerability

Brookswood and Abbotsford–Sumas aquifers are ranked in the top three. Most of the confined aquifers mapped by Makepeace and Ricketts (2000) would probably rank in the middle or lower levels of this scheme, although an assessment of demand versus productivity and recharge has not been carried out in most cases. The aquifer maps developed for the south Surrey–Langley area provide a basis for quantifying some of these variables.

PROJECT RESULTS

Synthesis of bulletin papers

The six papers that follow provide details for each component of the project. Basic data for some of this work, including the entire groundwater database, has been published as a GSC Open File (Ricketts and Makepeace, 2000). The database structure is outlined by Makepeace and Ricketts (2000), with emphasis on the methods developed for mapping of aquifers and aquitards using a GIS. Few geophysical studies in the Fraser lowland have been specifically targeted at groundwater. Therefore, in this project, several geophysical methods were evaluated with respect to groundwater exploration and definition of the hydrostratigraphic architecture. A variety of geological settings, extending throughout the lower Fraser River valley, are represented by the sites chosen for shallow, high-resolution seismic-reflection (Pullan et al., 2000) and electromagnetic (EM; Best and Todd (2000)) surveys. Ground-penetrating radar (GPR) surveys, on the other hand, concentrated on the Brookswood aquifer, providing detailed pictures of its internal architecture (Rea and Knight, 2000). Rea and Knight also outline research aimed at quantifying radar reflections with respect to water tables and electrical conductivities (the latter complementing the EM studies). Roberts et al. (2000) used GPR to illustrate critical hydrostratigraphic relationships on the western margin of Brookswood aquifer, particularly the northwestern seepage face and the stratigraphic onlap onto the White Rock upland. The final paper (Ricketts, 2000) outlines preliminary two- and three-dimensional groundwater-flow models for the Fraser River delta and the Brookswood aquifer.

Cone penetrometry

The utility of cone penetrometry for aquifer mapping in the Fraser lowland was investigated by the In-Situ Testing Group of the University of British Columbia and published as GSC open files (Campanella et al., 1994; Ricketts and Makepeace, 2000).

Aquifer maps to aid resource estimates

Detailed subsurface mapping in south Surrey–Langley has identified more than 30 confined aquifers in this area alone (Makepeace and Ricketts, 2000). Although the aquifers are known by virtue of the borehole intersections, estimates of their lateral extent and volume have not been possible until now. The new aquifer maps provide a means of assessing aquifer geometry, from which estimates can be made of resource potential versus demand. The maps will also provide the means for estimating recharge rates for the confined aquifers, by using simulated velocities for the aquifer and aquitard sediment types (Ricketts, 1998, 2000).

Volumes have been estimated for those aquifers for which there is a reasonable degree of control on map extent and top and bottom surfaces (Table 3). Several aquifers extend beyond the limits of the case study (marked with an * in

Table 3. Estimates of volumes and resources in confined aquifers (*from* Makepeace and Ricketts, 2000). Volume calculations, based on an average porosity of 30%, are to the nearest 1000 m^3. An * indicates that the calculations are only for the portion of the aquifer lying within the case-study area.

Aquifer		Total volume (m^3)	Volume of water (m^3)	Surface area (m^2)	Recharge rate (m^3/day)
XY	*	129 742	39 000	59 000	5.9
JZ		185 691	56 000	170 000	17.0
YA		223 476	67 000	127 000	12.7
TH		267 736	80 000	321 000	32.1
TG		536 980	161 000	378 000	37.8
JX		864 600	259 000	354 000	35.4
NG		867 824	260 000	1 731 000	173.1
NH		1 050 960	315 000	1 193 000	119.3
WA	*	1 093 756	328 000	295 000	29.5
XX	*	1 657 508	497 000	220 000	22.0
AV	*	1 747 796	524 000	368 000	36.8
Y		1 969 416	591 000	520 000	52.0
R	*	2 797 728	839 000	1 002 000	100.2
JY	*	3 277 808	983 000	449 000	44.9
JV		4 014 532	1 204 000	628 000	62.8
JW	*	7 236 464	2 171 000	1 343 000	134.3
C	*	7 293 136	2 171 000	2 052 000	205.2
D	*	13 838 944	4 152 000	3 467 000	346.7
NA		15 833 537	4 750 000	163 000	16.3
I	*	16 300 864	4 890 000	8 529 000	852.9
V	*	20 280 224	6 084 000	4 464 000	446.4
YY	*	30 889 142	9 267 000	195 000	19.5
T	*	47 010 176	14 103 000	10 236 000	1023.6
L	*	48 198 496	14 460 000	5 716 000	571.6
W	*	71 546 752	21 464 000	16 712 000	1671.2
N		136 860 928	41 058 000	9 904 000	990.4

Table 3; *see* Makepeace and Ricketts (2000, Fig. 9)); in these cases, the volume calculated is only for the portion of the aquifer mapped herein.

The total volume of water is calculated assuming an average porosity of 30%. These values represent only a static volume (i.e. they do not take inflow and outflow into account). Nevertheless, the numbers can be compared to groundwater withdrawal rates for specific aquifers, to determine approximate loading capacity. If recharge rates to the confined aquifers can be estimated (e.g. by vertical leakage from confining aquitards), then the optimum limits of groundwater withdrawal (i.e. rates that avoid mining of the aquifer) can be estimated.

The aquifer volumes in Table 3 vary widely. Dakin (1994) has estimated that, in 1987, about 46 000 000 m^3 of water were extracted throughout the lower Fraser River valley. This equates to the total static water volumes for confined aquifers T and L.

The simulated groundwater flow rate in the Fraser lowland aquitards is about 10^{-4} m/day, a value that may be too high for some of the dense diamictons. At this rate, vertical seepage through an aquitard 50 m thick will take about 1400 years.

Estimates of leakage recharge into the confined aquifers can also be made, using the flux of 10^{-4} m/day. For example, an aquifer surface area of 30 km^2 will permit a flux of about 3000 m^3/day into the aquifer, a rate similar to the water withdrawal required by communities such as Langley. Recharge has been calculated for each aquifer in Table 3 (to the limits of mapping), assuming a vertical flux of 10^{-4} m/day. The estimates do not account for groundwater loss by leakage into the underlying aquitard. However, the flow rates provide a reasonable approximation of aquifer supply potential (compared to demand).

Discovery of new aquifers

A significant result of the EM and seismic surveys is the potential they provide for discovering new aquifers. In addition to identifying confined aquifers, the EM results also give clues regarding aquifer quality, in particular that higher conductivity layers may indicate relatively high clay content or brackish groundwater. For example, resistivity values of a silty sand unit underlying the northern and central Brookswood aquifer indicate a potential confined aquifer. However, towards the southwest margin of the aquifer, the same unit becomes increasingly conductive because of increasing clay content (Best and Todd, 2000, Fig. 7, 9). Notably, only about 10% of water wells in the Brookswood area actually penetrate the base of the unconfined aquifer; therefore, there was little knowledge of possible confined aquifers in the area prior to the EM study.

Seismic reflections in a layered succession depend on the contrast in acoustic impedance of sedimentary units. Thus, it is possible to identify aquifers and aquitards, and to predict where coarse-grained deposits might occur, based on stratigraphic relationships. The seismic-reflection profile along 8th Avenue (southeast Surrey) is a good example, with reflections in Pleistocene and Tertiary strata to at least a depth of 500 m (Fig. 3; Pullan et al., 2000). Horizontal but laterally discontinuous reflections in the upper 100 m of section are characteristic of interbedded fine- and coarse-grained deposits in the Capilano and Fort Langley formations; most water wells in the area do not penetrate deeper than this layered package. The profile also contains a large channel structure (centred beneath shot point 460), possibly filled with coarse-grained deposits. At greater depths, strata onlapping a Pleistocene unconformity may also contain new aquifers. The layers possibly originated during a marine transgression. If this is the case, then landward migration of the ancient shoreline would have deposited beach and foreshore sand or gravel in a semicontinuous (diachronous) layer over the

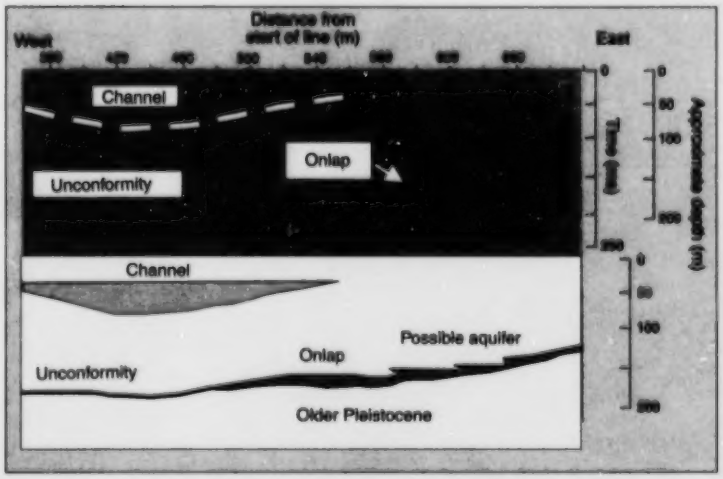

Figure 3.

Part of the 8th Avenue seismic profile (from *Pullan et al., 2000*), *showing potential new sources of groundwater. Note that the reflections onlapping the unconformity (arrow) are discontinuous, and disappear to the left (west) of the onlap surface; this can be interpreted as representing the transition from coarse-grained beach deposits, at the onlap, to finer grained silt and mud units offshore. The beach deposits would form a relatively continuous layer along the unconformity as onlap (or transgression) proceeded, resulting in an aquifer. The other potential new aquifer is located in the channel structure, which likely consists of sand and gravel.*

unconformity (Fig. 3). This layer is a potential aquifer, which could be intersected at conventional drilling depths toward the eastern end of the profile.

ACKNOWLEDGMENTS

Many people and organizations played pivotal roles in this project, from germination and inception to its completion. Foremost among these is Dirk Tempelman-Kluit, former Director of GSC Vancouver, whose enthusiasm and advice was indispensable. Database management and development of GIS mapping methods were major tasks undertaken by Dave Dunn and Andrew Makepeace. A significant component of the project involved geophysical field experiments, led by Susan Pullan, Ron Good, Mel Best, Brian Todd, Dave Seemann, Rosemary Knight, Jane Rea, and Bob McDonald. Lionel Jackson is thanked for reviewing this paper, and Bev Vanlier for shepherding it through the myriad editorial processes.

People who participated in the project, either directly or indirectly, include:

Geological Survey of Canada, Vancouver: J.L. Luternauer (Fraser River delta data and drilling), G.J. Woodsworth (database design), and D. Dunn and A. Makepeace (database management; GIS development);

Geological Survey of Canada, Sidney: M.E. Best (EM), R. McDonald (borehole geophysics), T. Hamilton (mapping of the sub-Quaternary bedrock surface), D. Seemann (gravity), and R. Conway (grain-size analyses);

Geological Survey of Canada, Calgary: L. Snowdon (organic analyses) and H. Abercrombie (inorganic analyses);

Geological Survey of Canada, Terrain Sciences, Vancouver and Ottawa: J.J. Clague (stratigraphic studies), L.E. Jackson (initial project setup), S.E. Pullan and R.L. Good (high-resolution seismic reflection), and S. Dallimore (stable-isotope analyses);

Geological Survey of Canada, Mineral Resources Division, Ottawa: G. Hall (trace-element analyses);

Environment Canada, Inland Waters Branch: H. Liebscher (advice during early stage of project; field work), B. Hii and L. Adamac (data files; GIS coverages of water-well co-ordinates);

Agriculture Canada: B. Zebarth (access to Agassiz Research Station for field experiments);

British Columbia Ministry of Health and Ministry Responsible for Seniors: S. Martin, K. Schneider, and V. Carmichael (water-quality data);

British Columbia Ministry of Energy and Mines, Petroleum Geology Branch: J. MacRea (oil-well data files);

British Columbia Ministry of Environment, Lands and Parks, Groundwater Division: A. Kohut, R. Zimmerman, M. Wei, and L. Ringham (water-well data and water-well maps);

British Columbia Ministry of Forests, Surrey Nursery: T. Willingdon (access to site for geophysical experiments; water analyses);

City of Surrey: K. Bennett (access to sites for geophysics; permission for roadside seismic; water analyses);

Municipality of Langley: N. Calver and P. Scales (access to sites and environmental data) and R. Walters, City Engineer (permission for roadside use);

Municipality of Matsqui: P. Andzans and E. Regts (access to sites; permission for roadside use);

Greater Vancouver Regional District: Engineering, Waste Management Department (water analyses);

City of Vancouver: Waste Management Department (access to Burns Bog data);

University of British Columbia (UBC), Department of Geological Sciences: R.J. Knight and J.M. Rea (GPR), K. Grimm and T. Mak (sedimentology), and L. Smith and R. Beckie (groundwater; UBC field site); **Department of Civil Engineering:** R. Campanella and M. Davies (cone penetrometry), and R. Dasika (denitrification experiments);

Simon Fraser University, Departments of Geography and Geology: M.C. Roberts and H.M. Jol (high-resolution seismic reflection; GPR; drilling);

University of Calgary, Department of Geology and Geophysics: I. Hutcheon (diagenesis; stable isotopes);

University College of the Fraser Valley: Sandy Vanderburgh (high-resolution seismic reflection);

British Columbia Groundwater Association: D. McNichol (advice on project development; data sources);

United States Geological Survey, Water Resources Division: S. Cox, Regional Aquifer Systems Analysis project; W. Staubitz, National Water Quality Assessment;

Industry: Predominantly transfer of data and technology between companies and the GSC: J. Psutka, BC Hydro; T. Sperling, Gartner Lee Ltd.; D. Tiplady, Piteau Associates; G. Rawlings, Golder Associates Ltd.; M. Davies, Klohn-Crippen Ltd.; R. Roussey, Sonic Drilling Ltd; W. Alderton, Novasol Inc.; Field Drilling Ltd.; Dandelion Geothermal; Harmony Gravel Pit (192nd St. gravel pit); Steelhead Aggregates Ltd.; R. Quinn, Terra Surveys Ltd.; J. Britton, Dynamic Oil Ltd.; and Conoco Canada Ltd.

REFERENCES

Armstrong, J.E.

1980a: Surficial geology, Mission, British Columbia; Geological Survey of Canada, Map 1485A, scale 1:50 000.

1980b: Surficial geology, Chilliwack, British Columbia; Geological Survey of Canada, Map 1487A, scale 1:50 000.

1981: Post-Vashon Wisconsin glaciation, Fraser Lowland, British Columbia; Geological Survey of Canada, Bulletin 322, 34 p.

1984: Environmental and engineering applications of the surficial geology of the Fraser Lowland, British Columbia; Geological Survey of Canada, Paper 83-23, 54 p.

Armstrong, J.E. and Clague, J.J.
1977: Two major Wisconsin lithostratigraphic units in southwestern British Columbia; Canadian Journal of Earth Sciences, v. 14, p. 1471–1480.

Armstrong, J.E. and Hicock, S.R.
1980a: Surficial geology, New Westminster, British Columbia; Geological Survey of Canada, Map 1484A, scale 1:50 000.
1980b: Surficial geology, Vancouver, British Columbia; Geological Survey of Canada, Map 1486A, scale 1:50 000.

Bertoldi, G.L., Johnston, R.H., and Evenson, K.D.
1991: Ground water in the Central Valley, California – a summary report; United States Geological Survey, Professional Paper 1401-A, 44 p.

Best, M.E. and Todd, B.J.
2000: Electromagnetic mapping of groundwater aquifers in the Fraser lowland; *in* Mapping, Geophysics, and Groundwater Modelling in Aquifer Delineation, Fraser Lowland and Delta, British Columbia, (ed.) B.D. Ricketts; Geological Survey of Canada, Bulletin 552.

Britton, J.R., Harris, J.B., Hunter, J.A., and Luternauer, J.L.
1995: The bedrock surface beneath the Fraser River delta from seismic measurements; *in* Current Research 1995-E; Geological Survey of Canada, p. 83–98.

Bryck, J.
1991: Drinking water – treat it with care; The BC Professional Engineer, October 1991, p. 8–10.

Bush, P.W. and Johnston, R.H.
1988: Ground-water hydraulics, regional flow, and ground-water development of the Floridan Aquifer System in Florida and in parts of Georgia, South Carolina, and Alabama; United States Geological Survey, Professional Paper 1403-C, 80 p.

Campanella, R.G., Davies, M., Boyd, T., Everard, J., Roy, D., Tomlinson, S., Jackson, S., Schrempp, H., and Ricketts, B.D.
1994: In-situ testing for the characterization of aquifers: demonstration project; Geological Survey of Canada, Open File 2940, 19 p.

Canadian Council of Resource and Environment Ministers (CCREM)
1987: Canadian Water Quality Guidelines; CCREM Task Force on Water Quality Guidelines, Environment Canada, Ottawa, Ontario.

Carmichael, V., Wei, M., and Ringham, L.
1995: Fraser Valley groundwater monitoring program, final report; British Columbia Ministry of Health and British Columbia Ministry of Environment, Lands and Parks, 104 p.

Clague, J.J.
1976: Quadra Sand and its relation to the late Wisconsin glaciation of southwest British Columbia; Canadian Journal of Earth Sciences, v. 13, p. 803–815.
1977: Quadra Sand: a study of the Late Pleistocene geology and geomorphic history of coastal southwest British Columbia; Geological Survey of Canada, Paper 77-17, 24 p.
1991: Quaternary glaciation and sedimentation; Chapter 12 *in* Geology of the Cordilleran Orogen in Canada, (ed.) H. Gabrielse and C.J. Yorath; Geological Survey of Canada, Geology of Canada, no. 4, p. 419–434 (*also* Geological Society of America, The Geology of North America, v. G-2).

Clague, J.J. and Luternauer, J.L.
1982: Excursion 30A: Late Quaternary sedimentary environments, southwestern British Columbia; International Association of Sedimentologists, 11th International Congress on Sedimentology, Hamilton, Ontario, Field Excursion Guidebook, 167 p.

Dakin, R.A.
1991: Groundwater contamination from agricultural sources in the Lower Fraser Valley, B.C.; The BC Professional Engineer, October 1991, p. 30–32.
1994: Coastal basins, lowlands and plains; *in* Groundwater Resources of British Columbia, (ed.) J. Atwater, L.V. Brandon, W.L. Brown, R.A. Dakin, H.D. Foster, J.C. Foweraker, R.A. Freeze, E.C. Halstead, H.G. Harris, W.S. Hodge, A.T. Holmes, B. Ingimundson, D. Johanson, A.P. Kohut, H. Liebscher, E. Livingston, H.W. Nasmith, M.L. Parsons, O. Quinn, K. Ronneseth, J.L. Smith, D.F. Van Dine, M. Wei, and M. Zubel; British Columbia Environment and Environment Canada, p. 9.1–9.30.

Gabrielse, H., Monger, J.W.H., Wheeler, J.O., and Yorath, C.J.
1991: Part A. Morphological belts, tectonic assemblages and terranes; *in* Chapter 2 of Geology of the Cordilleran Orogen in Canada, (ed.) H. Gabrielse and C.J. Yorath; Geological Survey of Canada, Geology of Canada, no. 4, p. 15–28 (*also* Geological Society of America, The Geology of North America, v. G-2).

Gordy, P.L.
1988: Evaluation of the hydrocarbon potential of the Georgia depression; British Columbia Ministry of Energy, Mines and Petroleum Resources, Geological Report 88-03, 40 p.

Halstead, E.C.
1957: Ground-water resources of Langley Municipality, British Columbia; Geological Survey of Canada, Water Supply Paper 327, 47 p.
1959: Ground-water resources of Matsqui Municipality, British Columbia; Geological Survey of Canada, Water Supply Paper 328, 43 p.
1960: Surficial geology of Sumas map-area, British Columbia; Geological Survey of Canada, Paper 59-9, 27 p.
1961: Ground-water resources of Sumas, Chilliwack, and Kent municipalities, British Columbia; Geological Survey of Canada, Paper 60-29, 37 p.
1978: Nicomekl–Serpentine Basin study, British Columbia; Fisheries and Environment Canada, Scientific Series no. 94, 36 p.
1986: Ground water supply – Fraser Lowland, British Columbia; Environment Canada, Inland Waters Directorate, National Hydrology Research Institute, Paper no. 26, Scientific Series no. 145, 80 p.

Hamilton, T.S. and Ricketts, B.D.
1994: Contour map of bedrock surface, Georgia Strait and Lower Mainland region; *in* Geology and Geological Hazards of the Vancouver Region, Southwestern British Columbia, (ed.) J.W.H. Monger; Geological Survey of Canada, Bulletin 481, p. 193–196.

Kreye, R. and Wei, M.
1994: A proposed aquifer classification system for groundwater management in British Columbia; British Columbia Ministry of Environment, Lands and Parks, Groundwater Section, Hydrology Branch, Victoria, British Columbia, 68 p.

Liebscher, H., Hii, B., and McNaughton, D.
1992: Nitrates and pesticides in the Abbotsford aquifer; Environment Canada, Inland Waters Directorate, British Columbia, 83 p.

Makepeace, A.J. and Ricketts, B.D.
2000: Aquifer mapping and database management using a geographic information system, Fraser lowland; *in* Mapping, Geophysics, and Groundwater Modelling in Aquifer Delineation, Fraser Lowland and Delta, British Columbia, (ed.) B.D. Ricketts; Geological Survey of Canada, Bulletin 552.

McNeely, R.N., Neimanis, V.P., and Dwyer, L.
1979: Water quality sourcebook, a guide to water quality parameters; Environment Canada, Inland Waters Directorate, Water Quality Branch, Ottawa.

Monger, J.W.H. and Journeay, J.M.
1994: Basement geology and tectonic evolution of the Vancouver region, southwestern British Columbia; *in* Geology and Geological Hazards of the Vancouver Region, Southwestern British Columbia, (ed.) J.W.H. Monger; Geological Survey of Canada, Bulletin 481, p. 3–25.

Mustard, P.S. and Rouse, G.E.
1994: Stratigraphy and evolution of Tertiary Georgia Basin and subjacent Upper Cretaceous sedimentary rocks, southwestern British Columbia and northwestern Washington State; *in* Geology and Geological Hazards of the Vancouver Region, Southwestern British Columbia, (ed.) J.W.H. Monger; Geological Survey of Canada, Bulletin 481, p. 97–169.

Pullan S.E., Good, R.L., Jarvis, K., Roberts, M.C., and Vanderburgh, S.
2000: Application of shallow seismic-reflection techniques to subsurface structural mapping, Fraser lowland; *in* Mapping, Geophysics, and Groundwater Modelling in Aquifer Delineation, Fraser Lowland and Delta, British Columbia, (ed.) B.D. Ricketts; Geological Survey of Canada, Bulletin 552.

Rea, J.M.A. and Knight, R.J.
2000: Characterization of the Brookswood aquifer using ground-penetrating radar; *in* Mapping, Geophysics, and Groundwater Modelling in Aquifer Delineation, Fraser Lowland and Delta, British Columbia, (ed.) B.D. Ricketts; Geological Survey of Canada, Bulletin 552.

Ricketts, B.D.
1998: Groundwater flow beneath the Fraser River delta, British Columbia: a preliminary model; *in* Geology and Natural Hazards of the Fraser River Delta, British Columbia, (ed.) J.J. Clague, J.L. Luternauer, and D.C. Mosher; Geological Survey of Canada, Bulletin 525, p. 241–256.
2000: Modelling of groundwater flow in the Fraser River delta and Brookswood aquifer; *in* Mapping, Geophysics, and Groundwater Modelling in Aquifer Delineation, Fraser Lowland and Delta, British Columbia, (ed.) B.D. Ricketts; Geological Survey of Canada, Bulletin 552.

Ricketts, B.D. and Jackson, L.E.
1994: Hydrogeology, Vancouver–Fraser Valley, southern British Columbia; *in* Current Research 1994-A; Geological Survey of Canada, p. 201–206.

Ricketts, B.D. and Liebscher, H.
1994: The geological framework of groundwater in the Greater Vancouver area; *in* Geology and Geological Hazards of the Vancouver Region, Southwestern British Columbia, (ed.) J.W.H. Monger; Geological Survey of Canada, Bulletin 481, p. 287–298.

Ricketts, B.D. and Makepeace, A.J. (ed.)
2000: Aquifer delineation, Fraser lowland and delta, British Columbia: mapping, geophysics and groundwater modelling; Geological Survey of Canada, Open File D3828.

Roberts, M.C., Vanderburgh, S., and Jol, H.M.
2000: Radar facies and geomorphology of the seepage face of the Brookswood aquifer, Fraser lowland; *in* Mapping, Geophysics, and Groundwater Modelling in Aquifer Delineation, Fraser Lowland and Delta, British Columbia, (ed.) B.D. Ricketts; Geological Survey of Canada, Bulletin 552.

Roddick, J.A.
1965: Vancouver North, Coquitlam, and Pitt Lake map-areas, British Columbia; Geological Survey of Canada, Memoir 335, 276 p.
1990: Bedrock geology of the Vancouver area; Geological Association of Canada, Annual Meeting, Vancouver, Field Trip Guide, Excursion B10, 14 p.

Wassenaar, L.I.
1994: Evaluation of the origin and fate of nitrate in the Abbotsford aquifer using the isotopes of ^{15}N and ^{18}O in NO_3^-; Final report to British Columbia Ministry of Environment, Fraser River Action Plan, NHRI Contribution No. CS-94009, 48 p.

Weeks, J.B., Gutentag, E.D., Heimes, F.J., and Luckey, R.R.
1988: Summary of the High Plains regional aquifer-system analysis in parts of Colorado, Kansas, Nebraska, New Mexico, Oklahoma, South Dakota, Texas, and Wyoming; United States Geological Survey, Professional Paper 1400-A, 30 p.

Wei, M., Kohut, A.P., Kalyn, D., and Chwojka, F.
1993: Occurrence of nitrate in groundwater, Grand Forks, British Columbia; Quaternary International, v. 20, p. 39–49.

Woodsworth, G.J. and Ricketts, B.D.
1994: A digital database for Fraser Valley groundwater data; *in* Current Research 1994-A; Geological Survey of Canada, p. 207–210.

APPENDIX A

Bibliography of the Fraser Lowland Hydrogeology Project (1993–1998)

Best, M.E. and Todd, B.J.

1996a: Fraser Valley Hydrogeology Project: time-domain EM surveys, August 4 to August 18, 1995 (supplement to Open File 3095); Geological Survey of Canada, Open File 3308, 7 p.

1996b: Electromagnetic soundings, pseudo-resistivity logs and implications for porosity and groundwater salinity; Proceedings of the Symposium on the Application of Geophysics to Engineering and Environmental Problems, Keystone, Colorado; Wheat Ridge, Colorado, p. 1061–1074.

2000: Electromagnetic mapping of groundwater aquifers in the Fraser lowland; *in* Mapping, Geophysics, and Groundwater Modelling in Aquifer Delineation, Fraser Lowland and Delta, British Columbia, (ed.) B.D. Ricketts; Geological Survey of Canada, Bulletin 552.

Best, M.E., Todd, B.J., and O'Leary, D.O.

1994: Fraser Valley Hydrogeology Project: time-domain EM surveys, June 20 to July 8, 1994; Geological Survey of Canada, Open File 3095, 19 p.

1995: Groundwater mapping using time-domain electromagnetics: examples from the Fraser Valley, British Columbia; *in* Current Research 1995-A; Geological Survey of Canada, p. 19–27.

Campanella, R.G., Davies, M., Boyd, T., Everard, J., Roy, D., Tomlinson, S., Jackson, S., Schrempp, H., and Ricketts, B.D.

1994: In-situ testing for the characterization of aquifers: demonstration project; Geological Survey of Canada, Open File 2940, 19 p.

Dunn, D. and Ricketts, B.D.

1994: Surficial geology of Fraser Lowlands digitized from GSC Maps 1484A, 1485A, 1486A, and 1487A (NTS 92G/1, /2, /3, /6, /7, and 92H/4); Geological Survey of Canada, Open File 2894 (3.5-inch diskette).

Hamilton, T.S. and Ricketts, B.D.

1994: Contour map of bedrock surface, Georgia Strait and Lower Mainland region; *in* Geology and Geological Hazards of the Vancouver Region, Southwestern British Columbia, (ed.) J.W.H. Monger; Geological Survey of Canada, Bulletin 481, p. 193–196.

Makepeace, A.J. and Ricketts, B.D.

2000: Aquifer mapping and database management using a geographic information system, Fraser lowland; *in* Mapping, Geophysics, and Groundwater Modelling in Aquifer Delineation, Fraser Lowland and Delta, British Columbia, (ed.) B.D. Ricketts; Geological Survey of Canada, Bulletin 552.

Pullan S.E., Good, R.L., Jarvis, K., Roberts, M.C., and Vanderburgh, S.

2000: Application of shallow seismic-reflection techniques to subsurface structural mapping, Fraser lowland; *in* Mapping, Geophysics, and Groundwater Modelling in Aquifer Delineation, Fraser Lowland and Delta, British Columbia, (ed.) B.D. Ricketts; Geological Survey of Canada, Bulletin 552.

Pullan, S.E., Good, R.L., and Ricketts, B.D.

1995: Preliminary results from a shallow seismic reflection survey, Lower Fraser Valley Hydrogeology Project, British Columbia; *in* Current Research 1998-A; Geological Survey of Canada, p. 11–18.

Rea, J.M.A. and Knight, R.J.

2000: Characterization of the Brookswood aquifer using ground-penetrating radar; *in* Mapping, Geophysics, and Groundwater Modelling in Aquifer Delineation, Fraser Lowland and Delta, British Columbia, (ed.) B.D. Ricketts; Geological Survey of Canada, Bulletin 552.

Rea, J., Knight, R., and Ricketts, B.D.

1994a: Ground-penetrating radar survey of the Brookswood aquifer, Fraser Valley, British Columbia; *in* Current Research 1994-A; Geological Survey of Canada, p. 211–216.

1994b: Ground penetrating radar, Brookswood aquifer, Lower Fraser Valley, British Columbia; Geological Survey of Canada, Open File 2821, 13 p.

1994c: Ground-penetrating radar survey of the Brookswood aquifer in southwestern British Columbia; American Geophysical Union, Annual Meeting, San Francisco, California, 1994 (abstract).

Ricketts, B.D.

1995: Progress report and field activities of the Fraser Valley Hydrogeology Project, British Columbia; *in* Current Research 1995-A; Geological Survey of Canada, p. 1–5.

1998: Groundwater flow beneath the Fraser River delta, British Columbia: a preliminary model; *in* Geology and Natural Hazards of the Fraser River Delta, British Columbia, (ed.) J.J. Clague, J.L. Luternauer, and D.C. Mosher; Geological Survey of Canada, Bulletin 525, p. 241–256.

2000: Modelling of groundwater flow in the Fraser River delta and Brookswood aquifer; *in* Mapping, Geophysics, and Groundwater Modelling in Aquifer Delineation, Fraser Lowland and Delta, British Columbia, (ed.) B.D. Ricketts; Geological Survey of Canada, Bulletin 552.

Ricketts, B.D. and Dunn, D.

1995: The groundwater database, Fraser Valley, British Columbia; *in* Current Research 1995-A; Geological Survey of Canada, p. 7–10.

Ricketts, B.D. and Jackson, L.E.

1994: Hydrogeology, Vancouver–Fraser Valley, southern British Columbia; *in* Current Research 1994-A; Geological Survey of Canada, p. 201–206.

Ricketts, B.D. and Liebscher, H.

1994: The geological framework of groundwater in the Greater Vancouver area; *in* Geology and Geological Hazards of the Vancouver Region, Southwestern British Columbia, (ed.) J.W.H. Monger; Geological Survey of Canada, Bulletin 481, p. 287–298.

Ricketts, B.D. and Makepeace, A.J. (ed.)

2000: Aquifer delineation, Fraser lowland and delta, British Columbia: mapping, geophysics and groundwater modelling; Geological Survey of Canada, Open File D3828.

Ricketts, B.D., Jackson, L.E., Halliwell, D.R., and Vanderberg, S.

1993: Unconfined aquifers, Fraser River Basin; Geological Survey of Canada, Open File 2624 (folio of 23 maps).

Roberts, M.C., Vanderburgh, S., and Jol, H.M.

2000: Radar facies and geomorphology of the seepage face of the Brookswood aquifer, Fraser lowland; *in* Mapping, Geophysics, and Groundwater Modelling in Aquifer Delineation, Fraser Lowland and Delta, British Columbia, (ed.) B.D. Ricketts; Geological Survey of Canada, Bulletin 552.

Woodsworth, G.J. and Ricketts, B.D.

1994: A digital database for Fraser Valley groundwater data; *in* Current Research 1994-A; Geological Survey of Canada, p. 207–210.

Aquifer mapping and database management using a geographic information system, Fraser lowland

Andrew J. Makepeace[1] and Brian D. Ricketts[2]

Makepeace, A.J. and Ricketts, B.D., 2000: Aquifer mapping and database management using a geographic information system, Fraser lowland; in *Mapping, Geophysics, and Groundwater Modelling in Aquifer Delineation, Fraser Lowland and Delta, British Columbia, (ed.) B.D. Ricketts; Geological Survey of Canada, Bulletin 552, p. 17–26.*

Abstract: The Fraser Lowland Hydrogeology Project groundwater database now permits the physical extent of aquifers to be represented using special database records called 'virtual wells'. Macro programs have automated analytical and mapping tasks in the geographic information system for a case study in the vicinity of Langley. Twenty-seven aquifers were modelled as triangulated irregular networks, which in turn enabled detailed mapping of the aquifers' horizontal extent at any elevation. Profiles generated from the database illustrate the locations of these aquifers in cross-section. Static-level data from the database were used to construct potentiometric contour maps for six of the largest aquifers.

Résumé : La base de données du projet d'hydrogéologie des basses terres du Fraser sur l'eau souterraine permet de représenter l'étendue physique des aquifères en utilisant des enregistrements spéciaux de la base de données appelés «puits virtuels». Des macroprogrammes dans le système d'information géographique ont permis d'automatiser l'analyse et la cartographie dans le cadre d'une étude de cas aux environs de Langley. On a modélisé en réseau triangulaire irrégulier 27 aquifères, ce qui a permis de cartographier en détail l'extension horizontale des aquifères au niveau souhaité. Les profils générés à partir de la base de données illustrent en coupe transversale l'emplacement de tous ces aquifères. On a utilisé les données de niveau statique de la base de données pour dresser des cartes potentiométriques de six des plus grands aquifères.

[1] Geological Survey of Canada, 101–605 Robson Street, Vancouver, British Columbia V6B 5J3
[2] Department of Earth Sciences, University of Waikato, Private Bag 3105, Hamilton, New Zealand

INTRODUCTION

The groundwater database was designed in 1993 as an integral part of the Fraser Lowland Hydrogeology Project (Woodsworth and Ricketts, 1994). The database initially contained about 4300 water-well records, from which diagrams depicting lithology were created as a means of determining the location of hydrostratigraphic units (Ricketts and Dunn, 1995). These diagrams consisted of lithological units for a series of wells that were selected along a transect. Drawing these wells to scale resulted in the portrayal of a geological cross-section of the transect. The database has since been expanded to include the well, location, and driller's log records for nearly 9000 wells (Fig. 1). In addition, its structure has been modified to allow the representation of aquifers themselves.

In order to determine the shapes of aquifers, an iterative routine was followed. Computer output of well maps and stratigraphic cross-sections was used alternately with hydrogeological interpretation, until the delineation of hydrostratigraphic units was refined to the point where they were distinguishable from one another. Units were then given an arbitrary designation so they could be entered in the database as aquifers.

The groundwater database is currently maintained in the ARC/INFO® geographic information system (GIS), in which commands can be programmed in the native macro language (AML). Programs (called AMLs) that were written to display individual wells and lithostratigraphic profiles (Ricketts and Dunn, 1995) have been enhanced to create and analyze three-dimensional models of aquifers, and to facilitate such day-to-day tasks of database management as data entry and editing.

For the purposes of detailed aquifer mapping, a case study was undertaken in the vicinity of the Brookswood aquifer near Langley. An exhaustive examination of well data in this area, which covers about 150 km^2, was the source for a representation of the hydrostratigraphic architecture in the database, which was in turn used to generate graphical products depicting the shape of aquifers.

GROUNDWATER DATABASE

Modifications to the structure

Changes to the database structure were made to integrate spatial and attribute data, and also to accommodate the modelling of aquifers. Woodsworth and Ricketts (1994) described the structure of the original database, which consisted of three spreadsheet tables of attribute data: general well characteristics (e.g. depth to water, screen depths), location information (e.g. street address, township), and the driller's log (lithology with elevations relative to sea level), each with a linking field (LINK1) for relating it to the other tables. The attribute tables were subsequently transferred to the GIS. Spatial data were collected by digitizing well locations from maps directly into the GIS (Ricketts and Dunn, 1995). This produced a fourth table consisting of point locations, also with a linking field for relating it to the three attribute tables (Fig. 2). The database was kept in the GIS for all subsequent analysis, and will continue to be curated at the GSC offices in Vancouver.

In order to represent aquifers efficiently in the database, an aquifer item and a surface item were added to the driller's log. The aquifer item is a character field containing an arbitrary designation (e.g. A, V, TF) that identifies a lithological unit as belonging to a specific aquifer, based on

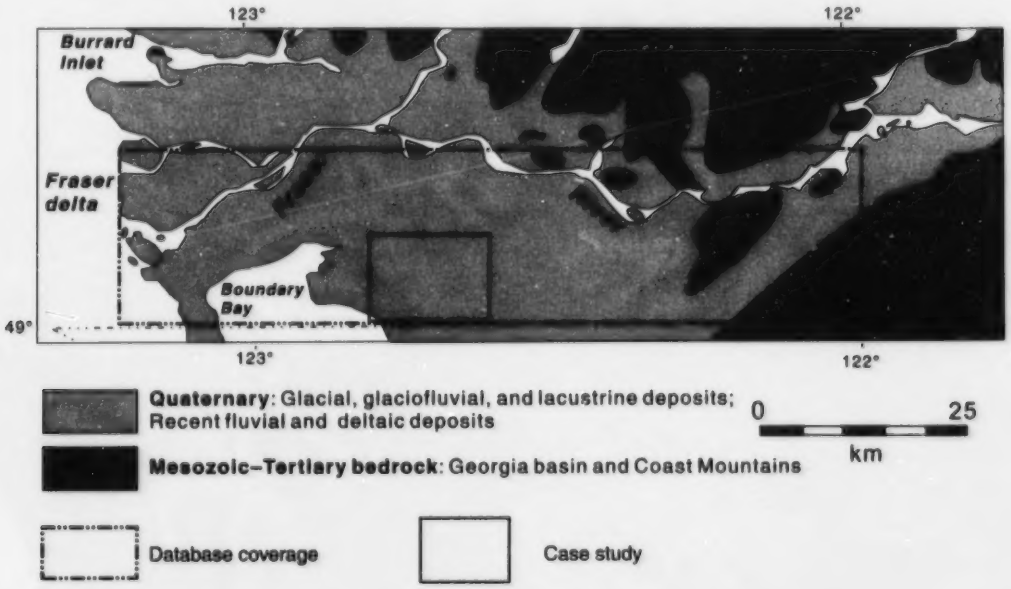

Figure 1. *Extent of database coverage and location of case study area.*

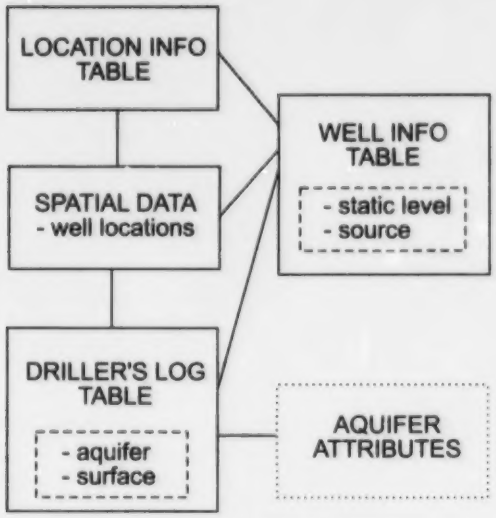

Figure 2. *Summary of the database structure. Dashed lines show additions to the original structure; dotted lines indicate possible future additions.*

hydrostratigraphic profiles. The surface item is a character field with a designation (e.g. T, B, TB) indicating the part of an aquifer's surface to which a lithological unit belongs: top, base, both, or neither. Thus, the locations of known points on an aquifer's surface are described by those units that form its top and its base, and by tagging the corresponding records in the driller's log with the appropriate character designation. Furthermore, the aquifer item can be used as a linking field to future tables, which might contain aquifer attributes.

Static levels of wells are implied by items giving the well-head elevation and the depth to water. These were used to calculate a new static level item (STAT_LVL) in the well-information table. This was done as a matter of convenience to allow the value of the static level at each well to be listed and queried directly. Since a well could penetrate more than one aquifer, a source item (SOURCE) was added to the well-information table to indicate which aquifer was the source of the hydrostatic pressure.

Input of remaining well data

To complete the database, the remaining well records (attribute data) for the lower Fraser River valley were transferred from a spreadsheet on an MS-DOS platform to the GIS on a UNIX platform (Fig. 3). Files were imported and exported in ASCII format, with intermediate editing of records done using awk scripts (a UNIX text-processing utility). Once imported into the GIS, each table was related via the linking field to the appropriate spatial data file representing well locations. The database is organized by British Columbia Geographic System map sheet number (e.g. 92G.005, 92G.006, etc.). Each map sheet has the four tables described above, although one or more of the tables may be empty or only partially complete for some map sheets (Table 1).

Table 1. Status of data tables, organized by British Columbia Geographic System (BCGS) map sheet.

BCGS map sheet	Well locations	Well information	Location information	Driller's log
92G.005		P	P	P
92G.006	P	P	P	P
92G.007	F	F	F	F
92G.008	F	P	P	P
92G.009	P	P	P	F
92G.010	F	F	F	F
92G.015		F	F	F
92G.016	P	F	F	F
92G.017	F	F	F	F
92G.018	P	P	P	F
92G.019	P	F	F	F
92G.020		F	F	F
92G.026	P			
92G.027	F			
92G.028	F			
92G.029	F			
92G.030	F			

F, full coverage; P, partial coverage.

Special records for aquifer modelling

To make full use in aquifer modelling of the information depicted in the hydrostratigraphic sections, two types of special records were introduced into the database: 'pseudolayers' and 'virtual wells'.

The need for the first type of special record arose due to omissions in some driller's logs. For a small number of wells, the driller's log listed entries for each unit within an aquitard, but no final entry when water-bearing material of a confined aquifer was intersected. In many cases, it could be determined, from depths of neighboring wells and from static level information, that the base elevation of one of these wells corresponded to the top of an aquifer. In this case, an extra record was added to the driller's log table, with top elevation equal to the base elevation of the overlying aquitard. This 'pseudolayer' was then tagged as the top of an aquifer, thus defining its vertical position.

The second type of special record, the 'virtual well', serves to represent the margins of an aquifer at locations where it is inferred to pinch out. In this case, the record fixes a position both horizontally and vertically. The horizontal position of a pinch-out was fixed by adding a virtual well to the spatial data file containing well locations. Entries in various fields of the record distinguish it from a real well. As with the real wells, however, virtual wells are linked to the driller's log table. Each virtual well has one corresponding record in the driller's log table: a pseudolayer, as described above, which fixes the vertical position of the pinch-out.

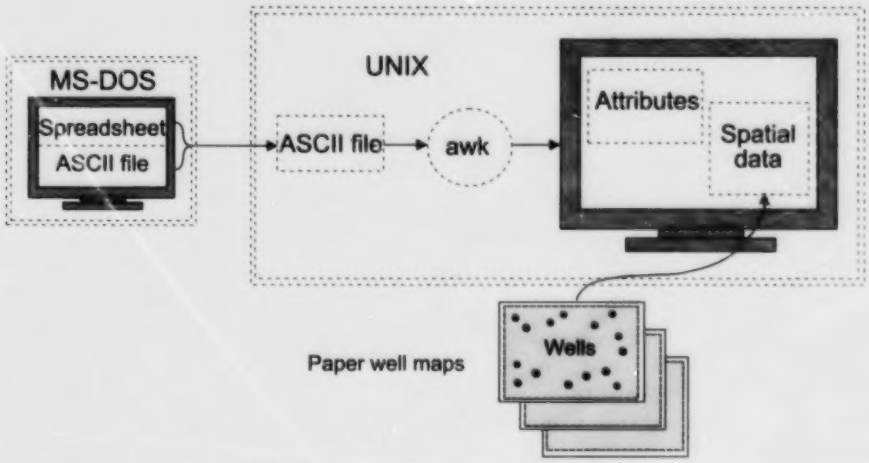

Figure 3. *Flowchart for completion of the database. Well-attribute tables were transferred from MS-DOS to UNIX as ASCII files, where they were processed by the awk utility before being imported into the GIS. Well locations were digitized from paper well maps directly into the GIS.*

METHOD

Using the groundwater database to extract, interpret, and store information for modelling aquifers in three dimensions involves an iterative procedure between operator and computer. Cross-section diagrams and well-location maps were produced to give a preliminary indication of the hydrostratigraphic architecture in the study area. Wells and cross-sections were examined visually so as to distinguish different, or apparently different, aquifers from one another. This initial interpretation of aquifer locations was added to the database and used to produce a working copy of an aquifer map. This map was again examined, using new cross-sections in different orientations, and the coded database description of the aquifers was refined. With each iteration, new aquifers were found, and existing aquifers split or merged.

Once all the wells intersecting an aquifer were identified, its horizontal extent was mapped. Any well intersecting a given aquifer necessarily lies within the aquifer boundary. The margin of the aquifer can be inferred to occur between one of these wells and a neighboring well that does not intersect the aquifer. For simplicity, the margin was assumed to be halfway between these two wells. For each inferred pinch-out, a virtual well at this location was then inserted into the database. The closer the spacing of neighboring wells, and the greater the number of virtual wells, the greater the accuracy in defining the aquifer margin. In some cases, a definite aquifer or aquitard in a neighboring well could not be discerned, so no pinch-out was assumed. Similarly, for deep aquifers or aquifers adjacent to the map boundary, there were no neighboring wells indicating an aquitard. Since no pinch-out could be assumed here, only real wells served to define the aquifer margin as a 'limit of information'.

This refinement procedure, shown schematically in Figure 4, can be broken down into the following steps:

1. Choose transects of interest, usually along major roads and other areas of densely spaced wells. Select wells in an organized fashion along each transect, using an AML-driven GIS routine, and print out a hard copy of the resulting lithostratigraphic cross-sections.
2. Inspect the cross-sections visually to identify and correlate hydrostratigraphic units. Assign an arbitrary designation to units that appear to be distinct.
3. Enter designations into the driller's log table (AQUIFER and SURFACE items). This is done with an AML that prompts for an aquifer designation, a well number, a layer number, and surface designation (top, base, or both). Generate and plot a well map (using an AML), with well symbology based on the data just entered in the driller's log table.
4. Re-examine sections visually. Find areas that imply the location of a pinch-out. Produce new cross-sections in specific orientations for areas in which correlations are difficult to discern.
5. Enter corrections and additions to the driller's log table as necessary. Plot a new well map. If not satisfactory, go back to step 4. Otherwise proceed.
6. Delineate aquifer margins on paper maps. Add virtual well records to the database to represent pinch-outs. An AML prompts for an aquifer designation and then allows the operator to select pairs of wells between which the aquifer is assumed to pinch out. Virtual wells and corresponding pseudolayer records are then added to the database automatically.

The result is that, for each aquifer, there is a series of records tagged as corresponding to the aquifer's top, base, or both, and which represents points, each with an x,y,z value.

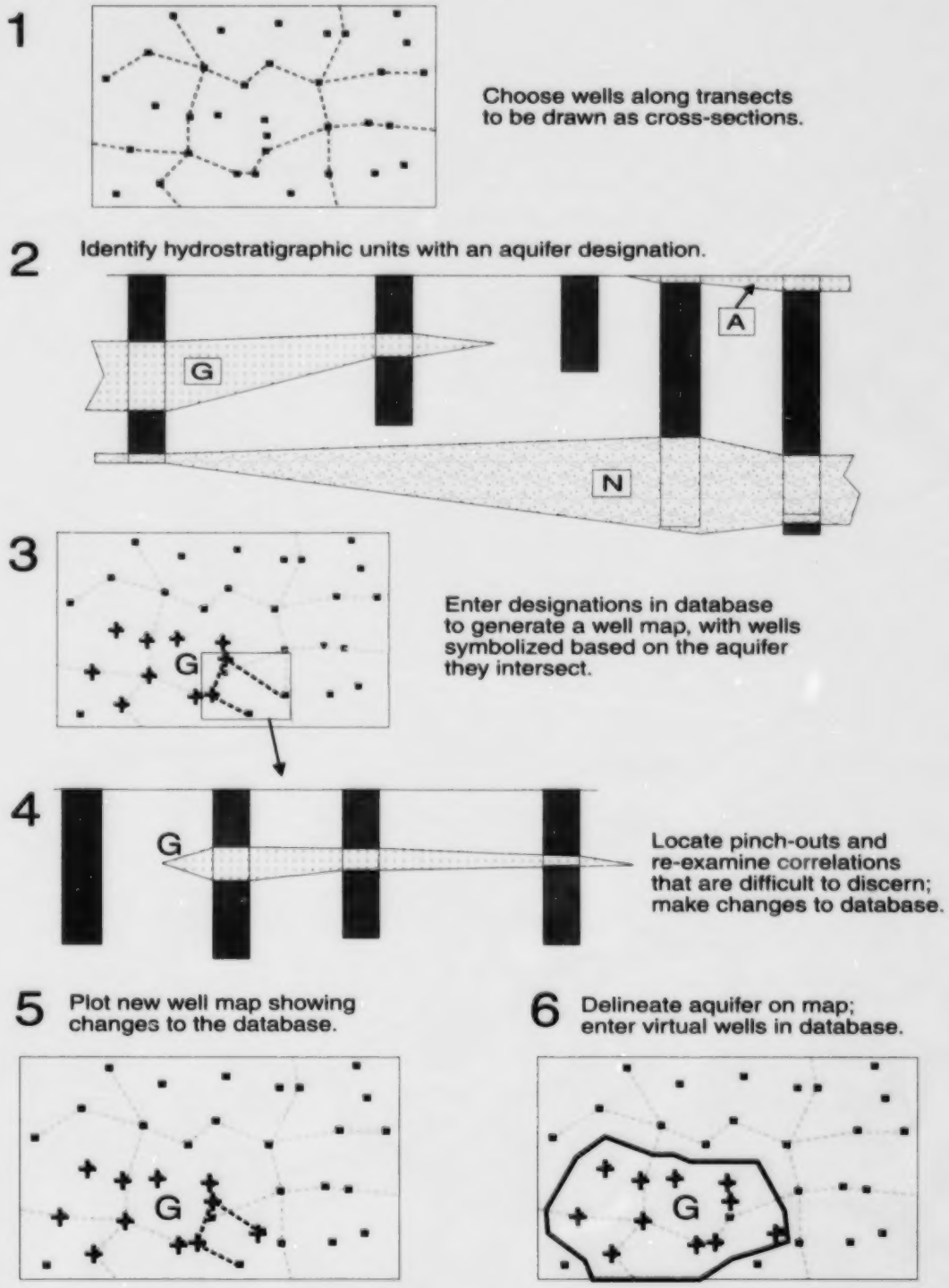

Figure 4. *Procedure for determining hydrostratigraphic architecture using lithological cross-sections and well-location maps.* See *text for details.*

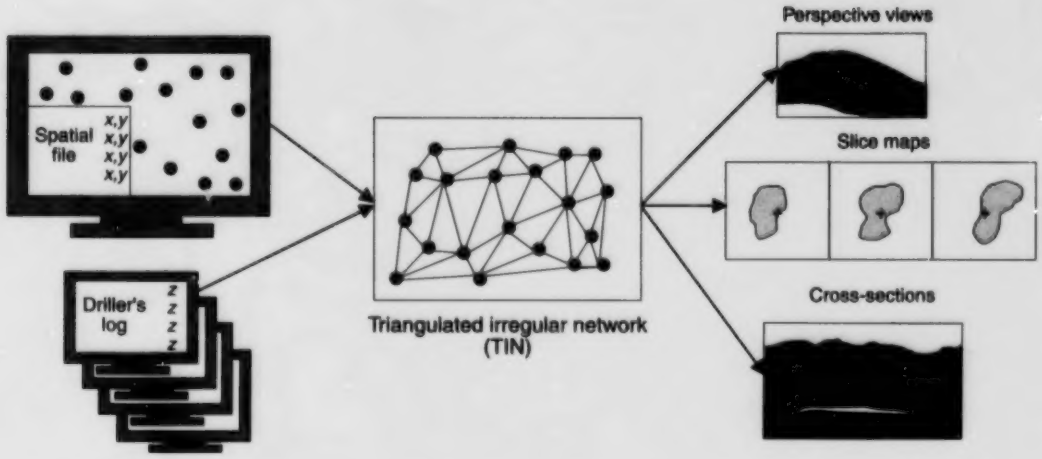

Figure 5. *Triangulated irregular network (TIN) integrates known x,y,z points of an aquifer into a single data structure, thus modelling the aquifer surface for subsequent output products.*

The x and y values are the well's UTM co-ordinates (from the spatial data file), and the z value is the elevation relative to sea level (from the driller's log table).

Construction of triangulated irregular networks

The last step in the compilation of aquifer data is the creation of a triangulated irregular network (TIN) for each aquifer surface. The TINs take as input the x,y,z co-ordinates known to coincide with the aquifer surface, namely the UTM co-ordinates from the spatial data file and the elevation data from the driller's log table. These co-ordinates are used as vertices of triangular facets by the GIS to model the entire surface (Fig. 5). Aquifer surfaces are represented as TINs because 1) the co-ordinates of an aquifer surface are consolidated into a single data structure, whereas before they were distributed between two database tables with much unrelated data; 2) this is an efficient method for storing irregularly spaced three-dimensional data points (as is the case here); and 3) a TIN is the basis for interpolation of z-values between data points when using the GIS to generate various products, such as slice maps, profiles (*see* 'Case Study' section, below), and oblique perspective views.

ALGORITHMS AND ARC MACRO LANGUAGE PROGRAMS

The groundwater database resides on the ARC/INFO® GIS running on a DEC™ Alpha workstation. In addition to the profusion of built-in commands and functions, ARC/INFO® permits programming in its native macro language (ARC Macro Language). Programs, or AMLs, were written to perform a number of analytical functions, and to expedite map creation and database editing and updating, as described below.

Generating cross-sections of the lithology

Creation of paper stratigraphic cross-sections from the mass of digital data was a fundamental step in determining the hydrostratigraphy. This was accomplished with a series of three AMLs (Fig. 6). The first displays a plan view of well locations overlain with roads for visual reference. The user is prompted to select wells with the mouse in the order in which they are to be drawn in cross-section. When the selection is complete, the first AML calls the second, which repeats once for each well. The second AML first adds annotations indicating well information, such as static level, address, and well number, at the top of the section. It then draws to scale the linework for each individual layer. Each time a layer is drawn, the second AML calls a third, which annotates the layer with the elevation and material type. When the diagram is complete, it is sent to the plotter for paper output.

Coded well map

In order to depict the horizontal extent of aquifers penetrated by each well, an AML was written to generate a well-location map in which each well was symbolized according to the aquifer recorded in its driller's log (Fig. 7). These maps served as an essential cross-reference when attempting to resolve the hydrostratigraphic units visually from cross-sections. Modifying the AML permitted aquifer symbols to be included in or excluded from the map, since new aquifers were found and others merged with each iteration. Where a well penetrated several aquifers, symbols were plotted one on top of the other, but with distinguishing colours, sizes, and shapes.

Pinch-out placement

When an aquifer was identified adjacent to a section depicting only an aquitard, the aquifer was assumed to pinch out halfway between the two wells. Pairs of wells around the

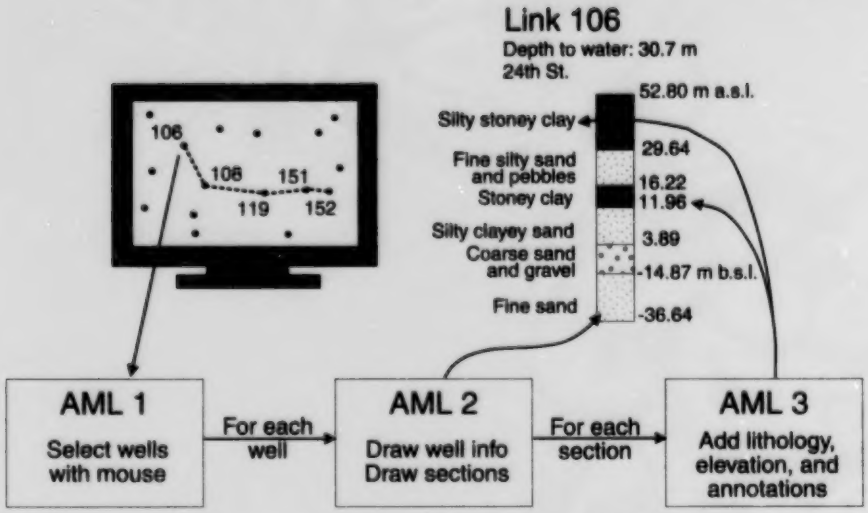

Figure 6. *Lithological cross-sections are constructed using a series of three ARC Macro Language (AML) programs. The first allows the user to select wells graphically, the second annotates the well and draws the cross-section linework, and the third annotates each unit with elevation and material type.*

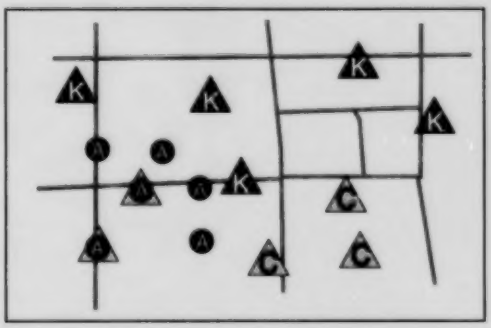

Figure 7. *Sample well-location map, with symbols indicating aquifers penetrated at each location.*

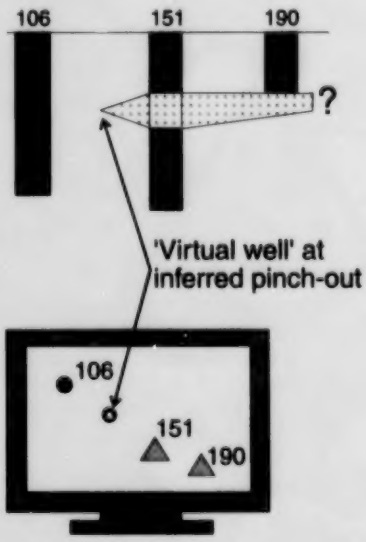

Figure 8. *Pinch-outs are stored in the database as virtual wells. The user selects two wells between which there is a pinch-out, and the records are added to the database automatically.*

aquifer margin were examined to find points where pinch-outs could be inferred (Fig. 8). Pinch-outs were then added to the database with an AML that prompted for an aquifer designation, and then displayed the wells in plan view. The user could then select a pair of wells, and the computer would automatically insert a virtual well between them and add a corresponding pseudolayer to the driller's log table. These records were used to define the margin of the aquifer, and contributed to the surface represented as a TIN.

CASE STUDY

Whereas the database covers a large area of the lower Fraser River valley, a smaller area was selected for detailed aquifer mapping (Fig. 1). The case study area coincides with BCGS map sheet 92G.007 (on the southern edge of NTS map sheet 92G/2) and includes the Brookswood aquifer near Langley. This area, extending about 13.5 km east-west, and about 11 km north from the United States border, has also been the study area for various geophysical methods for detecting groundwater. Since this was the only area mapped in detail, modifications to the groundwater database apply only to tables for map sheet 92G.007.

Table 2. Sample extract from driller's log table.

LINK1	AQUIFER	SURFACE	ELEV	BELEV	MATERIAL
158	NG	TB	101.2	99.4	Brown sand
158	ZZZ	*	99.4	92.1	Blue clay
158	ZZZ	*	92.1	86.0	Sandy blue clay
158	ZZZ	*	86.0	79.9	Coarse gravel and boulders with clay binder
158	N	T	79.9	72.3	Coarse gravel and sand
158	N	Int	72.3	64.7	Sand with some boulders
158	N	B	64.7	52.5	Fine grey sand
158	ZZZ	*	52.5	35.7	Boulders and gravel with clay binder
158	ZZZ	*	35.7	29.6	Hardpan
158	O	TB	29.6	18.9	Fine grey sand with boulders
158	ZZZ	*	18.9	-84.4	Silt

LINK1 – numerical well designation.
AQUIFER – designation of aquifer to which the lithological unit belongs.
SURFACE – part of the aquifer to which the lithological unit belongs: T, top; B, base; Int, intermediate unit; * indicates that the layer is an aquitard.
ELEV – elevation (m) of top of lithological unit.
BELEV – elevation (m) of base of lithological unit.

Initially, cross-sections were generated for main streets (running north-south) and avenues (running east-west) approximately 1.6 km apart. Hydrostratigraphic units identified on a cross-section were assigned an arbitrary designation, which was maintained in the correlations found in perpendicular cross-sections. These designations, once entered in the driller's log table, were the framework for the first map generated showing wells, which were symbolized according to the aquifer they penetrated. Table 2 is an extract from a driller's log record that shows entries flagging lithological units as belonging to an aquifer. Next, cross-sections were generated for wells located within each mile-square section. Viewing these cross-sections in conjunction with the plan-view map enabled further correlations to be found and entered in the database. The ability to identify distinct hydrostratigraphic units varied greatly across the study area, depending on the density of wells, well depth, completeness of well records, and amount of detail in the driller's log entries. In some areas, where it was particularly difficult to make correlations, additional cross-sections were generated in specific orientations to help visualize the hydrostratigraphy. Detail emerged as the examination became more localized, the result being that aquifers were split into separate units. Conversely, re-examination of the original framework with knowledge of the detail within each mile-square section showed that some aquifers had to be merged with others. There were many occurrences of a single hydrostratigraphic unit in one well for which no correlation could be found in neighboring wells. These are coded in the database with an aquifer designation of '?'.

Final aquifer and well map

With the database representation of aquifers in place, twenty-eight aquifers were mapped in detail (Table 3). Pinch-out locations were inferred for those portions of aquifers with sufficient control along their margins, and the corresponding virtual wells were added to the database. Virtual well records are designated by LINK1 numbers greater than 80 000 and a BCGS WELL_NUM entry beginning with 'V'. Margins were delineated by connecting virtual wells in sequence around the aquifer. In areas where pinch-outs could not be inferred, margin delineation was accomplished by joining real wells around the aquifer's outermost known extent. When completed, the margins were stored separately in the GIS for use in conjunction with the groundwater database.

Table 3. Aquifers mapped in detail. *See* Figure 9 for locations.

Margin delineated; TIN of top and base	A, I, NH, NG, NA, N, YY, JX, JY, JW, JZ, JV, XY, XX, WA, Y, YA, AV, TH, TG, T, V, C, R, D, L
TIN of top and base	W
TIN of top	J

The result of the detailed aquifer mapping was a map depicting well locations, the aquifers penetrated by each well, and the location of inferred margins (Fig. 9, in pocket). Each well is plotted with the symbol, colour, and designation of the aquifer it penetrates, and its LINK1 number is plotted beside it for reference purposes. Where a well penetrates a succession of aquifers, symbols for each are plotted one over the other in sequence, with the symbol and designation for the uppermost aquifer plotted on top. Aquifer margins are indicated by a line the same colour as the well symbols that represent the aquifer. A solid line represents an inferred margin based on pinch-outs; a dashed line shows the limit of information in areas for which there were no sufficiently deep wells to infer pinch-outs. As with well symbols, margins are plotted one over the other to indicate a succession of aquifers.

There are many aquifers for which detailed mapping was not practicable. This was the case for deep aquifers intersected by only a small number of wells (e.g. aquifer EE in the northeast corner of Fig. 9), or for two aquifers having overlapping boundaries and similar depths, which made it difficult to discern a margin (e.g. aquifers AK and AL in the

south-central part of Fig. 9). These aquifers are retained in the database and, where space permits, are symbolized on the map where they are intersected by a well.

Aquifer modelling

The next step in the detailed mapping was the creation of a TIN for the top and base of each aquifer. Elevations used as input for TINs were extracted from the database by selecting records based on the AQUIFER and SURFACE items in the driller's log table. Aquifer margins were used to define the horizontal extent of the TINs. Table 3 lists the aquifers for which TINs were created. Two products were generated from TINs to depict the shapes of aquifers, vertical profiles and horizontal slice maps. Both of these use TINs to estimate the elevation of aquifer surfaces between known points (i.e. well locations), by interpolating between the vertices of each facet of the TIN. The interpolation creates a smooth and continuous quintic surface, whose elevation at each TIN vertex is equal to the z-value of that vertex (Akima, 1978).

Vertical profiles

Vertical profiles (Fig. 10, in pocket), which were generated automatically along eight lines of section (*see* Fig. 9 for locations), are based on the TINs of each of the aquifers they cross. The quintic surfaces for the top and base of each aquifer were sampled at intervals of 50 m along each line, and the area between the resulting boundaries was shaded in the same colour used for margins and well symbols in Figure 9. Virtual wells contribute to the surfaces, and are reflected in the gradual pinching out of shading in aquifers (e.g. aquifer C in profile F-F′of Fig. 10). Where no pinch-out was inferred, a limit of information margin is represented by real wells, and is shown as an abrupt termination of the shaded profile (e.g. north end of aquifer V in profile F-F′of Fig. 10).

In some places, the interpolated surface for an aquifer's base was found to rise above the top surface. This tends to occur where the aquifer is very thin and where the slope of one surface is changing more rapidly than the other. Since this results in a profile that suggests a pinch-out in the middle of the aquifer where none is intended, a thin solid line is used to enforce shading across thin sections (e.g. aquifer T in profile B-B′of Fig. 10). Because aquifer J is relatively deep, there was insufficient data to represent its base. For this reason, only the top of aquifer J is shown, drawn as a solid yellow line below the other aquifers.

The profile of one aquifer occasionally intrudes on another (e.g. aquifers L and D in profile C-C′, and aquifers JW and JY in profile E-E′of Fig. 10). This suggests that the two aquifers may be a single hydrostratigraphic unit, and that the well data in these areas should be re-examined in detail.

The density of known data points (i.e. the density of TIN vertices) for all aquifer surfaces is less than that of the surface topography. For this reason, interpolation of aquifer surfaces occasionally produced values greater than the elevation of the land surface, resulting in small spikes above the topographic profile (e.g. profile E-E′in Fig. 10).

Slice maps

In order to visualize the extent of aquifers at different elevations in plan view, maps were created depicting the shape of a horizontal 'slice' through an aquifer at a specified elevation. For aquifers A, N, V, and I, the quintic surfaces for the top and base were contoured automatically by the GIS. Contours of each were written to separate files, each contour having been tagged with an item indicating its elevation. It was then possible to extract contours of a specified elevation for both the top and base and display them simultaneously to create slice maps for these four aquifers (Fig. 11a–d, in pocket). Slices are drawn as a solid line where they intersect the top of an aquifer and as a dashed line where they intersect the base. Cultural features in the area were drawn in the background for reference.

At many elevations, the shape of a horizontal slice is complex. However, the behaviour of the contour can be summarized by several typical shapes (Fig. 12). An isolated, closed solid line represents a slice through a local maximum on the top surface. An isolated, closed dashed line represents a slice through a local minimum on the base. A solid and dashed line meeting at the margin indicate that the aquifer dips toward the solid line. A closed solid line enclosed by a dashed line indicates that the slice passes through a local maximum on both surfaces. As with aquifer profiles, there are at some locations an artifact that arises from interpolated values of the base having greater z-values than the top. On the slice maps, it is seen

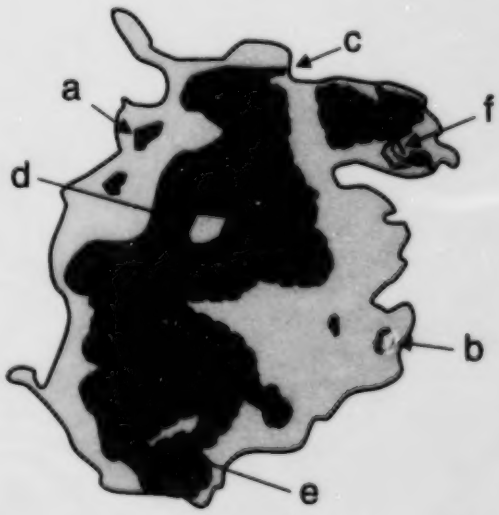

Figure 12. *Interpretation of typical features on a slice map: a, local maximum on the top; b, local minimum on the base; c, solid line and dashed line meeting at the margin indicate that the aquifer is dipping toward the solid line; d, enclosed solid line represents a local minimum on the top surface; e, enclosed dashed line represents a local maximum on the base; f, solid and dashed line cross where the interpolated surface of the base rises above the top; the edge of the slice in this case is taken to be halfway between the two lines (dotted line).*

as a dashed line that crosses a solid one. Here it is best to interpret the edge of a slice as running halfway between these two lines.

Potentiometric surface maps

Each record in the well-information table has an entry for the depth of water in the well due to hydrostatic pressure. This and the well-head elevation were used to calculate the static level relative to sea level for each well, which was assigned to the STAT_LVL item in the well-information table. Each well record also lists the depths of the top and bottom of the screen. If the elevation of a hydrostratigraphic unit overlapped that of a well's screen, it was taken to be the source of hydrostatic-pressure, and its aquifer designation assigned to the well information table in the SOURCE item. If more than one hydrostratigraphic unit fell within the screen depths, or if the original record had no depth to water information, the SOURCE item was assigned the value 'Unk', for 'unknown'.

For six aquifers (I, N, A, L, V, and T), static-level data were extracted and used as z-values for the construction of a TIN. A quintic interpolation performed on each TIN resulted in a potentiometric surface for each of the six aquifers. These surfaces were contoured at 2 m intervals as shown in Figure 13 (in pocket). Wells shown as black dots are those known to contribute to the surface; other wells are shown in grey.

The head contours for each aquifer permit inferences to be made about groundwater flow. Aquifers N and I (Fig. 13) are located on the south and north flanks, respectively, of a topographic high extending from White Rock to Hazelmere. Inferred regional flow in aquifers N and I is toward the south and north, respectively. Hydraulic gradients are high in these two aquifers: 14 m/km in N, and 8 m/km up to as much as 24 m/km in I.

Although locally complicated head-contour patterns emerge in the potentiometric surface of aquifer A (Brookswood aquifer water table), the contours show a radial distribution broadly similar to those of the measured water-table map and simulated potentiometric map in Ricketts (2000, Fig. 22, 23). Local variations in the head values probably result from a combination of 1) errors in the original static level measurements (e.g. under nonequilibium conditions) in the well, 2) local topography, 3) drawdown in neighboring wells during measurement of static level, and 4) seasonal variation in water-table elevations (particularly important in the unconfined Brookswood aquifer).

Many of the high and low points on the potentiometric surface appear to be controlled by single wells. Of the factors listed above, local drawdown effects from high-production wells (e.g. the community wells in Brookswood, and the Forest Nursery wells at 192nd St. and 36th Ave.) and seasonal variation likely have the most significant effects on individual static-level measurements.

CONCLUSIONS

Analysis of water-well records in a geographic information system was shown to be a practicable method for determining the extent of aquifers in three dimensions. Locations of points where wells penetrated aquifers and aquitards were used to define top and base surfaces of aquifers. These surfaces, which became part of the database, were used to depict aquifers in cross-section, and to draw plan views of horizontal slices through the aquifers at various depths. For wells in six aquifers within the case-study area, static level data were used to construct potentiometric surfaces. Contours of these surfaces were shown to be useful for making inferences about groundwater flow.

Data from this analysis could be exported in various formats to other computer platforms for use in database management, groundwater flow and contaminant modelling, and risk analysis. Graphical output could be used in concert with results from other geophysical methods to corroborate and refine aquifer locations. Furthermore, this study illustrates that a geographic information system is capable of successfully managing and analyzing hydrogeological data (e.g. water-well records, hydrostratigraphy) in most groundwater-mapping programs.

ACKNOWLEDGMENTS

The authors would like to acknowledge Al Kohut and Rod Zimmerman (British Columbia Ministry of Environment, Lands and Parks) and Larry Adamache, Hugh Liebscher, and Basil Hii (Environment Canada) for providing much of the raw water-well data for this study. Glenn Woodsworth is thanked for reviewing the manuscript. David Dunn worked on the initial stages of the groundwater database. Robert Cocking, Stephen Williams, and Murray Journeay provided useful advice along the way.

REFERENCES

Akima, H.
1978: A method of bivariate interpolation and smooth surface fitting for irregularly distributed data points; *in* ACM Transactions on Mathematical Software 4 (June 1978), p. 148–159.

Ricketts, B.D.
2000: Modelling of groundwater flow in the Fraser River delta and Brookswood aquifer; *in* Mapping, Geophysics, and Groundwater Modelling in Aquifer Delineation, Fraser Lowland and Delta, British Columbia, (ed.) B.D. Ricketts; Geological Survey of Canada, Bulletin 552.

Ricketts, B.D. and Dunn, D.
1995: The groundwater database, Fraser Valley, British Columbia; *in* Current Research 1995-A; Geological Survey of Canada, p. 7–10.

Woodsworth, G.J. and Ricketts, B.D.
1994: A digital database for groundwater data, Fraser Valley, British Columbia; *in* Current Research 1994-A; Geological Survey of Canada, p. 207–210.

Electromagnetic mapping of groundwater aquifers in the Fraser lowland

Melvyn E. Best[1] and Brian J. Todd[2]

Best, M.E. and Todd, B.J., 2000: Electromagnetic mapping of groundwater aquifers in the Fraser lowland; in *Mapping, Geophysics, and Groundwater Modelling in Aquifer Delineation, Fraser Lowland and Delta, British Columbia, (ed.) B.D. Ricketts; Geological Survey of Canada, Bulletin 552, p. 27–47.*

Abstract: Time-domain electromagnetic soundings were conducted in the Fraser lowland to investigate whether electromagnetic methods can distinguish groundwater aquifers (both confined and unconfined) from aquitards. A secondary purpose was to investigate whether electromagnetic methods can determine water quality (salinity) of the aquifers.

More than 100 electromagnetic soundings were conducted in the vicinity of Langley and Abbotsford using a Geonics EM-47™ system operating in the central-sounding mode. The sites were chosen to ensure a wide range of geological conditions related to different aquifer and seal types. Interpretation of these data indicates that electromagnetic methods can map surficial and deeper (>150 m) geological features associated with groundwater aquifers and seals. Geophysical interpretations of the soundings agree with available drillhole information and, where available, seismic-reflection, detailed gravity, and ground-penetrating radar data.

Résumé : On a effectué des sondages électromagnétiques à domaine temporel dans les basses terres du Fraser afin de déterminer si les méthodes électromagnétiques permettent de distinguer les aquifères (captifs ou libres) des aquitards. L'étude avait comme objectif secondaire d'établir si les méthodes électromagnétiques permettent de déterminer la qualité (salinité) de l'eau des aquifères.

Avec un système Geonics EM-47^{MC} exploité en mode sondage central, on a effectué plus de 100 sondages électromagnétiques aux environs de Langley et d'Abbotsford. On a sélectionné les sites de manière à obtenir une grande variété de conditions géologiques reliées aux différents types d'aquifères et de couches encaissantes. L'interprétation des données indique que les méthodes électromagnétiques peuvent être utilisées pour cartographier les entités géologiques de surface et plus profondes (>150 m) associées aux aquifères et aux couches encaissantes. L'interprétation de ces sondages géophysiques concorde avec l'information fournie par les forages et, le cas échéant, avec les données de sismique réflexion, de gravimétrie détaillée et du géoradar.

1 Bemex Consulting International, 5288 Cordova Bay Road, Victoria, British Columbia V8Y 2L4
2 Geoterra Geoscience, 6 Shady Lane, Halifax, Nova Scotia B3N 1T9

INTRODUCTION

Residential and agricultural growth in the Fraser lowland of southwestern British Columbia are putting stress on existing groundwater supplies in the region. Consequently, new aquifers must be identified and producing aquifers require better definition in order to develop their total potential. Many of the aquifers utilized at present are shallow, and therefore new aquifers will tend to be deeper and more expensive to delineate and develop. Groundwater contamination, particularly in unconfined aquifers, has also become a contentious issue. As a result, information is required on the direction and magnitude of groundwater flow, aquifer recharge and discharge, and location of impermeable boundaries, in order to better understand regional aquifer characteristics.

Regional geology is an essential component of the investigation of regional groundwater studies. The Geological Survey of Canada therefore initiated the Fraser Lowland Hydrogeology Project, in April 1993, to develop techniques for mapping the regional geology and groundwater flow (Ricketts and Jackson, 1994). The program consists of surface and subsurface hydrogeological mapping, geophysical investigations, and groundwater modelling. As part of this program, time-domain electromagnetic (TDEM) soundings were carried out at a number of sites. The objectives were to determine whether electromagnetic methods could provide information on such aquifer parameters as porosity, hydraulic conductivity, and water quality (salinity), as well as information on location and quality of aquitards (seals).

Electromagnetic methods measure the vertical and lateral resistivity structure of the Earth. The conductivity (inverse of resistivity) of earth materials depends on the conductivity of the pore fluids and on the mineralogy (particularly clay minerals) of the sediment or rock. Field test sites were chosen to investigate a range of geological environments, each with different aquifer and aquitard properties. In addition, some sites were selected to ensure that the electromagnetic surveys overlapped high-resolution seismic-reflection, ground-penetrating radar, and gravity surveys that were being carried out independently.

In particular, the present study investigated whether TDEM methods could differentiate good aquifers (e.g. sand and gravel with high porosity and permeability) from poor aquifers and impermeable boundaries (clay). The study also explored whether electromagnetic (EM) methods could map the bedrock topography beneath aquifers, in order to delineate preferential flow paths. Finally, the study investigated whether EM methods could distinguish fresh pore water from brackish or saline pore water.

Location maps (Fig. 1) and detailed geological and geographic descriptions of the test sites were reported by Best et al. (1994, 1995) and Best and Todd (1996a). This paper summarizes the results of the two-year EM study and, in addition, presents a geological interpretation that incorporates information from the entire data set.

GEOLOGICAL SETTING

The Fraser lowland has a complex geological history (Armstrong, 1957, 1980, 1981; Armstrong and Hicock, 1980; Clague et al., 1983). Late Quaternary Salish sediments, consisting of stream channel fill, floodplain and overbank deposits, lacustrine silt and clay deposits, bogs, swamps, shallow lake deposits, and Fraser River sediments, are scattered throughout the lowland. Thick Holocene sediments underlie the Fraser delta. Extensive regions east of the delta consist of Pleistocene glacial, fluvial, glaciomarine, and marine deposits up to 700 m thick. This complex package of Quaternary sediments sits on an irregular surface of Tertiary bedrock, which consists of clastic sedimentary rocks.

The resistivity structure of this sediment package is complex, consisting of conductive marine and lacustrine sediments, more resistive glacial sand and gravel, and highly resistive bedrock. In some instances, Pleistocene sediments contain pockets of saline pore water trapped during deposition. In such cases, the resistivity of the sediment is very low.

The electromagnetic study concentrated on two geological environments within the Fraser lowland, 1) the Abbotsford–Sumas and Brookswood aquifers, which are unconfined aquifers consisting of Sumas Drift (Late Pleistocene) and underlain by Pleistocene (Capilano or Fort Langley) marine and glaciomarine sediments; and 2) confined aquifers within Pleistocene sediments.

ELECTROMAGNETIC METHODS

Electromagnetic (EM) methods map conductivity variations within the Earth by inducing currents in the ground using a time-varying electromagnetic field. All EM systems consist of a transmitter, which generates an electromagnetic (primary) field, and one or more receivers, which measure the primary field and the (secondary) fields generated in the Earth by the induced eddy currents. The two types of EM system in use are frequency-domain EM and time-domain EM. The transmitter of a frequency-domain EM system generates sinusoidal electromagnetic fields at a number of fixed frequencies, usually between 100 and 20 000 Hz. The receiver(s) measure the amplitude and phase (relative to the

Figure 1.

Locations of EM-47 surveys in the Fraser lowland: ***a)*** *western Fraser lowland and Fraser delta,* ***b)*** *central Fraser lowland, and* ***c)*** *detailed locations near the Brookswood aquifer. Surveys 1, 2, 3, 10, 11, 12, and 13 are over the Brookswood aquifer; surveys 6 and 7 are over the Abbotsford–Sumas aquifer; and surveys 4 and 5 are over confined aquifers within Pleistocene sediments.*

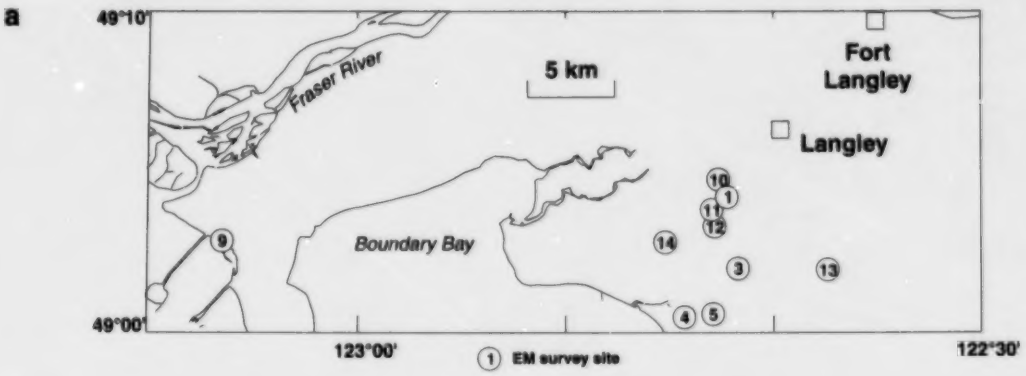
a
49°10'
Fraser River
5 km
Fort Langley
Langley
Boundary Bay
49°00'
123°00'
122°30'
1 EM survey site

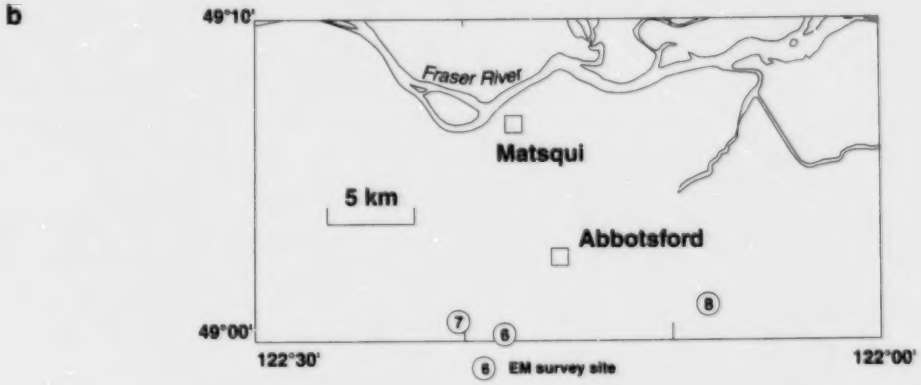
b
49°10'
Fraser River
Matsqui
5 km
Abbotsford
49°00'
122°30'
122°00'
6 EM survey site

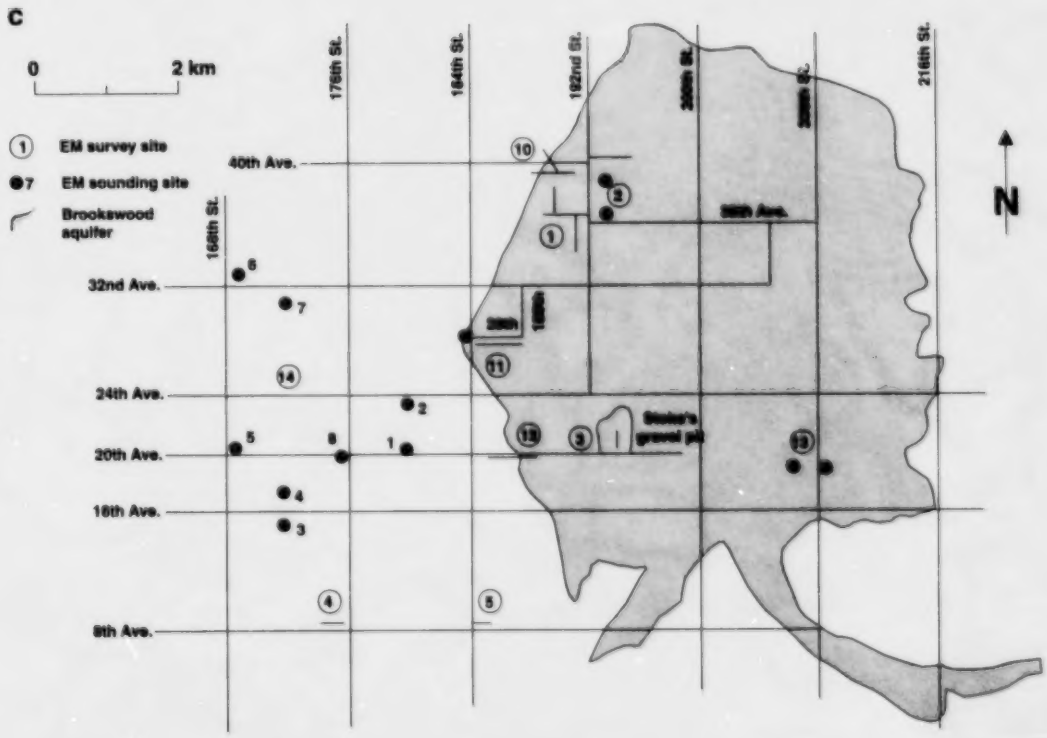
c
0
2 km
1 EM survey site
7 EM sounding site
Brookswood aquifer
176th St.
184th St.
192nd St.
216th St.
40th Ave.
32nd Ave.
24th Ave.
20th Ave.
16th Ave.
8th Ave.
N

transmitted magnetic field) of the in-phase and quadrature components of the secondary magnetic field at each fixed frequency. The transmitter of a time-domain EM system transmits square-wave or coded-pulse electromagnetic fields. The receiver(s) measure the magnetic field as a function of time, usually when the current (primary field) is off. Electromagnetic transmitters consist of a coil of area 'A' with 'N' turns of wire, each carrying a current 'I'. The strength of the transmitted electromagnetic field is proportional to the dipole moment (M) of the transmitter coil:

$$M = NIA \quad (1)$$

Electromagnetic receivers consist of coils with N turns of wire. They measure the voltage in the coil caused by the time-dependent magnetic field (Faraday's Law). In time-domain systems, the transmitter and the receiver(s) must be synchronized to ensure that time zero is known, whereas, in frequency-domain systems, the phase difference between the transmitted EM field and the secondary field caused by the Earth must be known.

The electromagnetic survey carried out as part of the Fraser Lowland Hydrogeology Project used a time-domain electromagnetic system, the Geonics EM-47™. Details of the EM-47™ system are provided in Best et al. (1994, 1995) and Best and Todd (1996a). Figure 2 depicts the layout of the transmitter and receiver for operating in the central-sounding mode. The transmitter dipole consists of a single wire deployed in a square loop. The survey used a loop with sides measuring 20, 40, or 80 m, and carrying a current of 2.1–2.3 A. The transmitter controls the shape of the current and the frequency of the transmitted square wave. The receiver coil has a diameter of approximately 1 m (coil area times the number of turns equals 31.4 m^2). A reference cable connects the transmitter and receiver to control the timing of the transmitted waveform and the time during which the received voltage is measured. The receiver measures the vertical component of the magnetic field.

Figure 3a illustrates the time-dependent current in the transmitter loop that generates the electromagnetic field, the voltage in the receiver coil caused by this primary current (V_p), and the secondary voltage in the receiver coil caused by the induced currents in the Earth (V_s). The transmitter current approximates a square wave with a sine-wave rise time and a linear ramp at the end of the square wave to turn off the current. The frequency of the square wave is equal to 1/T, where T is the period of the square wave pulse. The period consists of a positive square wave of duration T/4, followed by an off-time of duration T/4. These are then reversed to give a total period equal to T. Three frequencies are available with the EM-47 system: ultra high frequency (UH) of 285 Hz, very high frequency (VH) of 75 Hz, and high frequency (H) of 30 Hz.

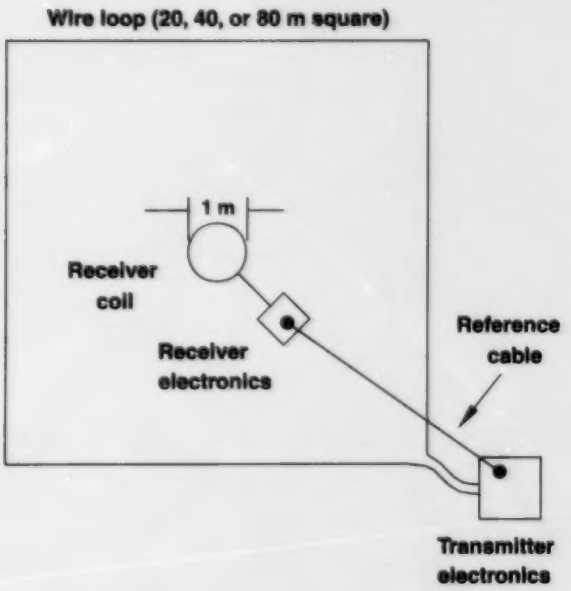

Figure 2. Schematic diagram of the Geonics EM-47™ system configuration used during the survey, in the central-sounding mode.

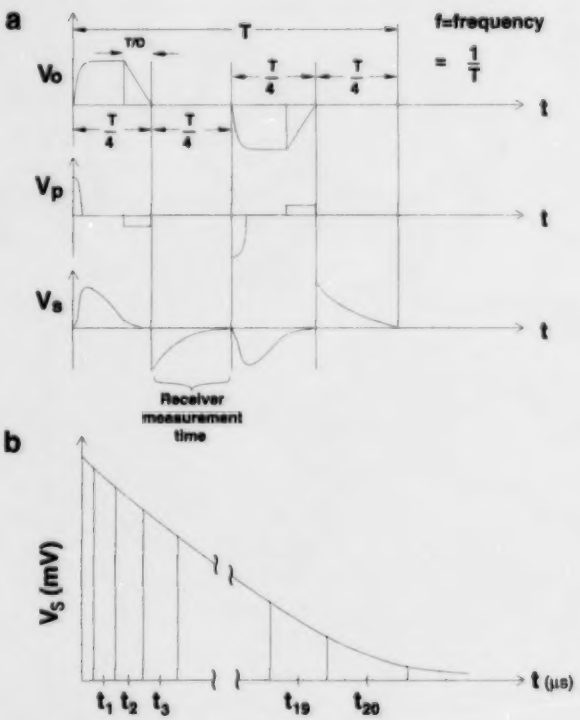

Figure 3. a) Voltage (V) versus time (t) plot of the transmitter current wave form and the corresponding wave form in the receiver. The iinear ramp turn-off time (T/O) depends on the size of the transmitter loop. The secondary voltage (V_s) is measured by the receiver when the transmitter is off. b) Expanded view of the secondary voltage at the receiver, showing the time windows increasing with time. The time of a window is defined to be the time at the centre of the window.

As already discussed, the receiver voltage is measured when the transmitter is off. Consequently, there is no primary voltage at the receiver to interfere with the secondary magnetic field generated by the induced eddy currents. The receiver voltage in the EM-47™ unit is measured in millivolts but is displayed as nanovolts (nV) per Am^2 (dipole moment) when plotted as a function of time using the TEMIXGL™ software from Interpex Limited. The receiver voltage is measured in 20 time windows for each of the three square-wave frequencies listed above. The total time window goes from about 6 to 7000 μs, with UH times from 6.85 to 701 μs, VH times from 48.3 to 2825 μs, and H times from 100 to 7040 μs. The receiver voltage is sampled logarithmically in time (Fig. 3b). Each voltage measurement is averaged over its time window, and the time at the centre of the averaging window is defined to be the time for that window. The windows increase at greater times because the voltages are usually smaller. Good conductors produce larger voltages that take longer to decay, whereas poor conductors produce smaller voltages that decay quickly.

The voltages are converted to apparent resistivity values using late-time normalized voltages (Fitterman and Stewart, 1986; Stoyer, 1990). The apparent resistivity is defined as the ratio of the measured voltage to the voltage that would be measured over a half-space of constant resistivity. Once the apparent resistivity versus time curves are computed, the data can be interpreted in terms of multilayered earth models using standard forward and inverse mathematical modelling programs.

FIELD ACQUISITION

The Geonics EM-47™ surveys were carried out over approximately six weeks during the summers of 1994 and 1995. More than 120 central-loop soundings were made in the three areas surveyed. Most of the soundings were made using 40 and 80 m square loops; a few were made using 20 m square loops. The transmitter current was kept as close as possible to 2.3 A for all soundings. Data were collected at the three frequencies of the EM-47 system (UH, VH, and H) for each sounding, even though the voltages from the longer times (H frequency range) were often within the noise window.

Three measurements were averaged at each frequency to increase the signal-to-noise ratio. Several of the soundings had noise that needed to be edited before interpretation. In general, the Fraser lowland data were relatively noisy (Todd et al., 1993; Best et al., 1994, 1995). There are numerous EM sources in the area due to the close proximity of airports (Vancouver International and Abbotsford), marine navigation and communication systems, and local industrial and construction noise (e.g. Stoke's gravel pit, site 3).

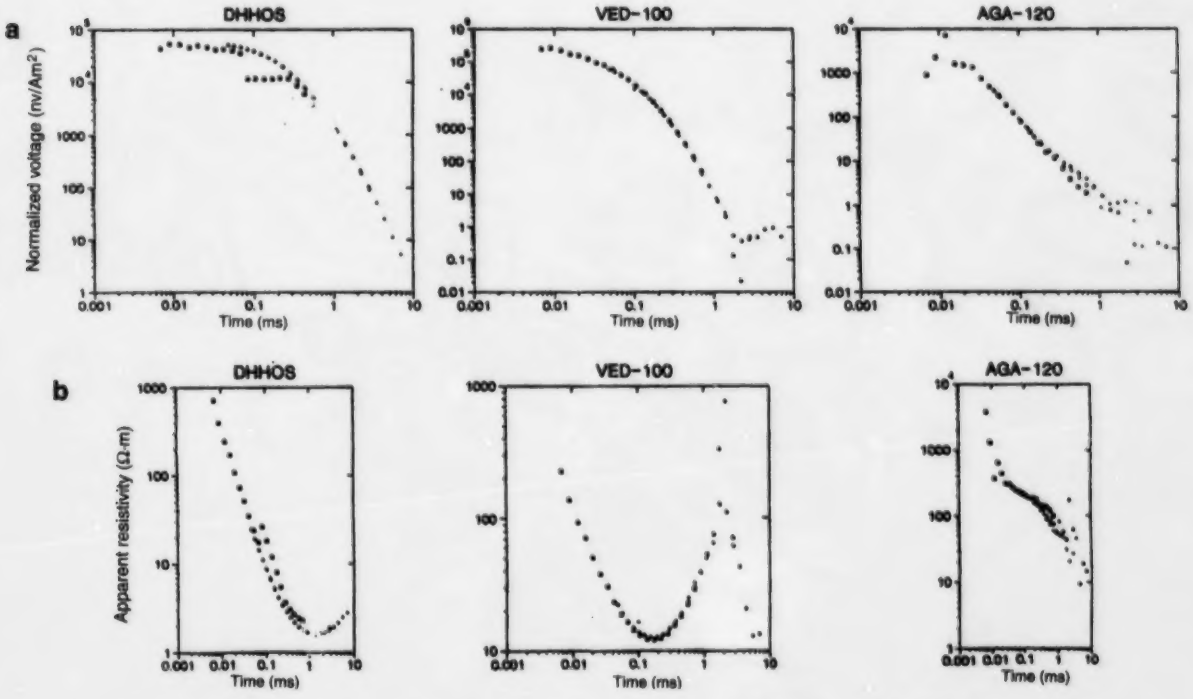

Figure 4. a) *Log-log plots of unedited normalized voltage (nV/Am^2) versus time for: DHH0S, Coal port dyke near drillhole 86-5 (site 9); VED-100, Vedder Mountain (site 8); and AGA-120, Agassiz Experimental Farm (site 7). Note the different scales for the three plots.* ***b)*** *Log-log plots of unedited apparent resistivity (Ω·m) versus time for the soundings in Figure 4a.*

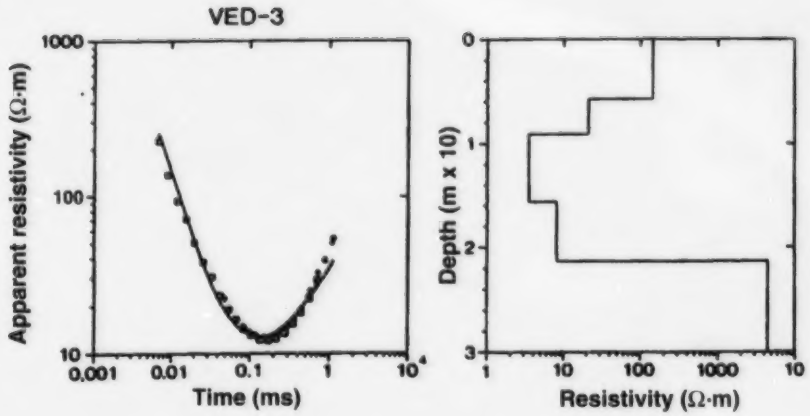
VED-3
Apparent resistivity (Ω·m)
1000
100
10
0.001
0.01
0.1
1
10
Time (ms)
Depth (m x 10)
0
1
2
3
1
10
100
1000
10
Resistivity (Ω·m)

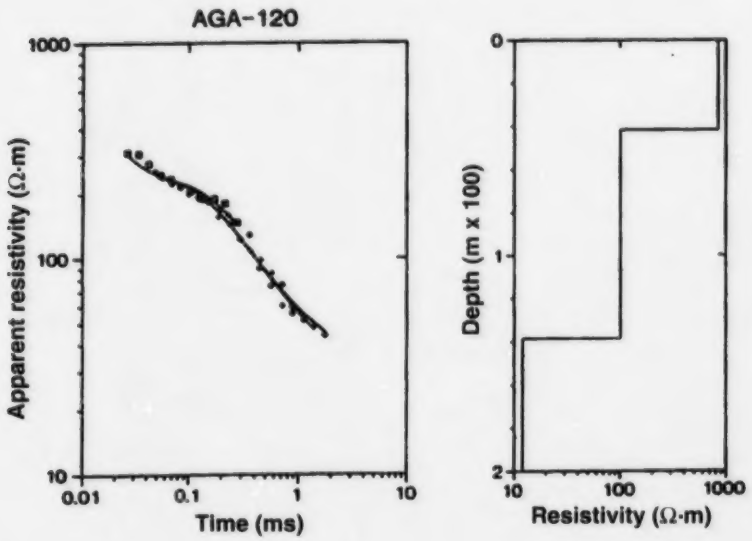
AGA-120
Apparent resistivity (Ω·m)
1000
100
10
0.01
0.1
1
10
Time (ms)
Depth (m x 100)
0
1
2
10
100
1000
Resistivity (Ω·m)

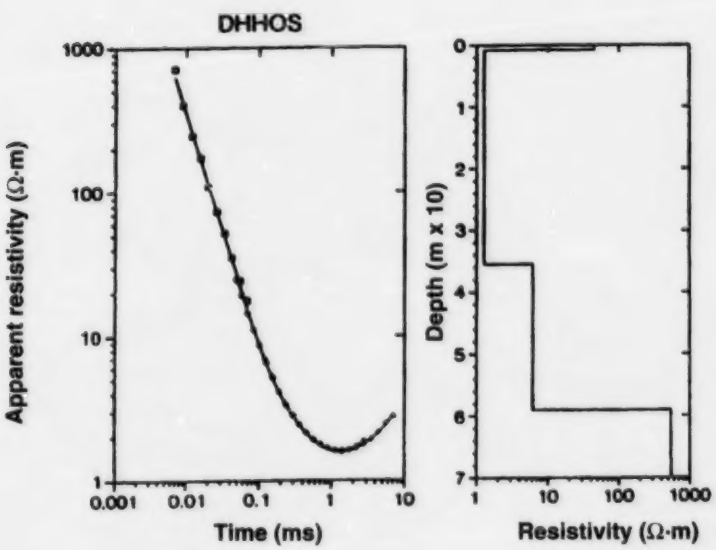
DHHOS
Apparent resistivity (Ω·m)
1000
100
10
1
0.001
0.01
0.1
1
10
Time (ms)
Depth (m x 10)
0
1
2
3
4
5
6
7
1
10
100
1000
Resistivity (Ω·m)

EDITING

Soundings shown in Best et al. (1994, 1995) and Best and Todd (1996a) are typical of the data obtained during the surveys. The data generally required editing before interpretation. Any saturated values (values greater than 5000 mV) at short times, and noisy values (usually less than 1 nV/Am^2) at long times were first removed from the data. Voltages related to specific noise at specific times were sometimes removed as well. Edited data were stored for future processing and interpretation. The effects of editing are illustrated by comparing the original data to the final edited data (Fig. 4, 5). Figure 4 also provides examples of conversion of the normalized voltage versus time plots into corresponding apparent resistivity versus time plots.

The solid line in each of the three edited apparent resistivity plots in Figure 5 is the apparent resistivity curve computed for the multilayer conductivity model shown graphically in the same figure. These models were computed using interactive graphics and Occam inversion. Inversion was performed only after the computed apparent resistivity values obtained from interactive graphics were relatively close to the measured data.

INTERPRETATION

Smooth-model inversion (Best and Todd, 1996b) of the data using 19 layers was carried out to obtain a general idea of the one-dimensional resistivity distribution associated with each sounding. Several soundings (e.g. site 1, NUR1-80 and NUR1-160) had cultural noise from buried pipes, cables, and metal. In such cases, forward modelling was the only option available. Fortunately, this occurred only at four soundings (two at site 1 and two at site 12; Fig. 1c).

The smooth-model results were used to develop simpler models consisting of two to four layers. The initial thicknesses and resistivities of each layer were estimated from the smooth model. These initial models were then inverted, using Occam inversion, to obtain best-fit estimates for the layer thicknesses and resistivities (Best and Todd, 1996a, b). In addition, equivalence analysis was performed for each inversion to provide resistivity and thickness (depth) ranges for all layers. Values of resistivity and thickness within these ranges produced fits to the data that have a standard error equal to, or somewhat larger than, that of the best-fit model.

The sounding data presented in this paper have been plotted as 1) best-fit layer thicknesses (depths) for each sounding, as a profile at a given site (e.g. Fig. 6a), with the range of possible depths represented by the shaded regions associated with the profile and best-fit values for layer resistivities included; and 2) best-fit layer resistivities for each sounding, as a profile at a given site (e.g. Fig. 6b), with the range of possible resistivities represented by the shaded regions. For both presentations, the darker shaded regions represent areas where the ranges of fit of adjacent layers overlap. These plots form the basis of the interpretation presented below. Examples of smooth-model inversions, layered-model inversions, and equivalence plots are given in Best et al. (1994, 1995) and Best and Todd (1996a).

The data collected in the Fraser lowland will be discussed first for the unconfined Brookswood and Abbotsford–Sumas aquifers and then for the confined aquifers associated with Capilano sediments.

Pore-water resistivity values in freshwater environments tend to vary from a few tens to thousands of ohm metres. Under such circumstances, some general comments can be made regarding the influence of clay on the bulk resistivity of a material (Keller and Frischknect, 1966). This is important, because a similar relationship exists between clay content and hydraulic conductivity (Fetter, 1988).

There are no hard and fast rules, but clean sand (coarse to medium) and gravel will generally have resistivities of 100 Ωm or more. Fine and silty sand with little clay content will be between 50 Ωm and 100 Ωm. As the clay content increases, the resistivity decreases to the point where clayey sand and clay have resistivities of less than 30 Ωm. By analogy, clean sand and gravel will have higher hydraulic conductivities than fine and silty sand, which in turn will be higher than clayey sand and clay. Indeed the hydraulic conductivity of clay layers is often so low that they are almost perfect seals. Leaky seals can consist of clay, clayey sand, and even silty sand.

Brookswood aquifer

The Brookswood aquifer (Fig. 1c) is an unconfined (phreatic) aquifer consisting mainly of coarse sand and gravel. Aquifer thickness varies from a few metres, near its southern and eastern edges, to more than 40 m in sections within its interior and northwest quadrant. Aquifer stratigraphy is variable, depending on its position relative to the old meltwater channel, which coincides approximately with the modern Campbell River (Ricketts, 2000). A pre-existing, west-trending topographic high (informally referred to as the White Rock–Hazelmere high; Ricketts (2000)), which abuts the southwest corner of the Brookswood aquifer, also influenced deposition. The Brookswood aquifer overlies a thick package (50 m or more) of silty sand containing clay lenses, which in turn overlies marine clay (Capilano and Fort Langley formations).

Figure 5.

Log-log plots of edited apparent resistivity (Ω·m) versus time for the three soundings in Figure 4 (VED-3 is identical to VED-100). Note the different scales for the three plots. Solid lines correspond to apparent resistivity computed for the layered earth models. When the overlapping data from the three frequencies are not identical, the TEMIXGL™ software fits each of the three curves separately. This leads to the two solid curves for AGA-120, where the UH and VH frequencies overlap around 0.2 ms (200 μs).

Figures 6 to 12 are layered-earth interpretations of the electromagnetic data for each site associated with the Brookswood aquifer. The coarse sand and gravel of the Brookswood aquifer is represented by the upper resistivity layer in these diagrams.

In the northwestern and western sections of the aquifer (sites 1 (Fig. 6), 2 (Fig. 8), 10 (Fig. 7), and 11 (Fig. 9a)), the west-central portion (site 3 (Fig. 10a)), and the westernmost of the two soundings at site 13 (Fig. 12a), the unconfined aquifer has resistivities (best-fit values) between 100 and 300 Ω·m. These values are consistent with other measurements in coarse sand and gravel, although the pore-water resistivity does affect the total or bulk resistivity (*see* section on 'Archie's Law' below). Sounding NDH at site 2 is the only exception, with a resistivity of approximately 500 Ω·m. The upper layer resistivity at sites 10 and 11 drops below 100 Ω·m about halfway down the topographic slope at the western end of the lines. This change in resistivity (dashed line in Fig. 7a, 9a) appears to be associated with changes in depositional environment (seepage face of Ricketts (2000)). The location

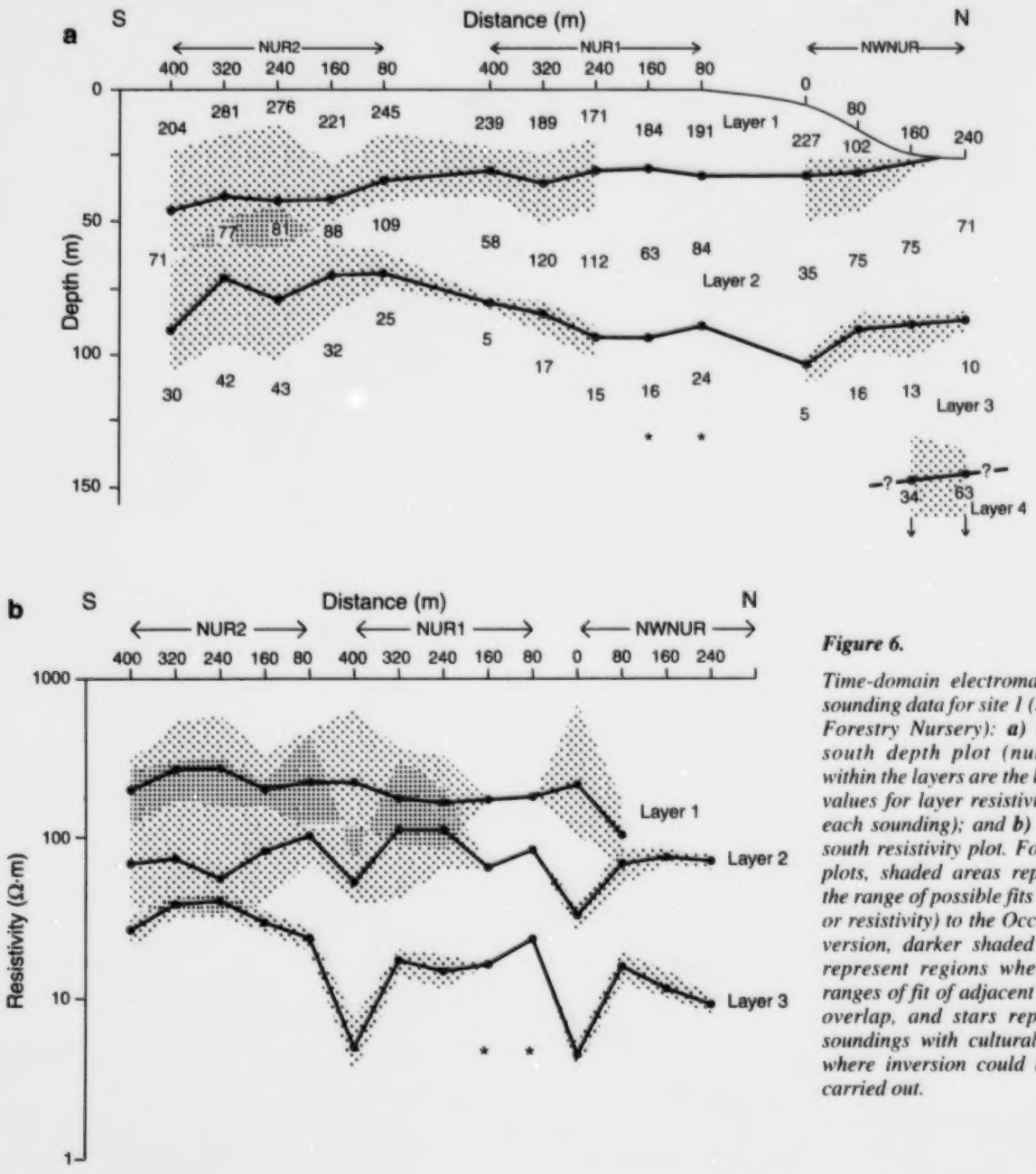

Figure 6.

*Time-domain electromagnetic sounding data for site 1 (Surrey Forestry Nursery): **a)** north-south depth plot (numbers within the layers are the best-fit values for layer resistivities at each sounding); and **b)** north-south resistivity plot. For both plots, shaded areas represent the range of possible fits (depth or resistivity) to the Occam inversion, darker shaded areas represent regions where the ranges of fit of adjacent layers overlap, and stars represent soundings with cultural noise where inversion could not be carried out.*

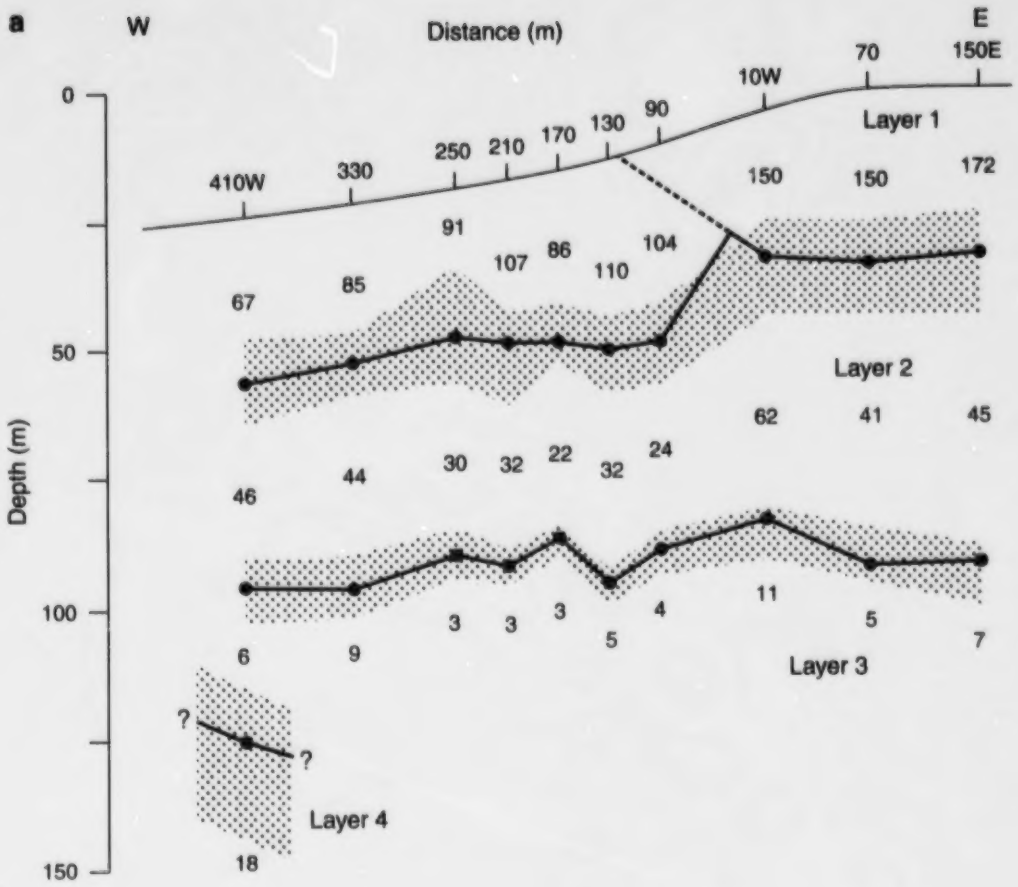

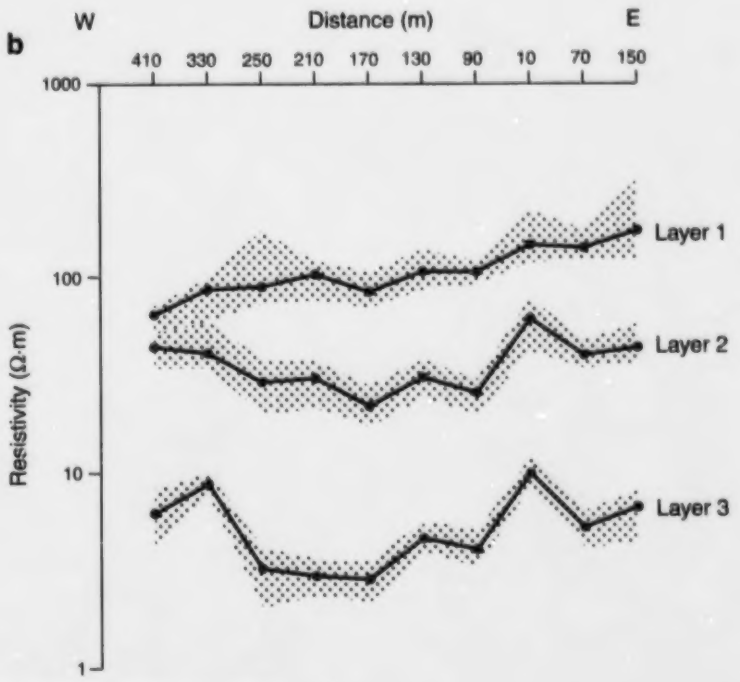

Figure 7.

*Time-domain electromagnetic sounding data for site 10 (40th Ave.): **a**) east-west depth plot (numbers within the layers are the best-fit values for layer resistivities at each sounding); and **b**) east-west resistivity plot. For both plots, shaded areas represent the range of possible fits (depth or resistivity) to the Occam inversion.*

is not precisely determined from the EM data because there is a zone across which the transition occurs. This transition is also confirmed by ground-penetrating radar data along the same lines (Roberts et al., 2000).

The resistivity of the aquifer at sites 12 (Fig. 11a) and 13 (Fig. 12a) is less than 100 Ω·m; the depositional environment in this portion of the Brookswood aquifer was influenced by the pre-existing White Rock–Hazelmere topographic high (west of 184th Ave.). Indeed, the two soundings at the west end of site 12 are not related to the Brookswood aquifer, but are associated with Vashon Drift (Armstrong and Hicock, 1980). The thickness of the Brookswood is consistently between 35 and 50 m at all sites, except where it changes character at the west end of sites 10 and 11.

Although the resistivity of the silty sand unit beneath the Brookswood aquifer is generally less than 100 Ω·m, it too changes from place to place. It is more resistive in the northern (sites 1 (Fig. 6a), 2 (Fig. 8a), and 10 (Fig. 7a)) and central (sites 3 (Fig. 10a) and 13 (Fig. 12a)) regions of the aquifer, with values greater than 30 Ω·m. Sites 11 (Fig. 9a) and 12 (Fig. 11a) have resistivity values less than 20 Ω·m. The silty sand unit in this area must contain more clay than in the northern and central areas. Based on the resistivity values, this unit can vary from being an aquifer, albeit not a good one, in the northern and central regions, to at best a leaky seal near sites 11 and 12. Infiltration from the Brookswood aquifer into this unit is therefore a distinct possibility, the rate depending on the difference in potentiometric head between the two units.

Based on its resistivity (less than 10 Ω·m), the marine clay unit underlying the silty sand is generally a good seal. The exception may be near the south end of sites 1 (Fig. 6a) and 2 (Fig. 8a), where the resistivity values are as high as 43 Ω·m. There is an indication of a deeper confined aquifer at the north end of site 1 (Fig. 6a) and the west end of site 10 (Fig. 7a). This layer can be observed at these locations because the sediment package above it is at its thinnest. The minimum thickness of the clay unit in this area is estimated to be about 50 m. However, according to the observed resistivity values, the confined aquifer would be poor.

The edge of the Brookswood aquifer coincides with the north end of site 1 (Fig. 6a), in an abandoned gravel pit. There is a lens of more conductive surface material at the east end of site 11 (Fig. 9a), but its origin is uncertain. The conductive surface material (clay) at the east end of site 13 (Fig. 12a) continues westward, according to ground-penetrating radar

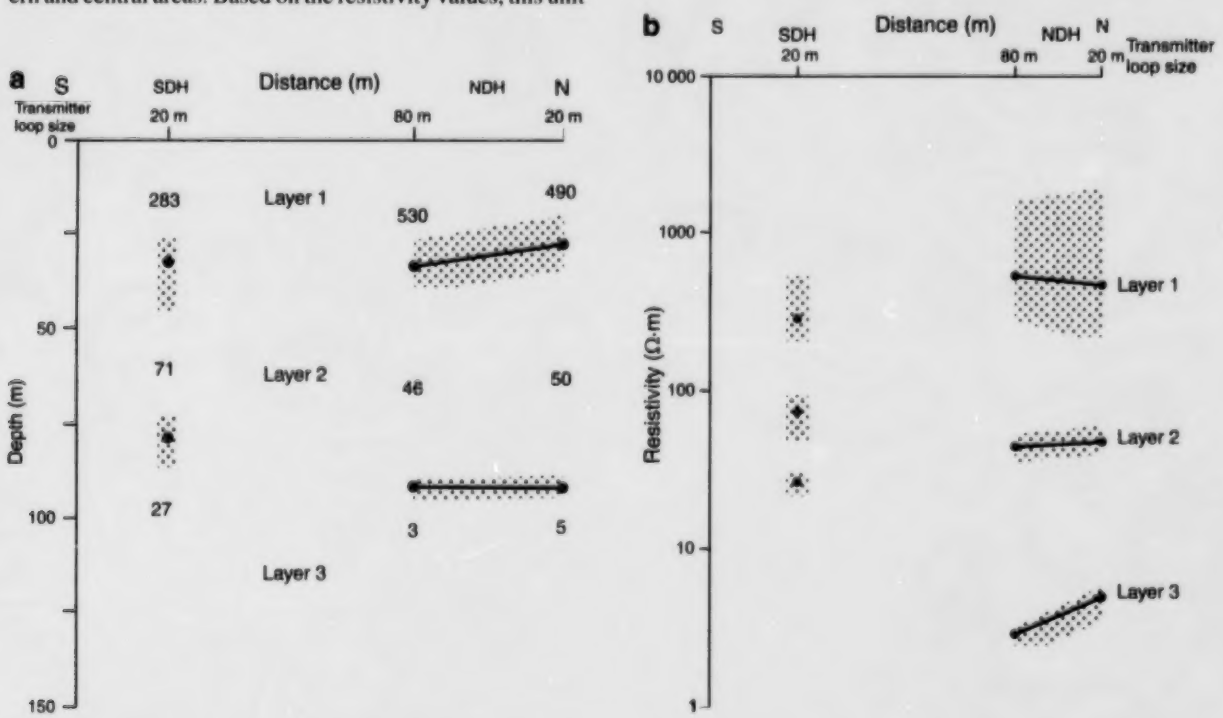

Figure 8. *Time-domain electromagnetic sounding data for site 2 (CRTC): **a)** depth plot (numbers within the layers are the best-fit values for layer resistivities at each sounding); and **b)** resistivity plot. For both plots, shaded areas represent the range of possible fits (depth or resistivity) to the Occam inversion. SDH and NDH indicate drill holes at the south and north ends, respectively, of the site.*

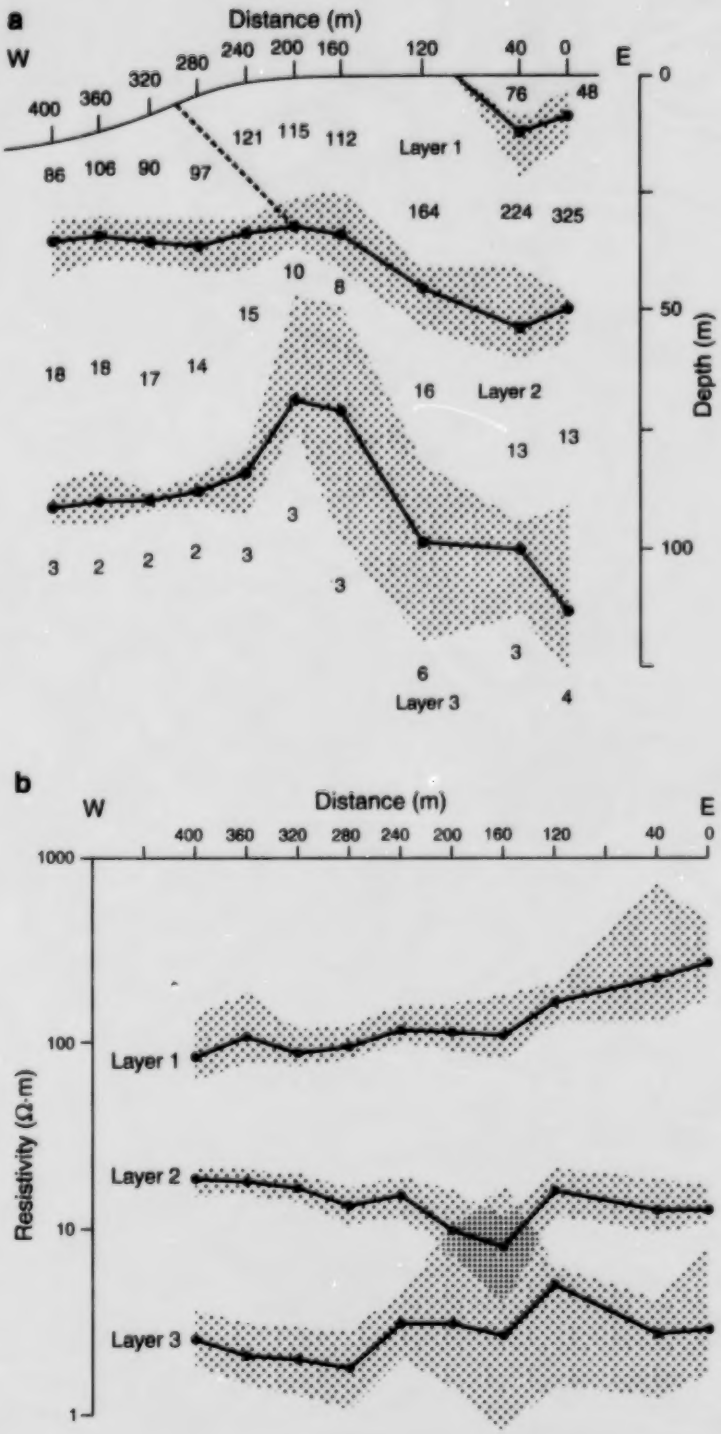

Figure 9.

*Time-domain electromagnetic sounding data for site 11 (28th Ave.): **a)** east-west depth plot (numbers within the layers are the best-fit values for layer resistivities at each sounding); and **b)** east-west resistivity plot. For both plots, shaded areas represent the range of possible fits (depth or resistivity) to the Occam inversion and darker shaded areas represent regions where the ranges of fit of adjacent layers overlap.*

data (Rea, 1996; Rea and Knight, 2000). The depositional environment in this part of the aquifer, being somewhat removed from the old meltwater channel, may have been a less energetic, lacustrine setting.

There are only two sites (1 and 11) where there is overlap between depth and resistivity ranges, thus making the results difficult to interpret. Site 1 (Fig. 6) has two soundings where depths overlap and eight soundings where resistivities overlap; site 11 (Fig. 9) has two soundings where resistivities overlap. Nevertheless, the data suggest that layer 1 is more resistive than layer 2, and that layer 1 is shallower than layer 2.

Abbotsford–Sumas aquifer

The Abbotsford–Sumas aquifer covers a much larger area than the Brookswood aquifer. It consists of coarse sand and gravel (Sumas Drift) underlain by silty sand and marine clay. Only two widely separated sites were investigated within the aquifer.

At site 6 (Fig. 13), the resistivity values of 100–300 Ω·m obtained for the upper layer of coarse sand and gravel are similar to those obtained for the Brookswood aquifer. Resistivity values for the underlying silty sand and clay layers are also similar to those obtained from the Brookswood aquifer, as are thickness estimates (cf. cone penetrometry results at Short Road; Campanella et al. (1994)). The resistivity values of the upper layer at site 7 (Fig. 14) are considerably higher than those at site 6 (and those within the Brookswood aquifer). Values for the silty sand and clay layers are similar to those of the Brookswood aquifer.

The resistivity values of the silty sand layer have a range that suggests it will be an aquifer but probably of poor quality. Therefore, hydraulic communication can be expected between the unconfined Abbotsford–Sumas aquifer and the deeper, silty sand layer.

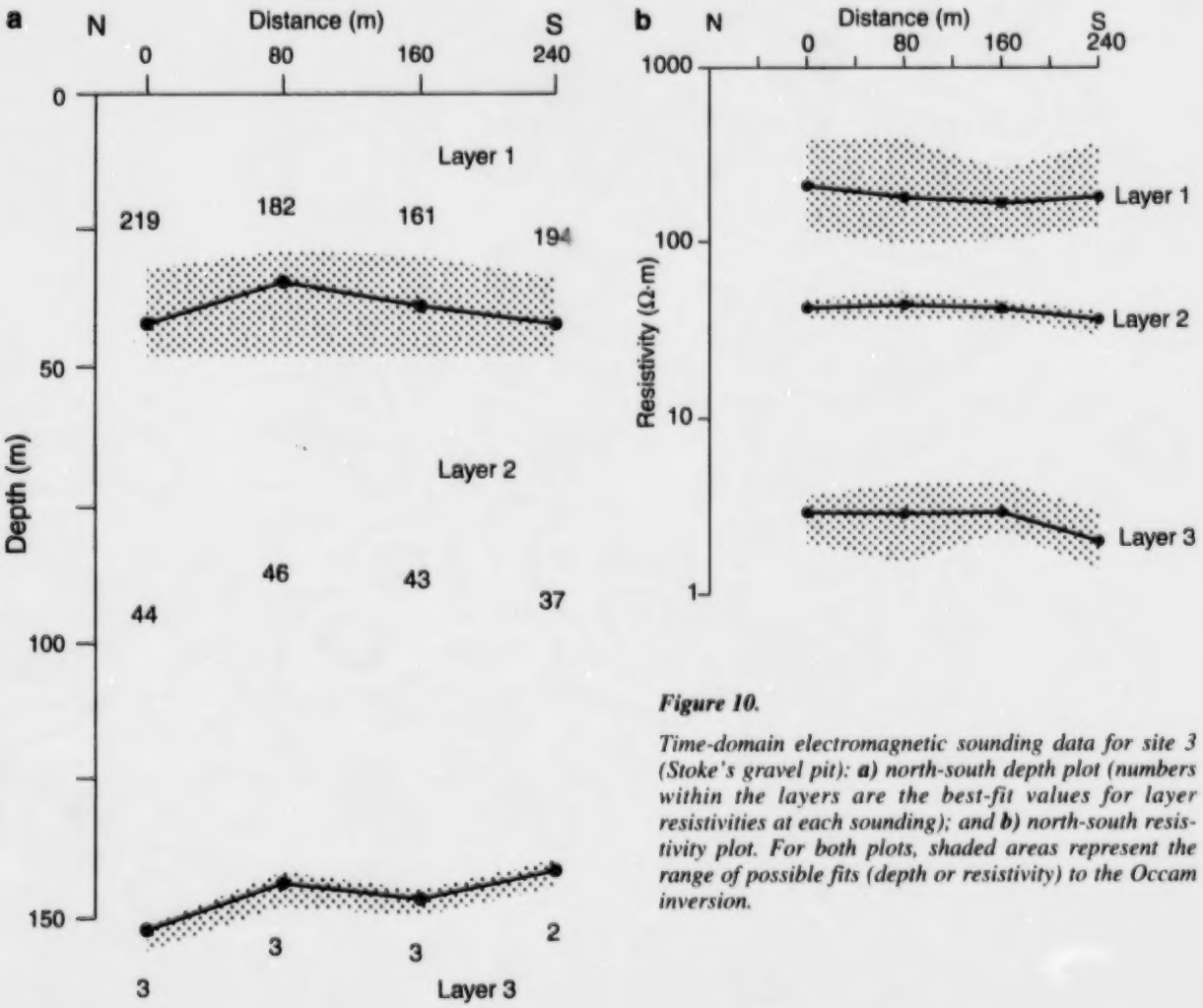

Figure 10.

*Time-domain electromagnetic sounding data for site 3 (Stoke's gravel pit): **a)** north-south depth plot (numbers within the layers are the best-fit values for layer resistivities at each sounding); and **b)** north-south resistivity plot. For both plots, shaded areas represent the range of possible fits (depth or resistivity) to the Occam inversion.*

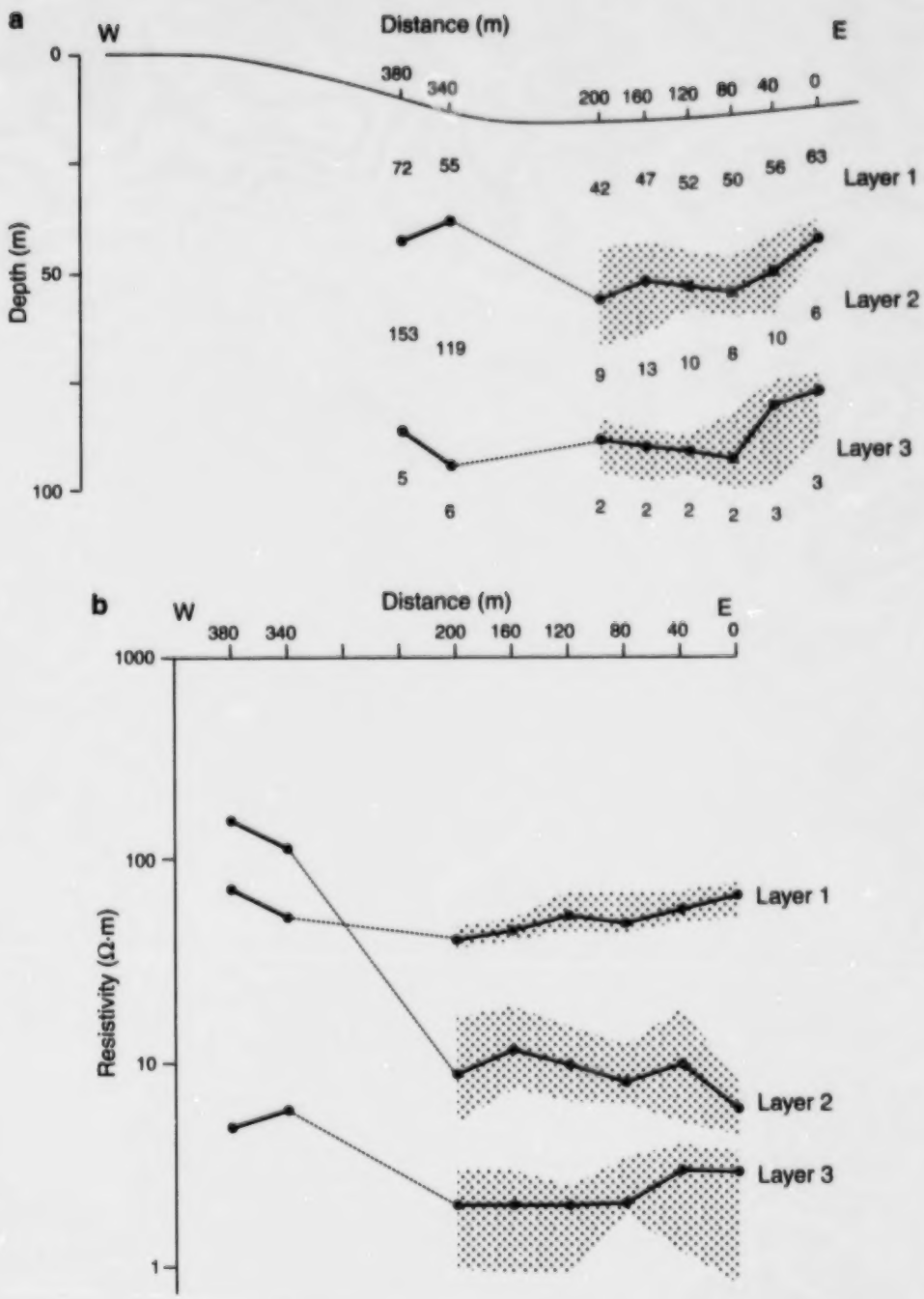

Figure 11. *Time-domain electromagnetic sounding data for site 12 (20th Ave.):* ***a)*** *east-west depth plot (numbers within the layers are the best-fit values for layer resistivities at each sounding); and* ***b)*** *east-west resistivity plot. For both plots, shaded areas represent the range of possible fits (depth or resistivity) to the Occam inversion. Dashed line indicates an inferred boundary.*

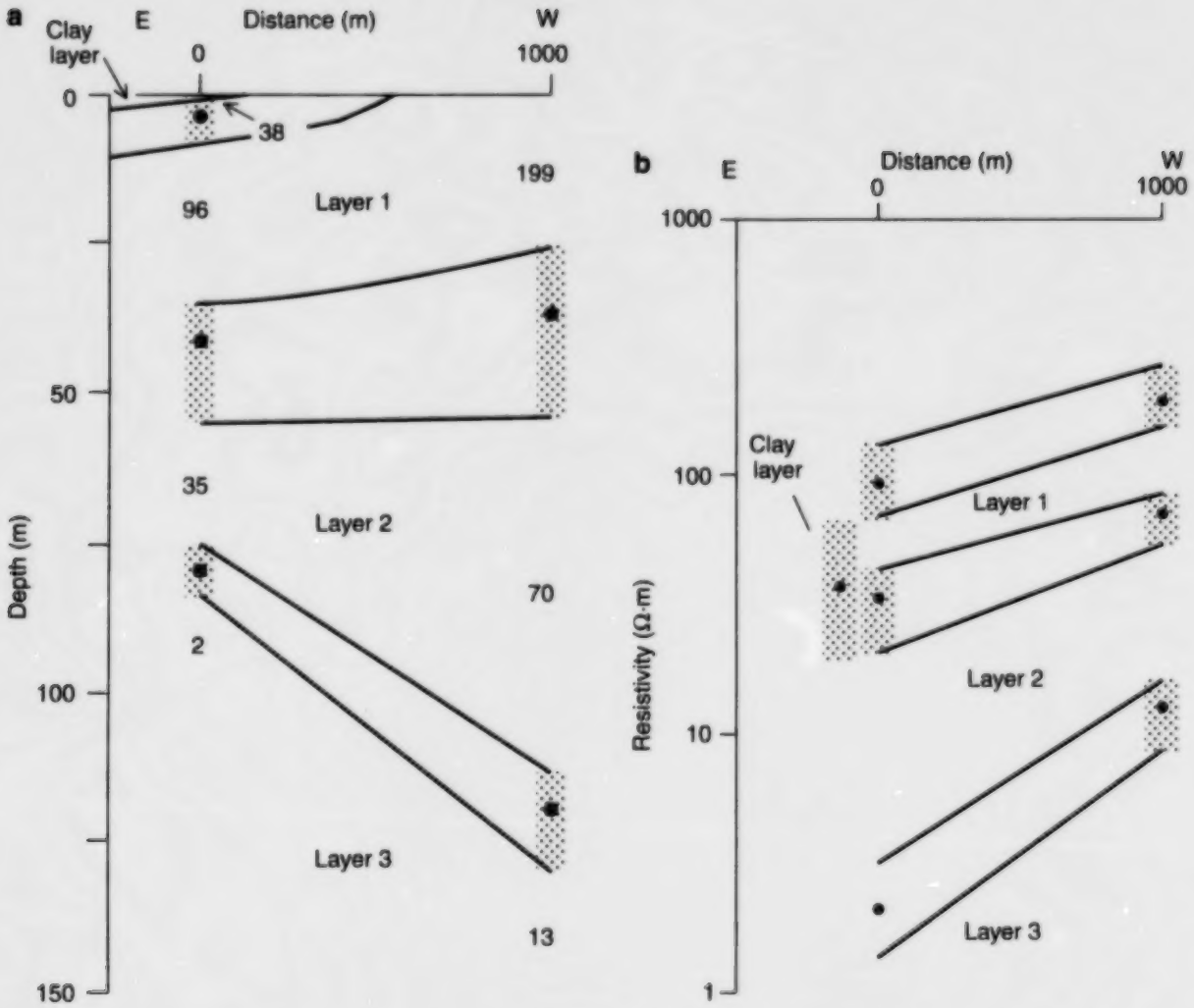

Figure 12. *Time-domain electromagnetic sounding data for site 13 (208th St.): **a)** depth plot (numbers within the layers are the best-fit values for layer resistivities at each sounding); and **b)** resistivity plot. For both plots, shaded areas represent the range of possible fits (depth or resistivity) to the Occam inversion.*

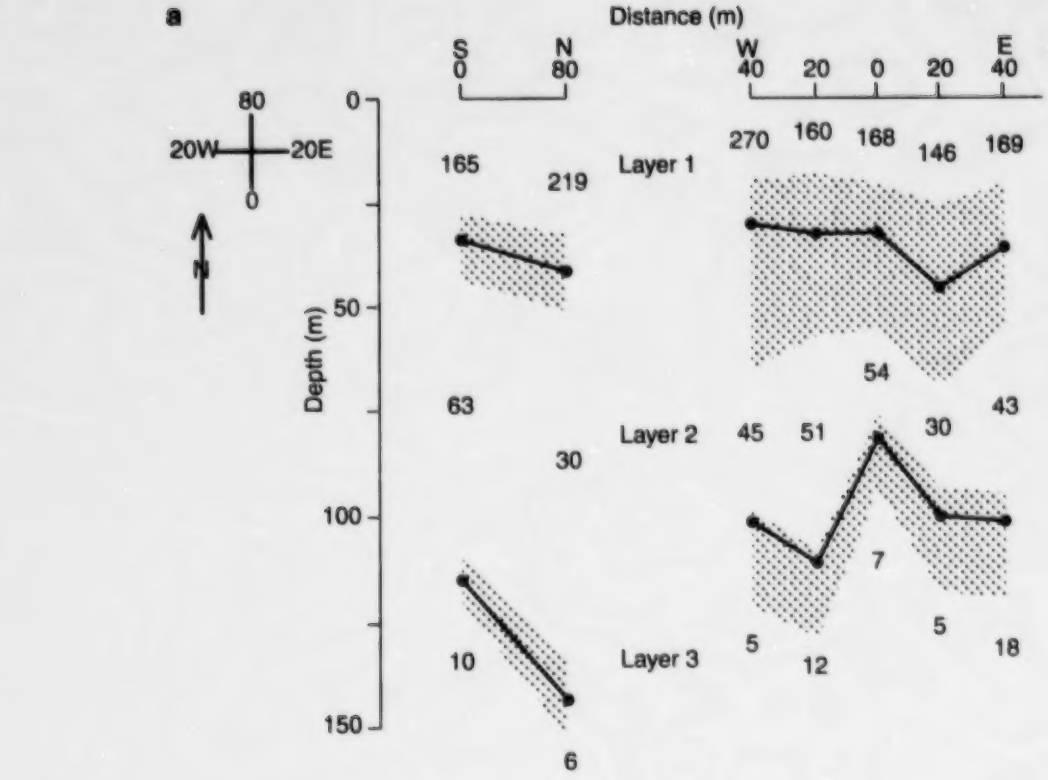

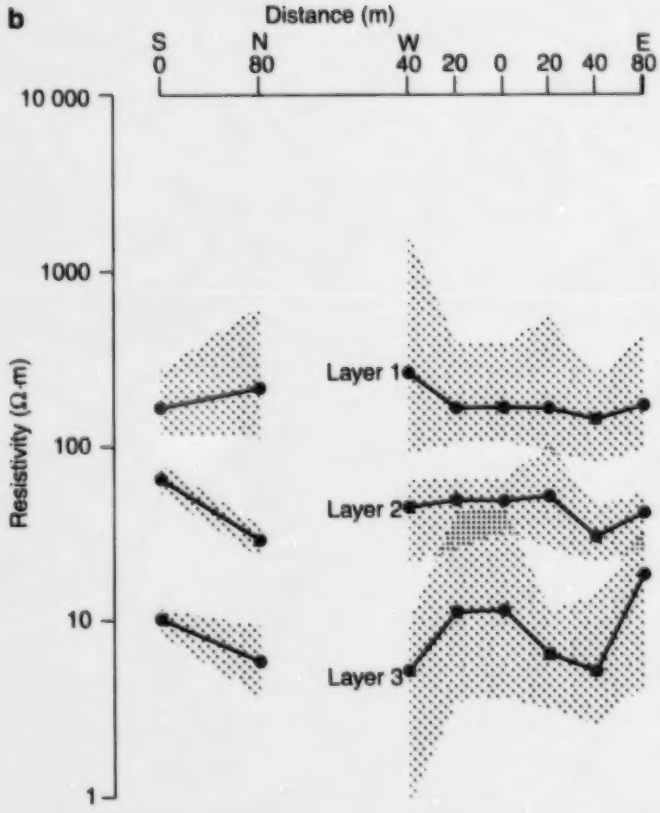

Figure 13.

*Time-domain electromagnetic sounding data for site 6 (Short St.): **a)** depth plot (numbers within the layers are the best-fit values for layer resistivities at each sounding); and **b)** resistivity plot. For both plots, shaded areas represent the range of possible fits (depth or resistivity) to the Occam inversion and darker shaded areas represent regions where the ranges of fit of adjacent layers overlap. The north-south soundings used 80 m transmitter loops and the east-west soundings used 40 m transmitter loops.*

Unconfined aquifers

The resistivity of the shallow layer at site 4 (Fig. 15) indicates that it may be an unconfined aquifer, 4 to 8 m thick, of poor quality. The layer below this is very conductive, indicating it is most likely a marine clay and hence a good seal. The layer below this is likely a confined aquifer, although the seal at its base cannot be seen because the conductive clays limit penetration of the EM signal.

Site 5 (Fig. 16) is an excellent example of the EM response from a confined aquifer (layer 3). In this case, the confining layers can be seen at the top and bottom of the aquifer, and the top confining layer is exposed at the surface near the east end of the line (sounding 320). The confined aquifer at this site appears to be of better quality than the one at site 4. There is an unconfined aquifer (approximately 10 to 15 m thick) at the surface between soundings 0 and 240 that appears to be of reasonable quality. Again, there is an indication of a possible deeper confined aquifer at sounding 320, although it appears to be of poor quality.

ARCHIE'S LAW

Hydrogeologists are not directly interested in the resistivity of unconsolidated sediments. They are interested in whether a package of sediments is an aquifer or an aquitard (including leaky aquitards) and, if it is an aquifer, its porosity and hydraulic conductivity. Estimates of porosity and hydraulic conductivity are difficult to obtain from geophysical data; however, recent work (Mosher et al., 1995; Mosher and Law, 1996) indicates that an apparent porosity may be obtained from bulk resistivity values using Archie's Law. To demonstrate the process, porosity has been estimated for the unconsolidated Brookswood sediments near sites 1, 2, and 10.

As discussed earlier, bulk resistivity of unconsolidated sediment (in other words, the resistivity obtained from inversion of the EM-47 soundings) is controlled predominantly by pore-water resistivity, porosity, and the amount of clay. Resistivity variations within the unconfined Brookswood aquifer (coarse sand and gravel) near sites 1, 2, and 10 should be mainly the result of porosity variations associated with grain size and compaction effects, because

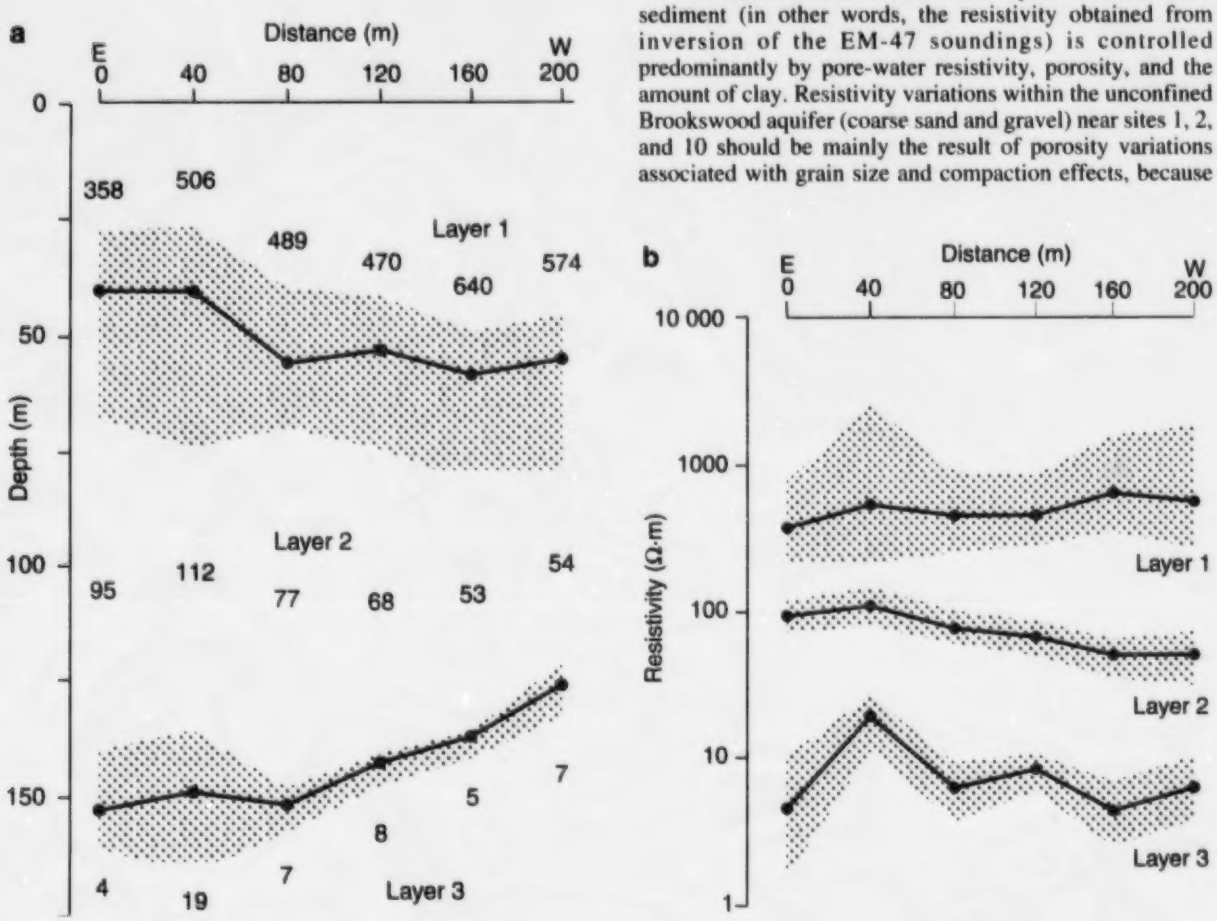

Figure 14. *Time-domain electromagnetic sounding data for site 7 (Agricultural Farm): **a)** east-west depth plot (numbers within the layers are the best-fit values for layer resistivities at each sounding); and **b)** east-west resistivity plot. For both plots, shaded areas represent the range of possible fits (depth or resistivity) to the Occam inversion. Note the rapid change in depth of the clay layer (layer 3) at the west end of the site and the general decrease in the resistivity of the silty sand layer (layer 2).*

the amount of clay contained in the deposits is very small. The average bulk resistivity varies from approximately 100 Ω·m to 550 Ω·m in this portion of the Brookswood aquifer. The average resistivity of pore water collected from the Surrey Forestry Nursery (site 1) over the last few years was approximately 22 Ω·m (T. Willingdon, pers. comm., 1996).

Archie's Law,

$$\Phi = F^{-1/m} = (\rho_b/\rho_w)^{-1/m} \quad (2)$$

relates bulk resistivity (ρ_b), porosity (Φ), and pore-water resistivity (ρ_w). The ratio of bulk resistivity to pore-water resistivity (F) is called the form factor and m is the cementation factor. The value of m depends on compaction and grain size, as well as clay content, and must be determined experimentally. It is between 1.5 and 2.0 for unconsolidated sediments, with 1.8 being a typical value (Mosher et al., 1995). Figure 17 illustrates the relationship between porosity and bulk resistivity for m values of 1.5 and 2.0 and pore-water resistivities of 20 and 25 Ω·m, respectively, wherein porosity increases with m for a given value of bulk resistivity. Similarly, for a given value of bulk resistivity, porosity increases as pore-water resistivity increases. Porosities vary between 10 and 40% for values of bulk resistivity between 600 and 100 Ω·m, respectively.

The apparent porosity of the unconfined Brookswood aquifer for sites 1 (Fig. 6), 2 (Fig. 8), and 10 (Fig. 7) was obtained using Archie's Law, with m = 1.8 and ρ_w = 22 Ω·m (Fig. 18). Bulk resistivity was assumed to that of the upper layer (unconfined aquifer). The apparent porosity values have not been calibrated with measured values, so there is no experimentally determined value of m. However, porosity variations are to be expected, subject to the pore-water resistivity remaining constant with position.

A significant increase in porosity occurs on both lines at the edge of the topographic slope of the aquifer (90W at site 10 and NWNUR80 at site 1). This may be related to a change in pore-water resistivity, a change in clay content, and/or a change in depositional environment. If pore-water resistivity is different for this section of the unconfined aquifer, then porosity values computed using ρ_w = 22 Ω·m will be incorrect. A change in clay content changes the value of m, which changes the porosity even for constant F (Fig. 17). At site 10,

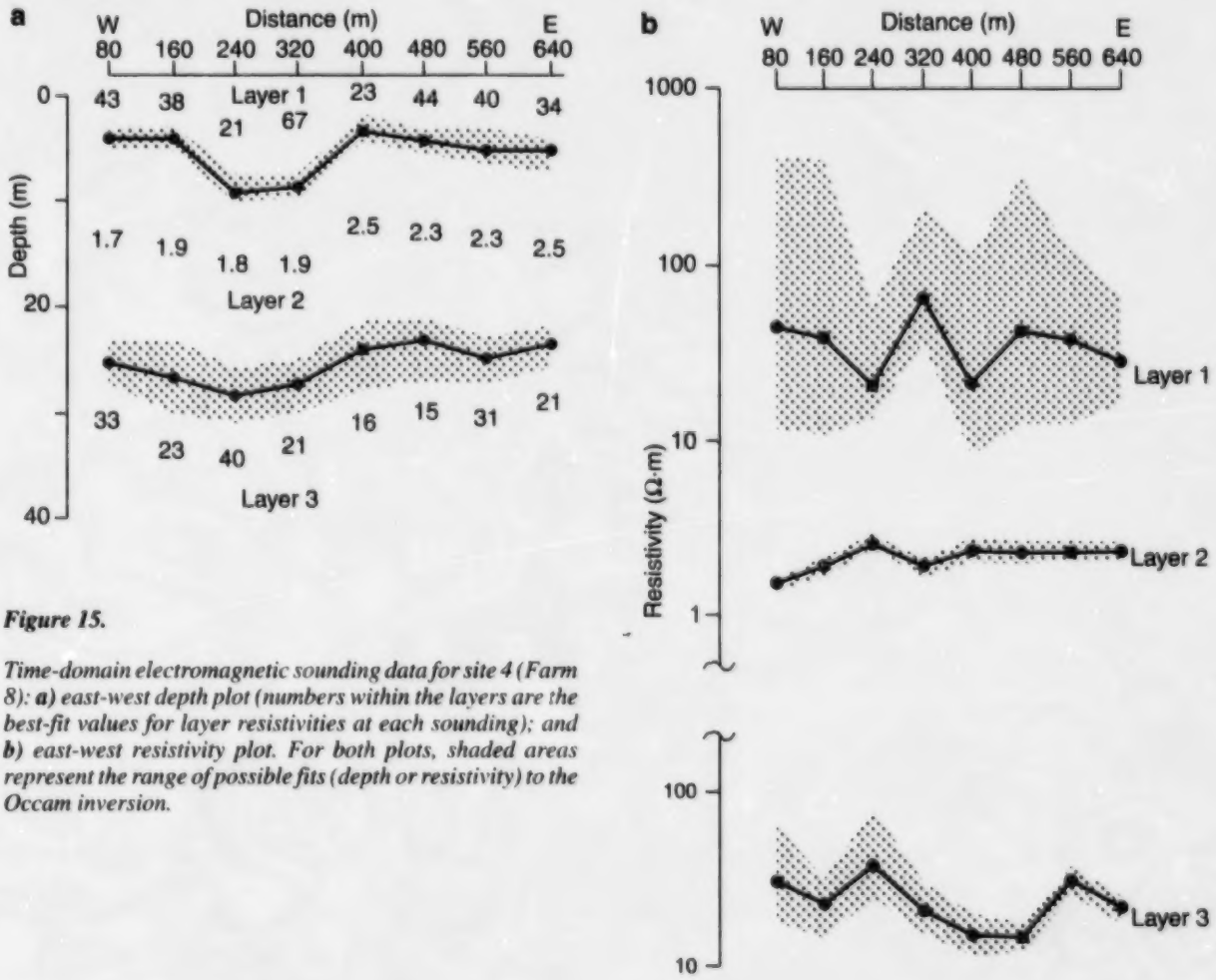

Figure 15.

*Time-domain electromagnetic sounding data for site 4 (Farm 8): **a)** east-west depth plot (numbers within the layers are the best-fit values for layer resistivities at each sounding); and **b)** east-west resistivity plot. For both plots, shaded areas represent the range of possible fits (depth or resistivity) to the Occam inversion.*

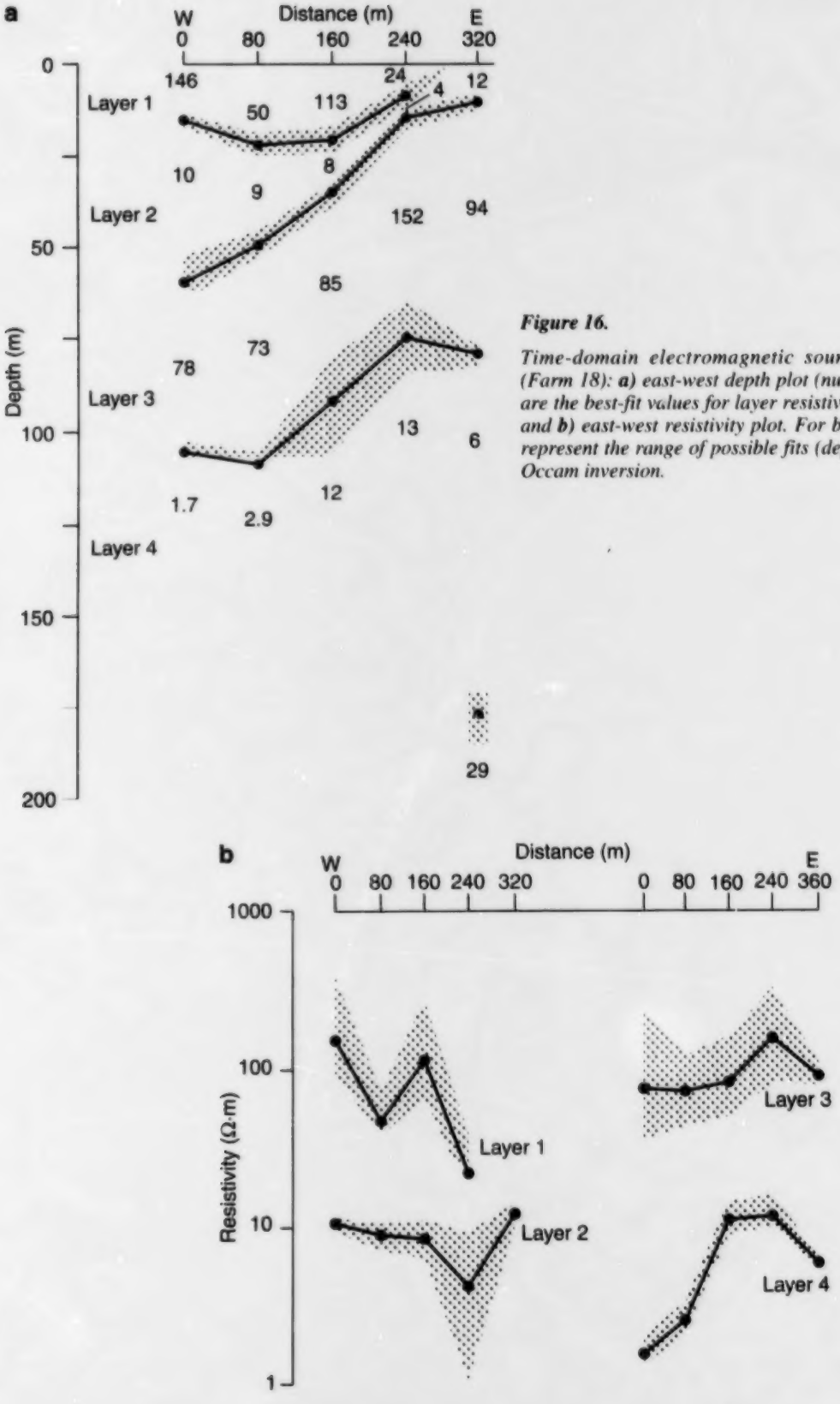

Figure 16.

*Time-domain electromagnetic sounding data for site 5 (Farm 18): **a)** east-west depth plot (numbers within the layers are the best-fit values for layer resistivities at each sounding); and **b)** east-west resistivity plot. For both plots, shaded areas represent the range of possible fits (depth or resistivity) to the Occam inversion.*

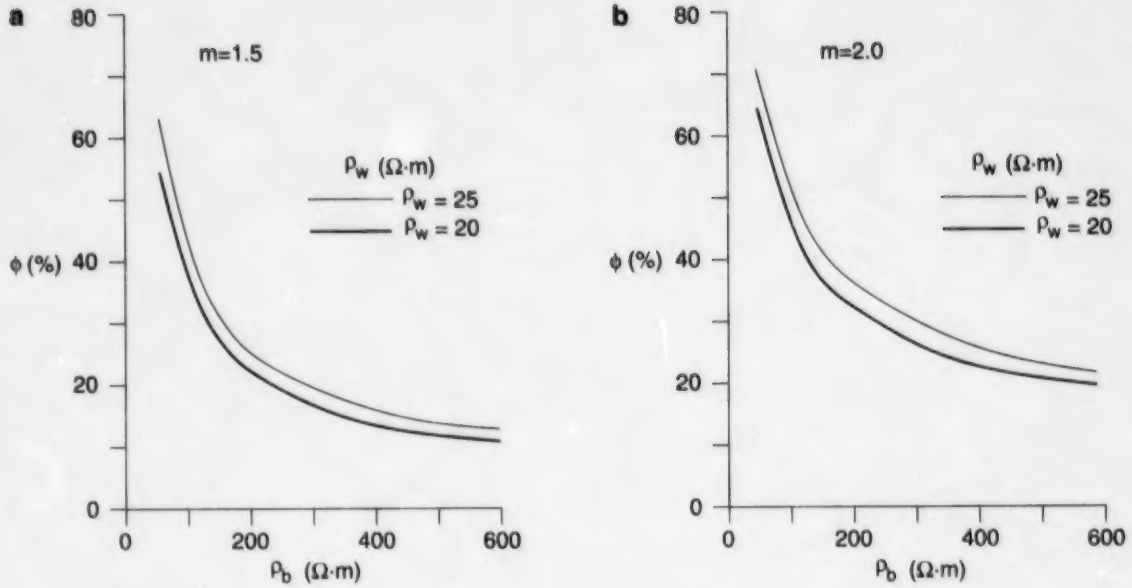

Figure 17. *Plot of porosity versus bulk resistivity, for pore-water resistivity values of 20 and 25 Ω·m and cementation factors of* ***a)*** *1.5 and* ***b)*** *2.0.*

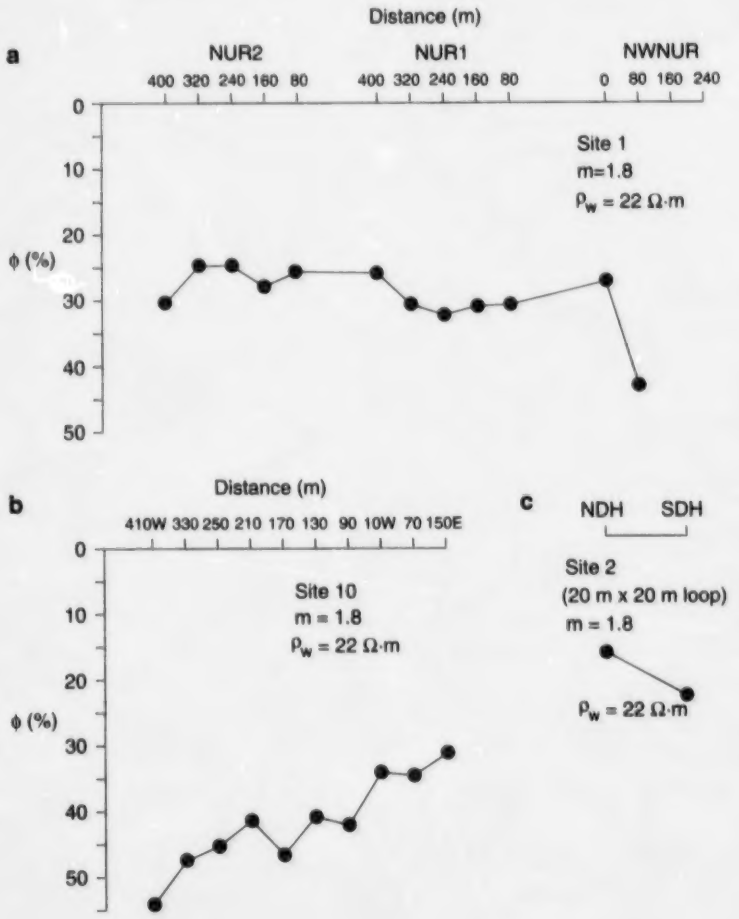

Figure 18.

Porosity of the unconfined Brookswood aquifer, obtained using Archie's Law with m = 1.8, ρ_w = 22 Ω·m, and ρ_b of the top layer in Figures 6, 7, and 8, for: ***a)*** *site 1 (Surrey Forestry Nursery),* ***b)*** *site 10 (40th Ave.), and* ***c)*** *site 2 (CRTC).*

ground-penetrating radar data indicate that a depositional change occurs at the break in slope (Roberts et al., 2000). Without additional information, it is impossible to determine which of the above effects is the most significant.

SUMMARY

Time-domain electromagnetic methods have proved very effective for mapping groundwater aquifers and seals (aquitards) in the Fraser lowland. Confined aquifers and seals as deep as 150 m were mapped in areas where geological and electrical noise conditions were optimal. Resistivity contrasts between good aquifers (coarse to medium sand and gravel), poor aquifers (fine sand and sand with clay), and seals (clay-rich sediments) were generally large enough to generate an EM response. With further calibration, electromagnetic methods will be capable of mapping, at least qualitatively, aquifer and seal characteristics.

The resistivity contrast between the unconfined Brookswood and Abbotsford–Sumas aquifers and the underlying fine sand and clay units made it possible to map the thickness of the two aquifers and, for the Brookswood aquifer, the relief on the contact between successive layers. Relief on these surfaces can have a marked influence on groundwater flow. Resistivity variations associated with aquifers and seals can be qualitatively used to estimate their sediment type, and hence overall aquifer quality.

This study showed that it is possible to map deep (up to 150 m) and shallow confined aquifers within the Pleistocene sediments. The resistivity of these aquifers suggests that they do not have high capacity for groundwater flow and storage, like the Brookswood and Abbotsford–Sumas aquifers. Several of these aquifers are presently used for domestic and agricultural water supply, so their characteristics and geometry are important considerations for future expansion.

The integration of electromagnetic soundings with other geophysical methods (e.g. high-resolution seismic reflection and ground-penetrating radar) will lead to a better understanding of the aquifers and seals within the Fraser lowland (*see* Pullan et al., 2000; Rea and Knight, 2000; Roberts et al., 2000). These methods complement one another, since they measure different physical properties of the sediments. The various methods also provide information from different depths, with ground-penetrating radar being the shallowest and seismic reflection the deepest.

ACKNOWLEDGMENTS

The field support of D. O'Leary and A. Best is gratefully acknowledged. B. Hill provided electronic support and equipment to the project during the three field seasons. We thank Brian Ricketts for providing geological guidance and field support, and the Ontario Geological Survey for lending us their Geonics EM-47 system for the study. Unpublished water chemistry data was kindly provided by T. Willingdon (B.C. Surrey Nursery, B.C. Ministry of Forestry). We thank L. Law and D. Mosher for their comments and review of this manuscript.

REFERENCES

Armstrong, J.E.
1957: Surficial geology of New Westminster map area, British Columbia; Geological Survey of Canada, Paper 57-5, 25 p.
1980: Surficial geology, Mission, British Columbia; Geological Survey of Canada, Map 1485A, scale 1:50 000.
1981: Post-Vashon Wisconsin glaciation, Fraser lowland, British Columbia; Geological Survey of Canada, Bulletin 327, 34 p.

Armstrong, J.E. and Hicock, S.R.
1980: Surficial geology, New Westminster, British Columbia; Geological Survey of Canada, Map 1484A, scale 1:50 000.

Best, M.E. and Todd, B.J.
1996a: Fraser Valley hydrogeology project: time-domain EM surveys, August 4 to 18, 1995 (supplement to Open File 3095); Geological Survey of Canada, Open File 3308, 7 p.
1996b: Electromagnetic soundings, pseudo-resistivity logs and implications for porosity and ground water salinity; *in* Proceedings of the Symposium on the Application of Geophysics to Engineering and Environmental Problems, (comp.) R.S. Bell and M.H. Cramer; Wheat Ridge, Colorado, p. 1061–1074.

Best, M.E., Todd, B.J., and O'Leary, D.
1994: Ground water mapping using time-domain electromagnetics: examples from the Fraser Valley, British Columbia; *in* Current Research 1994-A; Geological Survey of Canada, p. 19–27.
1995: Fraser Valley hydrogeology project: time-domain EM surveys, June 20 to July 8, 1994; Geological Survey of Canada, Open File 3095, 19 p.

Campanella, R.G., Davies, M., Boyd, T., Everard, J., Roy, D., Tomlinson, S., Jackson, S., Schrempp, H., and Ricketts, B.D.
1994: In-situ testing for the characterization of aquifers: demonstration project; Geological Survey of Canada, Open File 2940, 19 p.

Clague, J.J., Luternauer, J.L., and Hebda, R.J.
1983: Sedimentary environments and postglacial history of the Fraser Delta and lower Fraser Valley, British Columbia; Canadian Journal of Earth Sciences, v. 20, p. 1314–1336.

Fetter, C.W.
1988: Applied Hydrogeology; Prentice-Hall, New York, New York, 691 p.

Fitterman, D.V. and Stewart, M.T.
1986: Transient electromagnetic soundings for groundwater; Geophysics, v. 51, p. 995–1005.

Keller, G.V. and Frischknect, F.C.
1966: Electrical Methods in Geophysical Prospecting; Pergammon Press, Oxford, United Kingdom, 517 p.

Mosher, D.C. and Law, L.K.
1996: Application of concurrent marine electromagnetic and marine seismic high resolution profiling, British Columbia, Canada; Journal of Environmental and Engineering Geophysics, v. 1, p. 215–228.

Mosher, D.C., Law, L.K., and Quinn, R.
1995: Marine electromagnetic and seismic high resolution profiling results from coastal British Columbia; *in* Canadian Coastal Conference Proceedings, October 1995, Extended Abstracts, p. 621–635.

Pullan S.E., Good, R.L., Jarvis, K., Roberts, M.C., and Vanderburgh, S.
2000: Application of shallow seismic-reflection techniques to subsurface structural mapping, Fraser lowland; *in* Mapping, Geophysics, and Groundwater Modelling in Aquifer Delineation, Fraser Lowland and Delta, British Columbia, (ed.) B.D. Ricketts; Geological Survey of Canada, Bulletin 552.

Rea, J.M.A.
1996: Ground penetrating radar applications in aquifer characterization; Ph.D. thesis, Department of Earth and Ocean Sciences, University of British Columbia, Vancouver, British Columbia, 84 p.

Rea, J.M.A. and Knight, R.J.
2000: Characterization of the Brookswood aquifer using ground-penetrating radar; *in* Mapping, Geophysics, and Groundwater Modelling in Aquifer Delineation, Fraser Lowland and Delta, British Columbia, (ed.) B.D. Ricketts; Geological Survey of Canada, Bulletin 552.

Ricketts, B.D.
2000: Modelling of groundwater flow in the Fraser River delta and Brookswood aquifer; *in* Mapping, Geophysics, and Groundwater Modelling in Aquifer Delineation, Fraser Lowland and Delta, British Columbia, (ed.) B.D. Ricketts; Geological Survey of Canada, Bulletin 552.

Ricketts, B.D. and Jackson, L.E.
1994: Hydrogeology, Vancouver–Fraser Valley, southern British Columbia; *in* Current Research 1994-A; Geological Survey of Canada, p. 201–206.

Roberts, M.C., Vanderburgh, S., and Jol, H.M.
2000: Radar facies and geomorphology of the seepage face of the Brookswood aquifer, Fraser lowland; *in* Mapping, Geophysics, and Groundwater Modelling in Aquifer Delineation, Fraser Lowland and Delta, British Columbia, (ed.) B.D. Ricketts; Geological Survey of Canada, Bulletin 552.

Stoyer, C.H.
1990: Efficient computation of transient sounding curves for wire segments of finite length using an equivalent dipole approximation; Geophysical Prospecting, v. 38, p. 87–99.

Todd, B., Gupta, V.K., and Best, M.E.
1993: Oak Ridges Moraine electromagnetic project, October 18–26, 1993; Geological Survey of Canada, Open File 2797, 52 p.

Application of shallow seismic-reflection techniques to subsurface structural mapping, Fraser lowland

S.E. Pullan[1], R.L. Good[1], K. Jarvis[2], M.C. Roberts[3], and S. Vanderburgh[4]

Pullan, S.E., Good, R.L., Jarvis, K., Roberts, M.C., and Vanderburgh, S., 2000: Application of shallow seismic-reflection techniques to subsurface structural mapping, Fraser lowland; in *Mapping, Geophysics, and Groundwater Modelling in Aquifer Delineation, Fraser Lowland and Delta, British Columbia, (ed.) B.D. Ricketts; Geological Survey of Canada, Bulletin 552, p. 49–74.*

Abstract : Shallow seismic-reflection methods have been tested and applied in several areas of the lower Fraser River valley as a component of the Fraser Lowland Hydrogeology Project (1993–1996). A summary of the results of an initial testing phase, and of 12-fold common-midpoint continuous profiling, is presented in this paper. The quality of the seismic-reflection data obtained varied widely across the survey area, depending primarily upon surface geological conditions. In some areas where the surface materials were fine grained and water saturated, excellent data were obtained and continuous seismic profiles delineate subsurface structure to depths of greater than 500 m below surface; other areas proved to be unsuitable for the application of shallow seismic-reflection techniques. These data show that shallow seismic-reflection profiles provide information on the subsurface structure and seismic facies that will be crucial in exploring, defining, and possibly developing groundwater resources in the area.

Résumé : Dans le cadre du projet d'hydrogéologie des basses terres du Fraser (1993–1996), on a mis à l'essai et mis en application des méthodes de sismique réflexion à faible pronfondeur en plusieurs sites dans la vallée du bas Fraser. Dans cet article, on présente un résumé des résultats de la phase initiale des essais et du profilage sismique continu en point-milieu commun avec un ordre de couverture de 12. La qualité des données de sismique réflexion obtenues varie beaucoup dans la région étudiée, surtout en fonction des conditions géologiques en surface. À certains sites, où les matériaux en surface étaient de granulométrie fine et saturés en eau, on a obtenu des données excellentes et les profils sismiques continus permettent de délimiter les structures souterraines jusqu'à plus de 500 m sous la surface; d'autres sites ne conviennent pas aux techniques de sismique réflexion à faible profondeur. Les données montrent que les profils de sismique réflexion à faible profondeur fournissent de l'information sur la structure subsuperficielle et les faciès sismiques qui sera de toute première importance pour l'exploration, la définition et peut-être la mise en valeur des ressources en eau souterraine de la région.

[1] Terrain Sciences Division, Geological Survey of Canada, 601 Booth Street, Ottawa, Ontario K1A 0E8
[2] Department of Earth and Ocean Sciences, University of British Columbia, 129–2219 Main Mall, Vancouver, British Columbia V6T 1Z4
[3] Departments of Earth Sciences and Geography, Simon Fraser University, Burnaby, British Columbia V5A 1S6
[4] Department of Geography, University College of the Fraser Valley, 33844 King Road, Abbotsford, British Columbia V2S 7M9

INTRODUCTION

In 1993, the Geological Survey of Canada (GSC) reinstated a hydrogeological program with the establishment of two major projects, one in the Oak Ridges Moraine north of Toronto and one in the Fraser lowland southeast of Vancouver. The overall objective of the program was to build on the existing strengths of the GSC, and focus on studies that would provide information and an understanding of the basic geoscience framework of the area. Both projects have concentrated on the characterization of aquifers and aquitards in terms of their three-dimensional geometry, stratigraphic position and sedimentary character, hydraulic properties, recharge characteristics, and groundwater types (Ricketts and Jackson, 1994; Sharpe et al., 1996; Ricketts, 2000). This baseline information is crucial for understanding, evaluating, and protecting groundwater resources, and for dealing with any site-specific issues of groundwater quantity or quality (Sharpe et al., 1996).

Many different types of data and field surveys have been utilized in the Fraser Lowland Hydrogeology Project, including water-well records (Woodsworth and Ricketts, 1994; Ricketts, 1995; Ricketts and Dunn, 1995; Makepeace and Ricketts, 2000; Ricketts and Makepeace, 2000), new drilling and water sampling, cone penetrometry (Campanella et al., 1994), and geophysical surveys (Rea et al., 1994; Best et al., 1995; Pullan et al., 1995; Best and Todd, 2000; Rea and Knight, 2000; Roberts et al., 2000). Geophysical surveys provide a nondestructive means of obtaining data related to the physical properties of the subsurface, and of expanding one-dimensional information obtained from boreholes into a two- or three-dimensional picture.

Shallow seismic-reflection techniques provide a means of delineating and mapping the sedimentary architecture of unconsolidated sequences. Such seismostratigraphic information yields critical insight into past depositional environments and the lateral continuity (or inhomogeneity) of subsurface units, and in this sense plays an important role in hydrogeological studies (Pullan et al., 1994). This paper summarizes the results of an initial testing phase of the shallow seismic-reflection method in the area, and of 12-fold common-midpoint seismic-reflection surveys carried out by the GSC, Simon Fraser University (SFU), and the University of British Columbia (UBC). The results demonstrate the potential application of the shallow seismic-reflection technique in regional and/or site-specific hydrogeological studies in the Fraser lowland (noting the limitations and difficulties in applying this method), and provide data for comparison with the results of other geophysical surveys.

GEOLOGICAL AND HYDROGEOLOGICAL SETTING

The Fraser lowland lies in the Tertiary Georgia Basin, with the buried Tertiary sequence consisting of a sandstone-dominated Paleocene–Eocene succession, probably in excess of 1500 m thick (Mustard and Rouse, 1994). The early Tertiary sequence is overlain in places by up to several hundred metres of younger sediments (Miocene–Pliocene), consisting of weakly indurated, intercalated sandstone and mudstone (Mustard and Rouse, 1994), and then by a thick Quaternary sequence which almost completely masks the underlying bedrock topography (Clague, 1994). Information on the depth to bedrock is sparse, but available data suggest that much of the area south of the north arm of the Fraser River and west of New Westminster is underlain by 300–500 m of unconsolidated sediments (Dunn and Ricketts, 1994; Hamilton and Ricketts, 1994). Near Langley, a bedrock high (elevation close to sea level) is encountered at a depth of approximately 100 m (Conoco–Dynamic Oil Murray Creek borehole, 1993).

The Quaternary succession consists of a complex sequence of sediments deposited during several glaciations and intervening interglacial periods (Armstrong, 1984; Clague, 1994). Repeated glacial advances and retreats, and the resultant isostatic adjustments of the land, caused sea level to fluctuate up to 200 m relative to the land surface (Clague, 1994). As a result, sequences of diamictons and stratified drift exist in complex associations with marine and deltaic sediments. The present landscape and surface deposits are mainly a result of late glacial (late Wisconsinan, or Fraser Glaciation, ca. 30 000–11 000 BP) or postglacial processes (Armstrong, 1984; Clague, 1994). A simplified Quaternary stratigraphy of southwestern British Columbia is outlined in Figure 1; the distribution of surficial materials and the locations of the seismic-reflection profiles are shown in Figure 2.

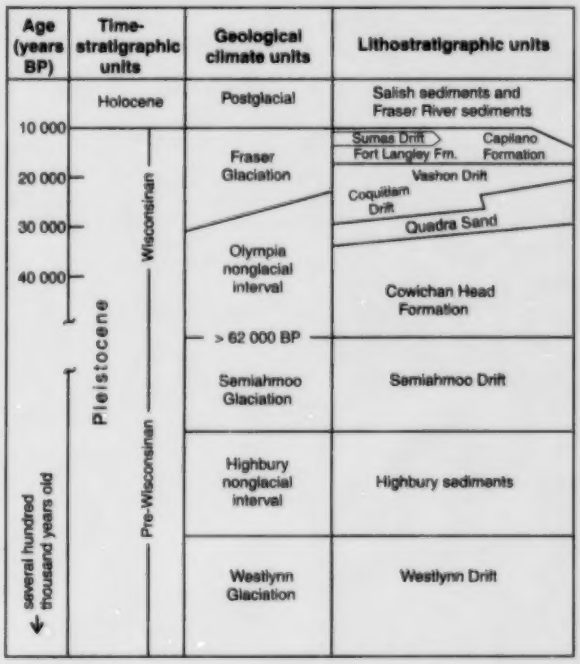

Figure 1. *Simplified Quaternary stratigraphy of the Fraser lowland (*modified from *Armstrong, 1984; Clague, 1994).*

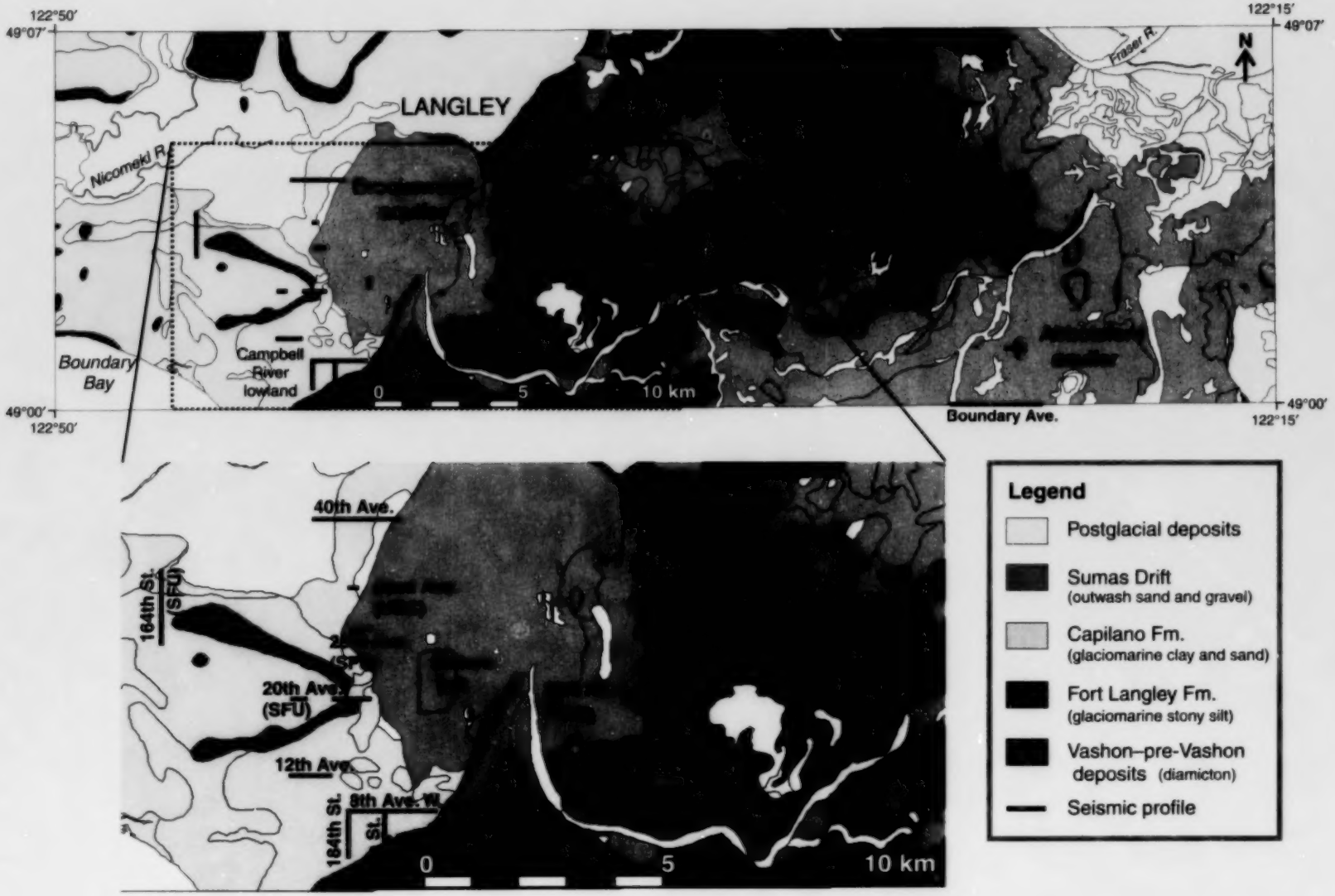

Figure 2. *Surficial geology of the Fraser lowland* (simplified from *Armstrong, 1980; Armstrong and Hicock, 1980*) *and locations of seismic profiles. Profiles obtained by Simon Fraser University and the University of British Columbia are designated as (SFU) and (UBC), respectively; those obtained by the Geological Survey of Canada are not designated.*

The western portion of the survey area is underlain primarily by Capilano sediments (glaciomarine sediments deposited beyond the retreating ice margin 13 000–10 000 BP; Clague (1994)). In the Nicomekl River valley, these sediments were deposited in what was an arm of the sea during the late Wisconsinan; today, the valley is underlain by thick (<300 m) sequences of marine silt, clay, and fine sand (Armstrong, 1984). In contrast, the upland areas to the south are covered by thin, discontinuous deposits of sandier Capilano sediments overlying Vashon Drift. Much of the eastern portion of the survey area is underlain by the Fort Langley Formation or a thin mantle of Sumas Drift (Fig. 1, 2). The Fort Langley Formation (approximately time equivalent to the Capilano sediments) is a diverse unit composed of interbedded glaciomarine and glacial sediments deposited in an area of fluctuating ice margins (Clague, 1994), and may include diamicton as well as glaciofluvial and ice-contact deposits (Armstrong, 1984). Fort Langley sediments range in thickness from 30 m to greater than 165 m (Armstrong, 1984). The slightly younger till and glaciofluvial gravel of the Sumas Drift (e.g. Brookswood aquifer) were deposited during a minor readvance of the retreating Fraser Glacier in the eastern Fraser lowland (Clague, 1994).

The surficial materials discussed above overlie Vashon Drift (Fig. 1), which was deposited during the maximum ice advance of the Fraser Glaciation (18 000–14 000 BP; Clague (1994)). The unit is complex, in places including up to three diamictons and interbedded glaciofluvial deposits (Armstrong, 1984). Aprons of thick, well sorted Quadra Sand were deposited in front of the advancing glaciers during the early stages of the Fraser Glaciation (Clague, 1994). Beneath these sediments lies the Cowichan Head Formation (Fig. 1), deposited during the middle Wisconsinan Olympia nonglacial interval and composed of gravel, sand, silt, and peat deposited in fluvial, estuarine, and marine environments (Armstrong and Clague, 1977).

Information regarding older Pleistocene stratigraphy is limited, but the sediments are interpreted to represent deposits related to two other glaciations (Semiahmoo and Westlynn drifts) and an intervening nonglacial period (Highbury sediments; Armstrong (1984), Clague (1994)). In the Fraser lowland, the principal aquifers are found in Quaternary sediments (Halstead, 1986). The Abbotsford and Brookswood aquifers are prominent unconfined aquifers composed predominantly of Sumas Drift deposits. These aquifers provide shallow sources of readily accessible water (Halstead, 1986) but are highly susceptible to surface contamination. Permeable units at depth can be high-quality, productive aquifers if they are confined and protected by diamict, glaciomarine, and glaciolacustrine deposits (e.g. there are a large number of flowing artesian wells in such deposits in the Nicomekl and Campbell River lowlands; Halstead (1986)). It is clear, from the preceding description of the stratigraphy of subsurface units (Armstrong, 1984; Halstead, 1986; Clague, 1994), that the location, depth, lateral continuity, and size of subsurface aquifers are extremely complex. This makes issues of aquifer evaluation and potential development difficult to address. Geophysical surveys, in conjunction with borehole information, provide a two- or three-dimensional picture of sedimentary architecture, information which is crucial in formulating models of groundwater flow.

PRINCIPLES AND APPLICATIONS OF SEISMIC-REFLECTION METHODS

Seismic-reflection methods involve measurement of the time taken for seismic energy to travel from the source, at or near the surface, down to an acoustic discontinuity in the ground and back up to a receiver or series of receivers (geophones) on the surface. Seismic energy is reflected from any interface across which there is a change in acoustic impedance (product of velocity and density). A large contrast in acoustic impedance (e.g. at a contact between unconsolidated sediments and competent bedrock) will cause much of the incident seismic energy to be reflected back toward the surface, rather than transmitted to deeper horizons; however, coherent reflections can result from relatively small changes in acoustic impedance, such as lithological boundaries within unconsolidated sediments. Shallow seismic-reflection methods can therefore be an effective means of delineating the subsurface structure of unconsolidated sediments, and also of mapping the overburden-bedrock contact.

Seismic-reflection methods require digitization of the seismic wave train and at least some degree of computer processing of the data. Data are usually acquired continuously along a survey line, and processed to produce a seismic section, which is a two-way travel-time cross-section of the subsurface. Velocity-depth functions calculated from the data (ideally supplemented with seismic or acoustic logs in nearby boreholes) are used to translate the two-way travel time into depth.

Seismic-reflection surveys have been the mainstay of hydrocarbon exploration since the 1930s, but their application to shallow (<100 m) targets only became technologically and economically viable in the 1980s. Details of the application and methods used in shallow seismic-reflection surveys can be found in Pullan and Hunter (1990) and Steeples and Miller (1990). These papers summarize the development of two different shallow seismic-reflection methods: the 'optimum-offset' technique, which in its simplest form is a single-channel, constant-offset profiling technique requiring a minimum of data processing; and the common-midpoint (CMP), or common-depthpoint (CDP), method, which is an adaptation of the methods employed extensively in the petroleum industry. Over the last decade, technological improvements in engineering seismographs, personal computers, and data storage capabilities, and the availability of new PC-based processing software packages have overcome many of the limiting factors that led to the development of the optimum-offset technique. Common-midpoint data are now routinely collected for most shallow applications, although full CMP processing may not always be required (Pullan et al., 1991).

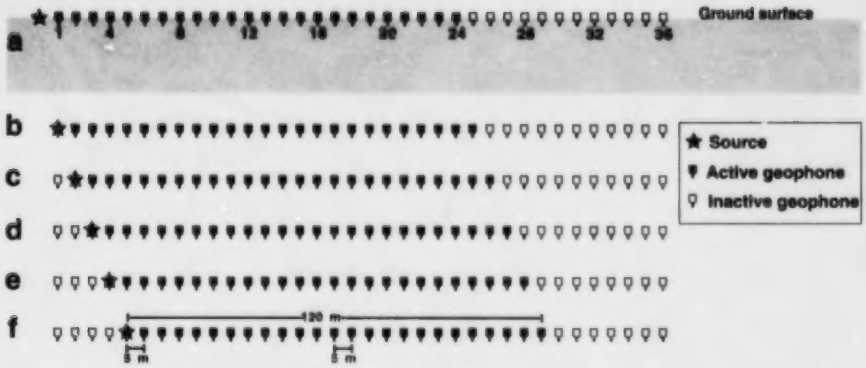

Figure 3. *Schematic layout of 36 geophones on the ground surface, and the source and receiver (active geophone) geometry for six consecutive 24-channel records (**a–f**). This geometry was used to acquire the Geological Survey of Canada and Simon Fraser University seismic data.*

In CMP surveys, multichannel (12, 24, or more) data are recorded for each shotpoint (Steeples and Miller, 1990). This is accomplished by laying out a large number of geophones and using a 'rollalong' switching box (either internal or external to the recording seismograph) that allows a multichannel record with the chosen offset and receiver geometry to be recorded for every shot (Fig. 3). During processing, the data are sorted according to their common midpoints or common depthpoints (Fig. 4). Each trace is corrected for offset according to a velocity-depth function determined from the data (normal moveout (NMO) corrections). Finally, the NMO-corrected traces in each CMP gather are stacked (summed). This stacking procedure is the essence of the CMP technique, and allows a potential improvement in the signal-to-noise ratio of the data according to the square root of the fold (where 'fold' refers to the number of traces stacked or summed to produce a single trace on the final section; *see* Steeples and Miller (1990)). The CMP technique requires the storage, handling, and processing of a large amount of data, but, in many study areas, the signal-enhancement capabilities of the CMP method are critical for successfully acquiring the desired subsurface information (Pullan et al., 1991).

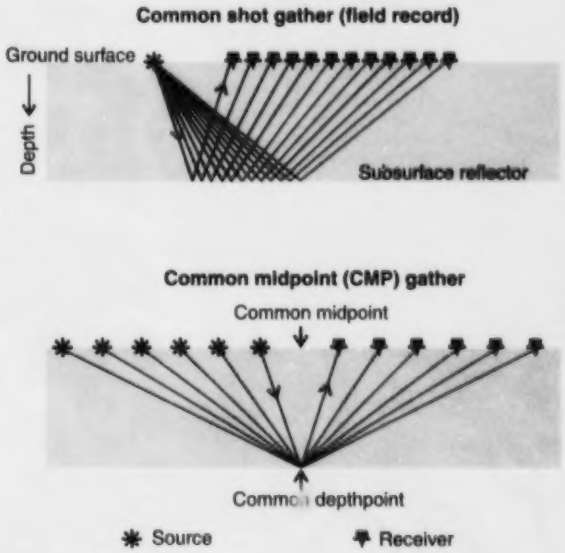

Figure 4. *Schematic diagrams showing the subsurface travel paths of reflections from field records (upper diagram) that have been sorted into a common-midpoint (CMP) gather (lower diagram). The traces in a CMP gather are processed and stacked together to form a single trace on a final CMP section.*

Resolution

The successful application of any shallow seismic-reflection survey depends on the detection of high-frequency energy reflected from subsurface velocity discontinuities. The dominant wavelength of the recorded data (wavelength = velocity / frequency) must be small enough to image the target reflector. The required frequency will depend on the objective of the particular survey. For example, high frequencies are required for imaging targets that are very shallow (i.e. 10–20 m in depth), small, or thin (i.e. a few metres in either lateral or vertical extent). Unfortunately, earth materials, especially unconsolidated sediments, are strong attenuators of high-frequency energy. Thus, seismic waves in the 10–90 Hz range, commonly used in hydrocarbon exploration, may be reflected from depths of thousands of metres, but waves with frequencies above 100 Hz normally have travel paths of only tens or hundreds of metres. The ability of a particular site to transmit high-frequency energy is a major factor in determining the quality and ultimate resolution of a shallow seismic-reflection survey.

Much of the attenuation of high-frequency energy occurs in the near-surface sediments where the seismic energy is produced. The optimum conditions for shallow reflection surveys are usually where the surface sediments are fine grained and water saturated; reflections with dominant

frequencies of 300–500 Hz can be obtained in such field situations. In unconsolidated, water-saturated overburden, these frequencies correspond to seismic wavelengths on the order of 3–5 m, with a corresponding potential subsurface resolution of approximately 1–2 m (one-third of the dominant wavelength; Miller et al. (1995)); however, when the surface materials are coarse grained and dry, the dominant frequencies of the recorded data can be less than 100 Hz. With such low-frequency data, seismic wavelengths may exceed 15 m in water-saturated, unconsolidated sediments. In such areas, the resolution of the data may not be sufficient to obtain the desired subsurface information.

Reflections from very shallow acoustic interfaces arrive at times that are close to the arrival times for energy that has travelled directly along the surface of the ground, or has been refracted from shallow interfaces such as the water table. For this reason, it is often impossible to separate shallow reflection signals from other interfering events. The depth to the first unequivocal reflection depends on the frequency of the signals and the source-receiver offsets, but horizons within 10–15 m of the surface generally cannot be easily delineated using the shallow seismic-reflection method.

Potential contributions of shallow seismic-reflection surveys

Shallow seismic-reflection surveys were carried out as part of the Fraser Lowland Hydrogeology Project in order to evaluate their potential usefulness in this particular geological environment. The aim of the seismic work was to map the subsurface structure of major lithological units in a number of different areas, with potential depths of investigation ranging from 20 m to greater than 500 m. As discussed above, the best results were expected where surface materials were fine grained and the water table was close to the surface (e.g. in lowland areas, on Capilano sediments, or on glaciomarine deposits of the Fort Langley Formation). It was anticipated that it would be more difficult to acquire good-quality seismic-reflection data on uplands or on Sumas Drift deposits, where surface materials were likely to be coarse grained and dry.

SURVEY METHODS AND RECORDING PARAMETERS

The Fraser lowland shallow seismic-reflection surveys carried out by the GSC in 1994 involved both a testing and a production phase. Figure 2 shows the locations of the profiles that were obtained during the production phase, along with the locations of the seismic profiles shot later by SFU and UBC. The locations of all test sites can be found in Pullan et al. (1995).

At each test site, one 24-channel geophone spread (5 m geophone spacing) was laid out in the ditch alongside the road, and data were recorded from five shotpoints (5 and 2.5 m off each end, and in the centre of the spread; *see* Pullan et al. (1995, Fig. 2)). The test data were used to evaluate the quality of reflected energy (frequency and signal strength), to determine the depths from which reflection signals were recorded, and to establish the recording parameters (source-receiver geometry, recording timescale, input filter settings, etc.) and line priorities for the production phase. Tests were carried out at 14 sites across the survey area in four general locations (Pullan et al., 1995). An effort was made to test sites located on all major surficial geological units (Armstrong, 1980, 1984; Armstrong and Hicock, 1980), as surface conditions strongly affect the frequency and signal strength of the energy that can be transmitted into the ground.

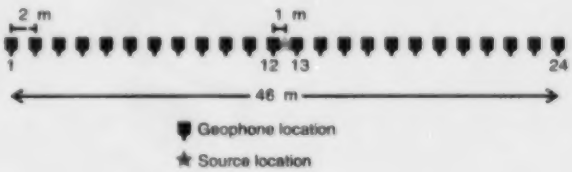

Figure 5. *Split-spread source-receiver geometry used by the University of British Columbia for acquisition of very high resolution data.*

Table 1. Recording parameters of seismic reflection surveys in the Fraser lowland in 1994 and 1995.

Year	Acquired by	Seismograph	No. of channels	Source	Geophones	Geophone spacing (m)	Source offset (m)	Record length (ms)	Total line-km
1994	GSC	Geometrics ES-2401™	24	12-gauge shotgun (black powder)	50 Hz	5	5 (off-end)	500 or 1000	12
1994	SFU	Geometrics SmartSeis™ S-24	24	12-gauge shotgun (black powder)	50 Hz	5	5 (off-end)	400	1
1995/ 1996	SFU	Geometrics SmartSeis™ S-24	24	12-gauge shotgun (black powder)	50 Hz	5	5 (off-end)	1000	3.6
1995	UBC	Geometrics SmartSeis™ S-24	24	12-gauge shotgun (poppers)	100 Hz	2	1 (split-spread)	250	0.6

The production phase involved the recording of continuous 12-fold CMP data along the chosen survey lines. This was accomplished by 'rolling' 24 channels through 36 geophones as the shotpoint was moved (Fig. 3). In 1994, the GSC collected approximately 12 line-km of 12-fold CMP data with 5 m shot and receiver spacings; an additional 1 line-km was recorded by a crew from SFU. In 1995, SFU recorded four more lines (totalling 3.6 line-km), using the same source and receiver geometry. Both the tests and the CMP data were recorded with a single 50 Hz vertical geophone per channel, and a 12-gauge black-powder blank shotgun shell, detonated at the bottom of a 0.5–1 m hole, was used as the seismic source (Pullan and MacAulay, 1987). University of British Columbia recorded some very high resolution data using higher frequency geophones (100 Hz), a smaller geophone spacing (2 m), and a split-spread geometry (i.e. with the source located in the middle of the spread; Fig. 5). All data were recorded on 24-channel engineering seismographs with instantaneous floating-point amplifiers and 15-bit analog-digital conversion. Elevations along the lines were surveyed so that elevation corrections could be made on the final processed sections. The recording parameters for the various surveys are listed in Table 1.

DATA PROCESSING

All data were processed by applying standard CMP sequences of processing steps, including trace editing, static corrections, bandpass filtering, gain scaling, velocity analyses, normal moveout corrections, and stacking of the corrected traces. An overview of the basic processing procedure can be found in Steeples and Miller (1990).

The test data were processed in-house on IBM-compatible microcomputers using Eavesdropper™ software. The limited data available from each site allowed only minimal processing, including bandpass filtering, mute of ground roll or air wave as necessary, re-sorting into common-midpoint (midpoint between source and receiver) gathers, velocity analysis, normal moveout corrections, and final stacking. The result for each site was a 96-trace (1-2 fold) seismic section (e.g. Fig. 6, 7; Pullan et al., 1995).

Most of the GSC and SFU profiles were processed under contract using more sophisticated routines developed in the petroleum industry to address near-surface effects such as ground coupling and statics, lateral velocity variations, and image enhancements (Schieck and Pullan, 1995). Advanced data-processing techniques, such as surface-consistent deconvolution, scaling analysis, residual static analysis, and structural modelling to enhance velocity and static analysis, have been applied to these data.

The UBC profiles were processed using their own Geophysical Research Processing Facility, which maintains a network of Sun workstations with ITA Insight™ seismic-processing software. The processing flow was essentially the same as that applied to the GSC and SFU data. Surface-consistent residual statics analysis and deconvolution were the key processes that resulted in the broad-bandwidth, high-frequency profiles.

The seismic profiles shown in this paper are sections in two-way travel time (not depth). Velocity functions were estimated from the seismic data at intervals along the line during the processing sequence, in order to calculate the normal moveout corrections applied to the data before the stacking procedure. An average of these velocity functions has

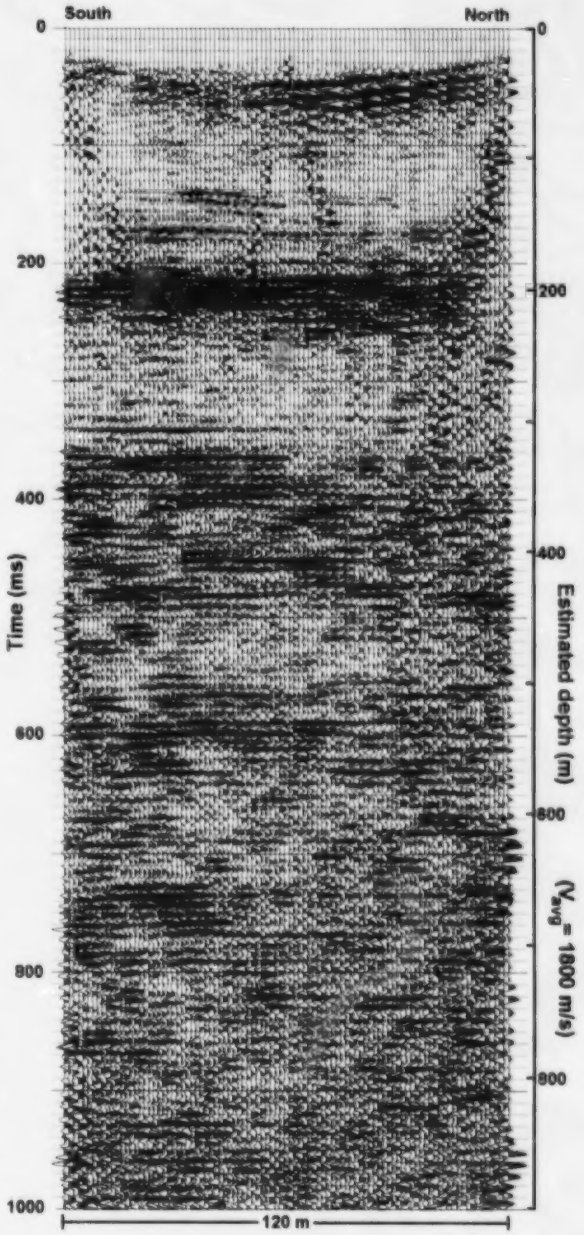

Figure 6. *Seismic section (96 trace, 1-2 fold), constructed from records acquired at test site 3* (from *Pullan et al., 1995*), *showing the excellent reflection data obtained in some areas where surface conditions were optimal. The depth scale has been calculated from the results of the velocity analysis conducted to create this stacked section.*

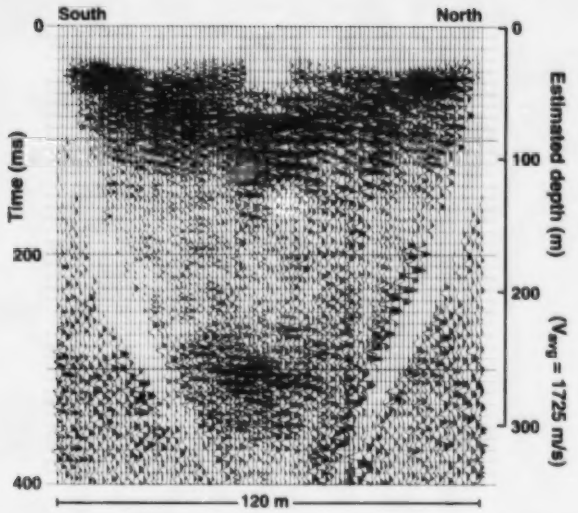

Figure 7. *Seismic section (96 trace, 1-2 fold), constructed from records acquired at test site 5 (from Pullan et al., 1995), showing typical reflection data obtained in areas where the water table was several metres below surface. The depth scale has been calculated from the results of the velocity analysis conducted to create this stacked section.*

been used to calculate the depth scales, shown alongside the sections discussed in this paper. It should be noted that the source-receiver geometry used in these surveys does not allow accurate determination of velocities below a depth of 100 m in the case of the GSC and SFU surveys, or 30 m in the case of the UBC surveys. Thus, the depth scales shown are only approximate, with the uncertainty increasing with depth.

TESTING-PHASE RESULTS

The data collected at the 14 test sites show that the quality of shallow seismic-reflection records varies widely across the survey area, depending primarily on the surface geological conditions (Pullan et al., 1995). The test results can be summarized on the basis of data quality and surficial geology units as follows:

1. Sites that were shot on the relatively fine-grained Capilano sediments (predominantly glaciomarine and fluvial deposits) and recent floodplain deposits produced excellent reflection records, with dominant frequencies in the 150 Hz range and visible reflections on the field records to 800 ms (corresponding to an estimated depth of 700 m below surface). The results from site 3 are shown in Figure 6.
2. Sites that were shot on the coarser grained Fort Langley Formation (glacial and deltaic deposits) and Sumas Drift (outwash, ice-contact, and deltaic deposits), where the surface sediments were typically drier and the water table was several metres below ground surface, produced fair to good reflection records having lower dominant frequencies (approx. 100 Hz). These data showed visible reflections on the field records down to 200–400 ms (estimated depths of 180–350 m below surface), but with considerably more interference from ground roll (low-frequency, large-amplitude surface waves). The results from site 5 are shown in Figure 7.
3. Sites that were shot in the Sumas valley (fine-grained lacustrine deposits) yielded extremely poor reflection records despite the seemingly good surface conditions. The reasons for the poor-quality data are still not understood. Because of the extremely poor test results, no seismic profiles were acquired in this area.

COMMON-MIDPOINT PROFILING RESULTS

Influence of surface conditions

As discussed above and demonstrated in the results of the testing phase of this survey, surface conditions can strongly influence the quality of seismic-reflection data, and hence the resolution and penetration depth of the survey. Figure 8 shows examples of field records obtained from various seismic lines, and illustrates the extreme variation in signal strength, dominant frequency of reflections (i.e. 'sharpness' of reflections), and ground-roll interference that characterize records from areas with differing surface sediments and depth to water table.

Profiles acquired on Capilano sediments

Several seismic profiles were acquired on Capilano sediments west of the Brookswood aquifer (Fig. 2). In general, data quality was excellent in the lowland areas where the surface sediments are fine grained and water saturated (Fig. 8a). In contrast, on the uplands, where the surface sediments tend to be sandier and the water table may be several metres below surface, data quality was usually poor (Fig. 8b). The following discussion deals with data acquired in 1) the Campbell River lowland (12th Ave., 184th St., 188th St., 8th Ave. W.), 2) the Nicomekl River lowland (40th Ave. (GSC), UBC line 32-184), and 3) the upland areas (SFU lines 20, 200, 164).

Campbell River lowland seismic profiles

Approximately 5 line-km of seismic profiles were recorded on the Campbell River lowland by the GSC and SFU in 1994. These include the four southernmost lines acquired on Capilano sediments (Fig. 2, 12th Ave. between 176th and 184th St., 8th Ave. between 184th and 192nd St., and 184th and 188th St. south of 8th Ave.). These data delineate the glaciomarine infilling of this valley (Capilano sediments), the underlying Pleistocene stratigraphy, and the interpreted Tertiary boundary.

Figure 9 is the upper 250 ms of the 12th Avenue profile, which was shot in the centre of the lowland area. The section delineates an upper unit (above 100 ms) of continuous subhorizontal reflections. This unit is interpreted as Capilano sediments, which reach a maximum thickness of 100 m along

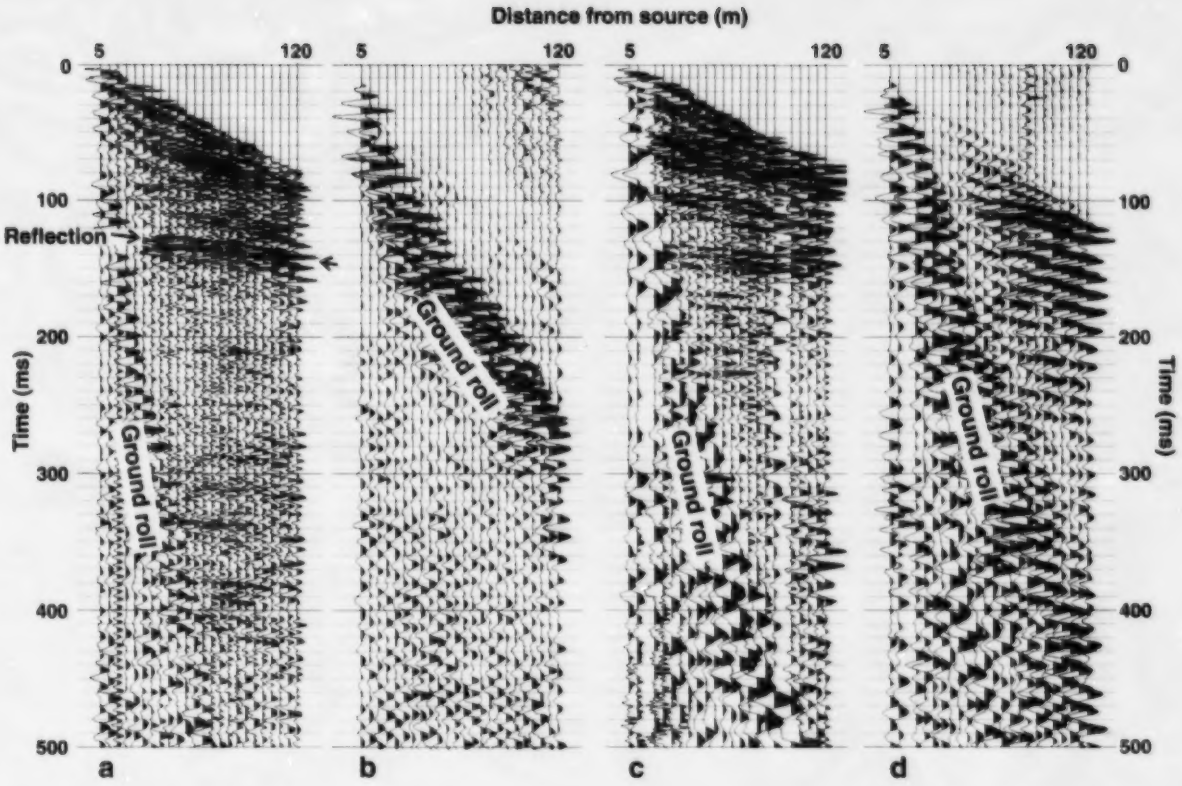

Figure 8. *Sample field files, recorded in various surficial geological settings, showing the wide variation in reflection data quality:* ***a)*** *excellent record from the Campbell River lowland (water-saturated, fine-grained Capilano sediments, 40th Ave.) showing strong, high-frequency reflection energy with little ground-roll interference;* ***b)*** *poor record from upland areas (low water table in thin, sandy Capilano sediments overlying Vashon Drift, 164th St.), showing virtually no reflection energy, low dominant frequencies, and strong ground roll;* ***c)*** *very good record from Fort Langley Formation (stony, clayey silt, damp near-surface horizons, 24th Ave.), showing strong reflection energy with slightly lower dominant frequency and more ground-roll interference than in (a); and* ***d)*** *fair record obtained on outwash floodplain of Sumas age deposits (dry sand and gravel, Boundary Ave.), showing some low-frequency reflection energy with strong ground roll.*

the section (at both the east and west ends of the line). The reflections within this unit are interpreted to represent alternating fine- and coarser grained sediment types, based on the sequence of alternating sand and clay intersected to a depth of greater than 150 m by a borehole on 8th Avenue, 1 km directly south of the centre of this profile (*see* Ricketts and Makepeace, 2000). A flowing artesian well less than 70 m deep has been drilled at the east end of this line (Halstead, 1986, Fig. 9), indicating that water can be obtained from the coarse-grained layers in this sequence.

A reflection at 100–120 ms (Fig. 9) is interpreted as the top of the underlying Vashon Drift. In the western half of the section, there is a mound or lobe of sediment lying above this surface. The lobe is 450 m in length along this section, and approximately 30 thick. The large amplitudes associated with this unit suggest that it contains a significant amount of coarse-grained sediment. The seismic signals coming from below a depth of 100 m are weak, and delineation of deeper stratigraphy becomes more speculative; however, there is a suggestion of flat-lying deposits in the eastern half of the section (*see* reflections at 210 and 250 ms at the east end of the line), with overlying sediments (120 to >250 ms) in the western half of the profile that are dipping to the west (possibly infilling an erosional valley). A large-amplitude reflection at 350 ms (below the section shown in Fig. 9) at the east end of the line (where data are exceptionally good) is interpreted to be the Tertiary surface at a depth of 350 m (*see below* for further discussion on the Tertiary surface).

Three intersecting lines were acquired at the southeast margin of the Campbell River lowland (Fig. 2). Figure 10 shows the northern portion of the seismic profile along the westernmost north-south line (184th St. south of 8th Ave.). This section shows a similar stratigraphy to that of 12th Avenue (Fig. 9). Again, the uppermost seismic unit is a sequence

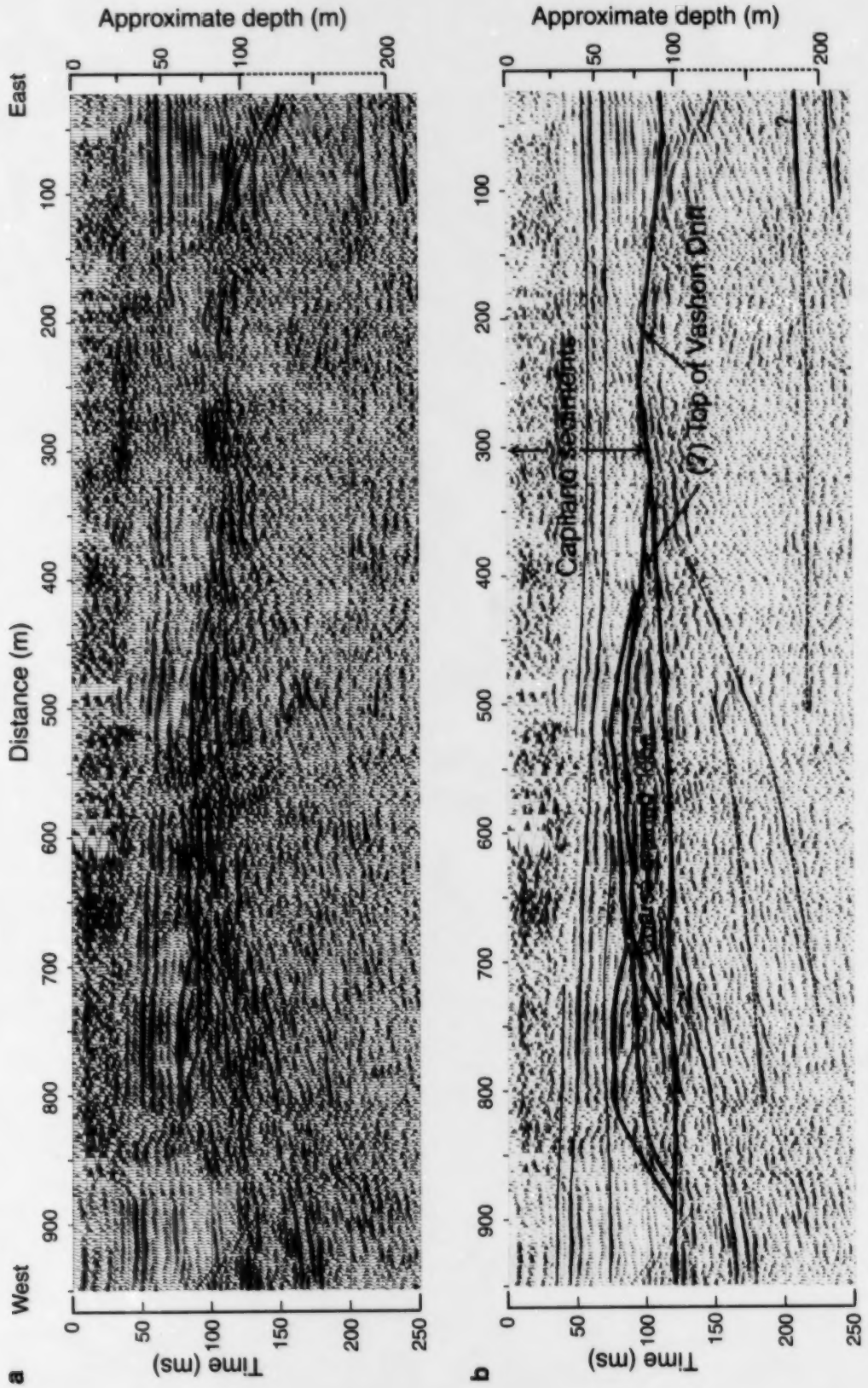

Figure 9. *Portion of the 12th Avenue profile (0–250 ms), shot in the centre of the Campbell River lowland, which shows a thick sequence of Capilano sediments above a large-amplitude, complex reflection package:* ***a****) processed seismic profile,* ***b****) interpreted section (vertical exaggeration approx. 1.2).*

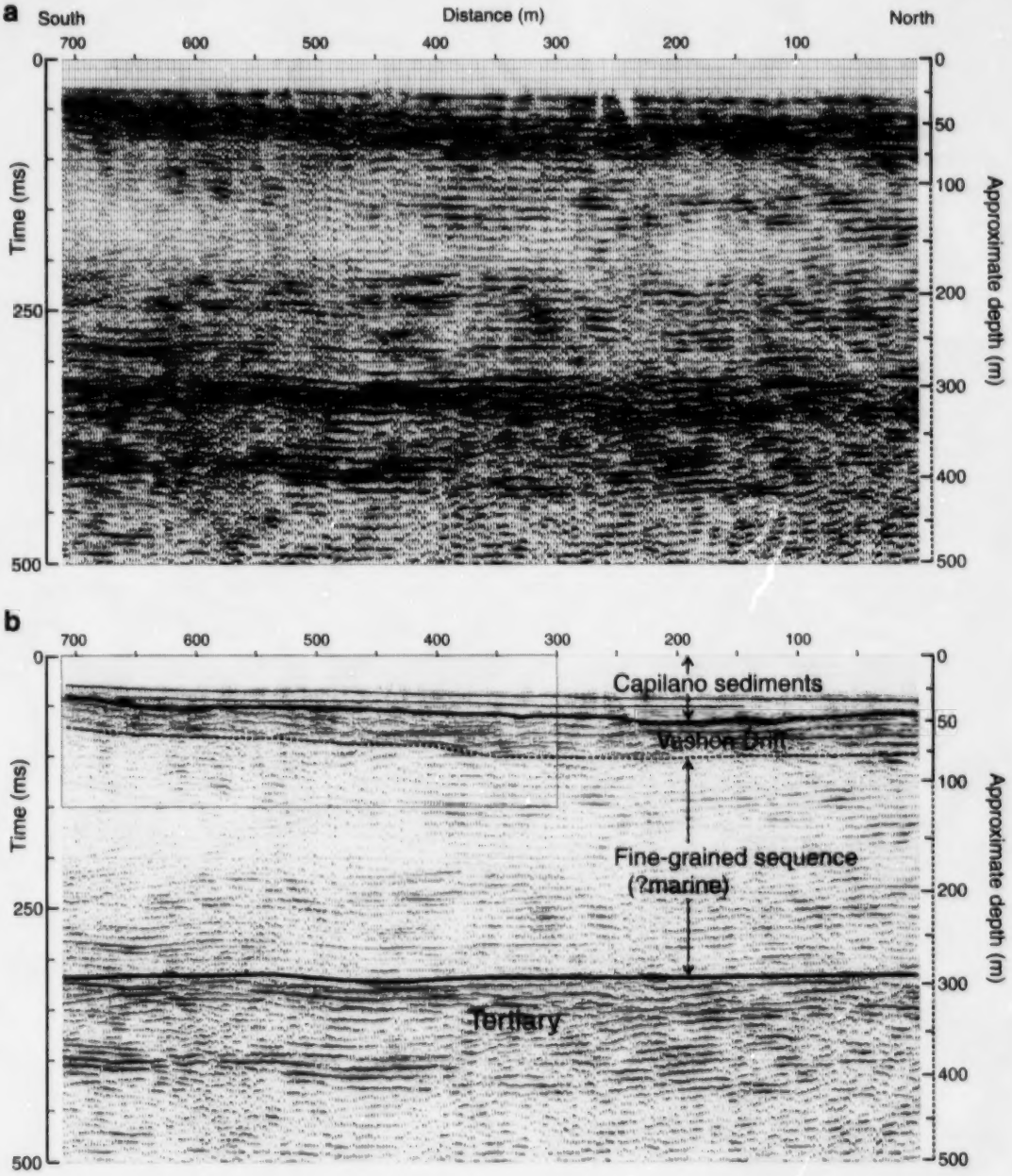

Figure 10. *North end of 184th Street profile (0–500 ms), showing the interpreted top of Tertiary bedrock:* ***a)*** *processed seismic profile,* ***b)*** *interpreted section (vertical exaggeration approx. 1.0). Box in upper left outlines the area detailed in Figure 11.*

of flat-lying continuous reflections interpreted to represent the Capilano sediments (to 60 ms), although the unit is somewhat thinner (approx. 50 m) than it was on 12th Avenue. It overlies a complex sequence of large-amplitude reflections (60–90 ms), which is interpreted as Vashon Drift. The irregular upper surface of the Vashon Drift appears to be eroded by channel processes (Fig. 11). Below 100 ms is a thick (>200 m) unit of subhorizontal continuous reflections, which suggests a low-energy marine or lacustrine sequence. The interpretation of the upper stratigraphy based on the seismic data is supported by a borehole log at the north end of the line (Ricketts and Makepeace, 2000), which indicates clay or silty sand and clay to a depth of 54 m (?Capilano), 25 m of diamict and sand (?Vashon), and then silty clay to a depth of 115 m (bottom of the borehole). Though unsupported by any borehole data, the major reflection boundary at 320 ms is interpreted to be the Tertiary surface at a depth of approximately 300 m.

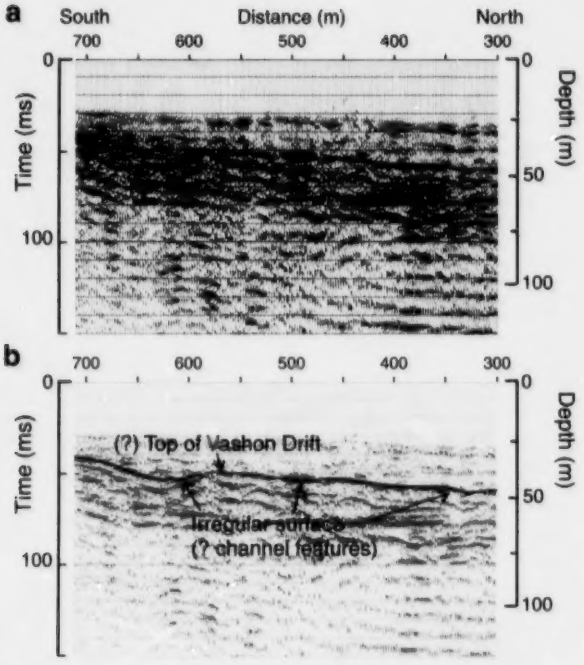

Figure 11. *Detail of shallow portion in centre of 184th Street profile (0–150 ms), showing irregularities (channel features?) in the surface of the unit that is interpreted to be Vashon Drift:* ***a)*** *processed seismic profile,* ***b)*** *interpreted section (vertical exaggeration approx. 2.2).*

Figure 12 shows part of the profile that runs east (along 8th Ave.) from the north end of 184th Street (Fig. 10). The west end of the figure is 550 m from the start of the line (SOL; i.e. from the intersection with the profile in Fig. 10). Two areas of poor data are observed along this line (700–800 m and 1400–1450 m from SOL); these are attributed to poor surface conditions (loss of the ditch for planting source and geophones due to built-up areas and road crossings). This section does not show any indication of the upper unit observed on 12th Avenue (Fig. 9) or 184th Street (Fig. 10). The surficial geology map indicates that the surficial deposits along this line are still Capilano sediments, but they are too thin (<20 m) in this area to resolve with the source-receiver geometries used for these seismic surveys. Instead, the uppermost unit observed on this line (30–80 ms) is characterized by a series of laterally continuous reflections that may indicate several lithological units varying considerably in thickness over the kilometre of line surveyed. The sequence is thickest in the centre of the figure (approx. 100 m) and thinnest at the eastern end of the line (<50 m). Below this unit is the thick succession of low-amplitude reflections that was observed on the previous two lines and interpreted as marine or lacustrine deposits.

Armstrong (1984, Fig. 10) constructed a 2 km long northwest-southeast cross-section across the contact between the Fort Langley Formation and the Capilano sediments just east of this profile. It indicates that the highlands are underlain by Fort Langley and Vashon deposits, and suggests that, below an elevation of 25 m a.s.l., the sediments are a complex sequence of Vashon Drift, Quadra Sand, Cowichan Head Formation, and Semiahmoo Drift overlying Highbury sediments (silt, silty sand, and minor gravel). The upper surface of the Highbury sediments is shown to vary between 50 and 100 m below the surface of the lowland area. Armstrong's interpretation of the subsurface stratigraphy bears a strong resemblance to the seismic profile in Figure 12. On this basis, the marine or lacustrine unit is interpreted as Highbury sediments, overlain by a complex sequence of younger diamictons and sand (Fig. 12b).

The most striking feature on this section is the large-amplitude reflection, below the interpreted Highbury sediments, that drops off sharply to the west between 550 and 800 m from the SOL. It is suggested that this reflection marks the top of a lobe of Westlynn–pre-Westlynn deposits. Below this unit (at 320 ms) is the same sequence of reflections observed on Figure 10 and interpreted as the Tertiary surface at a depth of approximately 300 m.

The north end of the third seismic profile in this series of intersecting lines is shown in Figure 13 (north-south line on 188th St. south of 8th Ave.). The south end of the figure shows yet another stratigraphic unit at an estimated depth of 150–200 m (175–250 ms). This appears to be a lobe of stratified sediments deposited on the Westlynn–pre-Westlynn surface (as interpreted above), but no ground truth from drillholes is available to provide more information on the stratigraphy or age of the unit.

Nicomekl River lowland seismic profiles

One GSC seismic line (Fig. 2, 40th Ave. crossing 184th St.) was shot in the Nicomekl River lowland southwest of Langley. The eastern portion of this line from just west of 184th Street is shown in Figure 14. It shows an upper seismic unit (above 120–150 ms) of continuous subhorizontal reflections similar to those observed in Figure 9. Again, this unit is interpreted as Capilano sediments, with the reflections representing a sequence of alternating fine- and coarser grained sediment types. The coarser grained layers may be water bearing (flowing artesian conditions exist along this line from a depth of less than 115 m; Halstead (1986, Fig. 9)). This unit ranges from 110 to 125 m in thickness along the section.

The east end of this line (Fig. 14) is at the base of the delta front of the Campbell River delta (Brookswood aquifer). As there is no indication of a thinning out or shallowing of the Capilano sediments, they clearly must underlie the Brookswood aquifer in this area. Halstead (1986) showed the northwestern portion of the Brookswood aquifer to be underlain by fine-grained marine or lacustrine deposits. This observation is also consistent with the results of electromagnetic and gravity surveys conducted in the same area (Best and Todd, 2000).

The base of the upper unit, interpreted here as Capilano sediments, is marked by a strong reflection at 120–150 ms. This is interpreted to be a major lithological boundary, presumably the top of a coarse-grained unit. Below this reflection,

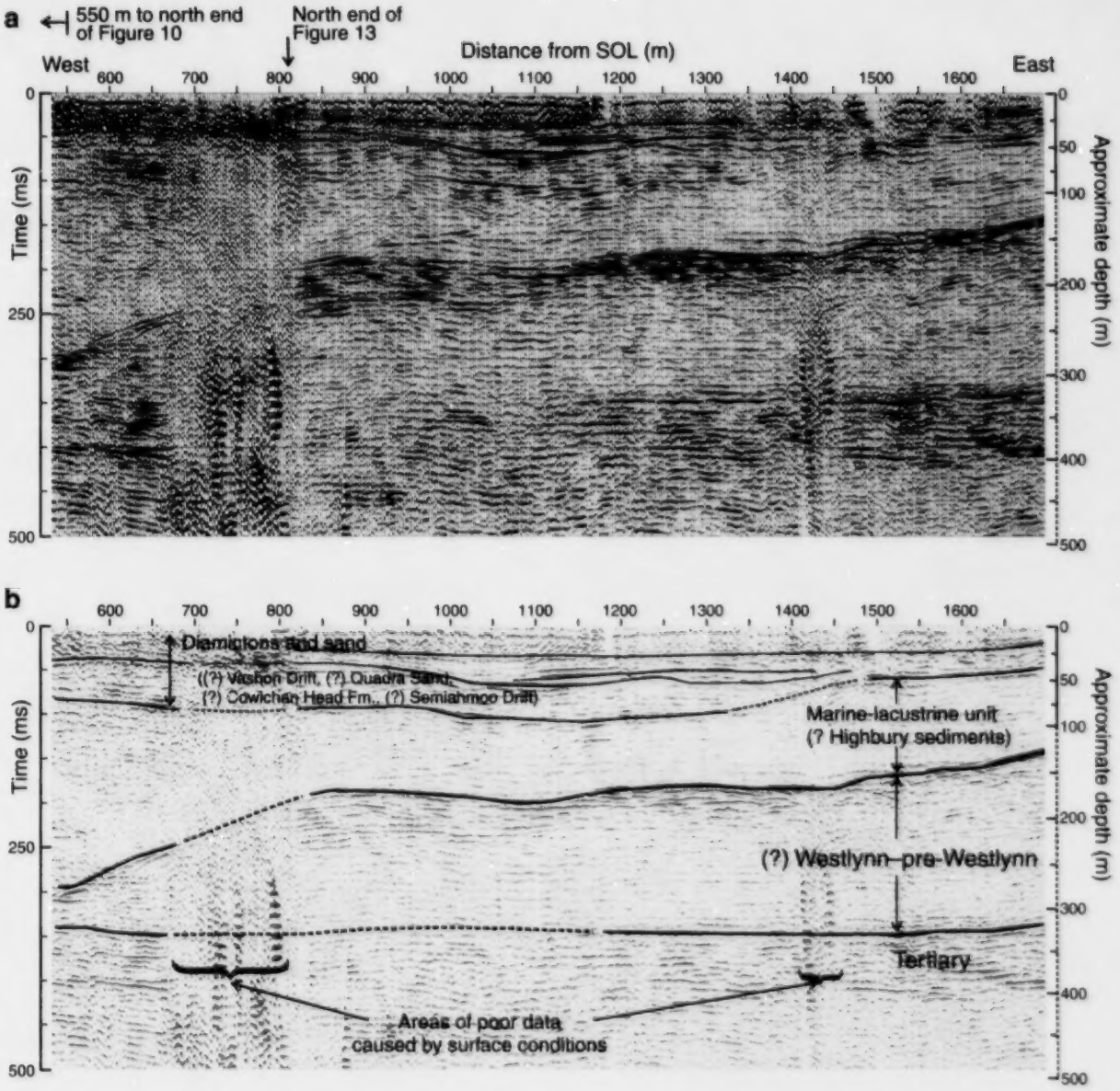

Figure 12. *Eastern end of 8th Avenue West line (0–500 ms):* ***a)*** *processed seismic profile,* ***b)*** *interpreted section (vertical exaggeration approx. 1.1). The stratigraphy is based on Figure 10 in Armstrong (1984). This section was shot on Capilano sediments, but they are too thin to be observed on the section. Areas of poor-quality data (700–800 m and 1400–1450 m) are attributed to a change in surface conditions. SOL means 'start of line'.*

the seismic signals are markedly weaker, suggesting that little energy is transmitted across this boundary and/or that contrasts in acoustic impedance at deeper horizons are small. The reflection package observed at 350 ms at the west end of Figure 14 is interpreted as the top of the Tertiary. At the east end of the figure, a reflection at 260 ms dips west and intersects the Tertiary reflection package. If this represents the Tertiary contact, it implies approximately 100 m of relief on the bedrock surface along this section. Alternatively, the dipping reflector could be interpreted as a lobe of older Pleistocene deposits overlying a relatively flat Tertiary surface.

A test borehole drilled 2 km north of the west end of this line (Armstrong, 1984, Fig. 15) showed that 100 m of Capilano sediments overlie a thin (<25 m) unit of Vashon Drift and approximately 175 m of older Pleistocene

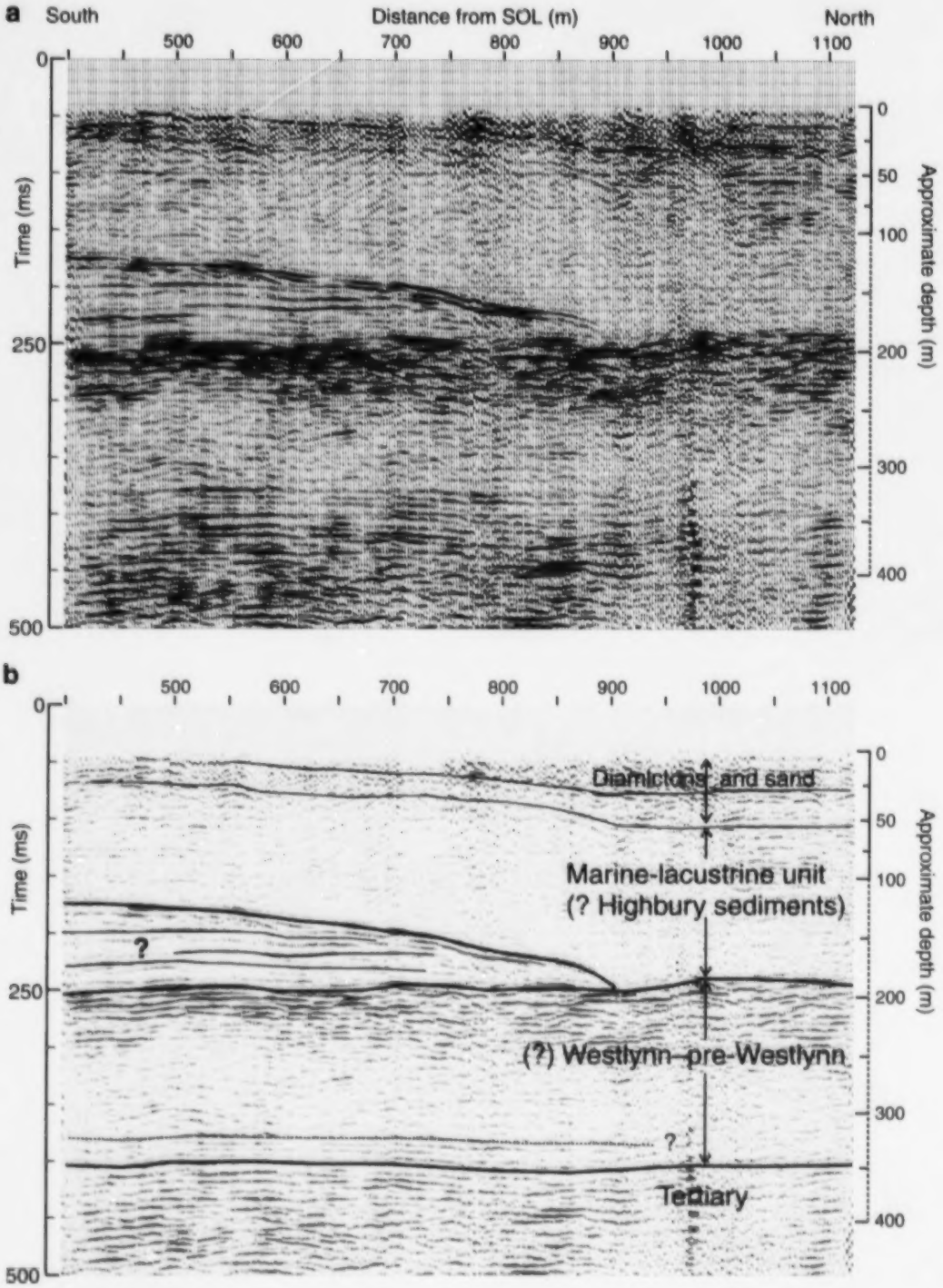

Figure 13. *Lowland portion (north end) of 188th Street profile:* ***a)*** *processed seismic profile,* ***b)*** *interpreted section (vertical exaggeration approx. 1.1). The interpretation is based on a correlation with Figure 14. The lobe of stratified sediments (0–80 m in thickness) at the south end of the figure is interpreted to be deposited on the Westlynn–pre-Westlynn surface, and to have an erosional surface. SOL means 'start of line'.*

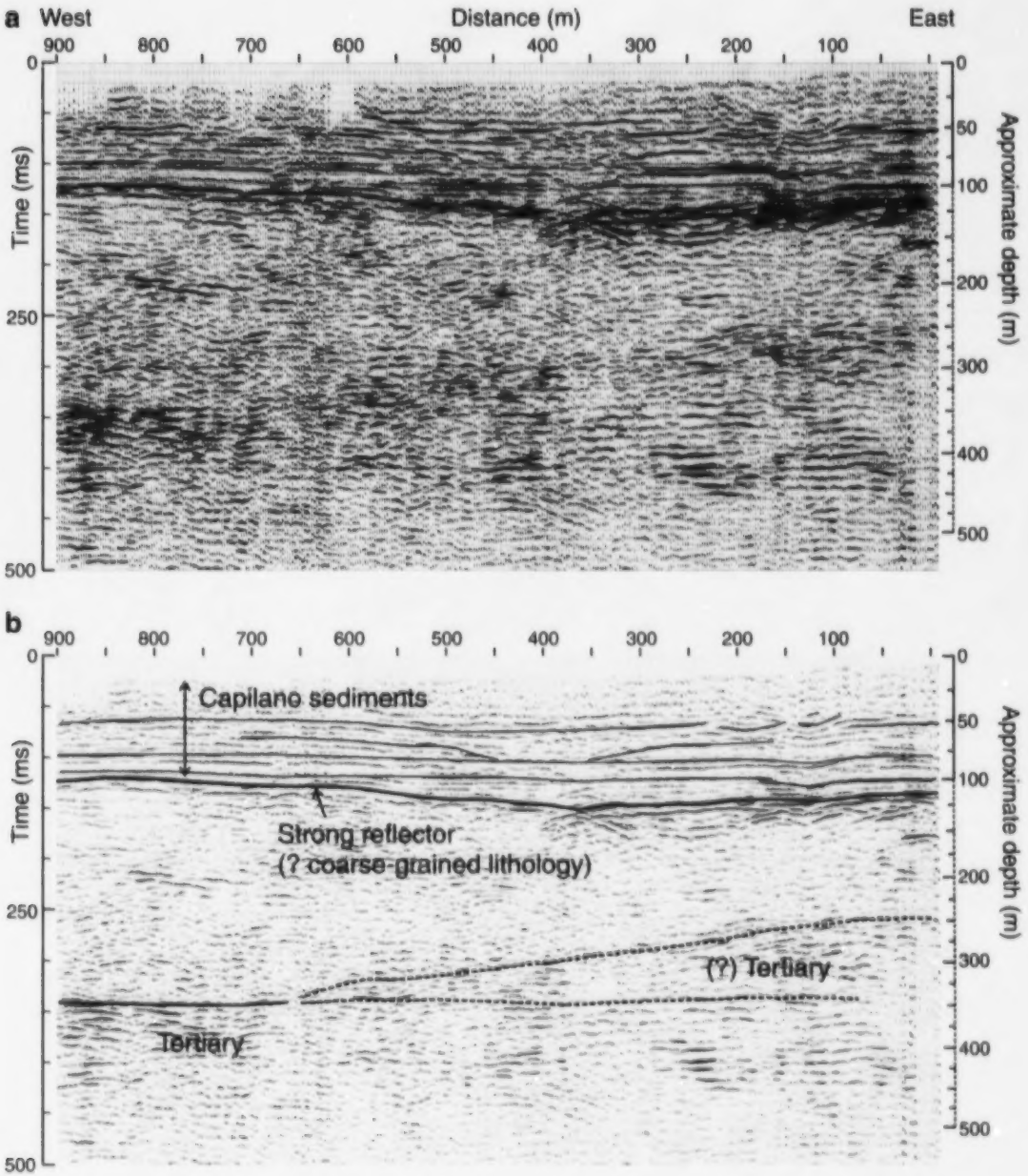

Figure 14. *West end of 40th Avenue profile (0–500 ms), shot on the Nicomekl River lowland:* ***a)*** *processed seismic profile,* ***b)*** *interpreted section (vertical exaggeration approx. 1.1). The sequence of Capilano sediments reaches thicknesses in excess of 100 m along this line. Deeper reflections are weaker, but suggest that there may be 100 m of relief on the bedrock surface in this area.*

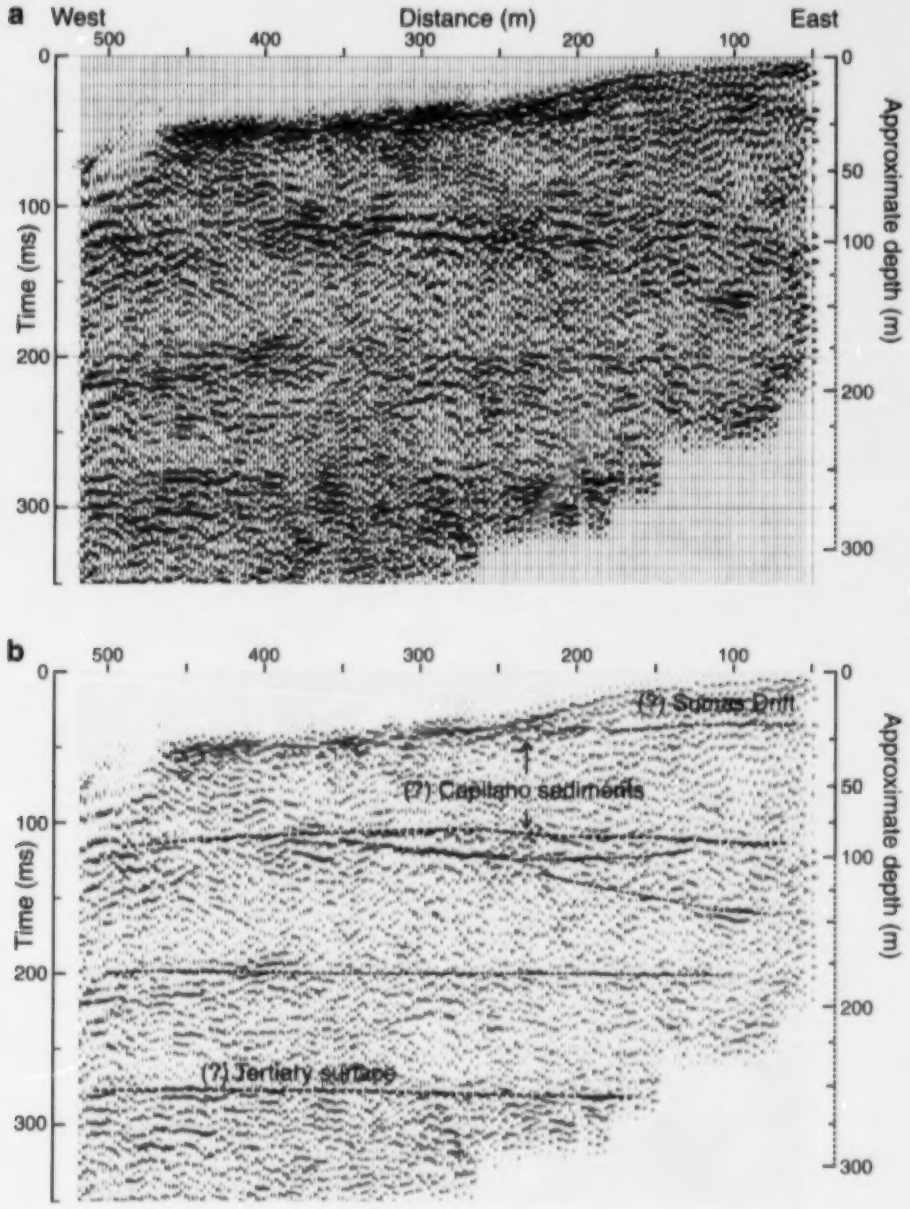

Figure 15. *Simon Fraser University line 300 (28th Ave.), acquired on the western edge of the Brookswood aquifer (note the 21 m increase in elevation from west to east):* ***a)*** *processed seismic profile,* ***b)*** *interpreted section (vertical exaggeration approx. 1.1). Data quality in this area was marginal; the blank area at the bottom right of the section is where there was excessive groundroll interference in the records which had to be surgically muted. Interpretation of the Tertiary surface is based on a correlation with Figure 16.*

sediments above the Tertiary contact at a depth of 300 m. This correlates well with the west end of the section shown in Figure 14. There are also indications in the borehole records of considerable relief on the Tertiary surface in the area, because another test hole drilled 3 km southeast of this seismic section (Armstrong, 1984, Fig. 11) showed the surface to be 140 m higher in elevation.

A high-resolution seismic line was shot by UBC on the Nicomekl River lowlands adjacent to the Brookswood aquifer and 2 km south of the line in Figure 14. This line showed a thinner sequence of Capilano sediments and a reflector at a depth of approximately 200 m (possibly the Tertiary surface; *see* 'Shallow high-resolution investigations (University of British Columbia)' section below).

Seismic profiles on upland areas

Attempts were made to collect data along two lines west of the Brookswood aquifer on the upland areas, where Capilano sediments form a veneer over Vashon Drift deposits (Fig. 2, 164th St. and 20th Ave.). However, the dry surface conditions led to poor data quality with low signal-to-noise ratio and limited penetration (Fig. 8b). Little information was obtained from these lines, so they will not be discussed further in this paper.

Profiles acquired on deposits of Sumas age

Several seismic profiles were acquired on the Brookswood aquifer, and one line was acquired on the Abbotsford aquifer south of Abbotsford Airport (Fig. 2). Data quality varied from very good under certain surface conditions (close to water table, or damp fine-grained sediments) to poor in areas where the surface materials were dry and coarse grained (Fig. 8d). The following discussion deals with data acquired on 1) the edge of the Brookswood aquifer, 2) the south-central Brookswood aquifer, and 3) the Abbotsford aquifer.

Profiles on the edge of the Brookswood aquifer

Simon Fraser University acquired two lines of seismic data on the western edge of the Brookswood aquifer (SFU lines 100 and 300), in an attempt to delineate the sedimentary structures at the margin of the delta deposit. Unfortunately, the frequency and signal strength were not high enough to resolve such shallow structure. However, some subsurface structural information has been obtained, as shown in Figure 15 (28th Ave. east of 184th St.). The fair data quality means that only major subsurface boundaries can be observed, with little information on reflection character within units. An interpretation of this section, based on a correlation of major reflections with Figure 14, suggests that the reflection observed at 110 ms (approximately 50 m below surface at the western end of the profile) is the base of a marine or lacustrine near-surface unit, whereas the reflections at 200 and 280 ms correlate with those at 260 and 380 ms on Figure 14 (the latter possibly being the Tertiary surface).

Profiles on the Brookswood aquifer

Good data were obtained on Sumas deposits in areas where surface conditions were more amenable to the application of shallow seismic-reflection techniques. One example is Stoke's gravel pit in the centre of the southwestern quadrant of the Brookswood aquifer (Fig. 2). In this case, data were obtained in the bottom of a gravel quarry where operations had been halted when the extraction of material reached the water table; the geophones and source were planted in water-saturated sand. The Stoke's pit profile, shown in Figure 16, correlates very closely with the data obtained on 12th Avenue, 3 km to the southwest (Fig. 9). The base of the sand and gravel of the Brookswood aquifer (Sumas age) is not evident on this section, presumably because it is within 25–30 m of the surface and too shallow to be resolved with the source-receiver geometries used for this survey. The upper unit observed is a thick (>100 m) sequence of continuous subhorizontal reflections interpreted as marine (Capilano sediments) or glaciolacustrine (Fort Langley Formation) deposits. It is underlain by a strong reflection at 140–170 ms that dips to the north, from approximately 125 to 150 m below surface. This reflection corresponds to a prominent electromagnetic horizon obtained along the same transect (Best and Todd, 2000). It is interpreted to be the top of an underlying sequence of coarse-grained deposits (possibly Vashon Drift plus older units). Between 200 and 320 ms, the data show the same character of low-amplitude, continuous, flat-lying reflections that are suggestive of marine or lacustrine deposition, and have been previously interpreted as Highbury sediments (Fig. 12). The reflection package at 320 ms (estimated depth of 350 m) is interpreted to be the top of Tertiary bedrock at this site.

Another example of good reflection data obtained on Sumas age deposits is seen in a high-resolution seismic line shot by UBC in the east-central quadrant of the Brookswood aquifer (Fig. 2, 20th Ave. East), 2.5 km west of the profile shown in Figure 16. In this case, the geophones and source were planted in partly saturated, fine to medium sand with some gravel and clay. This line is discussed in the 'Shallow high-resolution investigations (University of British Columbia)' section below.

Profile on the Abbotsford aquifer

One profile was shot on an outwash floodplain of Sumas deposits south of Abbotsford Airport (Fig. 2, Boundary Ave.). In this area, gravel and sand up to 30 m thick overlie an uneven surface of Fort Langley Formation deposits (Armstrong, 1984). The quality of the reflection data acquired on this line was poor, due primarily to the dry, coarse-grained surface materials (Fig. 8d). The eastern end of the line is shown in Figure 17; all that is evident on this section is a reflection at 90 ms which dips slightly to the west along the 2.5 km length of the line. This reflection is assumed to be due to a major stratigraphic boundary at a depth of approximately 80 m, but no borehole data are currently available to provide any information on the nature of the horizon.

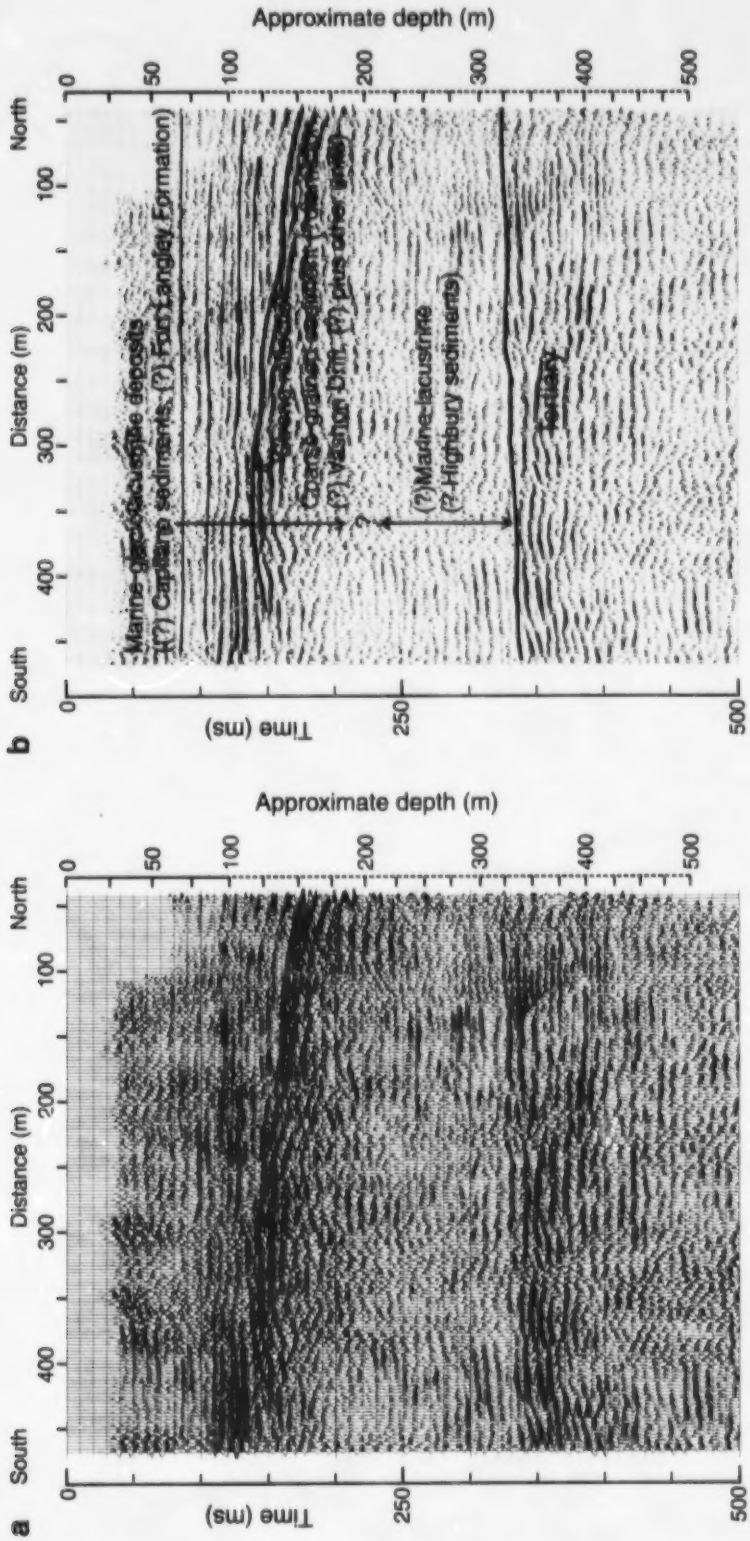

Figure 16. *Profile acquired on the Brookswood aquifer (Sumas deposits) in Stoke's gravel pit, under special conditions which allowed the source and receivers to be planted close to the water table:* ***a)*** *processed seismic profile,* ***b)*** *interpreted section (vertical exaggeration approx. 1.1).*

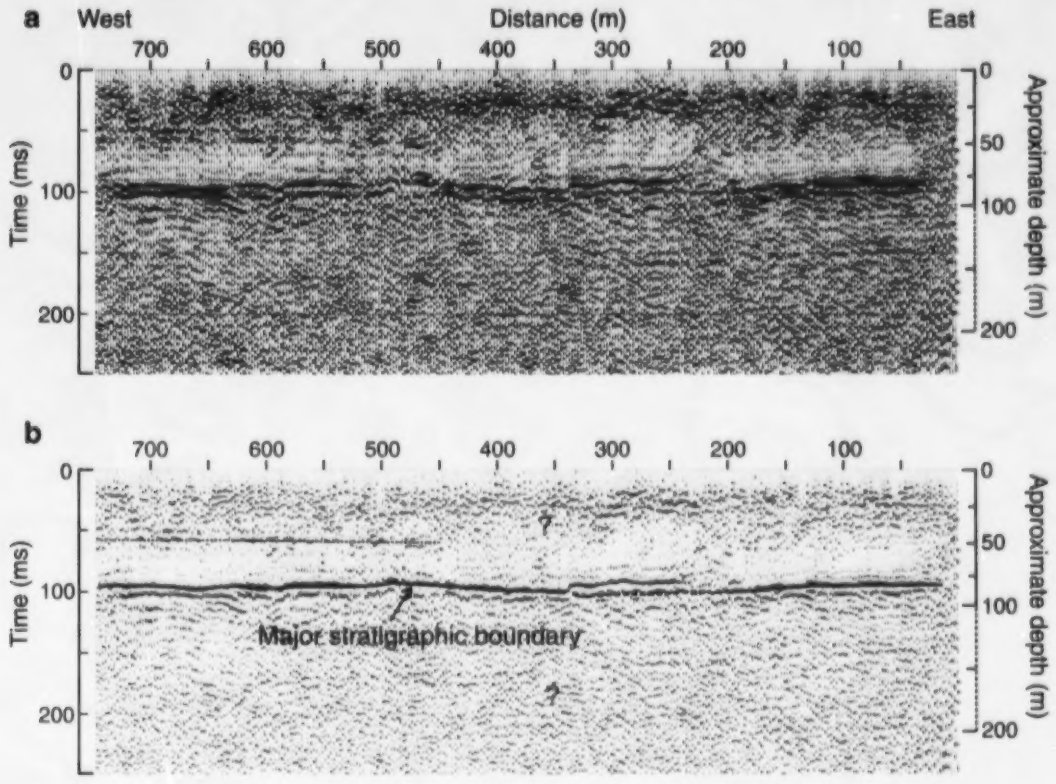

Figure 17. *East end of Boundary Avenue profile, shot on Sumas deposits in the eastern part of the survey area:* ***a)*** *processed seismic profile,* ***b)*** *interpreted section (vertical exaggeration approx. 1.1). The data are of marginal quality, but do indicate a stratigraphic horizon at a depth of approximately 80 m.*

Profiles acquired on the Fort Langley Formation

Two seismic profiles were acquired by the GSC on Fort Langley Formation deposits east and south of the Brookswood aquifer, and one high-resolution line was acquired by UBC immediately east of the Brookswood aquifer (Fig. 2, 216th St.). Data quality was good (Fig. 8c), and the sections delineate considerable subsurface structure.

Figure 18 shows the east-west profile along 24th Avenue east of the Brookswood aquifer. Considerable relief on subsurface horizons is evident at the east end of this section, but interpretation of the structures is difficult because of a lack of borehole information. A surface apparently dips to the east, from 150 m below surface in the centre of the line to a depth of more than 300 m over a distance of approximately 750 m. Halstead (1986) identified a Tertiary high 2.5 km north of the west end of this line. It is possible that this dipping structure delineates substantial topography on the Tertiary surface, which may only be 80–90 m below surface at the west end of the profile (*see also* Hamilton and Ricketts, 1994).

A very different subsurface structure is shown in Figure 19, the east-west profile along 8th Avenue located east and 3 km south of the 24th Avenue profile (Fig. 18). This section shows a thick unit characterized by relatively low reflectivity (50–150 m in depth at the west end of the profile and 50–90 m in depth at the east end). It appears to be similar in character to the unit interpreted as marine or lacustrine sediments on other sections (e.g. Fig. 10, 12, 16). A test hole 2 km east of the east end of Figure 19 (Armstrong, 1984, Fig. 11, Section 38) encountered more than 50 m of predominantly fine-grained sediments (interpreted to be deposits of Cowichan Head Formation, Semiahmoo Drift, and Highbury sediments) at a depth of about 75 m. Below that, 50 m of diamictons, interpreted as Westlynn–pre-Westlynn sediments, overlie Tertiary bedrock at a depth of approximately 200 m. This stratigraphy correlates well with the east end of the seismic section and, on that basis, the Tertiary surface is interpreted to be the major reflection package at 150 ms (approximately 150 m depth). This surface is an unconformable one: reflections from within the Tertiary sequence can be seen dipping slightly to the west. The area of no data in the middle of the seismic section corresponds to a road crossing (240th St.). West of the road, the section shows a thicker, low-reflectivity unit and a channel or basin in the Tertiary

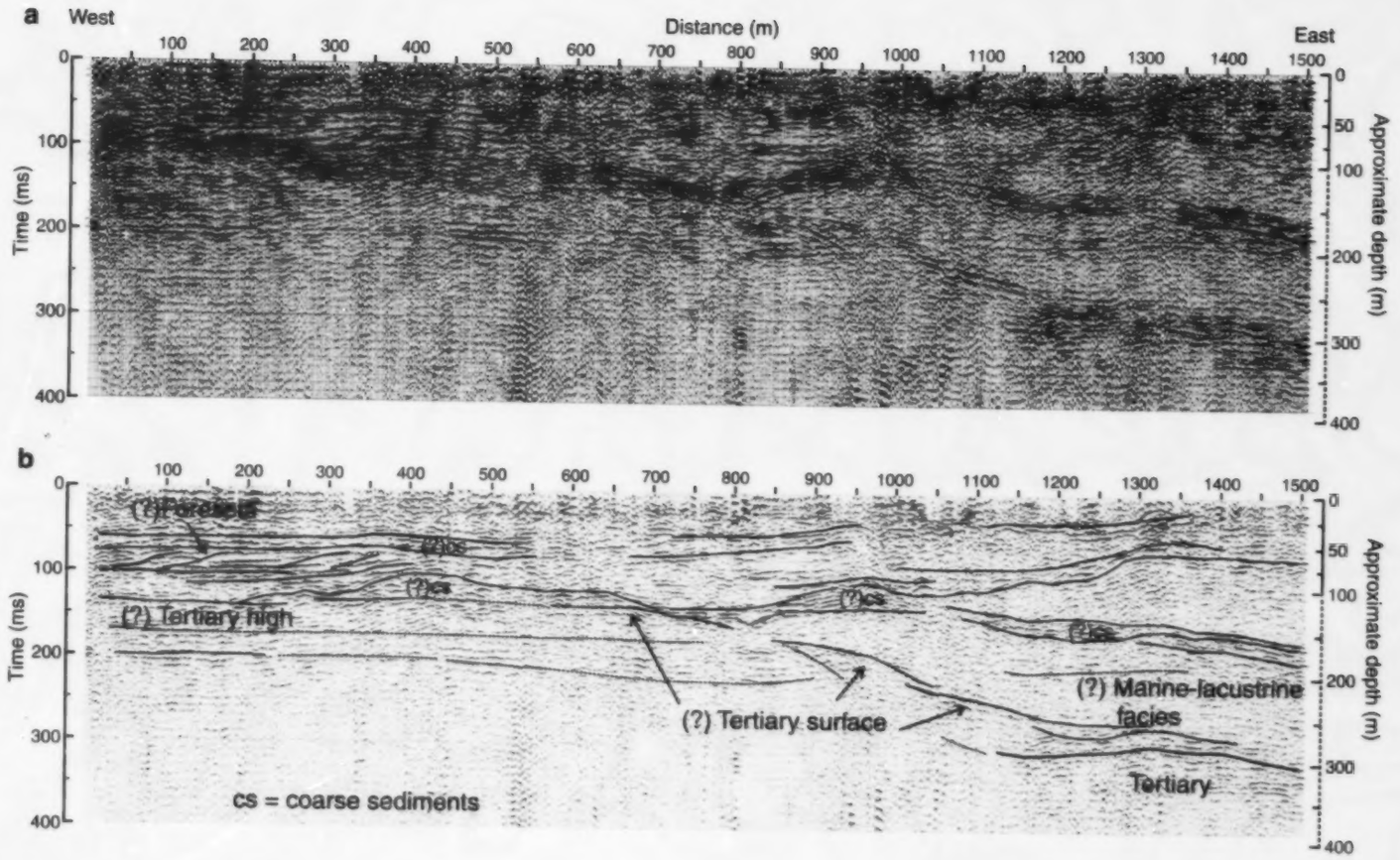

Figure 18. *Profile obtained along 24th Avenue between 224th and 232nd Streets on Fort Langley Formation glaciomarine deposits and delineating a complex subsurface structure:* ***a)*** *processed seismic profile,* ***b)*** *interpreted section (vertical exaggeration approx. 1.1).*

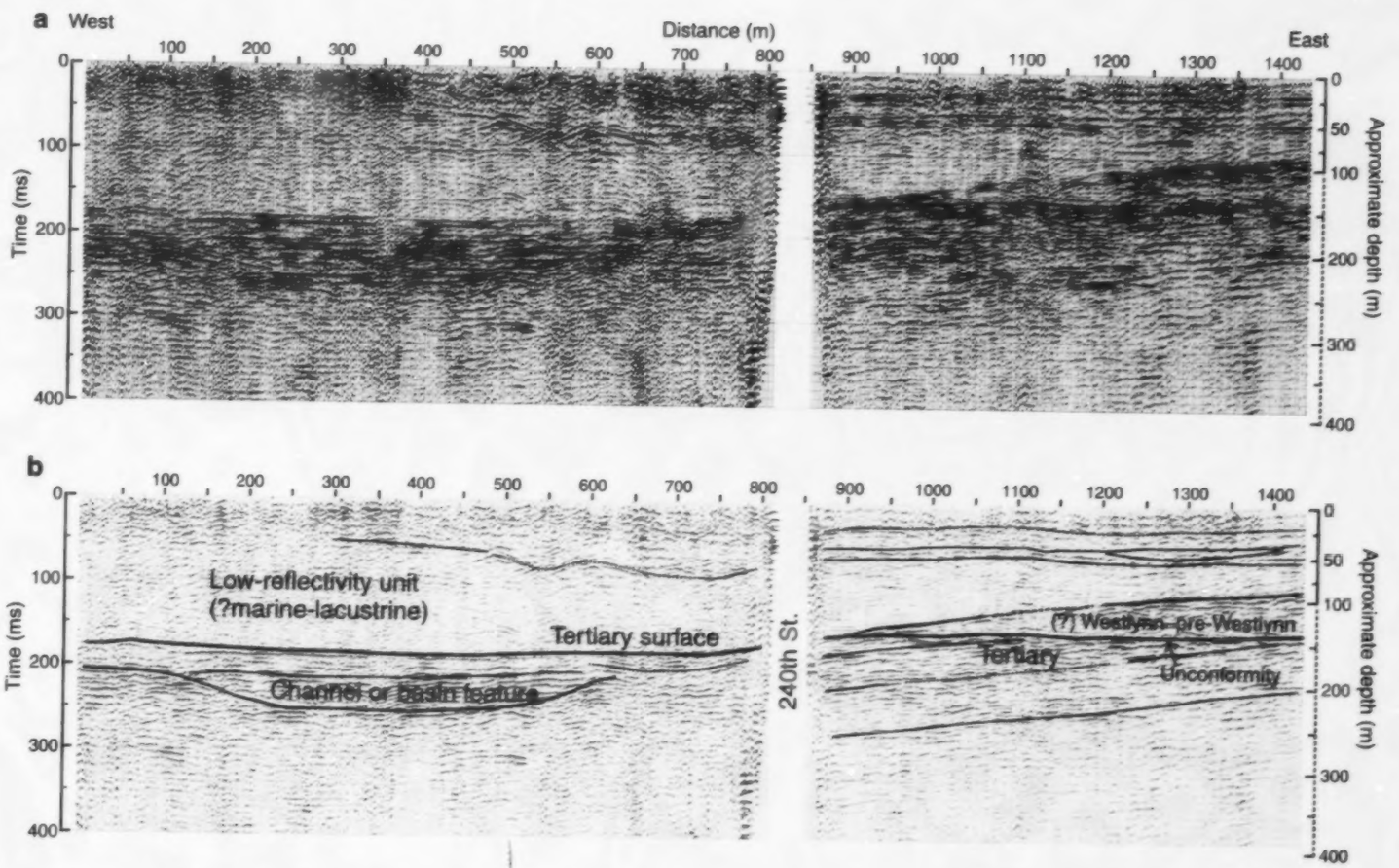

Figure 19. *Profile obtained along 8th Avenue East on Fort Langley Formation glaciomarine deposits:* ***a)*** *processed seismic profile,* ***b)*** *interpreted section (vertical exaggeration approx. 1.1). The interpreted stratigraphy is based on a nearby test hole (Armstrong, 1984).*

surface that has been infilled with deposits characterized by flat-lying, large-amplitude reflections. The channel is approximately 70 m deep and 500 m wide in the plane of the section.

University of British Columbia also acquired a short seismic line on Fort Langley Formation sediments immediately east of the Brookswood aquifer (*see* next section).

Shallow high-resolution investigations (University of British Columbia)

The University of British Columbia has recorded and processed three seismic profiles in different geological settings in the vicinity of the Brookswood aquifer (Fig. 2, 32nd Ave., 20th Ave. E., and 216th St.). These data were acquired with a source-receiver geometry (Fig. 5) that was designed to allow high resolution of the shallow subsurface. Care was taken in

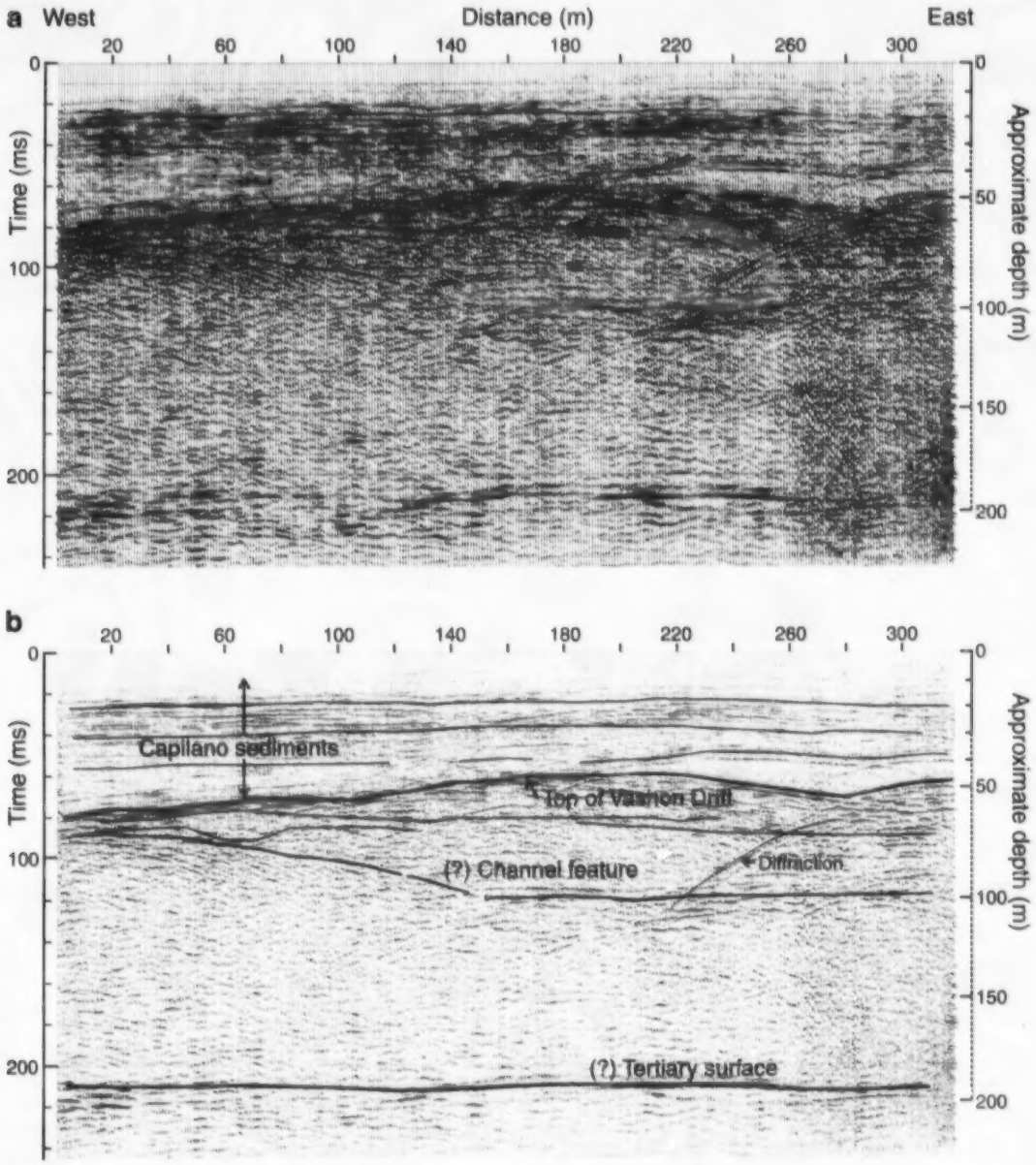

Figure 20. *University of British Columbia line 32-184, from the Nicomekl River lowland adjacent to the Brookswood aquifer:* ***a)*** *processed seismic profile,* ***b)*** *interpreted section (horizontal exaggeration approx. 1.1). This section shows very detailed structure of the upper 80–100 m.*

choosing the line locations and in the field procedures (e.g. use of 100 Hz geophones) to optimize the production and recording of high-frequency energy.

Figure 20 shows UBC line 32-184, acquired on the Nicomekl River lowland just west of the Brookswood aquifer (at the intersection of 32nd Ave. and 184th St.). At this site, the source and geophones were planted in water-saturated clay at the bottom of the ditch; the data are slightly noisier at the east end of the profile, possibly due to a near-surface peat layer. The upper unit observed on the section is a 40–50 m thick sequence of Capilano sediments, characterized by sub-horizontal reflections. The resolution of the data in this upper unit is on the order of 1 m. The Capilano sediments have been deposited on a slightly undulating surface, which is interpreted to be the top of Vashon Drift. The high frequencies of the data allow depositional structure within this deposit to be observed. This unit appears to overlie a large, infilled, channel-shaped feature. The west edge of this feature is the dipping surface at 100 ms on the west side of the profile. It is not known at this time what is represented by the deep reflection at 210 ms, but other sections in the area (Fig. 14) have suggested that the Tertiary surface can be expected in this depth range.

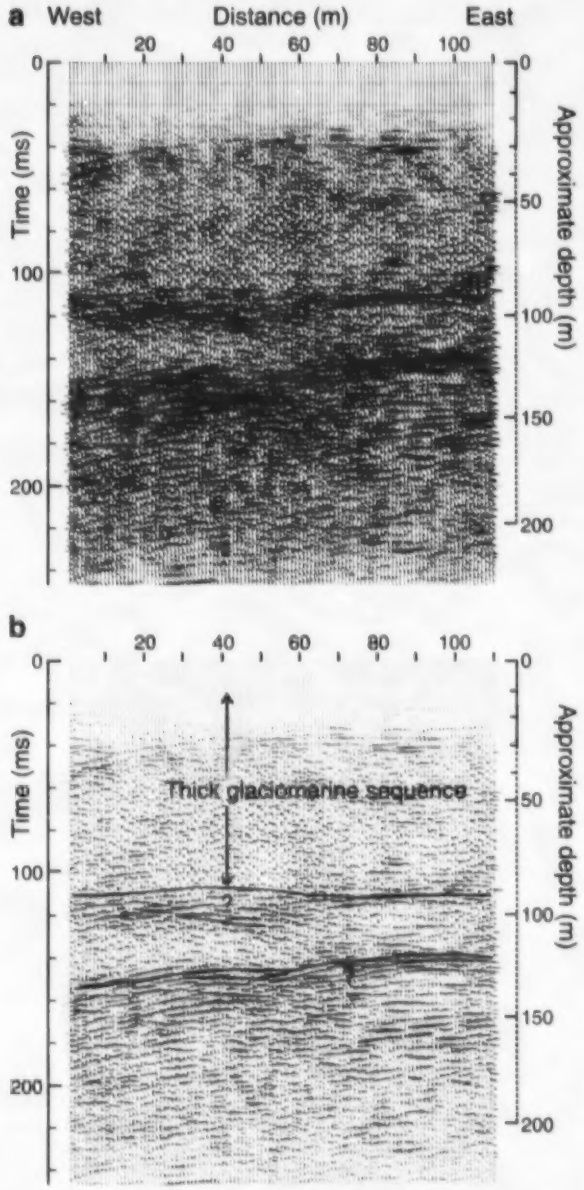

Figure 21. *University of British Columbia line 20-206, from the east-central quadrant of the Brookswood aquifer where the surface sediments are rich in clay and good quality data can be acquired:* ***a)*** *processed seismic profile,* ***b)*** *interpreted section (horizontal exaggeration approx. 1.5).*

A short, high-resolution line (UBC line 20-206), acquired on the Brookswood aquifer, is shown in Figure 21. Although other test-spread data generally indicate that fair to poor data are to be expected on the Sumas Drift deposits, this line shows that excellent data can be acquired in some areas. The surface materials are partly saturated, fine- to medium-grained sand with some gravel and clay, providing fairly good ground coupling. The Sumas Drift deposits at this site are expected to be only a few metres thick, and underlain by potentially thick, fine-grained, glaciomarine sediments of the Fort Langley Formation (Armstrong and Hicock, 1980). The absence of any significant reflection energy on the seismic section above 110 ms is consistent with a 90 m thick glaciomarine sequence at this site.

Figure 22 shows UBC line 216-28, a short north-south profile obtained on Fort Langley Formation deposits just east of the Brookswood aquifer. Again, excellent high-resolution data were recorded, this time with the source and geophones planted in partly saturated, fine-grained sand with a clay matrix. The subsurface structure is very different from that observed in Figure 21; in this case, the fine-grained Fort Langley Formation sediments appear to be only 30–35 m thick, their base being represented by the first major reflection (at 40 ms). Below this reflection is a layered sequence of large-amplitude reflections dipping slightly to the south, which may represent a sequence of coarser grained deposits. The deepest reflection is observed at 110 ms (approx. 100 m). This reflection is interpreted to be the Tertiary bedrock surface, as bedrock has been reported at approximately this depth in the area (Halstead, 1986, Fig. 14).

INTEGRATION OF RESULTS WITH OTHER DATA

Several seismic-reflection profiles were obtained along lines where other geophysical surveys were carried out: 1) in Stoke's gravel pit (Fig. 16), where time-domain electromagnetic soundings were conducted (Best and Todd, 2000, Fig. 10); 2) on UBC line 20-206 (Fig. 21), where ground-penetrating radar data were collected (Rea and Knight, 2000); and 3) in the extreme eastern portions of 40th Avenue, 28th Avenue (Fig. 15), and 20th Avenue on the western flank of the Brookswood aquifer, where ground-penetrating radar data

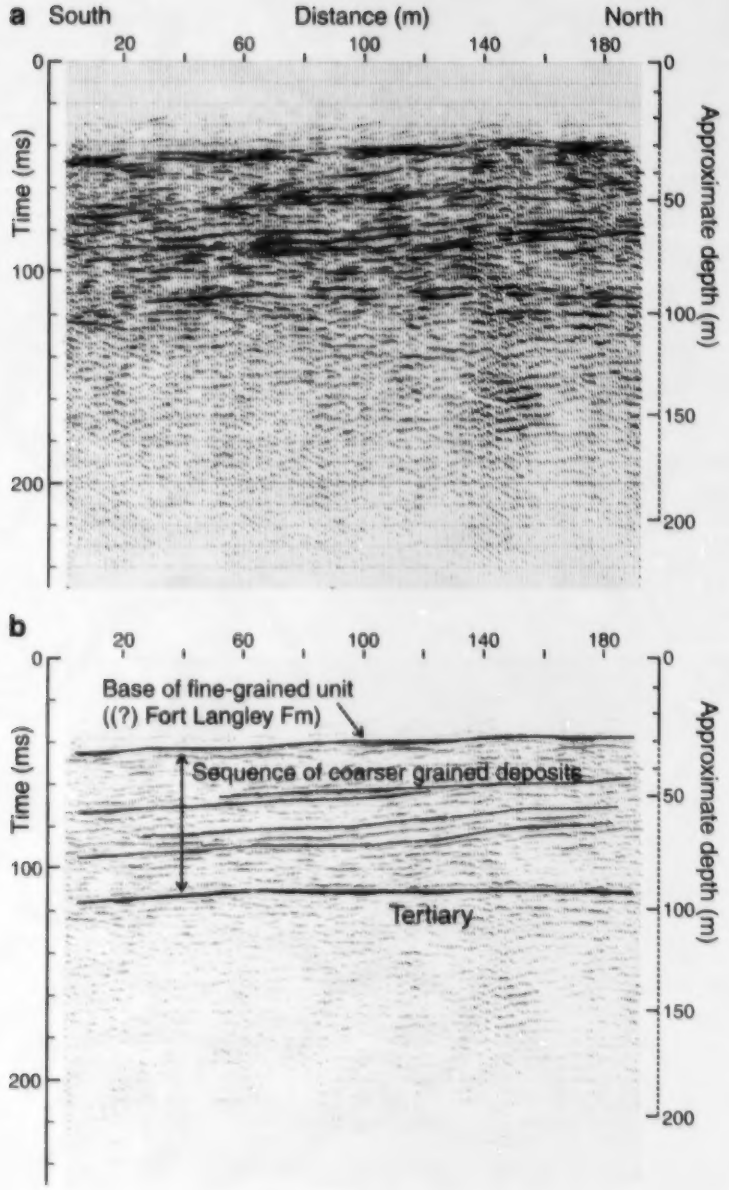

Figure 22.

University of British Columbia line 216-28, from the eastern edge of the Brookswood aquifer, on Fort Langley Formation glaciomarine deposits: ***a****) processed seismic profile,* ***b****) interpreted section (horizontal exaggeration approx. 1.2). This section was shot close to a bedrock high, and the relatively flat-lying reflector at 110 ms is interpreted as the top of Tertiary deposits.*

were also collected (Roberts et al., 2000, Fig. 3–6). It is often difficult to make direct comparisons between the results of different geophysical surveys, as they measure different physical properties of the subsurface and may have different depths of investigation. Nevertheless, an integration of results can provide helpful insights in interpreting the results of all surveys.

The seismic and electromagnetic data acquired in Stoke's gravel pit (Fig. 2) show an excellent agreement in mapping a northward-dipping layer at a depth of 150 m (Fig. 16). The interpretation of the electromagnetic data indicates that this is a boundary between sediments characterized by a resistivity of 40–45 Ω·m (suggestive of a silty clay) and underlying sediments of even lower resistivity (3 Ω·m; i.e. more clay-rich sediments and/or higher salinity pore water). This corroborates the interpretation of the upper unit observed on the seismic sections as being a thick sequence of marine or glaciomarine sediments, but does not support the interpretation of the large-amplitude reflection associated with the boundary as being an underlying diamicton or coarse-grained deposit. The seismic data do not delineate the upper layer indicated by the electromagnetic data at a depth of 35–40 m, as this is close to the shallow limit of detection with the source-receiver geometries used in this survey. Similarly, the boundary observed on the seismic section at 300–350 m depth is beyond the detection limit of the electromagnetic system used.

It is more difficult to directly compare seismic and radar results. This is because, although both surveys produce a cross-section related to subsurface stratigraphy, the methods differ by orders of magnitude in subsurface resolution, and are therefore rarely able to image the same depth range. Even though the UBC seismic surveys were designed to maximize the resolution of the shallow subsurface, there is little information on the sections that corresponds to the depths imaged by the radar (0–20 m).

DISCUSSION AND SUMMARY

This paper has presented the results of shallow seismic-reflection surveys carried out in the Fraser lowland to evaluate the potential and limitations of using this geophysical technique for mapping subsurface structure and aquifer hydrostratigraphy. The few kilometres of line surveyed are very small in comparison to the size of the project area, and the subsurface stratigraphy is complex and highly variable; therefore, these data can provide only glimpses into regional stratigraphic and structural relationships.

It has been shown that the quality of seismic-reflection data (in terms of signal strength and dominant frequency) varies from excellent to very poor across the survey area. The surface conditions strongly affect the ability to transfer high-frequency seismic signals into the ground, and are therefore a critical factor in determining the quality of seismic data obtained at a particular site. In general, the best areas for seismic-reflection surveying are where the surface materials are fine grained and water saturated (although this is not always the case, as shown by the poor test results in the Sumas valley), whereas poorer data are obtained on upland areas or in dry, coarse-grained surface materials. A field test is the only way to evaluate data quality at a particular site. The data quality ultimately determines the attainable subsurface resolution.

The seismic profiles gathered as part of this study have delineated subsurface structure from depths of 30 to 500 m, through the Quaternary sequence and into Tertiary bedrock. It has been shown that, with careful data acquisition, subsurface resolution on the order of 1 m can be obtained in areas of good data. Infilled channels, erosional surfaces, bedrock topography, and complex stratigraphic sequences have all been delineated in the profiles presented here. Although detailed geological interpretation of the results is hampered by a lack of deep borehole information, an attempt has been made to suggest possible interpretations based on the information available. The variation in subsurface structure and stratigraphy shown by these results makes it clear that any evaluation of deep groundwater resources in the area will be a difficult task; however, the seismic data do provide a reasonable basis for predicting new aquifers and groundwater resources. In areas where good quality data can be obtained, seismic-reflection profiles provide critical information for building two- or three-dimensional hydrostratigraphic models.

ACKNOWLEDGMENTS

The GSC and SFU work reported in this paper was funded through the Fraser Lowland Hydrogeology Project of the Geological Survey of Canada. Thanks are due to Brian Ricketts for encouraging and supporting this work. Geophysical Applications Processing Services Ltd. of Guelph, Ontario carried out most of the processing of these data. University of British Columbia's data were collected and processed under a Natural Sciences and Engineering Research Council of Canada (NSERC) collaborative grant to R.J. Knight, Department of Earth and Ocean Sciences, University of British Columbia. The data were acquired with the help of several dedicated field crews who worked long, hard hours in ditches; thanks are due to Eric Gilson, Deirdre O'Leary, and Jamie Rosen, who made up the GSC crew in 1994; Harry Jol and Ev Roberts, who worked on the SFU crew over several seasons; and Gwenn Flowers, Andrew Gorman, Kevin Kingdon, Wendi Milner, Sean Rastead, Jane Rea, Paulette Tercier, and Dan Woznow, who all contributed to UBC's field program.

REFERENCES

Armstrong, J.E.
1980: Surficial geology, Mission, British Columbia; Geological Survey of Canada, Map 1485A, scale 1:50 000.
1984: Environmental and engineering application of the surficial geology of the Fraser Lowland, British Columbia; Geological Survey of Canada, Paper 83-23, 54 p.

Armstrong, J.E and Clague, J.J.
1977: Two major Wisconsin lithostratigraphic units in southwest British Columbia; Canadian Journal of Earth Sciences, v. 14, p. 1471–1480.

Armstrong, J.E. and Hicock, S.R.
1980: Surficial geology, New Westminster, British Columbia; Geological Survey of Canada, Map 1484A, scale 1:50 000.

Best, M.E. and Todd, B.J.
2000: Electromagnetic mapping of groundwater aquifers in the Fraser lowland; *in* Mapping, Geophysics, and Groundwater Modelling in Aquifer Delineation, Fraser Lowland and Delta, British Columbia, (ed.) B.D. Ricketts; Geological Survey of Canada, Bulletin 552.

Best, M.E., Todd, B.J., and O'Leary, D.
1995: Ground water mapping using time-domain electromagnetics: examples from the Fraser Valley, B.C.; *in* Current Research 1995-A; Geological Survey of Canada, p. 19–27.

Campanella, D., Davies, M., Boyd, T., Everard, J., Roy, D., Tomlinson, S., Jackson, S., Schrempp, H., and Ricketts, B.D.
1994: In-situ testing for the characterization of aquifers: demonstration project; Geological Survey of Canada, Open File 2940, 19 p.

Clague, J.J.
1994: Quaternary stratigraphy and history of south-coastal British Columbia; *in* Geology and Geological Hazards of the Vancouver Region, Southwestern British Columbia, (ed.) J.W.H. Monger; Geological Survey of Canada, Bulletin 481, p. 181–192.

Dunn, D. and Ricketts, B.D.
1994: Surficial geology of Fraser Lowlands digitized from GSC Maps 1484A, 1485A, 1486A, and 1487A (92G/1, /2, /3, /6, /7, and 92H/4); Geological Survey of Canada, Open File 2894 (3.5-inch diskette).

Halstead, E.C.
1986: Ground water supply – Fraser Lowland, British Columbia; Environment Canada, Inland Waters Directorate, National Hydrology Research Institute, Paper no. 26, Scientific Series no. 145, 80 p.

Hamilton, T.S. and Ricketts, B.D.
1994: Contour map of the sub-Quaternary bedrock surface, Strait of Georgia and Fraser Lowland; *in* Geology and Geological Hazards of the Vancouver Region, Southwestern British Columbia, (ed.) J.W.H. Monger; Geological Survey of Canada, Bulletin 481, p. 193–196.

Makepeace, A.J. and Ricketts, B.D.
2000: Aquifer mapping and database management using a geographic information system, Fraser lowland; *in* Mapping, Geophysics, and Groundwater Modelling in Aquifer Delineation, Fraser Lowland and Delta, British Columbia, (ed.) B.D. Ricketts; Geological Survey of Canada, Bulletin 552.

Miller, R.D., Anderson, N.L., Feldman, H.R., and Franseen, E.K.
1995: Vertical resolution of a seismic survey in stratigraphic sequences less that 100 m deep in southeastern Kansas; Geophysics, v. 60, p. 423–430.

Mustard, P.S. and Rouse, G.E.
1994: Stratigraphy and evolution of Tertiary Georgia Basin and subjacent Upper Cretaceous sedimentary rocks, southwestern British Columbia and northwestern Washington State; *in* Geology and Geological Hazards of the Vancouver Region, Southwestern British Columbia, (ed.) J.W.H. Monger; Geological Survey of Canada, Bulletin 481, p. 97–169.

Pullan, S.E. and Hunter, J.A.
1990: Delineation of buried bedrock valleys using the optimum offset shallow seismic reflection technique; in Geotechnical and Environmental Geophysics, Vol. III – Geotechnical, (ed.) S.H. Ward; Society of Exploration Geophysicists, Tulsa, Oklahoma, p. 75–87.

Pullan, S.E. and MacAulay, H.A.
1987: An in-hole shotgun source for engineering seismic surveys; Geophysics, v. 52, p. 985–996.

Pullan, S.E., Good, R.L., and Ricketts, B.D.
1995: Preliminary results from a shallow seismic reflection survey, Lower Fraser Valley Hydrogeology Project, British Columbia; *in* Current Research 1995-A; Geological Survey of Canada, p. 11–18.

Pullan, S.E., Miller, R.D., Hunter, J.A., and Steeples, D.W.
1991: Shallow seismic reflection surveys – CDP or "optimum offset"?; *in* Expanded Abstracts, 61st International Meeting of the Society of Exploration Geophysicists, November 10–14, 1991, Houston, Texas, v. 1, p. 576–579.

Pullan, S.E., Pugin, A., Dyke, L.D., Hunter, J.A., Pilon, J.A., Todd, B.J., Allen, V.S., and Barnett, P.J.
1994: Shallow geophysics in a hydrogeological investigation of the Oak Ridges Moraine, Ontario; *in* SAGEEP '94, Proceedings of the Symposium on the Application of Geophysics to Engineering and Environmental Problems, March 27–31, 1994, Boston, Massachusetts, v. 1, p. 143–161.

Rea, J.M. and Knight, R.J.
2000: Characterization of the Brookswood aquifer using ground-penetrating radar; *in* Mapping, Geophysics, and Groundwater Modelling in Aquifer Delineation, Fraser Lowland and Delta, British Columbia, (ed.) B.D. Ricketts; Geological Survey of Canada, Bulletin 552.

Rea, J.M., Knight, R.J., and Ricketts, B.D.
1994: Ground-penetrating radar survey of the Brookswood aquifer, Fraser Valley, British Columbia; *in* Current Research 1994-A; Geological Survey of Canada, p. 211–216.

Ricketts, B.D.
1995: Progress report and field activities of the Fraser Valley Hydrogeology Project, British Columbia; *in* Current Research 1995-A; Geological Survey of Canada, p. 1–5.
2000: Overview of the Fraser Lowland Hydrogeology Project; *in* Mapping, Geophysics, and Groundwater Modelling in Aquifer Delineation, Fraser Lowland and Delta, British Columbia, (ed.) B.D. Ricketts; Geological Survey of Canada, Bulletin 552.

Ricketts, B.D. and Dunn, D.
1995: The groundwater database, Fraser Valley, British Columbia; *in* Current Research 1995-A; Geological Survey of Canada, p. 7–10.

Ricketts, B.D. and Jackson, L.E., Jr.
1994: An overview of the Vancouver–Fraser Valley Hydrogeology Project, southern British Columbia; *in* Current Research 1994-A; Geological Survey of Canada, p. 201–206.

Ricketts, B.D. and Makepeace, A.J. (ed.)
2000: Aquifer delineation, Fraser lowland and delta, British Columbia: mapping, geophysics and groundwater modelling; Geological Survey of Canada, Open File D3828.

Roberts, M.C., Vanderburgh, S., and Jol, H.
2000: Radar facies and geomorphology of the seepage face of the Brookswood aquifer, Fraser lowland; *in* Mapping, Geophysics, and Groundwater Modelling in Aquifer Delineation, Fraser Lowland and Delta, British Columbia, (ed.) B.D. Ricketts; Geological Survey of Canada, Bulletin 552.

Schieck, D.G. and Pullan, S.E.
1995: Processing a shallow seismic CDP survey: an example from the Oak Ridges Moraine, Ontario, Canada; in SAGEEP '95, Proceedings of the Symposium on the Application of Geophysics to Engineering and Environmental Problems, April 23–26, 1995, Orlando, Florida, p. 609–618.

Sharpe, D.R., Dyke, L.D., Hinton, M.J., Pullan, S.E., Russell, H.A.J., Brennand, T.A., Barnett, P.J., and Pugin, A.
1996: Groundwater prospects in the Oak Ridges Moraine area, southern Ontario: application of regional geological models; *in* Current Research 1996-E; Geological Survey of Canada, p. 181–190.

Steeples, D.W. and Miller, R.D.
1990: Seismic reflection methods applied to engineering, environmental, and groundwater problems; *in* Geotechnical and Environmental Geophysics: Volume 1 – Review and Tutorial, (ed.) S.H. Ward; Society of Exploration Geophysicists, Tulsa, Oklahoma, p. 1–30.

Woodsworth, G.J. and Ricketts, B.D.
1994: A digital database for groundwater data, Fraser Valley, British Columbia; *in* Current Research 1994-A; Geological Survey of Canada, p. 207–210.

Characterization of the Brookswood aquifer using ground-penetrating radar

Jane M. Rea[1] and Rosemary J. Knight[1]

Rea, J.M. and Knight, R.J., 2000: Characterization of the Brookswood aquifer using ground-penetrating radar; in *Mapping, Geophysics, and Groundwater Modelling in Aquifer Delineation, Fraser Lowland and Delta, British Columbia, (ed.) B.D. Ricketts; Geological Survey of Canada, Bulletin 552, p. 75–93.*

Abstract: Ground-penetrating radar has been used to characterize a shallow, unconfined aquifer in southwestern British Columbia. Traditional methods of aquifer characterization rely on data provided by borehole logs, pumping tests, and slug tests; however, these data are insufficient to fully characterize the heterogeneity in an aquifer. This paper presents the application of a technique that uses ground-penetrating radar to augment borehole data and provide broader spatial information for use in groundwater modelling.

A total of 12 km of 100 MHz radar data was collected over the Brookswood aquifer in southwestern British Columbia. Using the data, large-scale hydraulic features such as the aquifer-aquitard boundary and the water table have been identified. The sedimentological concept of architectural element analysis has been drawn upon to subdivide the aquifer into sedimentary units that can be used as the basic building blocks in a groundwater model.

Résumé : On a utilisé le géoradar pour caractériser un aquifère libre peu profond dans le sud-ouest de la Colombie-Britannique. Les méthodes classiques de caractérisation des aquifères utilisent des données tirées des rapports de forage, des essais de pompage et des essais de puits, toutefois, les données ainsi obtenues ne caractérisent pas complètement l'hétérogénéité d'un aquifère. Cet article présente l'application d'une technique qui utilise le géoradar pour compléter les données de forages et qui fournit davantage d'information spatiale à utiliser en modélisation des eaux souterraines.

On a recueilli au géoradar à 100 MHz des données sur une distance totale de 12 km sur l'aquifère de Brookswood dans le sud-ouest de la Colombie-Britannique. En utilisant les données recueillies, on a reconnu des entités hydrauliques à grande échelle comme l'interface aquifère–aquitard et la nappe phréatique. On a utilisé le concept sédimentologique de l'analyse des éléments architecturaux pour subdiviser l'aquifère en unités stratigraphiques qui peuvent être utilisées comme éléments de base en vue de l'élaboration d'un modèle des eaux souterraines.

[1] Department of Earth and Ocean Sciences, University of British Columbia, 2219 Main Mall, Vancouver, British Columbia V6T 1Z4

INTRODUCTION

The Geological Survey of Canada (GSC) has undertaken an extensive study to characterize and delineate the hydrogeology of the Fraser lowland of southwestern British Columbia (Fig. 1). The motivation is to provide a better understanding of the regional hydrogeology, in order to protect existing groundwater resources and explore for and exploit new resources. One of the main concerns in the Fraser lowland is the delineation of potential contaminant flow paths; this is of critical importance in the prevention and remediation of groundwater contamination.

In a previous hydrogeological investigation, the Fraser lowland was divided into hydrostratigraphic units, defined on the basis of lithology, permeability, and porosity data obtained from drilling records (Halstead, 1986). The resulting interpretations were presented in the form of fence diagrams, which are useful for delineating large-scale variations in hydrogeological properties; however, this gross structure may not be sufficient to fully characterize the region, particularly when attempting to understand and model contaminant transport. This requires knowledge of the finer scale structure and spatial heterogeneity of hydrogeological properties.

To improve upon the large-scale hydrogeological model and to fully characterize the heterogeneity of the region, further information about the spatial variability of hydrogeological properties, such as hydraulic conductivity, must be obtained. Traditional methods for obtaining data, such as pumping tests and slug tests, provide direct measurements of hydraulic conductivity but are expensive and sample only a very small fraction of the total aquifer volume. Therefore, they are inadequate for characterizing a heterogeneous system. Additional data may be acquired using geophysical techniques, which do not measure hydrogeological properties directly but provide important insights into the value and spatial distribution of these properties.

As part of the aquifer delineation study, the GSC initiated a series of investigations into the use of geophysics to extract information about the hydrogeology of the Fraser lowland, including cone penetrometry (Campanella et al., 1994), seismic reflection (Pullan et al., 1995), time-domain electromagnetic techniques (Best et al., 1994), and ground-penetrating radar (Rea et al., 1994; Roberts et al., 2000). The scale, depth, and type of information obtained from these geophysical techniques vary considerably. The time-domain electromagnetic (TDEM) and seismic techniques are capable of investigating to depths of several hundred metres, but differ in resolution, with the TDEM method resolving to depths of 200 m and the shallow seismic technique to depths of 1 km. In addition, the seismic technique maps variations in elastic wave properties, whereas the TDEM technique maps changes in electrical conductivity. The cone penetrometry (CPT) and ground-penetrating radar (GPR) surveys provide data of much higher resolution, but are normally used when information is required for lesser depths. In the case of the CPT surveys, the maximum depth of penetration in the study area was about 32 m and vertical resolution was between 2.5 and 75 cm, depending upon the cone tool being used. The GPR surveys had a depth of penetration of up to 30 m and a resolution of roughly 0.3 m. The CPT tool measures a variety of properties, including electrical resistivity, point resistance, and friction. The GPR technique, on the other hand, maps changes in electrical properties (dielectric permittivity and electrical conductivity).

The focus of this paper is the interpretation and assessment of GPR data for improving the hydrogeological characterization of the near surface. Accurate, high-resolution characterization is required, given the concern about potential contamination in the Fraser lowland. Ground-penetrating radar can provide this information because it is a high-resolution technique capable of obtaining images of the subsurface rapidly and inexpensively. The goal of this study was to determine if and how GPR could be used to extend the large-scale hydrogeological interpretation presented in the

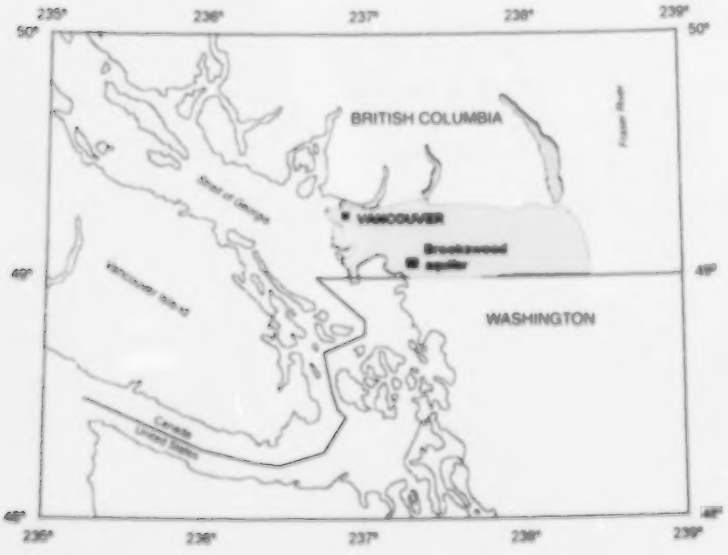

Figure 1.

Location of the Brookswood aquifer in the Fraser lowland (shaded area) of southwestern British Columbia.

hydrostratigraphic fence diagrams of Halstead (1986). The present analysis focused on assessing the ability of GPR to map the important hydraulic boundaries needed to model groundwater flow. These include the aquifer-aquitard boundary, the top of the saturated zone, and internal boundaries marking changes in hydraulic properties. To do this, hydrogeological units were identified in the subsurface. A hydrogeological unit is defined as a package of sediments that can be considered homogeneous with respect to its hydraulic properties. Hydraulic boundaries are therefore defined as the interfaces between hydrogeological units.

The GPR data for this paper were collected in two field studies over the Brookswood aquifer, a shallow, unconfined aquifer that covers an area of approximately 50 km^2 in the Fraser lowland (Fig. 1; Ricketts and Liebscher, 1994). The first involved a 12 km reconnaissance survey in which the hydrogeological structure, including aquifer-aquitard boundaries and internal sedimentary structures, was investigated (Rea et al., 1994; Rea, 1996). The second study was designed to identify and map the top of the saturated zone.

Interpretation of ground-penetrating radar data

A ground-penetrating radar (GPR) survey is conducted by transmitting electromagnetic waves into the subsurface and recording the reflected energy. The transmitted electromagnetic waves are affected by changes in the subsurface dielectric constant and electrical conductivity. Changes in dielectric constant cause electromagnetic energy to be reflected back to the surface. The electrical conductivity of the subsurface causes attenuation of the electromagnetic waves. The result of a radar survey is therefore an image of the subsurface, with reflectors marking changes in dielectric constant and the depth of penetration providing information about the electrical conductivity.

An image of changes in electrical properties, such as that produced in a GPR survey, is not itself useful for groundwater modelling. Changes in electrical properties are, however, related to changes in both sedimentary and hydraulic parameters, which can be used to identify the saturated zone boundary and hydrogeological units. In order to identify the hydrogeological units in GPR data, it is necessary to assess the ability of the technique to outline hydraulic and sedimentary boundaries in the subsurface. This involves establishing relationships between sedimentary and hydraulic parameters, and the parameters recorded in GPR data. The usefulness of determining sedimentary parameters is based on the assumption that a sedimentary unit will be composed of grains with similar size, packing, and orientation. Since these parameters are related to hydraulic properties, it is reasonable to assume that each sedimentary unit will possess characteristic hydraulic properties, and therefore can serve as a useful, large-scale building block for the hydrogeological model. Hydraulic properties, although assumed to be the same throughout a given unit, may be anisotropic due to bedding structure and grain orientation within the unit.

Recent studies have improved the methods of interpreting radar data in sedimentological terms (Jol and Smith, 1992; Stephens, 1994; Olsen and Andreasen, 1995). Identification of sedimentary features in radar data is predicated on establishing a relationship between sedimentary properties and electrical properties. For this purpose, it is useful to recognize that sedimentary classification is based on five fundamental properties of the sedimentary material: grain composition, grain size, grain shape, grain orientation, and grain packing. Electrical properties are determined by the composition and geometry of the solid and liquid components of the earth materials. As the composition and geometry of the solid component are clearly related to the five sedimentary properties, it is reasonable to assume that a change in sedimentary properties will correspond to a change in electrical properties, and thus will be observed in the GPR data. A change in sedimentary properties may be manifested in the radar data as 1) a reflection if the sedimentary change corresponds to a change in dielectric constant, or 2) an attenuation of the signal if the sedimentary change corresponds to a change in electrical conductivity. In describing the link between electrical properties and sedimentary properties, we have ignored any effects of changes in fluid composition. Whereas fluid chemistry would have little direct effect on the dielectric constant, increases in fluid salinity will give rise to greater attenuation of the GPR signal (due to increased electrical conductivity). Thus, changes in salinity can affect the appearance of the GPR profile in terms of the penetration depth and the amplitude of the reflectors.

A second relationship used in interpreting radar data for hydrogeological modelling is the link between electrical conductivity and hydraulic conductivity. In freshwater environments, an increase in clay content increases the electrical conductivity of the material and concomitantly decreases the hydraulic conductivity. Electrical conductivity increases the attenuation of the radar signal and can therefore serve as a good indicator of the hydraulic properties of the material being imaged.

The relationships between electrical parameters and sedimentary and hydraulic parameters provide the basic tools for our interpretation of the Brookswood data set; however, a framework in which to interpret GPR data is needed if the data are to be used in aquifer characterization. The framework adopted here is based on the identification of radar architectural elements (AEs) in the subsurface (Stephens, 1994). Radar AEs are similar to sedimentary AEs, a concept introduced by Miall (1985). A sedimentary AE is a two- or three-dimensional sedimentary package described by its bounding characteristics, external geometry, scale, and internal characteristics. In a similar manner, a radar AE is defined as a two- or three-dimensional package of radar reflections described by its bounding characteristics, external geometry, scale, and reflection characteristics. It is suggested here that radar AEs can be used as hydrogeological units for the purpose of groundwater modelling.

As part of the interpretation of the Brookswood data set, the radar AEs were related to sedimentary units using drill and outcrop data to provide lithological information. The sedimentary information can be used to determine the depositional environment, thereby providing insight into the spatial distribution and expected occurrence of hydrogeological features. In addition, it has been suggested that

sedimentary units possess characteristic hydraulic properties and anisotropies, and so can serve as useful large-scale building blocks for the hydraulic model (Anderson, 1989).

The one boundary which is not included in the above classification scheme is the top of the saturated zone (TSZ). The TSZ should create a strong reflection in the radar survey due to the large contrast between the dielectric constant of water (80) and those of other earth materials (4 to 15). The water table is differentiated from the top of the saturated zone because, in finer grained materials, a capillary fringe may occur above the water table in which the sediments are fully saturated. Therefore, there may be no difference in dielectric constant at the water table itself, only at the TSZ. In practice, the difference between the TSZ and the water table in coarse-grained aquifer sediments is small enough that it will not be discernible in a radar survey.

A strong horizontal reflector in a radar survey is often interpreted as the TSZ; however, this rule of thumb does not always work. For example, in areas of poorly drained soil, the capillary fringe created above the water table may be so diffuse as to create a gradual change in dielectric constant. In this case, the TSZ will be indistinct and no reflection will occur. Further misinterpretation arises in areas where the stratigraphy is horizontal. Two sedimentary units with markedly contrasting dielectric constants can cause a strong reflection which may be incorrectly interpreted as the TSZ. This issue was investigated by considering the processing techniques that can be particularly useful in enhancing radar reflections.

GEOLOGY OF THE BROOKSWOOD AQUIFER

The Brookswood aquifer is a shallow, unconfined aquifer in the Fraser lowland area of southwestern British Columbia, and is composed of sand and gravel from a large fan-type delta deposited between 11 500 and 11 000 BP. Five hydrostratigraphic units occur in and around the Brookswood aquifer (Halstead, 1986). The sediments of the Brookswood aquifer itself are classified as hydrostratigraphic unit C. Unit C is described as glaciofluvial and deltaic sand and gravel, locally covered by clay (Halstead, 1986; summarized *in* Ricketts, 2000b, Table 1). The Brookswood aquifer is underlain by marine sediments interbedded with estuarine and fluvial deposits (unit E). The aquitards surrounding the Brookswood are classified as unit A (clay, stony clay, and silty clay), glaciomarine stony clay of unit B, and a small area of unit D (till and diamicton) on the eastern boundary. Details of the stratigraphy in profiles and boreholes through the Brookswood aquifer are illustrated in Makepeace and Ricketts (2000).

RECOGNIZING HYDROGEOLOGICAL UNITS IN THE BROOKSWOOD DATA SET

Data acquisition

Radar data were collected using a PulseEKKO IV™ ground-penetrating radar unit with 100 MHz antennas. This system, shown in Figure 2, consists of a transmitter, receiver, control box, and power sources connected by fibre-optic cables. Acquisition is controlled using a laptop computer, which allows the data to be displayed as collected. Most radar lines were collected along the shoulders of roads and in a gravel pit. Common-midpoint (CMP) surveys were undertaken to determine the velocity of the radar waves, allowing conversion of time sections to depth sections. In all sections, a constant velocity is assumed for the entire GPR profile.

Data processing

Careful processing of radar data is needed for use in aquifer characterization. The main goal during processing is to ensure that important hydrogeological features, such as the top of the saturated zone, are clearly imaged. In addition, care must be taken to ensure that changes in the texture of the reflections, which indicate changes in a sedimentary unit, are not removed during processing. Data were processed using PulseEKKO Tools™ and a seismic-processing package called ITA Insight™ (Inverse Theory and Application).

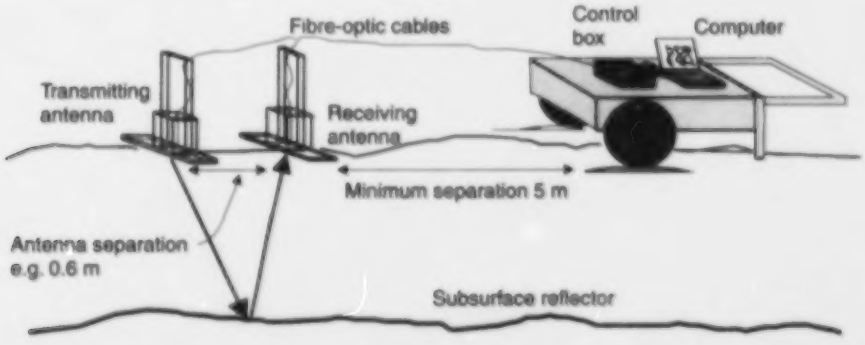

Figure 2. *Schematic diagram of the PulseEKKO IV™ ground-penetrating radar unit.*

The basic processing steps included a correction for time-zero drift and a 'dewow' process to correct for signal saturation. If necessary, an elevation correction was applied to adjust for topographic variations. Point scattering, for example by boulders, creates hyperbolic reflections (diffraction hyperbolas) in the data. A process called migration can, in some cases, prove beneficial for collapsing these diffractions; however, the diffractions themselves can provide information about the texture of the sediments being imaged. Migration can mute characteristic reflection patterns and so should be used with care; it was not used in this study.

The final step in processing radar data was applying a gain to the data. The two most useful types of gain for processing of GPR data are automatic gain control (AGC), and spreading and exponential compensation (SEC). Automatic gain control amplifies all reflectors so that they have equal strength. This gain function is useful for providing a clear image of all reflections to determine the overall structure and trend. Spreading and exponential compensation accounts for spherical spreading and attenuation from the electrical conductivity of the sediments being imaged. Relative amplitudes are preserved when applying this gain function. The type of gain applied to the data will be explained in the section dealing with each survey.

Interpretation of radar data as hydrogeological units

The technique of radar architectural element (AE) analysis was used to divide the subsurface into hydrogeological units. The following four radar AEs were identified in the Brookswood GPR data set:

1. **Steeply dipping reflectors** – a package of reflectors dipping at an angle greater than 10°;

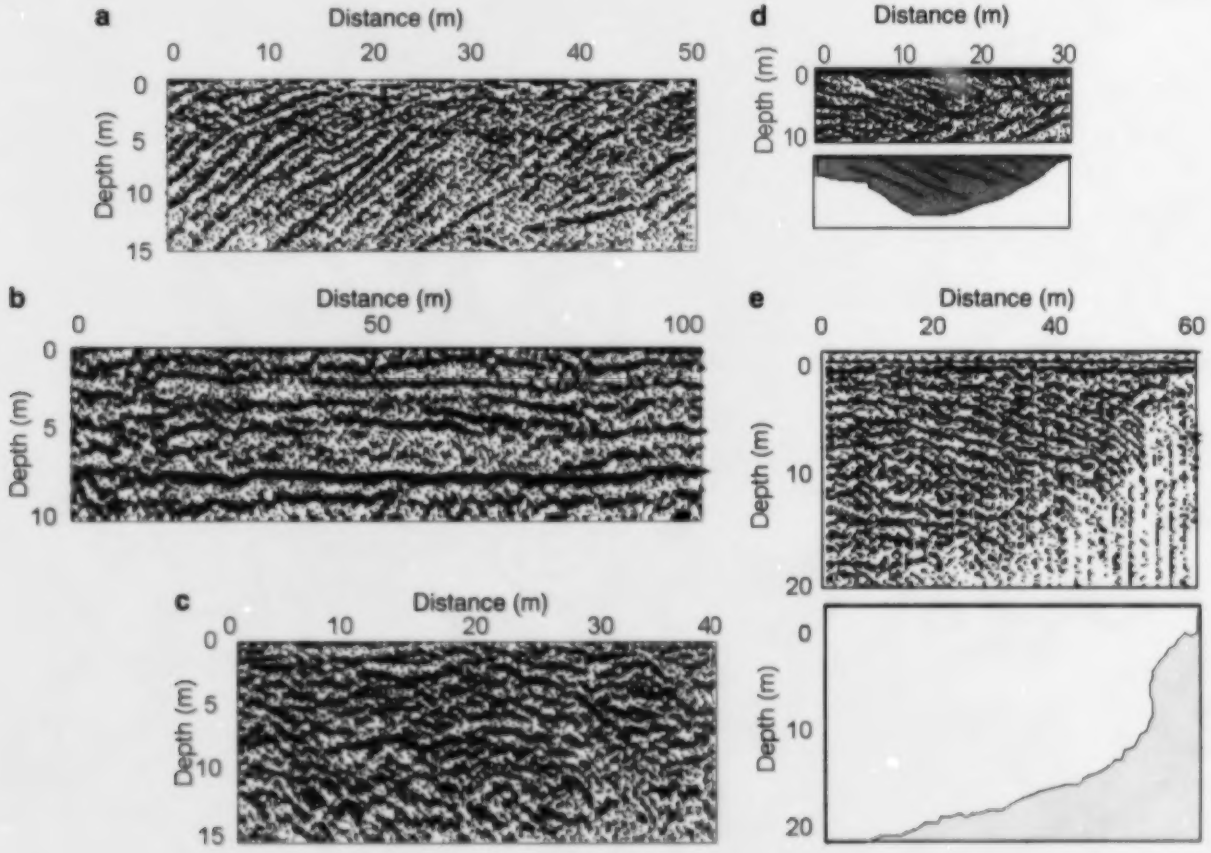

Figure 3. *Examples of radar architectural elements from the Brookswood data set.*

a) *dipping element (element 1);*

b) *horizontal element (element 2) with long reflectors;*

c) *horizontal element (element 2) with short reflectors;*

d) *channel element (element 3) with interpretive diagram (shading indicates location of element 3);*

e) *attenuation element (element 4) with interpretive diagram (shading indicates location of element 4).*

2. **Horizontal reflectors** – a package of reflectors which are horizontal or slightly dipping; the reflectors can have a range of lengths;

3. **Channel-shaped structures** – a distinct channel-shaped reflector which bounds a group of internal reflections; the internal reflections are commonly shallow dipping and onlap the channel boundary reflector; and

4. **Zones of attenuation** – regions in the data where there are few or no reflectors due to lack of signal penetration.

For the sake of brevity, these elements will be referred to by the above numbers throughout the discussion that follows.

Figure 3a shows a dipping element (element 1) that is interpreted as foreset beds. Two examples of element 2, in Figure 3b and c, show the variation in length of reflectors in this element. Figure 3d shows an example of the channel element (element 3), consisting of a bounding reflection with internal reflections dipping to the right. The first three elements have low attenuation and have been shown in a previous study to occur in regions composed of sand and gravel. They are therefore considered to be aquifer units. Element 4 (Fig. 3e) has a much higher attenuation and is inferred to have lower hydraulic conductivities than the first three. This element is therefore considered to be an aquitard unit. The alternative interpretation, that attenuation is due to saline groundwater, was discounted because only fresh water is encountered in the Brookswood aquifer (e.g. Halstead, 1986).

The Brookswood data set is discussed in three parts, each of which exhibits a different overall character. The first is an area in the southwestern portion of the aquifer, in and around Stoke's gravel pit (Fig. 4). There are four radar sections in this area: lines N, S, W, and E, located in the north, south, west, and east sectors of the pit. In addition, a three-dimensional (3-D) radar data set was collected. The second part of the Brookswood data set is a north-south line running almost the full length of the aquifer along 192nd Street. The third part consists of isolated radar sections from the eastern part of the aquifer, close to or at the aquifer boundary. These are located along 208th Street, 20th Avenue, and 24th Avenue (Fig. 4). The municipalities of Langley and Brookswood lie over the northeast quadrant of the aquifer. Radar data were not collected in this area due to cultural noise, which makes GPR data acquisition and interpretation difficult.

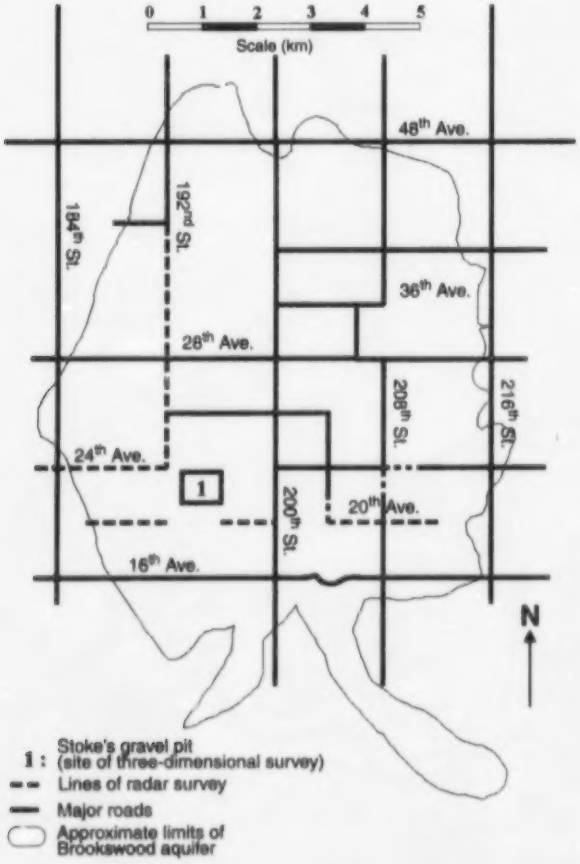

Figure 4. Locations of radar sections conducted over the Brookswood aquifer.

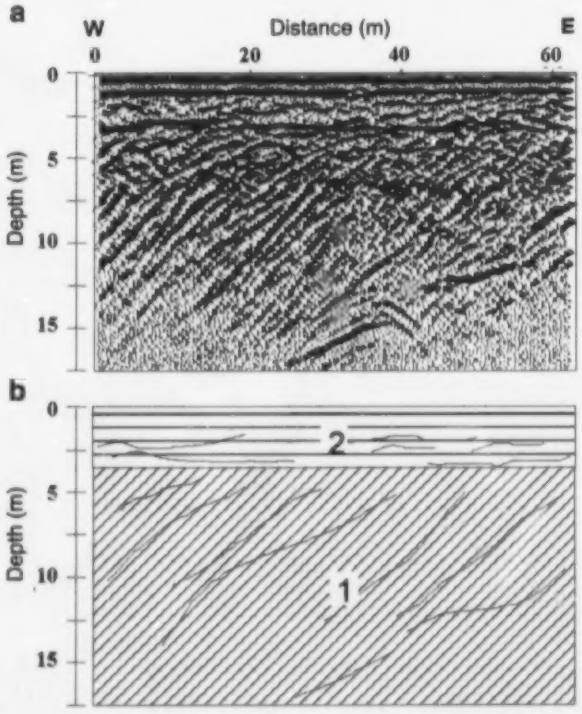

Figure 5. Ground-penetrating radar survey along line N, Stoke's gravel pit: a) radar section; b) interpretation showing radar architectural elements: 1, steeply dipping reflectors; 2, horizontal reflectors (see text for explanation).

Stoke's gravel pit

Stoke's municipal gravel pit in Surrey has been active for 40 years, with the top 6 m having been excavated. The most striking features in the Stoke's pit radar data are the prominent dipping reflectors (element 1), which appear in all four radar lines. Line N, shown in Figure 5, contains a typical example of the dipping radar element in the vicinity of Stoke's pit. As with subsequent figures, this consists of a radar section (Fig. 5a) and an interpretive schematic (Fig. 5b). On this line, the dipping reflectors are clearly visible from a depth of 3 to 15 m. Overlying these reflectors are long, horizontal reflectors of element 2.

Other examples of long, dipping reflectors are seen in line S (Fig. 6).The dipping reflectors (element 1) are the most prominent feature and occur at two locations along the survey

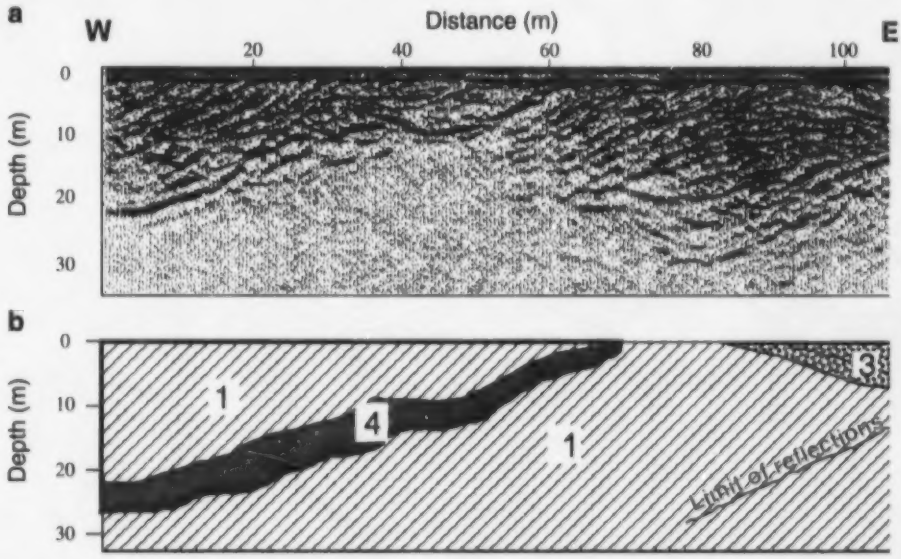

Figure 6. *Ground-penetrating radar survey along line S, Stoke's gravel pit:* ***a)*** *radar section;* ***b)*** *interpretation showing radar architectural elements: 1, steeply dipping reflectors; 3, channel-shaped structure; 4, zone of attenuation* (see *text for explanation).*

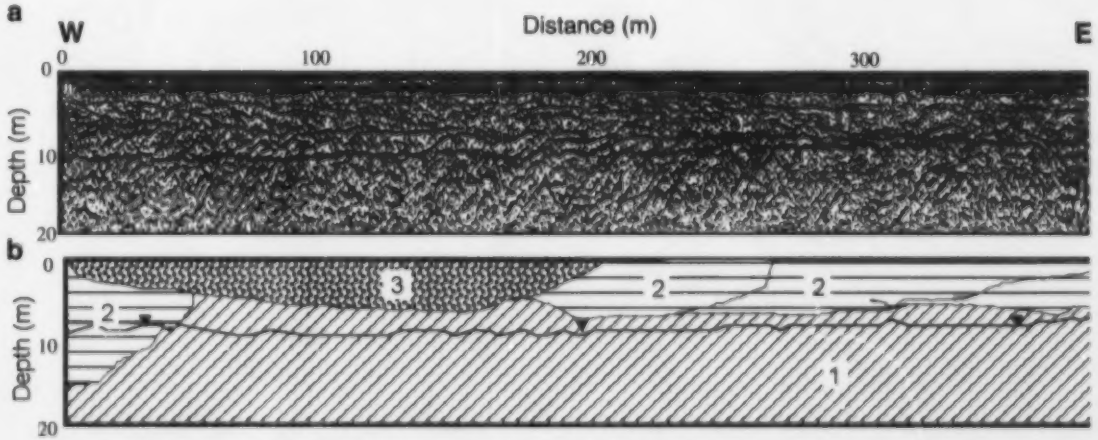

Figure 7. *Ground-penetrating radar survey along line E, located east of Stoke's gravel pit along 20th Avenue between 196th and 200th streets:* ***a)*** *radar section;* ***b)*** *interpretation showing radar architectural elements: 1, steeply dipping reflectors; 2, horizontal reflectors; 3, channel-shaped structure; solid line with inverted triangle ornamentation is the interpreted top of the saturated zone* (see *text for explanation).*

line: between 0 and 60 m, and between 60 and 110 m. A channel element (element 3) and a zone of high attenuation (element 4) mark the boundaries of the dipping elements. The thickness of element 4 is unknown, since the attenuation obscures any underlying reflectors that may exist.

In line E (Fig. 7), element 1 is less distinct than in lines N and S due to lower signal power reaching the depth of 8 to 20 m at which these reflectors occur; this is likely due to increased clay content. Element 1 is overlain by elements 2 and 3. A horizontal reflector occurs at a depth of about 10 m and is interpreted as the TSZ.

Line W (Fig. 8) contains additional examples of the dipping element all along the survey line. Note the diffraction hyperbolas in this section, coinciding approximately with the outer edges of each element 4, which are probably due to the presence of coarse-grained gravel or small boulders. There is an example of element 4 in the top 3 m from 350 to 700 m. A

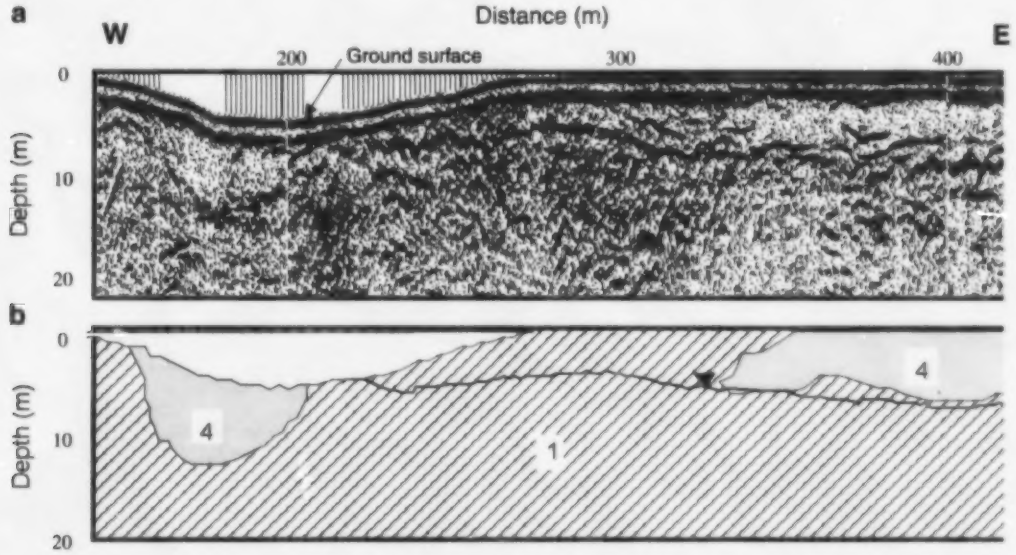

Figure 8. *Ground-penetrating radar survey along line W, located just west of Stoke's gravel pit along 20th Avenue: **a)** radar section; **b)** interpretation showing radar architectural elements: 1, steeply dipping reflectors; 4, zone of attenuation; solid line with inverted triangle ornamentation is the interpreted top of the saturated zone (see text for explanation).*

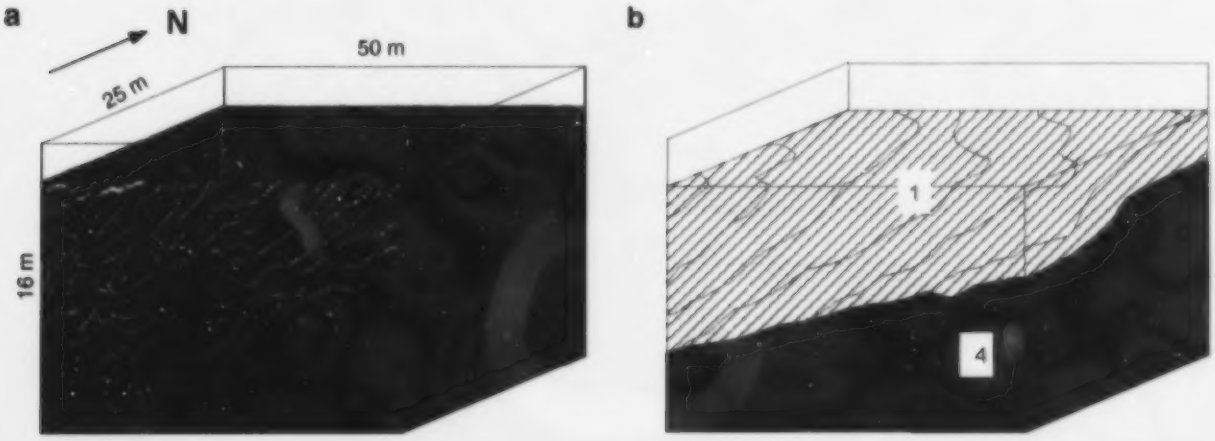

Figure 9. *Three-dimensional ground-penetrating radar survey of Stoke's gravel pit: **a)** radar data; **b)** interpretation showing radar architectural elements: 1, steeply dipping reflectors; 4, zone of attenuation (see text for explanation).*

channel-shaped region with no internal reflections occurs between 150 and 200 m; this has been classified as element 4 (zone of attenuation) rather than element 3 because the hydraulic conductivity of the zone corresponds to that of an aquitard rather than an aquifer. A strong, continuous reflector at a depth of about 6 m has been interpreted as the TSZ.

The true strike and dip of the dipping radar element was found by conducting a pseudo 3-D survey over the westernmost dipping radar element shown in line S. This data set was obtained by collecting a series of 50 parallel two-dimensional (2-D) lines, each 50 m long. The lines were spaced 0.5 m apart and station spacing along each line was also 0.5 m, so the resulting data set consists of 2500 radar traces in a 25 m by 50 m grid. The 3-D survey shown in Figure 9 contains two radar AEs: a zone of high attenuation (element 4) and steeply dipping reflectors (element 1). The strike of the dipping reflectors is to the northwest, and they dip to the west at about 25°.

Trenching and drilling in the area provided sedimentological data with which to calibrate the GPR data. A borehole near the east end of Stoke's gravel pit indicates that the top 3 m is a well compacted, medium-grained sand, underlain by coarse-grained sand and gravel. A trench close to the western end of the pit uncovered a 1 m thick layer of soft blue-grey clay, underlain by sand and gravel. The water table is about 1 m below the bottom of the pit.

North-south transect

The north-south transect was collected along 192nd Street, southwest of Langley, and represents an almost complete transect of the aquifer. The radar AEs observed along its length are horizontal reflectors (element 2), channels (element 3), and zones of attenuation (element 4). The northern half of the line consists mainly of attenuation zones interspersed with limited regions of the horizontal element. Figure 10 is a typical section from the northern part of the transect. Few reflectors can be seen in this section. The origin of the strong reflection at a depth of 5 m is unknown, although it may be the TSZ. Penetration improves toward the southern end of the line, where short and long horizontal elements and channel elements were found. An example of the response in the southern section of the 192nd Street transect is shown in Figure 11. Drill data along 192nd Street indicate that the

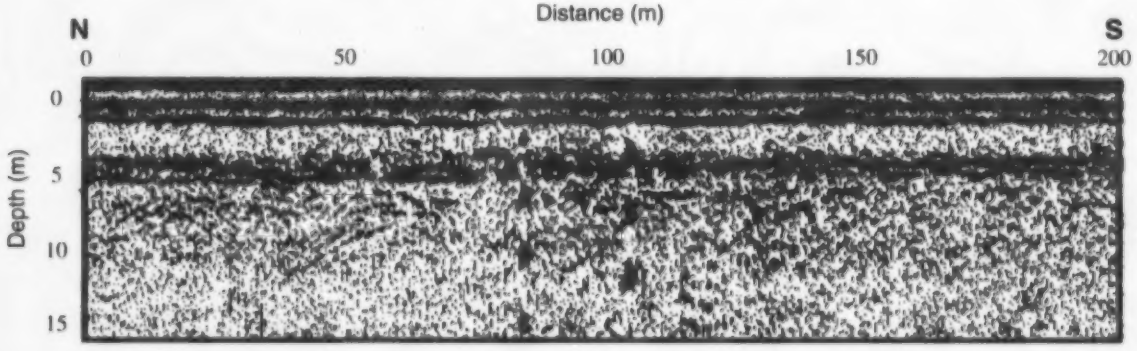

Figure 10. Typical ground-penetrating radar section from the northern part of the 192nd Street transect, just south of 40th Avenue.

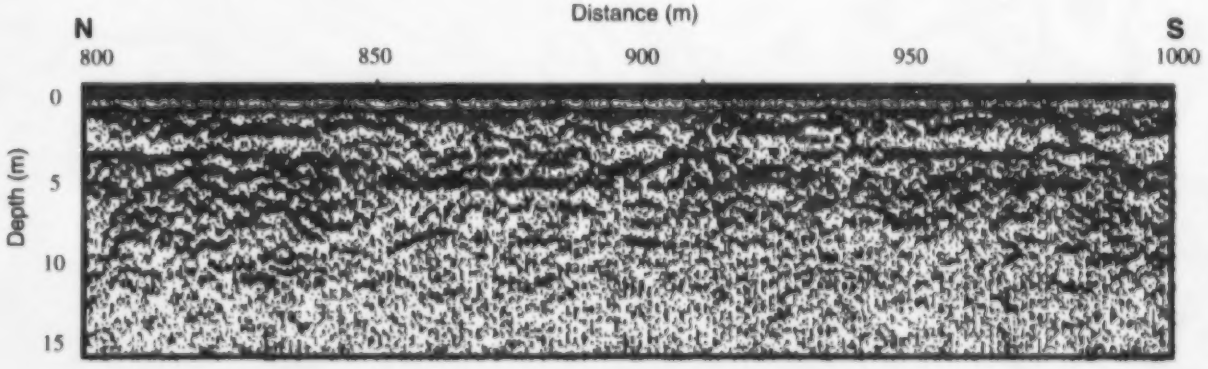

Figure 11. Typical ground-penetrating radar section from the southern part of the 192nd Street transect, just south of 24th Avenue.

sediments are predominantly sand and gravel, with isolated regions of silty sand and sand containing some clay; the aquifer here contains only fresh water.

Eastern Brookswood

Four radar lines were run over the southeastern part of the Brookswood aquifer, near the aquifer boundary. Line EW20208 extended east along 20th Avenue from its intersection with 204A Street; the first 300 m of this 600 m line are shown in Figure 12. Line SN24208 ran south along 208th Street from its intersection with 24th Avenue; this 400 m line is shown in Figure 13. Line EW24208 extended east along 24th Avenue from its intersection with 208th Street; the first 200 m of this 500 m line are shown in Figure 14. Line SN20204 ran north along 204A Street from its intersection with 20th Avenue; most of this 400 m line is shown in Figure 15.

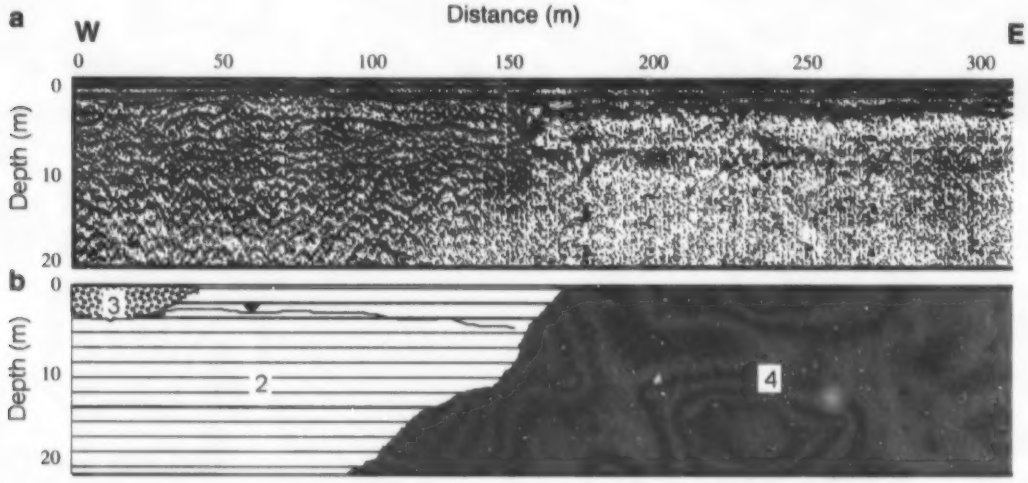

Figure 12. *Ground-penetrating radar survey along line EW20208, running east along 20th Avenue from its intersection with 204A Street:* ***a)*** *radar section;* ***b)*** *interpretation showing radar architectural elements: 2, horizontal reflectors; 3, channel-shaped structure; 4, zone of attenuation; solid line with inverted triangle ornamentation is the interpreted top of the saturated zone* (see *text for explanation).*

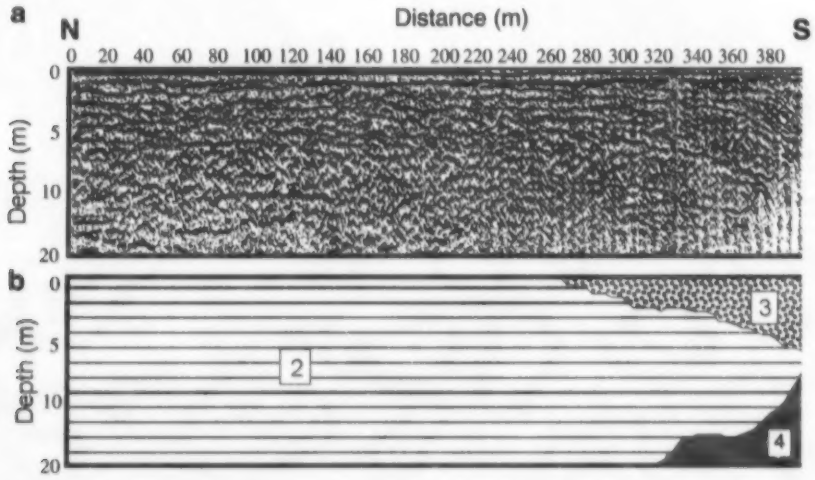

Figure 13. *Ground-penetrating radar survey along line SN24208, running south along 208th Street from its intersection with 24th Avenue:* ***a)*** *radar section;* ***b)*** *interpretation showing radar architectural elements: 2, horizontal reflectors; 3, channel-shaped structure; 4, zone of attenuation* (see *text for explanation).*

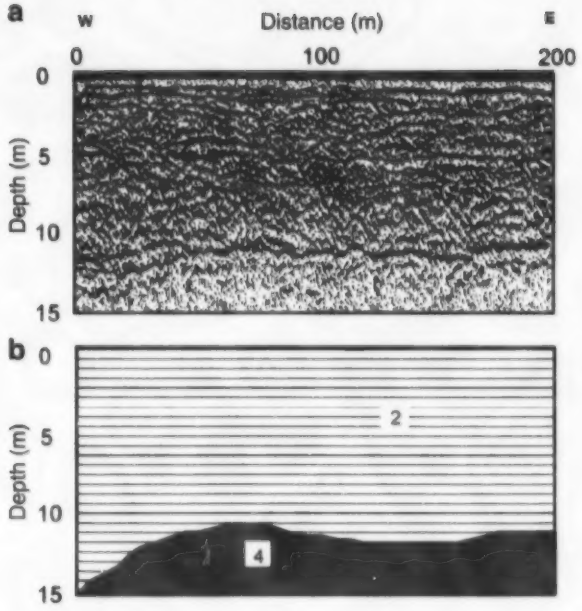

Figure 14. Ground-penetrating radar survey along line EW24208, running east along 24th Avenue from its intersection with 208th Street: a) radar section; b) interpretation showing radar architectural elements: 2, horizontal reflectors; 4, zone of attenuation (see text for explanation).

Some features of particular interest in this area include two striking examples of element 4, the high attenuation zone, in lines EW20208 (Fig. 12) and SN24208 (Fig. 13). In both cases the boundary between element 4 and the other elements is very distinct. Also present in these two sections are horizontal elements, of various lengths, and channel elements. A strong horizontal reflection at a depth of 3 to 5 m in line EW20208 is interpreted as the TSZ reflection.

Line EW24208 (Fig. 14) exhibits another interesting feature: a strong reflector at a depth of about 12 m, underlain by a zone of high attenuation. The upper portion of this section is composed predominantly of long horizontal reflectors, with some short horizontal reflectors.

The final survey line over the eastern Brookswood aquifer, SN20204 (Fig. 15), contains a large channel element between 200 and 250 m and several occurrences of elements 2 and 4. No evidence of the dipping reflectors can be seen.

Drill data along line EW20208 indicate that radar elements 2 and 3 are composed of sand and gravel, and element 4, the zone of attenuation, is composed of stony clay and till. Similar sediment types are indicated from borehole data along SN24208: elements 2 and 3 are described as sand and gravel, and element 4 corresponds to sticky grey clay and till. Drill data near line EW24208 indicate that elements 2 and 3 are composed of sand and gravel, and element 4 is composed of clay till.

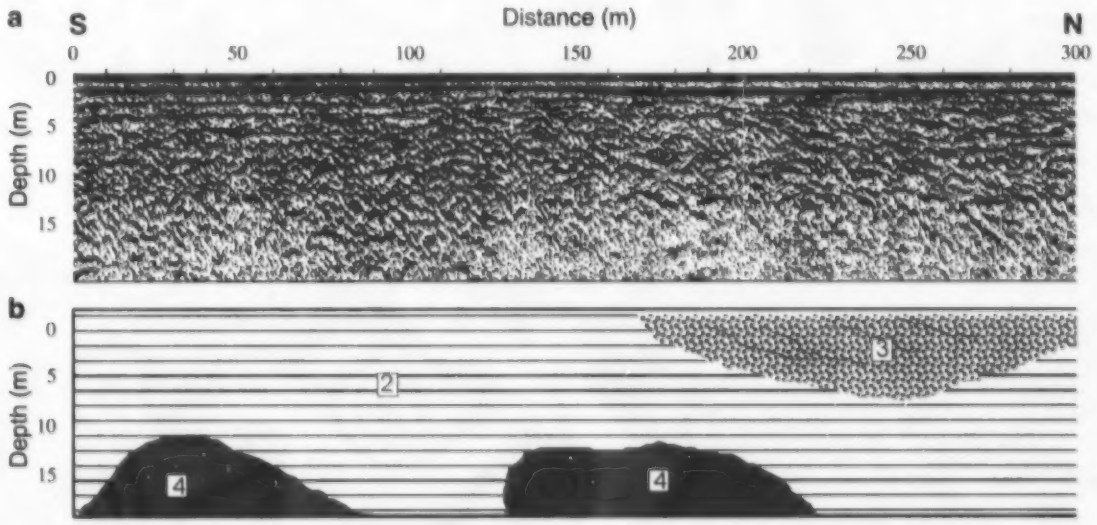

Figure 15. Ground-penetrating radar survey along line SN20204, running north along 204A Street from its intersection with 20th Avenue: a) radar section; b) interpretation showing radar architectural elements: 2, horizontal reflectors; 3, channel-shaped structure; 4, zone of attenuation (see text for explanation).

Sedimentary interpretation of radar data

Reconstruction of the paleodepositional environment can be of great use in developing predictive models for the spatial distribution of hydrogeological facies. In this section, the radar AEs are put to this use.

Stoke's gravel pit

The drilling and trenching data from Stoke's gravel pit suggest that the horizontal reflectors in the upper part of line N are sheet sands and that the dipping reflectors are sand and gravel foreset beds. Similarly, the dipping reflectors in line S and in the 3-D survey are interpreted as sand and gravel foreset beds. The zones of high attenuation in line S and in the 3-D survey are caused by a clay layer. There is no direct information about the composition of the channel-shaped radar element in line S; however, based on the good penetration of radar waves, it is probably a channel composed of clean sand and/or gravel.

The dipping reflectors in line W are interpreted as sand and gravel foreset beds. The zones of moderate attenuation above the dipping reflectors in line W suggest that the topset beds in the region have significant amounts of silt or some clay. This interpretation is based solely on the character of the radar data, because borehole coverage is poor along this line. The dipping reflectors in line E are also interpreted as sand and gravel foreset beds. The elements overlying the foreset beds are interpreted as sand and gravel channels and other fluvial elements.

The slope and scale of the clinoforms suggest that they are foreset beds from a deltaic rather than a fluvial environment. The strike and dip of these beds, determined from the 3-D survey, indicate that the influx of sediments was from the southeast into a body of water to the west. The horizontally bedded sand units are topset beds deposited as the delta prograded toward the ocean. The fact that the foreset beds in line E are deeper than those in the western lines supports the interpretation that the delta prograded from east to west; *see* Roberts et al. (2000) for an interpretation of regional depositional trends.

The clay layer has several possible origins. One possibility is that a lake was formed in the delta due to damming from sediment buildup farther downstream. In this low-energy environment, the fine clay sediments came out of suspension and were deposited conformably with the underlying foreset beds. The channel feature has high vertical relief and is therefore likely to be of deltaic origin, perhaps an outwash channel that was filled by lateral accretion.

North-south transect

Interpretation of this radar line is challenging due to the indistinct nature of many of the reflections. In addition, the resolution and accuracy of the drillers' logs along this transect make exact correlation with the sediments difficult. There is no outcrop in the area to augment the drill-log information.

Several sections along this transect show very poor penetration of the radar signal, indicating that the sediments, at least at surface, contain significant amounts of clay. The examples of element 4 along this line may be overbank deposits, or clay and silt from flooding of marsh or swamp environments formed behind natural levees in the delta. The reflectors in the sand and gravel sections at the south end of the transect all tend to be short and discontinuous. Included in these are several localized areas of moderate attenuation.

There is no evidence of the dipping element (element 1) along any part of this line. This suggests either that the sediments were not deposited in the same manner as those in and around Stoke's gravel pit, or that the sediments were reworked after deposition to produce the present sedimentary structure.

Eastern Brookswood

The eastern lines of the Brookswood data set are located at or near the edge of the aquifer. The locations of zones of high attenuation in lines SN24208 and EW20208 correspond to the locations of aquifer pinch-outs in Halstead's (1986) fence diagram. Drill data also confirm that a transition from sand and gravel to clay and clay-rich till occurs in these areas. The zone of high attenuation at a depth of 13 m in line EW24208 is also interpreted as an aquifer-aquitard boundary on the basis of drill data in the nearby area. The other elements in the area are horizontal and channel elements, and are consistent with a fluvial environment.

The eastern edge of the aquifer is very distinct, marked by a steeply dipping boundary. This boundary may have been created by ice coverage of the glaciomarine sediments of the Fort Langley Formation, which would have caused erosion of sediments at the ice-water boundary by wave and tidal action. Subsequently, sediments from the retreating Sumas glaciers were transported to the sea and deposited in a fan delta. The sediments were reworked by wave and tide to form structures such as gravel bars and crossbedded sand deposits.

IMAGING THE TOP OF THE SATURATED ZONE USING GROUND-PENETRATING RADAR

The goals of this part of the study were to: 1) determine whether ground-penetrating radar (GPR) can be used to positively identify the top of the saturated zone (TSZ), 2) determine which processing method can be used to enhance response from the TSZ, and 3) investigate temporal variations in the TSZ. These issues were investigated with data obtained from three sites in the lower Fraser River valley. The first two sites were used to develop and assess processing techniques. The third site was used to study temporal variations in the TSZ over a period of 10 months.

Data were collected using a PulseEKKO IV™ ground-penetrating radar unit using both 100 and 200 MHz antennas. Station spacing was either 0.50 m or 0.25 m. Common-midpoint surveys were conducted over each site to determine the velocity of the electromagnetic waves.

Site locations and descriptions of surveys

Site 1 – Environment Canada site

The Environment Canada site is located at 500 Clearbrook Road in Matsqui. A strong horizontal reflector is clearly visible at a depth of 4 m, in a GPR line 20 m long collected with 100 MHz antennas (Fig. 16a). Other horizontal and slightly dipping reflectors are visible to a depth of about 6 m. Lithological data from wells indicate sand and gravel between 2 and 36 m in depth; lithological variations over this interval are due to changes in grain size. From the available data, there is no significant lithological change that might account for the strong reflection seen at 4 m. Data from nearby piezometer wells indicate that the water table at the time of the survey was at a depth of 18 m. As the sediments are not fine grained, the capillary fringe should be small and therefore the water table should approximate the level of the TSZ.

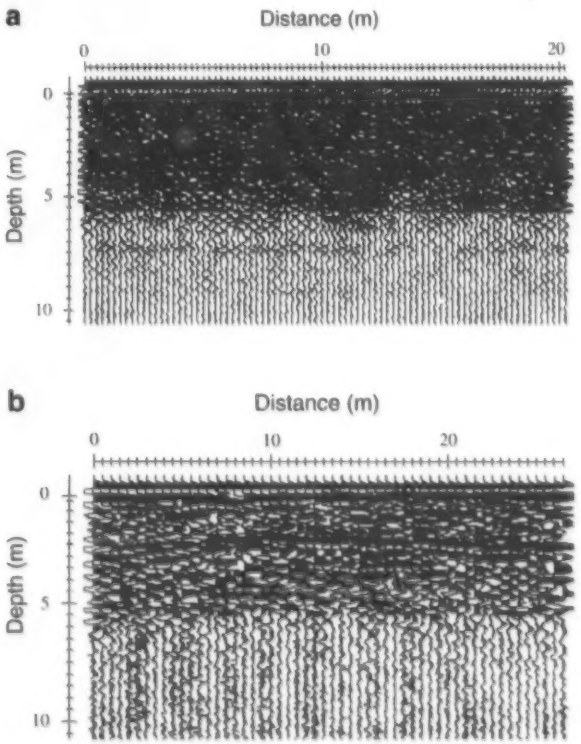

Figure 16. *Ground-penetrating radar data from* ***a)*** *site 1 (Environment Canada site), and* ***b)*** *site 2 (Stoke's gravel pit).*

Site 2 – Stoke's gravel pit

Data at the Stoke's gravel pit were collected along a line 20 m long, on a cliff 2 m above the pit floor (Fig. 16b). Processing with automatic gain control (AGC) reveals a strong reflector at a depth of 2.5 m. Shorter horizontal reflectors are visible across the survey, to a depth of about 5.5 m. A second survey of this line was collected 2 weeks after the first in order to compare the response from the TSZ.

The cliff is composed of coarse-grained sand and gravel. Previous GPR surveys in this pit have identified large sand and gravel foreset beds, together with some conformable clay layers. The gravel pit has been excavated down to the level of the water table. The water table is therefore well known as the level of ponding in trenches in the pit floor. Again, the water table should approximate the level of the TSZ.

Site 3 – Telecommunications Canada

The third site is at the Telecommunications Canada property at the corner of 36th Avenue and 192nd Street in Langley. Radar data were collected at four different times over a 10-month study period, on June 17, 1994; October 5, 1994; February 8, 1995; and April 10, 1995. The data, processed with AGC, are shown in Figure 17a–d. The surveys conducted on June 17 and October 5 were both 100 m long, whereas those conducted on February 8 and April 10 were 30 m long. A strong horizontal reflector is visible in the June 17 and October 5 profiles at depths of 6.5 and 7.5 m, respectively. The data from February 8 and April 10 do not have such an obvious, strong, horizontal reflector.

Independent measurements of the water table were obtained using data from R. Dasika (pers. comm., 1995), who measured the water level in a fully screened well located approximately 20 m from the survey line. The static level data were collected at monthly intervals from July 26, 1994 to June 26, 1995. The water levels at the dates of radar collection were estimated from monthly readings. On April 10, 1995, the water level was measured so it could be compared with Dasika's from the following day; after taking the stand-pipe height into account, the two measurements were similar.

Methods of identifying reflections from the top of the saturated zone

A key problem in interpreting GPR data is determining whether a strong horizontal reflector corresponds to the top of the saturated zone (TSZ) or to a geological boundary. In this section, two radar surveys are presented in which a strong horizontal reflection exists. In one case (site 1), this reflection is not due to the TSZ, whereas at site 2, it is a confirmed TSZ reflection. The goal was to establish a means of differentiating between true and false TSZ reflections. Four techniques were investigated for accomplishing this: 'gaining' the data, instantaneous phase and frequency, subtraction of data lines, and common-midpoint analysis.

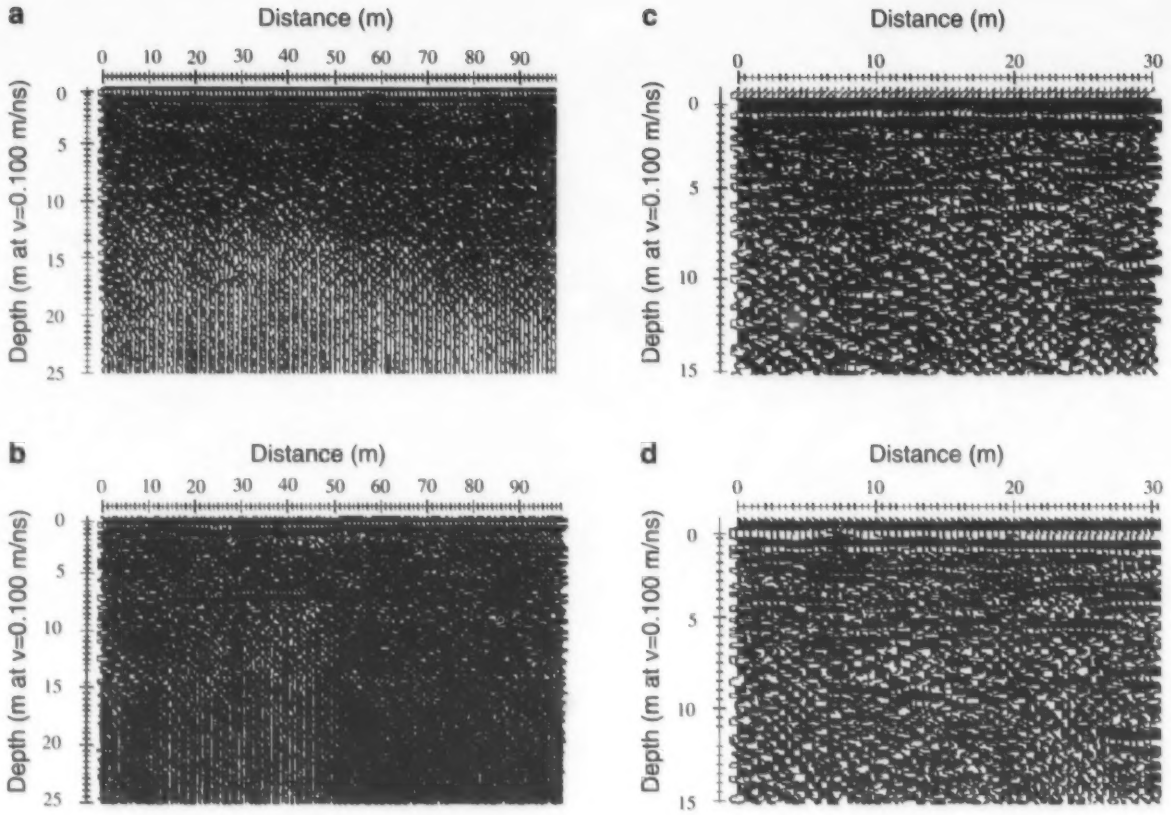

Figure 17. *Ground-penetrating radar data collected at site 3 (Telecommunications Canada site) at the corner of 36th Avenue and 192nd Street on:* ***a)*** *June 17, 1994;* ***b)*** *October 5, 1994;* ***c)*** *February 8, 1995; and* ***d)*** *April 10, 1995.*

'Gaining' of the data

The type of gain applied can dramatically change the way a data set is interpreted. Automatic gain control (AGC) amplifies all reflections to the maximum possible level in a given window. Therefore, a data set to which AGC has been applied has no variation between strong and weak reflectors. A reflection from the TSZ may have the same appearance as that from an interface between two materials which have only a small dielectric contrast. Spreading and exponential compensation (SEC) attempts to remove the effect of spherical spreading and attenuation. Estimated attenuation and velocity of the electromagnetic waves are needed for SEC.

Figure 18 shows the data from sites 1 and 2 with SEC applied. At site 2, it enhances the 2.5 m reflection and clearly marks this as a significant reflection, as very little else is seen in this plot except for the air and ground arrivals. The site 1 data do not show a similar differentiation between reflections. There is a reflection at a depth of 4 m that is continuous over the first 12 m of the survey, but no other significant features are apparent.

Figure 19 shows the uncorrected data. The reflection at 2.5 m is faintly visible in the site 2 data, even without amplification; however, the horizontal reflection from site 1 seen in the corrected data is not visible.

The type of gain applied to the data is critical to interpretation. The results of this study suggest that SEC may be the best way to discriminate between the TSZ and geological reflections.

Instantaneous frequency and phase

The software package PulseEKKO Tools™ can calculate the instantaneous phase and frequency plots for radar traces. The instantaneous phase of the radar data tends to emphasize continuous reflections, even those that have considerable interference obscuring them. Therefore, it may be a means of extracting the continuous TSZ reflection when other geological reflections are present. The instantaneous frequency of the radar response will change at this interface (Davis and Annan, 1989) and was therefore also investigated as a means of enhancing TSZ reflections.

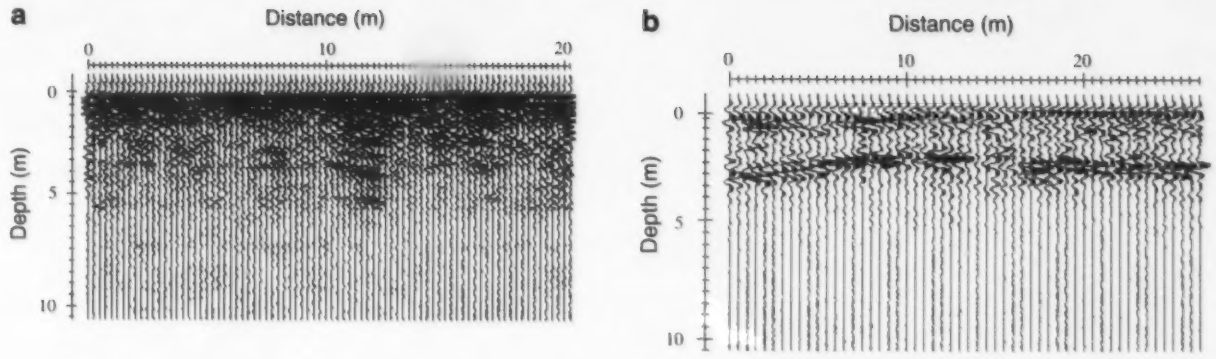

Figure 18. *Ground-penetrating radar data, with spreading and exponential compensation gain applied, from* ***a)*** *site 1 (Environment Canada site), and* ***b)*** *site 2 (Stoke's gravel pit).*

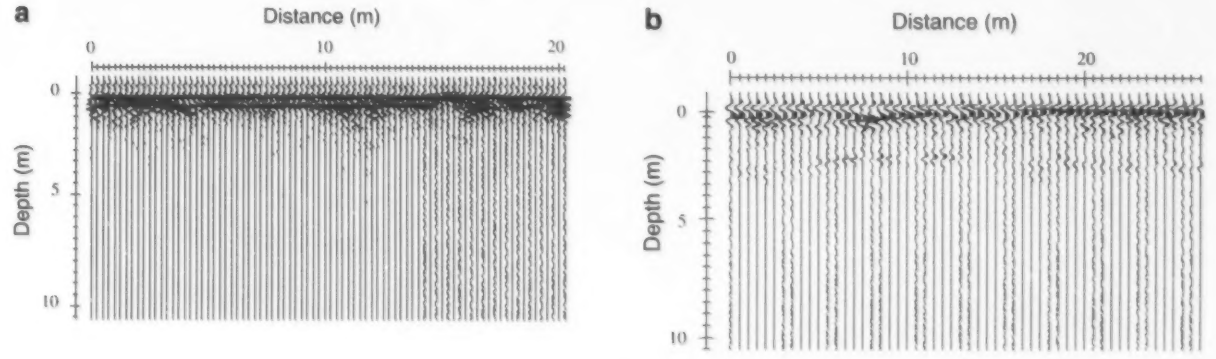

Figure 19. *Ground-penetrating radar data, with no gain applied, from* ***a)*** *site 1 (Environment Canada site), and* ***b)*** *site 2 (Stoke's gravel pit).*

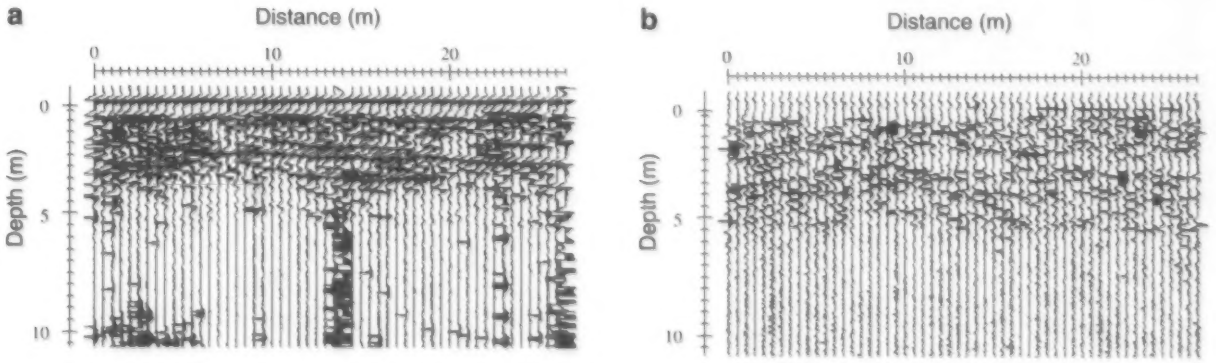

Figure 20. ***a)*** *Instantaneous phase plot of ground-penetrating radar data from site 2 (Stoke's gravel pit);* ***b)*** *instantaneous frequency plot of ground-penetrating radar data from the same site.*

Figure 20a shows the instantaneous phase plot of data from site 2 (Stoke's gravel pit). The strong continuous feature at 2.5 m depth is caused by the TSZ. The continuous feature at 1 m depth is the ground arrival. Figure 20b is an instantaneous frequency plot of the same data. There is a faintly discernible line of spikes at about 2.5 m depth which corresponds to the TSZ. The first two spikes at a depth of 0.5 m and 1.0 m are caused by the air and ground arrivals.

Figure 21a is an instantaneous phase plot of a line from site 1 (Environment Canada site), where the water table is quite deep. There is a continuous feature at a depth of 4 m which appears similar to the one in Figure 20a that was caused by the TSZ. However, the instantaneous frequency plot in Figure 21b does not show the sharp spikes observed at the depth marking the feature in the instantaneous phase plot.

The results suggest that instantaneous phase and frequency plots may be used to discriminate between TSZ reflections and geological reflections; however, further work is needed to confirm the general applicability of this method in other geological environments.

Subtraction of data lines

One way to investigate variations in the TSZ is to subtract data sets obtained from the same site over a period of time, as was done in this survey. Knowing that the depth of the TSZ changes seasonally (Halstead, 1986; *see* Ricketts, 2000a, Fig. 10), and that the surveys have been conducted at exactly the same position, the reflections from geological features will cancel out, leaving only the change in TSZ reflections. Figure 22c shows the difference between the two data sets in Figure 22a and b, which were collected at Stoke's gravel pit two weeks apart. In Figure 22c, there is a strong reflector visible at a depth of 0.5 m. This is interpreted as a change in the character of the ground arrival due to changes in the surficial water content. The parallel set of reflectors at a depth of about 2.5 m is due to the change in position of the TSZ reflection.

The difficulty with the subtraction method is ensuring that the data lines are collected at exactly the same location. Slight variations in antenna positioning can vary the reflected signals so that the geological reflections do not cancel out when subtracted from each other; however, if the antennas are positioned correctly, the subtraction of two data sets should not only give changes in the TSZ, but also changes in water content in the unsaturated zone.

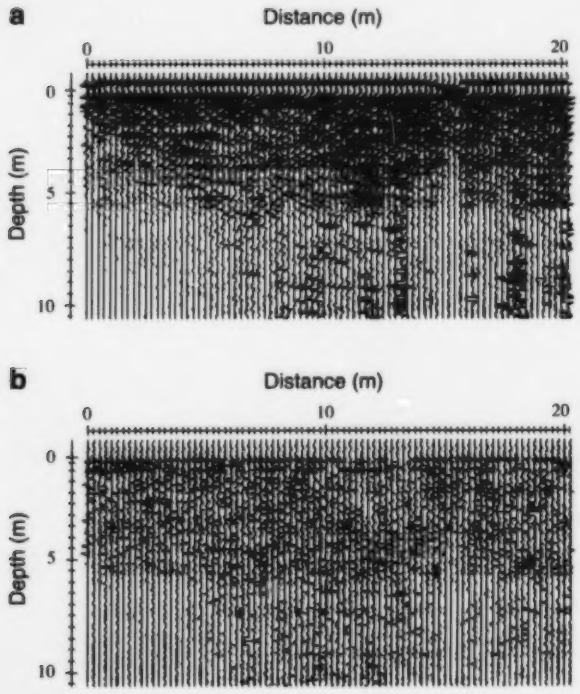

***Figure 21. a)** Instantaneous phase plot of ground-penetrating radar data from site 1 (Environment Canada site); **b)** instantaneous frequency plot of ground-penetrating radar data from the same site.*

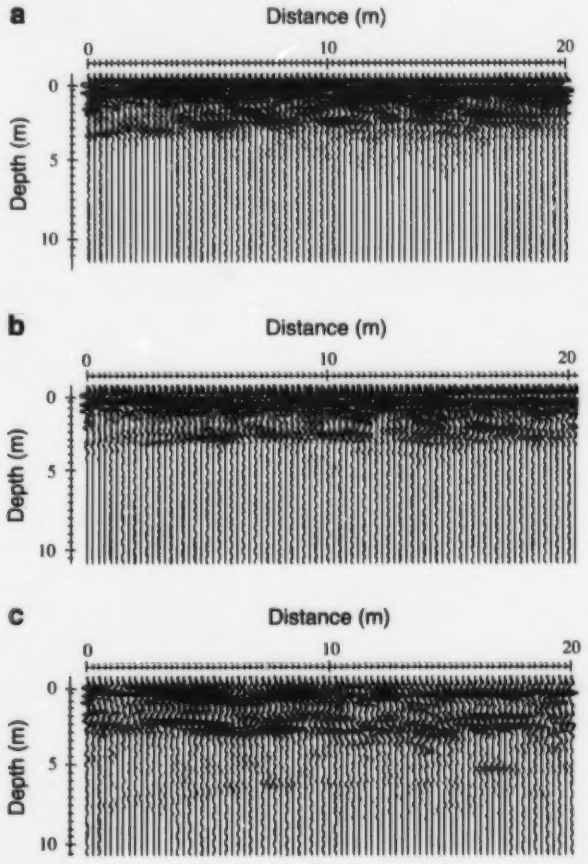

***Figure 22. a, b)** Sets of ground-penetrating radar data, processed using spreading and exponential compensation, collected at site 2 (Stoke's gravel pit) 2 weeks apart. **c)** Subtraction of data in Figure 22a and b provides an indication of the temporal variation in the top of the saturated zone (see text for explanation).*

Common-midpoint analysis

A common-midpoint (CMP) survey should be carried out and analyzed to determine the average velocity of radar waves through the subsurface. Such surveys are time consuming but essential for time-to-depth conversion. The velocity in water-saturated sand is typically 0.06 m/ns, quite different from that in unsaturated sand (1.5 m/ns). Therefore, the velocity determined from a reflection above the TSZ should be greater than one from below. Theoretically, the TSZ could be identified by comparing the velocities above and below the reflector.

The results of CMP surveys from site 1 and site 2 are summarized in Table 1. Velocities were calculated using both the direct ground arrivals and the hyperbolic reflections. The velocities obtained from site 1 are between 0.054 and 0.091 m/ns; velocities from site 2 are between 0.073 and 0.100 m/ns.

In theory, CMP data may be the most definitive way of confirming the existence of the TSZ in radar surveys; however, there are many drawbacks. In a wet area (e.g. after a rainfall), the unsaturated zone may have enough water in it to make its velocity similar to that in the saturated zone. Common-midpoint analysis can be difficult at times and therefore may produce misleading results. The technique becomes more difficult for deeper reflectors as phase shifts and other factors interfere with the ability to pick the reflector.

The data do show a decrease in velocity at site 2 above and below the TSZ; however, the velocities vary between common-midpoint surveys carried out at the same time, so the accuracy of the CMP data is in question. At site 1, velocities also decrease with depth, suggesting an increase in water content. The low velocities suggest that the material has a high water content.

Table 1. Common-midpoint survey results.

Site	Date	Frequency	Depth (m)	Velocity (m/ns)
Site 1	17-Jan-94	100 MHz	1.51	0.0756
Site 1	17-Jan-94	100 MHz	2.57	0.0694
Site 1	17-Jan-94	200 MHz	Ground	0.0910
Site 1	17-Jan-94	200 MHz	2.59	0.0763
Site 1	17-Jan-94	100 MHz	2.98	0.0543
Site 1	09-Mar-94	100 MHz	1.17	0.0783
Site 1	09-Mar-94	100 MHz	4.61	0.0693
Site 1	09-Mar-94	200 MHz	1.33	0.0829
Site 2	02-Feb-94	100 MHz	1.96	0.0849
Site 2	02-Feb-94	200 MHz	Ground	0.0820
Site 2	02-Feb-94	200 MHz	1.92	0.0853
Site 2	14-Feb-94	100 MHz	Ground	0.0910
Site 2	14-Feb-94	100 MHz	2.06	0.0868
Site 2	14-Feb-94	100 MHz	3.61	0.0825
Site 2	14-Feb-94	200 MHz	1.95	0.0822
Site 2	14-Feb-94	100 MHz	3.59	0.0732
Site 2	09-Mar-94	100 MHz	2.18	0.0927
Site 2	09-Mar-94	200 MHz	2.36	0.1005
Site 2	23-Mar-94	100 MHz	1.93	0.0770

Temporal variations in the top of the saturated zone

Temporal variation in the top of the saturated zone (TSZ) was studied at site 3 (Telecommunications Canada site) by means of surveys run on June 17, 1994; October 5, 1994; February 8, 1995; and April 10, 1995 (Table 2). The strong horizontal reflectors in the data from June 17 and October 5 are interpreted as being from the TSZ. These reflectors are the only ones that are continuous across the survey. The depth of the

Table 2. Temporal variations in the top of the saturated zone.

Date	Water level from ground-penetrating radar (m)	Water level determined by other means (m)
17-Jun-94	6.5	6.8
5-Oct-94	7.5	8.0
08-Feb-95	6.0	6.5
10-Apr-95	5.5	5.9

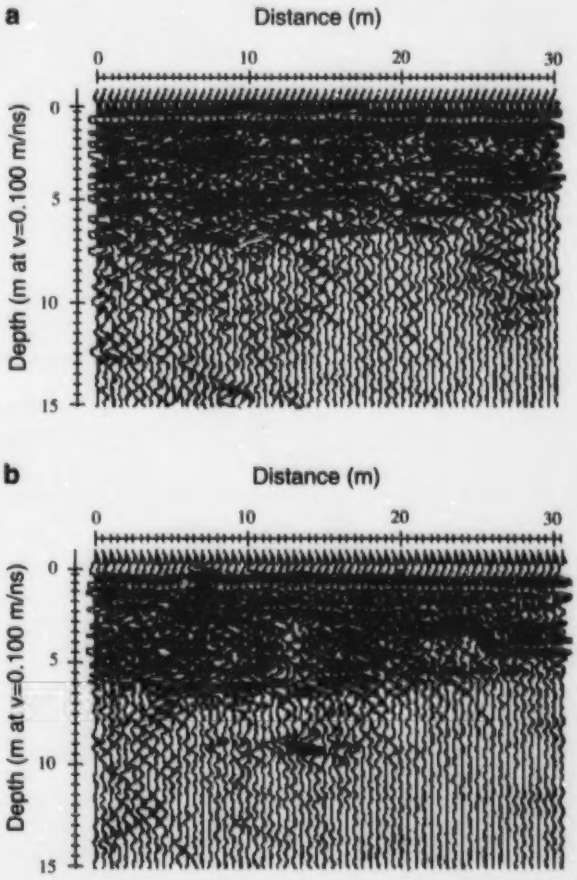

Figure 23. Ground-penetrating radar data, processed using spreading and exponential compensation, collected from site 3 (Telecommunications Canada site) on ***a)*** *February 8, 1995 and* ***b)*** *April 10, 1995.*

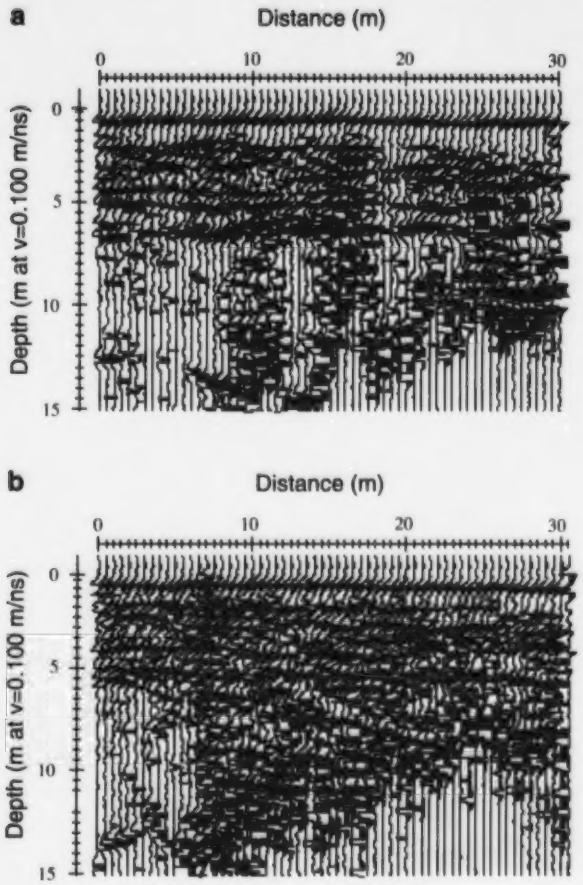

Figure 24. *Instantaneous phase plots of ground-penetrating radar data collected from site 3 (Telecommunications Canada site) on* ***a)*** *February 8, 1995 and* ***b)*** *April 10, 1995.*

reflector in the data from June 17 (6.5 m) matches the depth to the water table (6.8 m). Similarly, the depth to the reflector in the data from October 5 (7.5 m) matches the independent water-level measurement.

The data from February 8 and April 10 are more difficult to interpret. There are several very long horizontal reflectors that could correspond to the TSZ. Several of the processing methods described in the previous section were therefore applied to enhance TSZ reflections. With SEC applied, there is a distinct base to the visible reflections in both of the sections, at depths of 6.5 m and 6.0 m, respectively, that may correspond to the TSZ (Fig. 23a, b). This is to be expected, because the presence of water generally increases the electrical conductivity of a material. The independent water-table measurements for these two sections are 6.5 m and 5.9 m, respectively.

The plots of instantaneous phase (Fig. 24a, b) show distinct horizontal events in both of the processed sections, particularly at a depth of 6 m in the data from February 8. The horizontal event occurs at a depth of 5.5 m in the data from April 10. These events are interpreted as corresponding to the TSZ. In both instances, there is a reasonable match with the independently measured water-table depth.

DISCUSSION AND CONCLUSIONS

The analysis of the Brookswood data set demonstrates some applications of ground-penetrating radar (GPR) to aquifer characterization. This technique can be used to define and map many hydrogeological features in the subsurface, including the aquifer-aquitard boundary, internal heterogeneities caused by changes in hydraulic properties of sedimentary units, and the top of the saturated zone.

The aquifer-aquitard boundary was identified at two locations in the Brookswood GPR data. These correspond roughly to the location of boundaries between hydrostratigraphic units C and D identified by Halstead (1986). Boundaries identified by the GPR data are believed to be more accurate than those of Halstead, who relied on interpolation between wells separated by 100 m or more; however, one of the problems with the GPR method is its inability to determine the thickness of an aquitard unit. In addition, the depth of penetration is often too shallow to completely map a boundary. In both examples of aquifer-aquitard boundaries presented here, it is unclear whether these are true boundaries or simply represent local zones of clay that may not greatly affect aquifer continuity. Notably, Best and Todd (2000) showed, in their electromagnetic survey at 20th Avenue and 208th Street, that one of the clay units is discontinuous and underlain by aquifer sand and gravel. Clearly, a combination of both types of geophysical survey will provide the best results.

Boundaries within the aquifer may also be identified using GPR. This study demonstrates a method of aquifer characterization based on the identification and mapping of radar architectural elements (AEs) in the subsurface. Radar AEs can be identified as hydrogeological units, which are used to provide building blocks for a groundwater model. Four different radar AEs have been identified in the case of the Brookswood aquifer. The data set was separated into these four elements as the first step toward creating a hydrogeological model of the Brookswood aquifer. In addition, the information from the radar AEs was combined with data from drillers' logs to reconstruct the depositional environment. The interpretive method can clearly identify heterogeneities within the aquifer. Again, however, lack of penetration is a concern. Lower frequency antennas may provide a means of obtaining deeper penetration.

The top of the saturated zone (TSZ) can be clearly identified in the radar data throughout most of the aquifer. The most useful method for identifying the TSZ may be to apply different gains in order to enhance reflectors. It is a fast, simple method that, at least in this study, produced reasonable results. If time and resources permit, several of the methods outlined in this paper should be attempted.

The high level of heterogeneity in the Brookswood aquifer is clearly seen in the GPR data. In particular, no-flow boundaries, interpreted as electrically conductive clay

bodies, are shown to exist within the aquifer (e.g. in line S from Stoke's gravel pit). Such localized no-flow regions may have a significant effect on groundwater flow, particularly at the local scale. These heterogeneities may play an important role in the performance of nearby wells, as well as in the movement of contaminants.

The basic method demonstrated here can be applied at both small (contaminant transport modelling) and large (regional aquifer modelling) scales. At the scale of most contaminant studies (tens to hundreds of metres), a completely deterministic approach using GPR may be feasible. The technique can be used to image in detail the three-dimensional (3-D) stratigraphy of the region and can map exactly the location of no-flow boundaries. At a larger, regional scale, where detailed 3-D coverage is impractical, lines of radar data crossing the aquifer can pinpoint critical features in the subsurface and identify sedimentary AEs, which can be used to interpret the sedimentary environment. Facies models can then be used to interpolate between sampled lines and assign reasonable sedimentary elements to the unsampled areas. It is likely, however, that the high-resolution data provided by GPR surveys will be of more use in local rather than regional studies.

ACKNOWLEDGMENTS

This research was conducted within the four years of Jane Rea's Ph.D. program. Funding for the research came from various sources in the first two years: Geological Survey of Canada (Fraser Lowland Hydrogeology Project), United States Environmental Protection Agency, Environment Canada's Innovation Program, Canadian Space Agency, and Natural Resources Canada. During the last two years, the completion of portions of the study was funded by the United States Air Force Office of Scientific Research, under grant number F49620-95-I-0166. The United States Government is authorized to reproduce and redistribute reprints of this paper for government purposes, notwithstanding any copyright notation thereon. The views and conclusions contained herein are those of the authors and should not be interpreted as necessarily representing the official policies or endorsements, either expressed or implied, of the Air Force Office of Scientific Research or the United States Government.

This paper has benefited from the reviews and criticisms of Alan Judge (Terrain Sciences Division, GSC, Ottawa) and Brian Ricketts (formerly GSC, Vancouver).

REFERENCES

Anderson, M.P.
1989: Hydrogeologic facies models to delineate large-scale spatial trends in glacial and glaciofluvial sediments; Geological Society of America Bulletin, v. 101, p. 501–511.

Best, M.E. and Todd, B.J.
2000: Electromagnetic mapping of groundwater aquifers in the Fraser lowland; *in* Mapping, Geophysics, and Groundwater Modelling in Aquifer Delineation, Fraser Lowland and Delta, British Columbia, (ed.) B.D. Ricketts; Geological Survey of Canada, Bulletin 552.

Best, M.E., Todd, B.J., and O'Leary, D.
1994: Fraser Valley Hydrogeology Project: time-domain EM surveys, June 20 to July 8, 1994; Geological Survey of Canada, Open File 3095, 31 p.

Campanella, R.G., Davies, M., Boyd, T., Everard, J., Roy, D., Tomlinson, S., Jackson, S., Schrempp, H., and Ricketts, B.D.
1994: In-situ testing for the characterization of aquifers: demonstration project; Geological Survey of Canada, Open File 2940, 19 p.

Davis, J.L. and Annan, A.P.
1989: Ground penetrating radar for high-resolution mapping of soil and rock stratigraphy; Geophysical Prospecting, v. 37, p. 531–551.

Halstead, E.C.
1986: Ground water supply – Fraser Lowland, British Columbia; Environment Canada, Inland Waters Directorate, National Hydrology Research Institute, Paper no. 26, Scientific Series no. 145, 80 p.

Jol, H.M. and Smith, D.G.
1992: GPR results used to infer depositional processes of coastal spits in large lakes; *in* Proceedings, Fourth International Conference on Ground Penetrating Radar, Espoo, Finland; Geologian tutkimuskeskus, p. 169–177.

Makepeace, A.J. and Ricketts, B.D.
2000: Aquifer mapping and database management using a geographic information system, Fraser lowland; *in* Mapping, Geophysics, and Groundwater Modelling in Aquifer Delineation, Fraser Lowland and Delta, British Columbia, (ed.) B.D. Ricketts; Geological Survey of Canada, Bulletin 552.

Miall, A.D.
1985: Architectural element analysis: a new method of facies analysis applied to fluvial deposits; Earth-Science Reviews, v. 22, p. 261–308.

Olsen, H. and Andreasen, F.
1995: Sedimentology and ground-penetrating radar characteristics of a Pleistocene sandur deposit; Sedimentary Geology, v. 99, p. 1–15.

Pullan, S.E., Good, R.L., and Ricketts, B.D.
1995: Preliminary results from a shallow seismic reflection survey, Lower Fraser Valley hydrogeology project, British Columbia; *in* Current Research 1995-A; Geological Survey of Canada, p. 11–18.

Rea, J.M.A.
1996: Ground penetrating radar applications in aquifer characterization; Ph.D. thesis, Department of Earth and Ocean Sciences, University of British Columbia, Vancouver, British Columbia, 84 p.

Rea, J.M., Knight, R.J., and Ricketts B.D.
1994: Ground penetrating radar, Brookswood aquifer, Lower Fraser Valley, British Columbia; Geological Survey of Canada, Open File 2821, 13 p.

Ricketts, B.D.
2000a: Modelling of groundwater flow in the Fraser River delta and Brookswood aquifer; *in* Mapping, Geophysics, and Groundwater Modelling in Aquifer Delineation, Fraser Lowland and Delta, British Columbia, (ed.) B.D. Ricketts; Geological Survey of Canada, Bulletin 552.

2000b: Overview of the Fraser Lowland Hydrogeology Project; *in* Mapping, Geophysics, and Groundwater Modelling in Aquifer Delineation, Fraser Lowland and Delta, British Columbia, (ed.) B.D. Ricketts; Geological Survey of Canada, Bulletin 552.

Ricketts, B.D. and Liebscher, H.
1994: The geological framework of groundwater in the Greater Vancouver area; *in* Geology and Geological Hazards of the Vancouver Region, Southwestern British Columbia, (ed.) J.W.H. Monger; Geological Survey of Canada, Bulletin 481, p. 287–298.

Roberts, M.C., Vanderburgh, S., and Jol, H.M.
2000: Radar facies and geomorphology of the seepage face of the Brookswood aquifer, Fraser lowland; *in* Mapping, Geophysics, and Groundwater Modelling in Aquifer Delineation, Fraser Lowland and Delta, British Columbia, (ed.) B.D. Ricketts; Geological Survey of Canada, Bulletin 552.

Stephens, M.
1994: Architectural element analysis within the Kayenta Formation (Lower Jurassic) using ground-penetrating radar and sedimentological profiling, southwestern Colorado; Sedimentary Geology, v. 90, p. 179–211.

Radar facies and geomorphology of the seepage face of the Brookswood aquifer, Fraser lowland

M.C. Roberts[1], S. Vanderburgh[2], and H. Jol[3]

Roberts, M.C., Vanderburgh, S., and Jol, H., 2000: Radar facies and geomorphology of the seepage face of the Brookswood aquifer, Fraser lowland; in *Mapping, Geophysics, and Groundwater Modelling in Aquifer Delineation, Fraser Lowland and Delta, British Columbia, (ed.) B.D. Ricketts; Geological Survey of Canada, Bulletin 552, p. 95–102.*

Abstract : The main geomorphic elements of the unconfined Brookswood aquifer include the Campbell River meltwater channel (Late Wisconsinan), the delta plain and delta front, and the tidally influenced receiving basin seaward of the delta. Ground-penetrating radar was used to identify four delta radar facies across the seepage face (delta front) of the aquifer. Topset, foreset, bottomset, and distributary channel facies are each defined by a characteristic set of reflections, based on orientation, continuity, and length. The radar profiles indicate that there is hydraulic continuity between the foreset and bottomset units. The aquifer becomes confined where the fine sediments of the bottomset beds cover the gravel deposits of the foreset beds. Domestic wells along the lower part of the seepage face are commonly flowing artesian.

Résumé : Les principales entités géomorphologiques de l'aquifère libre de Brookswood sont le chenal d'eau de fonte (Wisconsinien supérieur), la plaine deltaïque et le front du delta de la rivière Campbell, ainsi que le bassin récepteur du côté océanique du delta qui est soumis à l'action des marées. On a utilisé le géoradar pour reconnaître quatre faciès deltaïques dans la zone de suintement (front du delta) de l'aquifère. On a ainsi identifié les faciès de sommet, de front, de base et de défluent, chacun reconnaissable d'après un ensemble de réflecteurs d'orientations, de continuités et de longueurs caractéristiques. Les profils radar indiquent qu'il y a une continuité hydraulique entre les unités de front et les unités de base. L'aquifère devient captif à l'endroit où les sédiments fins des couches de base recouvrent les graviers des couches de front. Les puits domestiques qui sont situés dans la partie inférieure de la zone de suintement sont souvent des puits artésiens jaillissants.

[1] Departments of Earth Sciences and Geography, Simon Fraser University, Burnaby, British Columbia V5A 1S6
[2] Department of Geography, University College of the Fraser Valley, 33844 King Road, Abbotsford, British Columbia V2S 7M9
[3] Department of Geography, University of Wisconsin–Eau Claire, Eau Claire, Wisconsin, U.S.A. 54702-4004

INTRODUCTION

The geographic extent of the Brookswood aquifer is largely coincident with the raised delta of the Campbell River. The delta was deposited where the Campbell River entered the ocean waters of the Nicomekl–Serpentine embayment of the Strait of Georgia (Fig. 1). Morphologically, the raised delta is a small plateau nestled against the flank of the Langley upland. Crossing the surface of the plateau are the incised valleys of the Campbell River and Anderson Creek. The western edge of the delta is marked by a steep hillslope, the paleodelta front, that dips into the Nicomekl–Serpentine embayment. The southwestern part of the paleodelta front slopes southward toward a lowland where the modern Campbell River flows after leaving the delta (Fig. 1).

The delta was formed when the Campbell River was an active meltwater channel during the Sumas Stade (from ca. 11 500 to 11 100 BP) of the Fraser Glaciation (Armstrong, 1981). High meltwater discharges from the melting Sumas ice transported an abundant supply of coarse clastic sediment to the delta, which, in response, grew rapidly into the Nicomekl–Serpentine marine embayment (Fig. 2). These coarse sediments, deposited in water depths of approximately 35 m, formed a Gilbert delta with clearly defined topset and foreset beds (Ricketts and Jackson, 1994). It is the coarse clastic sediments of this delta that constitute and largely define the Brookswood aquifer.

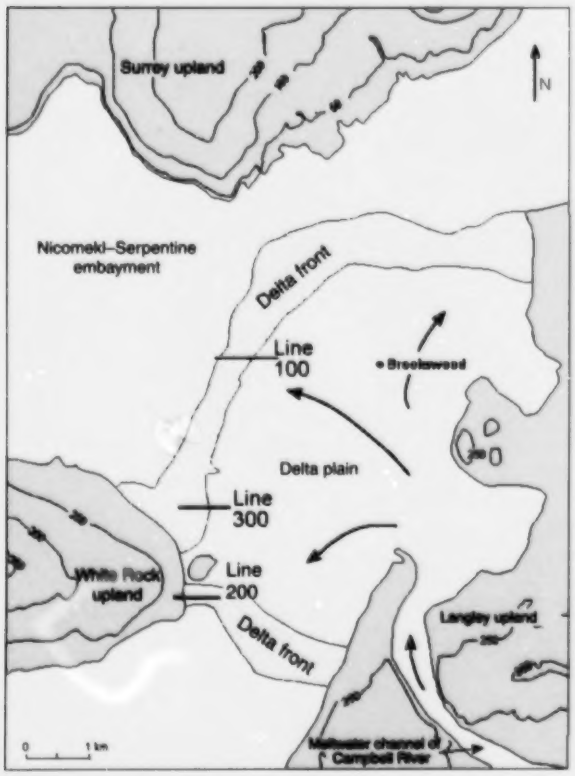

Figure 1. *Geomorphic elements and extent of the Campbell River delta. Locations of the three radar profiles are shown. Elevation contours in metres.*

OBJECTIVES

This component of the Brookswood aquifer study focused on the boundary conditions along the delta front (seepage face) and where the delta-front sediments interfinger with the fine-grained deposits (silt and sand) of the marine receiving basin (Nicomekl–Serpentine embayment). The specific objectives of this study were to: 1) describe the geomorphic setting of the Campbell River delta, in order to delineate the aquifer and its seepage face; 2) establish the depositional architecture of the seepage face and the adjacent delta plain, along the western flank of the aquifer, using ground-penetrating radar (GPR); and 3) locate the water table in the GPR lines for input to the groundwater database (Ricketts, 2000).

GEOMORPHIC SETTING OF THE DELTA

Predeltaic sediments

The eastern edge of the delta (Fig. 1) is bounded by glaciomarine stony clay of the Fort Langley Formation, which underlies the Langley upland. To the southwest, the delta onlaps the White Rock upland, which consists largely of glaciomarine and marine Capilano sediments. The silt- and clay-rich Capilano sediments also form an aquitard below the Brookswood aquifer.

Campbell River meltwater channel

The valley of the Campbell River has the typical morphology of a meltwater channel: steep (up to 35°) valley walls and a topographically flat floor. The width of the present river channel (8 m at 16th Avenue, Langley) is unusually narrow when compared with the size of the valley floor (650 m). The modern river is flowing in a valley that was originally eroded by meltwater discharges large enough to turn the whole valley into a river channel. Dury (1964) coined the term 'underfit' to describe this condition of discordance between a valley and the active channel that is too small to have eroded it. Shallow excavations reveal an upper valley fill of sand and gravel; the valley bottom is probably the site of a linear aquifer linked to the Brookswood aquifer.

Delta plain

The surface of the delta plain is flat to gently undulating. The delta plain has a slope of less than 1° from the place where the Campbell River emerges from the Langley upland (Fig. 1) to the upper edge of the delta front. Forming the delta surface are topset beds composed of sand and sandy gravel.

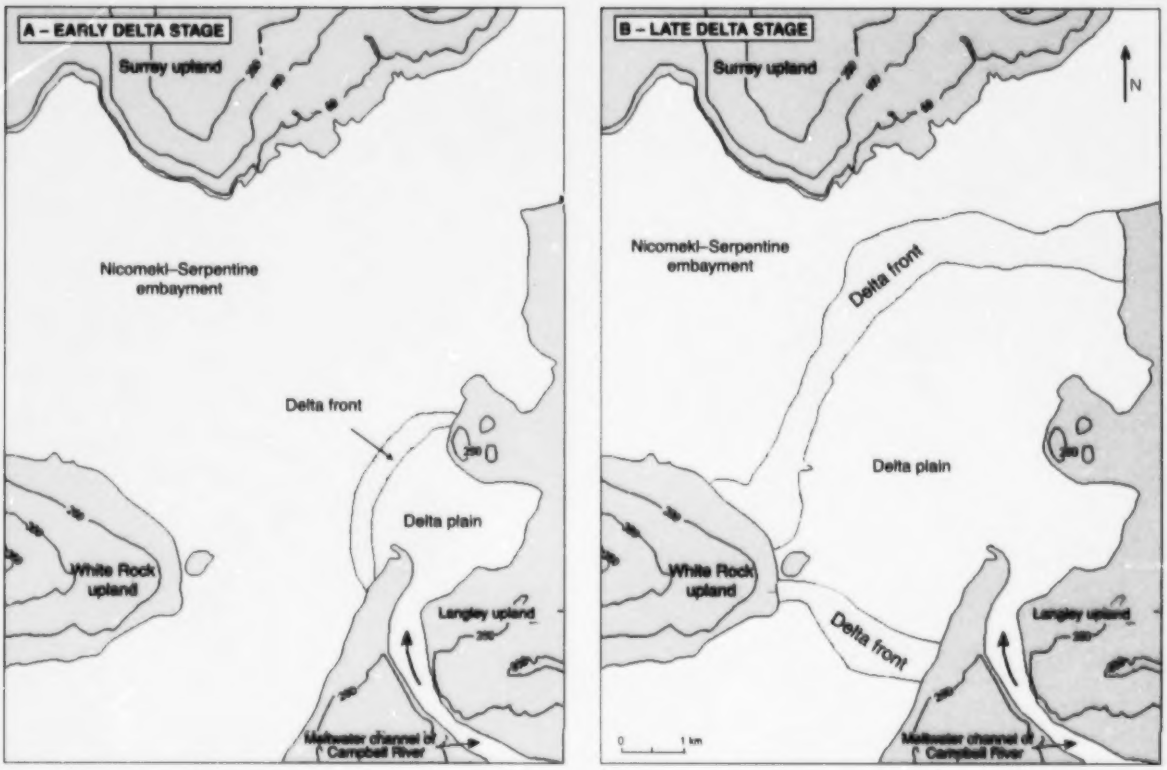

Figure 2. *Stages in the growth of the Campbell River delta. Elevation contours in metres.*

Delta front

The delta front can be divided into two parts (Fig. 1). The first consists of the main delta front, extending north and east from the White Rock upland to the Langley upland (Fig. 1). This steep portion of the front has slopes reaching about 9°, close to the 11° dip of the foreset reflections measured in the radar profiles. The slight difference between these two values results from the exposed foreset units of the delta having undergone continuous subaerial erosion once sea level dropped, resulting in a delta-front slope angle that is now slightly less than when it was first exposed.

The second section of the delta front consists of a gently sloping area that extends from the White Rock upland to the higher land west of the Campbell River meltwater channel (Fig. 1). The low slopes (1–1.5°) of this part of the delta front are indicative, in a Gilbert delta such as this, of slow growth resulting from a reduced sediment supply. The flow of sediment-laden meltwater was controlled by a protruding upland, located west of the meltwater channel (Fig. 1), which deflected it toward the northwest (and the steepest part of the delta front), and therefore away from this part of the delta front.

Receiving basin

The delta prograded into the approximately 35 m deep seawater of the Nicomekl–Serpentine embayment. The silt and sand forming the delta bottomset beds were deposited on the glaciomarine and marine silt and clay of the Capilano Formation.

Growth of the delta

During the Late Wisconsinan, the delta advanced into a tidal embayment, where its progradation was limited only by an offshore island that now constitutes the White Rock upland (Fig. 2). This island deflected delta growth away from the southwest and toward the north and west. With the final retreat of the Sumas ice, there was a decrease in meltwater flow in the Campbell River valley and, probably coevally, the start of isostatic rebound of the region. The combination of these two factors led to the cessation of delta growth and the emergence of the delta above sea level.

RADAR METHODS

A pulseEKKO IV™ radar system was used to obtain the radar lines across the Brookswood aquifer. Antennae with a centre frequency of 100 MHz were used, with antenna spacing being 1 m and station spacing ranging from 0.5 to 1 m. Traces at each station were collected at a sampling interval of 800 ps in a time window of 500 ns, and were vertically stacked 64 times. For plotting purposes, automatic gain control, topographic corrections, and down-trace averaging were applied to the data sets. Common-midpoint gathers were used to obtain velocities for converting time to depth (an average velocity of 0.1 m/ns was used in all the lines). Three radar lines were run (*see* Fig. 1 for locations): line 100 along 40th Avenue west of 192nd Street; line 200 along 20th Avenue east of 184th Street; and line 300 along 28th Avenue east of 184th Street.

RADAR FACIES OF THE DELTA

Topset facies

This facies is represented by horizontal to gently undulating, continuous reflections (Fig. 3). The radar signature of the facies is poorly defined because the topset beds are generally less than 1 m thick and the resolution of GPR at 100 MHz, with a velocity of 0.1 m/ns, is approximately 0.25–0.50 m. Locally, the reflections are truncated where distributary channels cross the delta plain (Fig. 3). The sedimentary structures of the topset beds have been described by Ricketts and Jackson (1994), who found crossbedded sand and gravel associated with the facies.

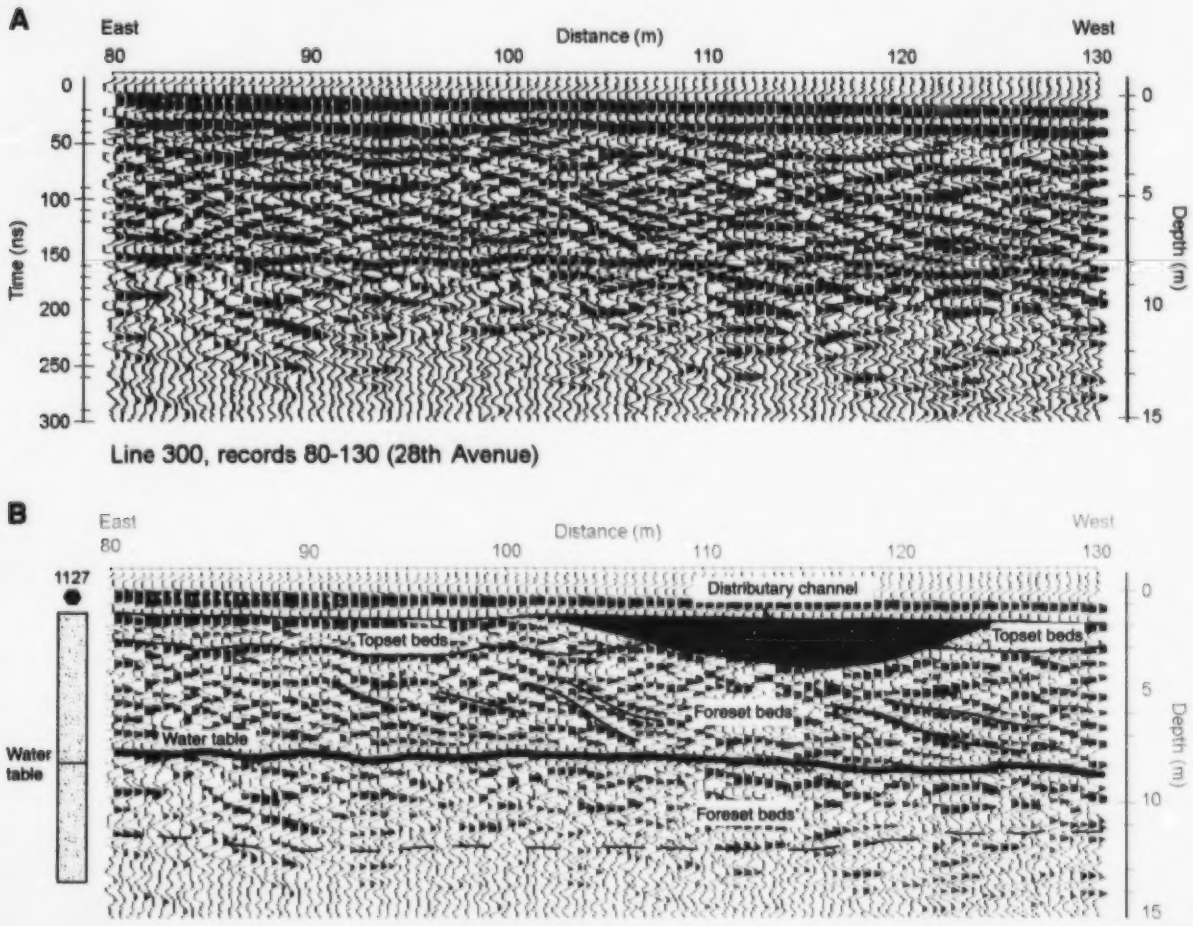

Figure 3. *Section of a radar profile (line 300 (28th Avenue), records 80–130) run along the delta plain: **A)** radar reflections; **B)** interpretation superimposed on radar reflections; water well (see Makepeace and Ricketts (2000) Fig. 9, LINK1 #1127 (UTM 521716E 5433330N)) is composed completely of sand (driller's log) and has a water-table level that correlates closely with the water table identified in the radar profile; the lowest foreset reflections have a tendency to flatten downdip.*

Foreset facies

The diagnostic feature of this facies is the steeply dipping, parallel, and continuous reflections of the foreset beds. The reflection configuration of this facies is similar to that identified in the seismic literature as oblique tangential clinoforms (Fig. 3, 4; *see* Mitchum et al., 1977). Lithological control for the identification and interpretation of the facies is provided by roadcuts in the delta front and from exposures in various gravel pits (Ricketts and Jackson, 1994). The radar profiles were run along roads that crossed the delta but were not necessarily parallel to maximum dip, so many of the foreset beds in the radar profiles have less than true dip. In the distal section of the delta front, as shown in the western end of line 300 (Fig. 3), the reflections have low dips (1–5°) and become increasingly undulating in geometry. Indeed, in this distal area, there is commonly a transition zone between the low-dip foreset beds and the bottomset beds.

Distributary channel facies

This facies is defined by a set of concave, continuous reflections that commonly truncates the reflections of the underlying radar stratigraphic unit. The widest distributary channel measured on the radar profiles was located on the western edge of the delta along 28th Avenue, where it attained a width of 22 m and a depth of 2.5 m (Fig. 3).

Bottomset facies

This facies is represented by mainly parallel, continuous reflections (Fig. 5, 6). The fine-grained sand and silt of this facies are portrayed on line 100 (Fig. 5) as reflections that dip toward the centre of the receiving basin. Locally, the foreset beds interfinger with the bottomset beds, but the radar signature is difficult to interpret because of signal attenuation and increased electrical conductivity from the high silt and clay content in the bottomset beds. Peat, exposed at the west end of line 100 (40th Avenue), has a continuous, horizontal to subhorizontal reflection pattern similar to that of the fine-grained sand and silt, but with significantly less signal attenuation.

GROUND-PENETRATING RADAR PROFILES ACROSS THE SEEPAGE FACE

Radar lines were run from the western edge of the delta plain and down the seepage face in order to characterize the relationship between the water table and the radar stratigraphy.

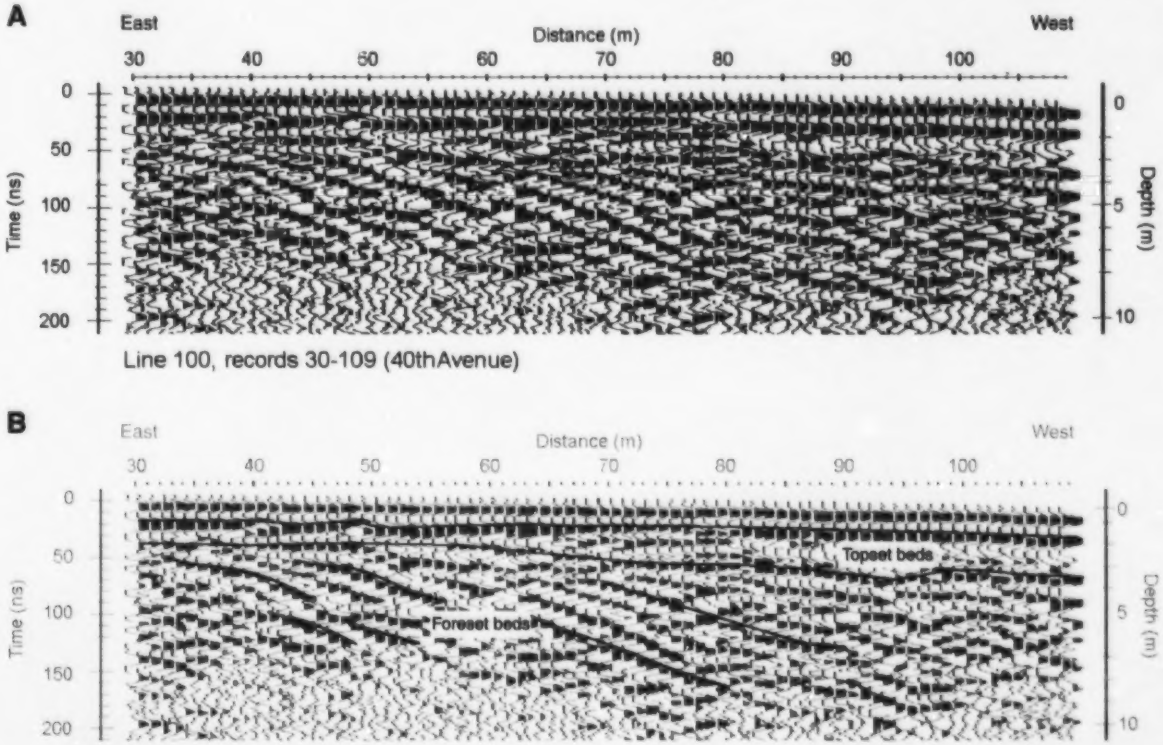

Figure 4. *Section of a radar profile (line 100 (40th Avenue), records 30–109) run along the western edge of the delta plain to the position where the slope of the delta front begins:* ***A)*** *radar reflections;* ***B)*** *interpretation superimposed on radar reflections.*

The water table is identified on the radar lines by a straight and continuous reflection, as shown on line 300 (Fig. 3). A large, 40 m deep gravel pit adjacent to 40th Avenue and line 100 has lowered the water table below the depth of radar penetration. This accounts for the absence of a prominent water-table reflection on line 100 (Fig. 4). Where the water table crosses foreset reflections, there can be a small step where it drops 20–30 cm. Whether this drop is a function of changes in the dielectric response of the radar signals from dense sand to gravel, or the result of a permeability change within the same unit, is not known. When the radar survey was run during the summer of 1995, seepage was observed at, or close to, the contact between the exposed face of the unconfined aquifer and the bottomset beds.

GROUND-PENETRATING RADAR PROFILE ACROSS A CONFINED AQUIFER

The Brookswood aquifer undergoes a transition, from an unconfined state (seepage face) to a confined state, where the fine-grained clastic sediments of the bottomset beds cover the sandy gravel aquifer (Fig. 5, 6). The nature of the change is commonly in the form of a transition zone (Fig. 5), where the lowest parts of the foreset reflections have very shallow dips and become increasingly parallel. Such reflection geometries are almost identical to the bottomset reflections where the two facies are intercalated.

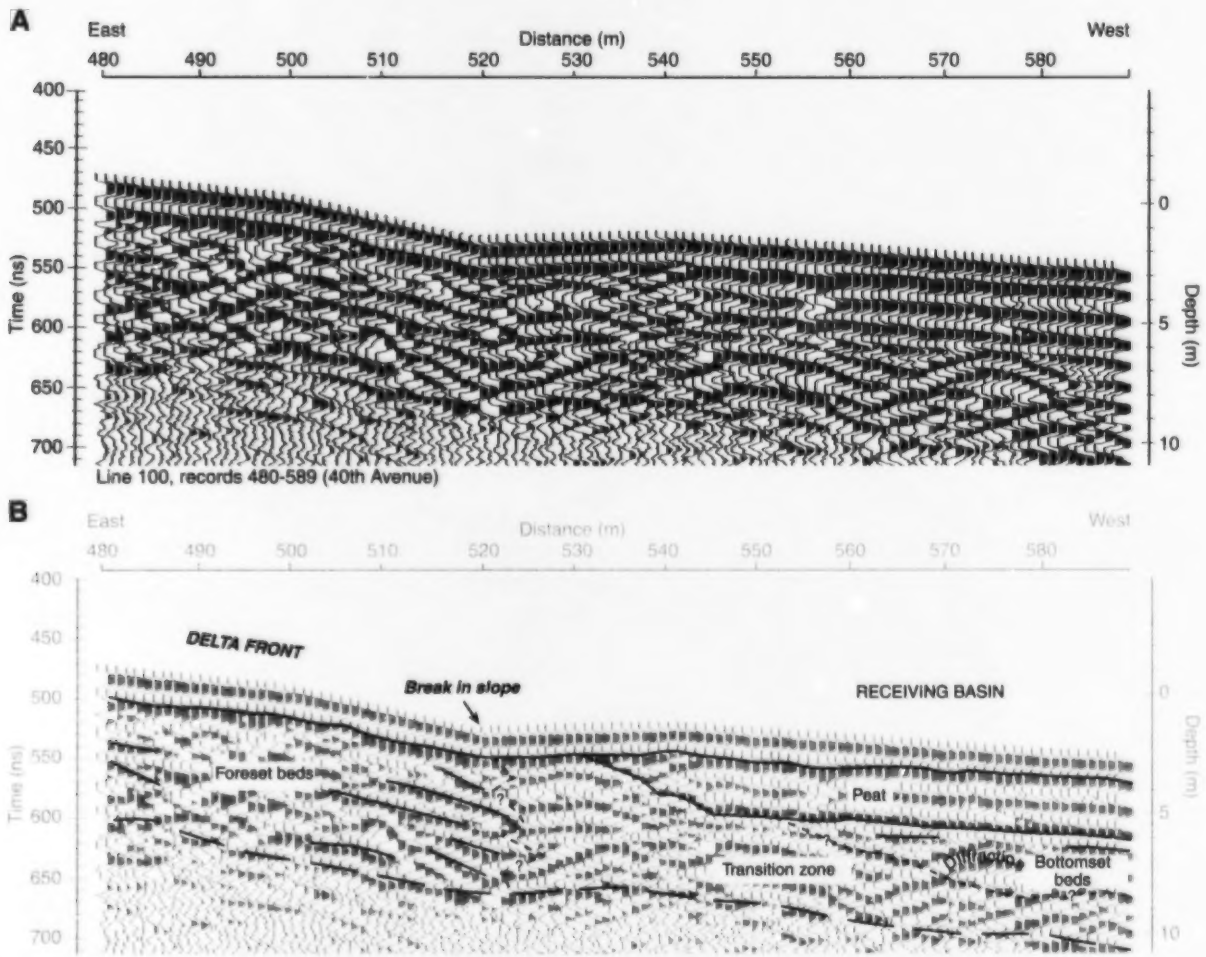

Figure 5. *Section of a radar profile (line 100 (40th Avenue), records 480–589) run where the dipping delta front merges into the bottomset beds and the receiving basin:* ***A)*** *radar reflections;* ***B)*** *interpretation superimposed on radar reflections; peat ranges from purely organic to organic-rich silt.*

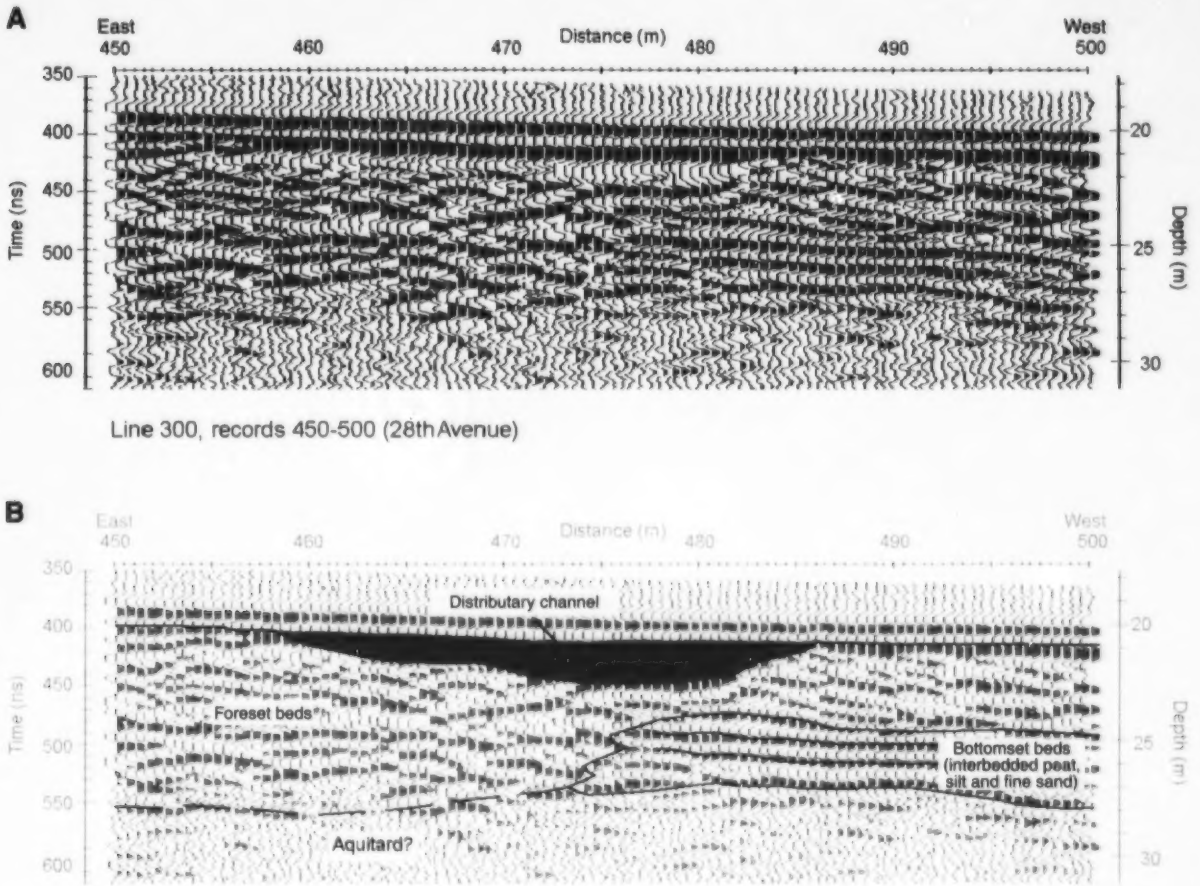

Figure 6. *Section of a radar profile (line 300 (28th Avenue), records 450–500) showing low-angle foreset beds and the bottomset beds of the delta:* ***A)*** *radar reflections;* ***B)*** *interpretation superimposed on radar reflections; high electrical conductivity of the aquitard (Capilano sediments) produces a transparent zone beneath the delta.*

SUMMARY

Ground-penetrating radar lines were run across the seepage face of the Brookswood aquifer (Rea et al., 1994; Rea and Knight, 2000). From an analysis of the radar reflections, it is possible to resolve four radar facies. These facies provide an insight into the stratigraphic architecture of the delta, and include topset, foreset, and bottomset beds, and distributary channels. The water table is defined by a strong radar reflection.

ACKNOWLEDGMENTS

The support of Brian Ricketts, formerly of the Geological Survey of Canada, in underwriting some of the costs of this work is gratefully acknowledged. We thank James MacEachern (Simon Fraser University) and Brian Ricketts for their helpful critiques of the paper, and our field assistant Ev Roberts.

REFERENCES

Armstrong, J.E.
1981: Post-Vashon Wisconsin glaciation, Fraser Lowland, British Columbia; Geological Survey of Canada, Bulletin 322, 34 p.

Dury, G.H.
1964: Principles of underfit streams; United States Geological Survey, Professional Paper 452-A, 67 p.

Makepeace, A.J. and Ricketts, B.D.
2000: Aquifer mapping and database development using a geographic information system, Fraser lowland; *in* Mapping, Geophysics, and Groundwater Modelling in Aquifer Delineation, Fraser Lowland and Delta, British Columbia, (ed.) B.D. Ricketts; Geological Survey of Canada, Bulletin 552.

Mitchum, R.M., Jr., Vail, P.R., and Sangree, J.B.
1977: Seismic stratigraphy and global changes of sea level, part 6: stratigraphic interpretation of seismic reflection patterns in depositional sequences; *in* Seismic Stratigraphy – Application to Hydrocarbon Exploration, (ed.) C.E. Payton; American Association of Petroleum Geologists, Memoir 26, p. 117–133.

Rea, J.M.A. and Knight, R.J.
2000: Characterization of the Brookswood aquifer using ground-penetrating radar; *in* Mapping, Geophysics, and Groundwater Modelling in Aquifer Delineation, Fraser Lowland and Delta, British Columbia, (ed.) B.D. Ricketts; Geological Survey of Canada, Bulletin 552.

Rea, J.M.A., Knight, R., and Ricketts, B.D.
1994: Ground-penetrating radar survey of the Brookswood aquifer, Fraser Valley, British Columbia; *in* Current Research 1994-A; Geological Survey of Canada, p. 211–216.

Ricketts, B.D.
2000: Modelling of groundwater flow in the Fraser River delta and Brookswood aquifer; *in* Mapping, Geophysics, and Groundwater Modelling in Aquifer Delineation, Fraser Lowland and Delta, British Columbia, (ed.) B.D. Ricketts; Geological Survey of Canada, Bulletin 552.

Ricketts, B.D. and Jackson, L.E.
1994: An overview of the Vancouver–Fraser Valley hydrogeology project, southern British Columbia; *in* Current Research 1994-A; Geological Survey of Canada, p. 201–206.

Modelling of groundwater flow in the Fraser River delta and Brookswood aquifer

Brian D. Ricketts[1]

Ricketts, B.D., 2000: Modelling of groundwater flow in the Fraser River delta and Brookswood aquifer; in *Mapping, Geophysics, and Groundwater Modelling in Aquifer Delineation, Fraser Lowland and Delta, British Columbia, (ed.) B.D. Ricketts; Geological Survey of Canada, Bulletin 552, p. 103–130.*

Abstract: Numerical simulations of groundwater flow have been made for the Fraser River delta and the unconfined Brookswood aquifer, using three- and two-dimensional models.

Shallow groundwater beneath the Fraser delta is recharged by precipitation on the delta and topography-driven flow from the adjacent uplands. Simulated hydraulic gradients at the water table are 0.1–0.25 m/km. Flow velocities increase toward the delta front, with maxima of 1.1–1.4 m/d.

The possibility of groundwater flow to the delta front is supported by electrical conductivity data, which show mixing of seawater and fresh water as far west as the low-tide limit. Zones of submarine seepage could raise pore pressures and increase the susceptibility of the delta front to failure.

Groundwater flow in the Brookswood aquifer is quasi-radial. Hydraulic gradients north of an east-west hydraulic divide are 6–7 m/km and compare with measured gradients. About 15% of the total discharge occurs at the aquifer seepage face.

Résumé : On a fait des simulations numériques du débit de l'eau souterraine pour le delta du Fraser et pour l'aquifère libre de Brookswood en utilisant des modèles bi- et tridimensionnels.

La nappe d'eau souterraine située à faible profondeur dans les dépôts du delta du Fraser est alimentée par les précipitations et le ruissellement provenant des hautes terres adjacentes. Les gradients hydrauliques simulés à la surface de la nappe phréatique sont de 0,1 à 0,25 m/km. Les vitesses d'écoulement augmentent en direction du front du delta, pour atteindre un maximum de 1,1 à 1,4 m/jour.

La possibilité d'un écoulement d'eau souterraine au front du delta est appuyée par les données de conductivité électrique qui indiquent qu'il y a un mélange d'eau douce et d'eau salée aussi loin vers l'ouest que la limite de la marée basse. Les zones de suintement sous-marin pourraient faire monter la pression interstitielle et accroître la susceptibilité du front deltaïque aux ruptures.

L'écoulement de l'eau souterraine dans l'aquifère de Brookswood est presque radial. Au nord d'une ligne de partage hydraulique orientée est-ouest, les gradients hydrauliques sont de 6 à 7 m/km, ce qui est comparable aux gradients mesurés. Environ 15 p. 100 de l'écoulement total de l'aquifère se font à la zone de suintement.

[1] Department of Earth Sciences, University of Waikato, Private Bag 3105, Hamilton, New Zealand

INTRODUCTION

Geological models, like those of other disciplines, provide tools for predicting what will happen to a particular physical or chemical system when stresses are applied to it. Groundwater-flow models can predict the effects of withdrawing water from, or injecting it into, an aquifer; the velocity and direction of contaminant plume migration; and the effects of streams, drains, recharge, and evapotranspiration. To maximize its predictive power, a groundwater model should duplicate the hydrogeological conditions using as few boundary conditions as possible. For example, a particular aquifer model would have little predictive value if constant heads (i.e. water-table elevations measured in wells) were applied across the entire model grid, so that hydraulic potential could never vary even when stresses such as water withdrawal were applied.

There are very few published groundwater-flow models for aquifers in the Fraser lowland and none in the Fraser River delta. Investigations in this project were conducted in two areas: the Fraser River delta and the Brookswood unconfined aquifer. The models are preliminary, but will provide the basis for future investigations. The Brookswood area corresponds to the quadrant used as a template for database development and subsurface hydrostratigraphic mapping (Makepeace and Ricketts, 2000; Ricketts and Makepeace, 2000), and contains several hundred water wells that provide reasonable stratigraphic control and hydraulic data for model calibration. Data from ground-penetrating radar, time-domain electromagnetic, and high-resolution seismic-reflection surveys have also been incorporated into the models.

General attributes of the models

A three-dimensional numerical-simulation program (MODFLOW), originally developed for the United States Geological Survey by M. McDonald and A. Harbaugh, was used to model groundwater flow in the two areas; the version used here (Visual MODFLOW™) was developed by Waterloo Hydrogeologic Software. Each model consists of a three-dimensional grid in which cells are assigned aquifer-aquitard properties (hydraulic-conductivity and storage values) and boundary-head conditions. A constant-head boundary, for example, regulates the flow in and out of cells to maintain a constant (specified) hydraulic head throughout the simulation. A no-flow boundary, on the other hand, does not permit flow into or out of a cell. Two-dimensional streamflow simulations on profiles through the Brookswood aquifer were also performed to examine the effects of local anisotropy.

Co-ordinates in the model layers were specified as Universal Transverse Mercator (UTM) values, thus enabling easy import of map overlays (e.g. digital surficial geology and topography) from other sources and export of results (e.g. simulated heads for each layer) to other applications (e.g. geographic information system, or GIS, mapping). Maximum and minimum elevations were specified relative to sea level. Layer thickness was also specified but could be changed from one simulation to another. The hydraulic properties were defined for each cell within a layer, thus making it possible to represent lithological heterogeneity within a layer (e.g. changes from sand to silt or mud) by varying hydraulic conductivity and porosity.

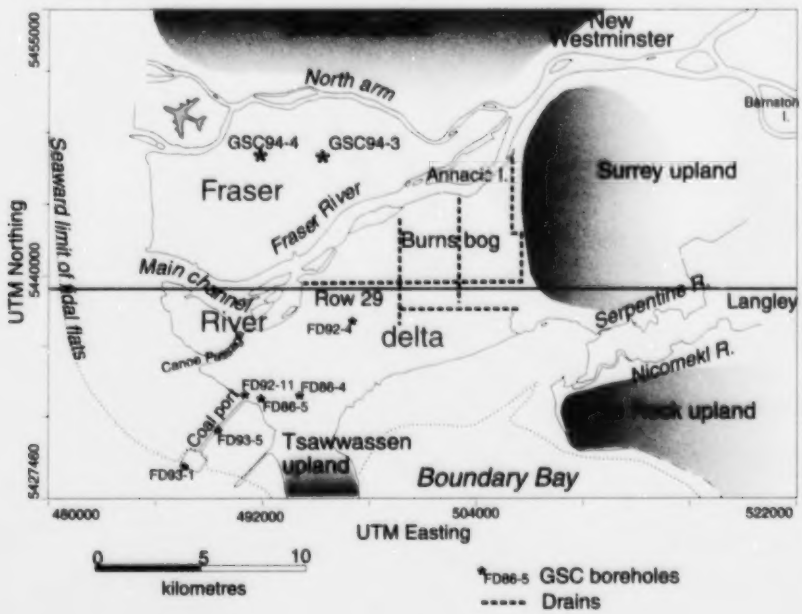

Figure 1. *Location of the Fraser River delta and surrounding uplands.*

Subsurface data relating to aquifer and aquitard lithology, elevation, well co-ordinates, and static level were derived from the database developed for the Fraser Lowland Hydrogeology Project (*see* Woodsworth and Ricketts, 1994; Ricketts and Dunn, 1995; Makepeace and Ricketts, 2000). Overlay maps of surficial geology for each model were extracted (Dunn and Ricketts, 1994) from digitized versions of the original Geological Survey of Canada (GSC) A-series maps (Armstrong and Hicock, 1980a, b).

FRASER RIVER DELTA

The Fraser River delta (Fig. 1) is the modern, actively growing extension of the Fraser lowland, which is the region of glacial and interglacial sedimentation at the margin of the Strait of Georgia. There is little groundwater use on the Fraser River delta plain because seawater intrudes the shallow aquifers and most of the area is linked to the regional district (surface) water supply. Consequently, little is known about the water table, groundwater recharge, or flow beneath the delta. Nevertheless, the hydrogeological conditions in the delta plain sediments are an important consideration for foundation construction (e.g. excess pore pressure in areas of artesian flow), assessment of seismic risk and sediment surface stability (liquefaction of shallow, saturated sediment), and river flood-management (rising water tables).

Groundwater flow and seepage at the delta front and slope may also play a significant role in delta-slope failure. Sediment failure of the Fraser River delta front and slope is a common and potentially costly phenomenon (Luternauer and Finn, 1983; Hart et al., 1992; McKenna et al., 1992; Luternauer et al., 1994; Harris et al., 1995). Slope failure is usually attributed to one or more of seismic activity, storms, sediment loading at distributary mouth bars, tidal currents, and interstitial gas. Although direct observations of submarine seepage have not been made, preliminary examination of groundwater flow beneath the delta plain indicates that seepage is indeed a possible cause of delta-front failure (Ricketts, 1998).

Groundwater flows from regions of high fluid potential to regions of low fluid potential. The driving force for regional groundwater flow is topography (Toth, 1963; Bredehoeft et al., 1982). Consequently, areas of high elevation tend to be characterized by groundwater recharge, whereas those of low elevation are characterized by discharge. Subsurface flow can be divided into nested systems of recharge and discharge on the basis of their local, intermediate, and regional extent. A conceptual picture of groundwater flow beneath the Fraser lowland and delta is shown in Figure 2. Local, shallow flow on the delta is likely recharged by precipitation on the delta plain itself. The residence time of groundwater in local systems is usually on the order of months to years. Freshwater seepage at the delta front is also depicted as part of a local flow system (Fig. 2). Here, a saline wedge also flows landward under the freshwater lens. Other examples of local flow systems in the Fraser lowland are the unconfined Abbotsford–Sumas and Brookswood aquifers.

Intermediate systems include flow within the Pleistocene sediment wedge and deeper portions of the delta (e.g. groundwater flow from the Surrey, Burrard, White Rock, and Tsawwassen uplands adjacent to the delta and the Nicomekl–Serpentine drainage basin). The residence time of groundwater in these systems probably ranges from hundreds to thousands of years.

Regional flow systems derive from groundwater recharge in the Coast Mountains, mostly through fractured metasedimentary and intrusive rocks, and flow deep within the Tertiary and older bedrock (Ricketts and Liebscher, 1994). The residence time of connate water at these depths (hundreds of metres) is unknown but may be on the order of hundreds of thousands of years. It is therefore unlikely that the regional system plays a significant role in short-term groundwater discharge to either subaerial or submarine environments.

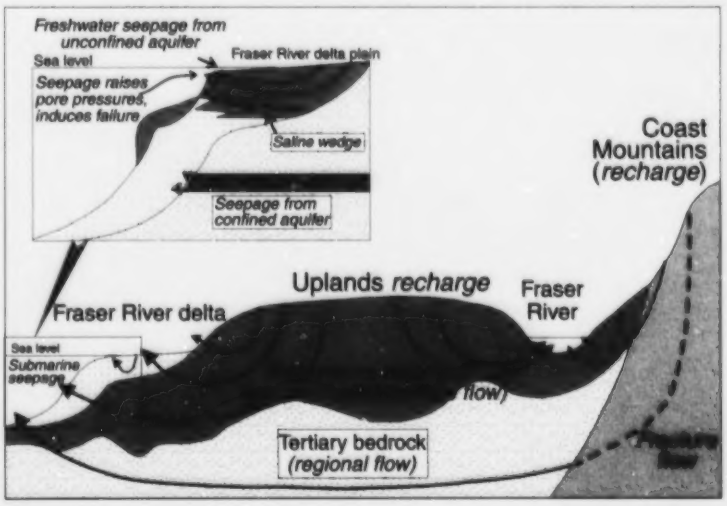

Figure 2.

*Conceptual picture of groundwater flow, showing local, intermediate, and regional flow systems (*from *Ricketts, 1998). Inset depicts effects of submarine seepage on the delta front.*

Delta stratigraphy and hydrostratigraphy

Hydrostratigraphy refers to both the material properties of a rock or sediment body and its hydraulic properties (e.g. porosity, hydraulic conductivity, degree of heterogeneity). Therefore, the boundaries of a hydrostratigraphic unit (aquifer, aquitard) may not coincide with formal lithostratigraphic boundaries. This situation occurs in the Fraser lowland, where more than one formation may be included in a single aquifer, or a single formation (e.g. Capilano Formation) may contain several, hydraulically separate aquifers. Examples pertinent to the Fraser River delta and adjacent groundwater regions include Pleistocene units such as the Quadra Sand and Semiahmoo Drift (Clague, 1977; Armstrong, 1984). In places, these two units are in direct contact and constitute a single aquifer, whereas, at other locations, they are separated by diamicton aquitards.

The modelling process requires simplification of aquifer-aquitard stratigraphy. In Figure 3, aquifers are grouped into aquifer and aquitard complexes; in the simplest case, these are treated as regionally homogenous and isotropic units. The thick, coarse-grained aquifers consist of interbedded sand, gravel, and fine-grained deposits, and the aquitard complexes typically consist of clay, silt, and diamictons.

The stratigraphic scheme illustrated in Figure 3 is a simplification based on lithological and hydraulic criteria. Aquifer and aquitard depths are averages determined from sections illustrated by Armstrong (1984) and the GSC water-well database (Ricketts, 1995).

The stratigraphic succession beneath the modern Fraser River delta comprises three unconformity-bound sequences (Fig. 3):

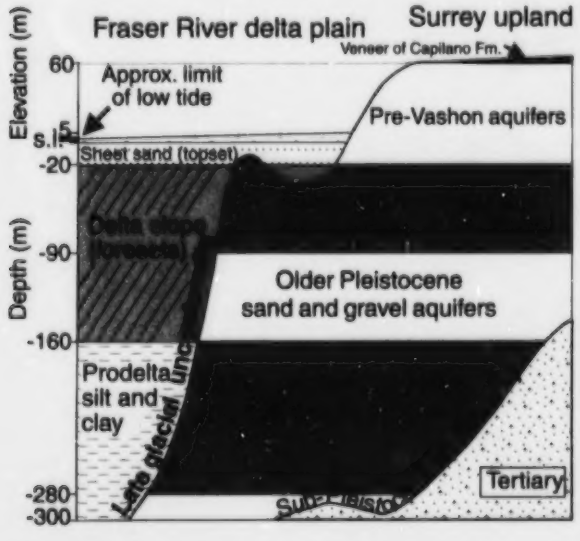

Figure 3. *Generalized hydrostratigraphic-lithostratigraphic architecture, Fraser River delta and uplands (*from *Ricketts, 1998). Abbreviation: s.l., sea level.*

1. The Holocene delta (postglacial) consists of a sediment wedge, up to 300 m thick near the seaward margin of the delta plain and pinching out where it onlaps the Pleistocene Burrard, Surrey, and Tsawwassen uplands (Fig. 1). Relief on the late-glacial unconformity (>300 m) provides evidence of considerable differential erosion during the final stages of the Fraser Glaciation and Sumas glacial advance (Fig. 4; Luternauer and Hunter, 1996). For the purpose of constructing the delta model, the succession was divided into three broad units:

   a) A topset sand unit (sheet-sand aquifer) occurs over a wide area of the delta plain, based on borehole and cone penetrometer coverage (Monahan et al., 1993) and subhorizontal reflections in seismic profiles (Pullan et al., 1989). The sand sheet consists of one or more fining-upward, sand-silt packages that represent a complex amalgamation of laterally migrating distributary channels (Clague et al., 1991). This unit is overlain by a veneer of modern overbank, peat bog, floodplain, and tidal flat deposits.

   b) A delta-slope unit, up to 170 m thick, consists of alternating fine sand, silt, and mud foreset layers that dip 5–7°. This geometry is best seen in seismic profiles (Jol and Roberts, 1988; Pullan et al., 1989).

   c) Prodelta silt and mud total more than 100 m in thickness in a recent, deep borehole (J.L. Luternauer, pers. comm., 1996). The transition from delta slope to prodelta deposits is gradational.

2. Pleistocene deposits beneath and adjacent to the delta represent the western extent of the Fraser lowland wedge. A veneer of Capilano Formation glaciomarine silt, clay, sand, and diamicton covers most of the upland surfaces, but this layer is not included in the model. The Capilano deposits overlie Vashon Drift and pre-Vashon units such as the Quadra Sand (Fig. 5), Cowichan Head Formation, Semiahmoo Drift, and older Pleistocene units (Clague, 1977; Armstrong, 1981). The pre-Vashon aquifer extends into the subsurface and may be represented beneath the delta in borehole GSC 94-3 (Fig. 1; Dallimore et al., 1995).

3. The overall thickness of the Pleistocene succession is controlled by erosion on the late-glacial unconformity and relief on the sub-Pleistocene unconformity (Fig. 3, 4). Depths to the top of the Tertiary bedrock in places exceed 800 m (Hamilton and Ricketts, 1994; Britton et al., 1995). The Pleistocene sediments are at least 700 m thick in some areas.

4. Pleistocene glaciogenic deposits in the Fraser lowland and delta unconformably overlie Neogene and older sandstone, conglomerate, and mudrock (Fig. 3, 4; Mustard and Rouse, 1994).

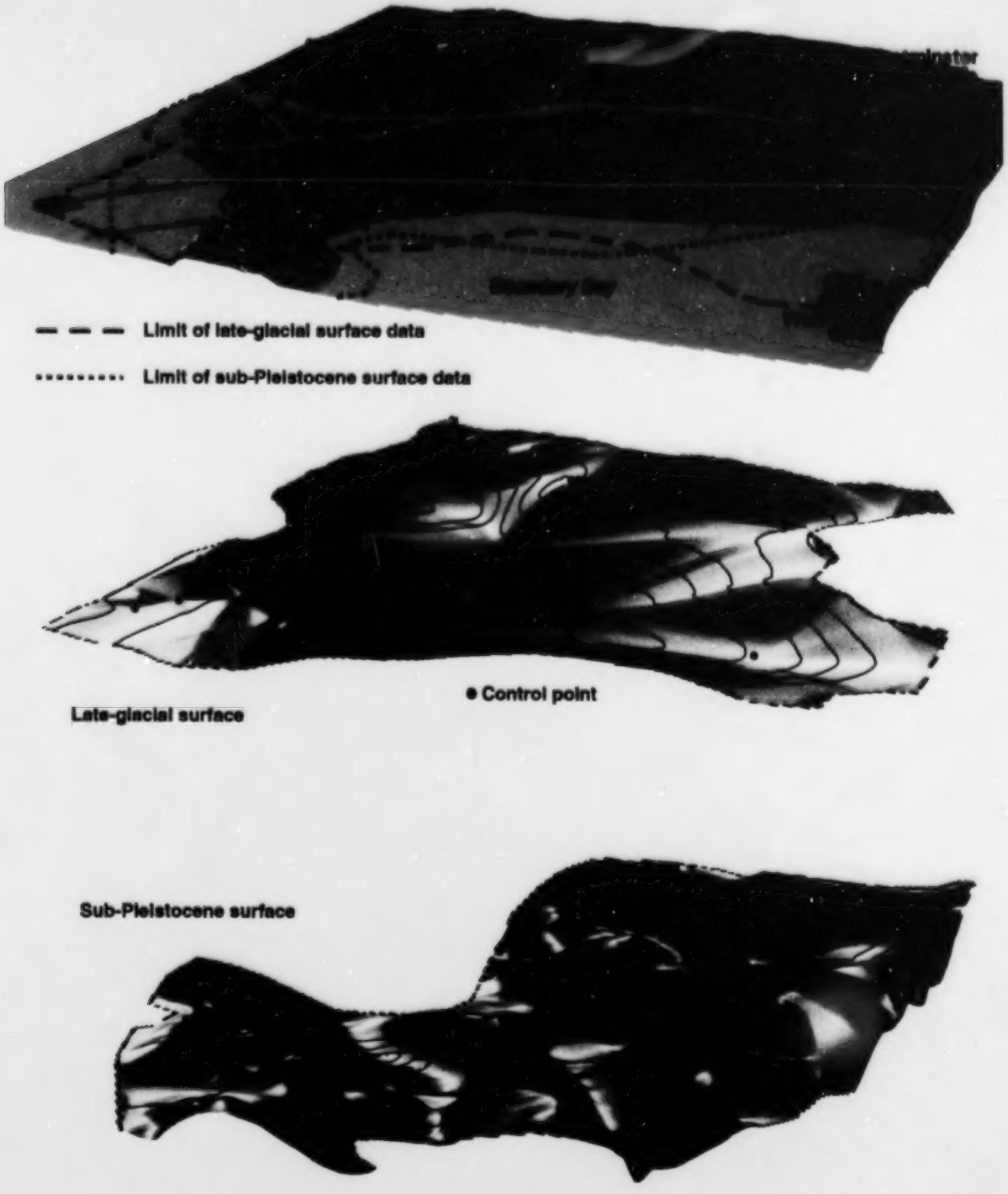

Figure 4. *Graphical reconstruction of the late-glacial and sub-Pleistocene (Tertiary) unconformities relative to modern topography of the Fraser River delta* (from *Ricketts, 1998*)*, viewed from the southeast. Drainage and coastline have been added to the sub-Pleistocene surface for reference. Vertical exaggeration is 5x for the two digital terrain models.*

Figure 5. Quadra Sand, Point Grey. Photograph by J.J. Clague. GSC 1999-063

Flow modelling

Model parameters

A typical example of grid and layer structure, and hydraulic properties–lithology distribution is shown in Figure 6. The model parameters applied are summarized in Table 1. Details on the model parameters can be found in Ricketts (1998).

Results of three-dimensional simulations

Very few groundwater data are available to calibrate the Fraser delta models. Therefore, the model was adjusted to simulate a water table (for layer 3) that approximates the delta plain topography. Groundwater in the sheet-sand aquifer flows toward the Fraser River and the coast from two hydraulic divides (Fig. 7). As expected, the hydraulic potential decreases seaward, with gradients steepest in the upland areas and decreasing gradually across the delta plain. Hydraulic gradients along the divides in the south delta and north delta areas are 0.25 and 0.1 m/km, respectively. Local flow systems are present beneath the delta and uplands. Artesian pressures in the eastern part of the delta plain, which are 2–3 m above the topographic surface in this model, are generated from local flow systems originating in the Surrey and Burrard uplands. These artesian conditions correlate reasonably well with pressures encountered in geotechnical boreholes near the Alex Fraser Bridge over Annacis Island (Bazett and McCammon, 1986). Artesian flow conditions in the Nicomekl–Serpentine valley (derived from uplands recharge) are also simulated, although the modelled head values are higher than observed values. Modelled head values for the pre-Vashon aquifer in layers 3 and 4 also correlate

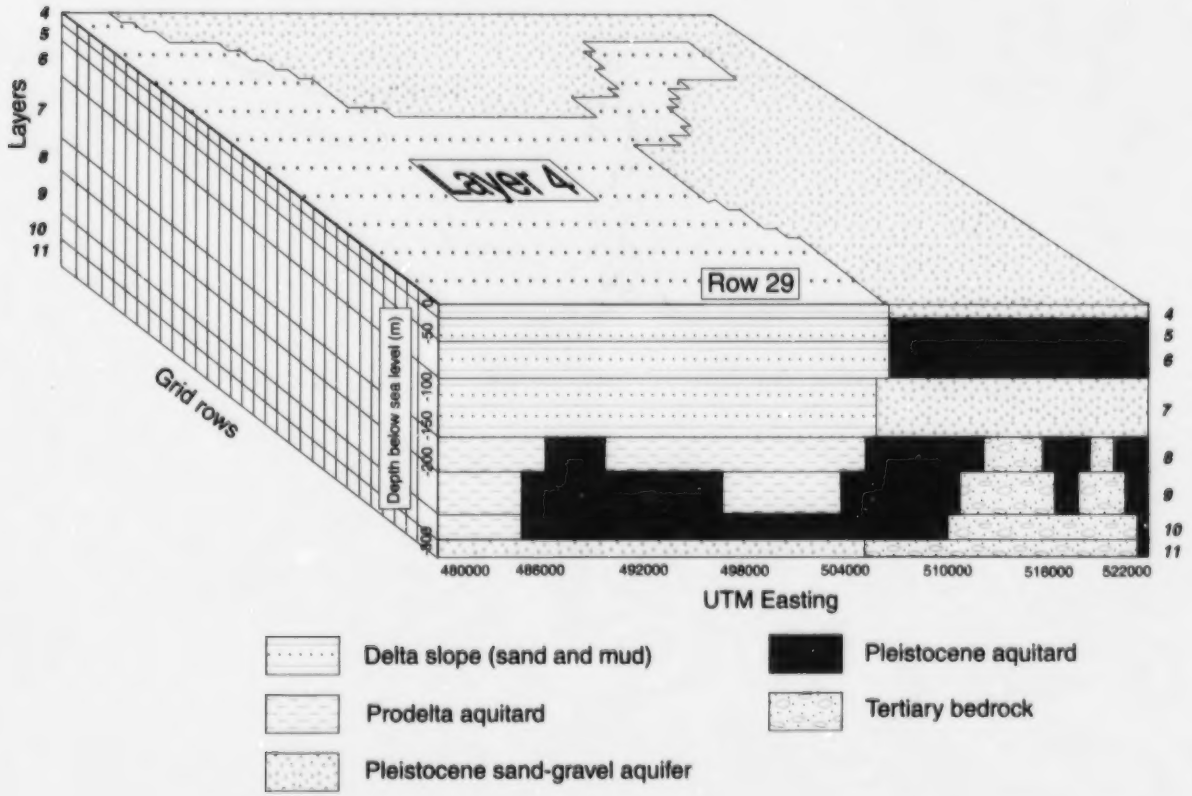

Figure 6. Example of a typical model grid for layer 4 (sheet-sand aquifer) and row 29. Drainage and coastline added for reference.

Table 1. Model parameters for the Fraser River delta.

Model parameter	Values for Fraser River delta model
Elevation	60 m above sea level to 300 m below sea level
Grid size	50 rows by 60 columns, equally spaced
Number of layers	11
Cell faces	Approximately 0.5 km wide
Model boundaries	Coincide approximately with low-tide limits on delta plain and drainage divide, and with recharge areas on uplands
Heads	Constant heads applied to main channel, north arm, and Canoe Passage of the Fraser River, with a maximum of 3.0 m in Parsons channel (Barnston Island); head values in the Fraser River decrease regularly to zero at the low-tide limit (*data from* Ages and Woollard, 1994); constant head of 1.0 m at eastern boundary of Nicomeki–Serpentine valley, decreasing to zero at the coast; constant head of zero applied to the coastal water bodies
Tidal fluctuations	Not taken into account
Recharge	Total recharge over the delta set at 130 mm/a (sum of direct inflow to the water table, minus surface runoff and evapotranspiration); total precipitation in Ladner area averages 950 mm/a); higher recharge rates result in unrealistically high model heads; recharge east of New Westminster set at 250 mm/a
Drains	Delta plain transected by many drains (*see* Fig. 1), used primarily to control the shallow water table by removal of water to the coast; seven drains added to model to simulate removal of water from aquifer
Water withdrawal	Water withdrawal by pumping assumed to be zero (there are very few active wells in the area)

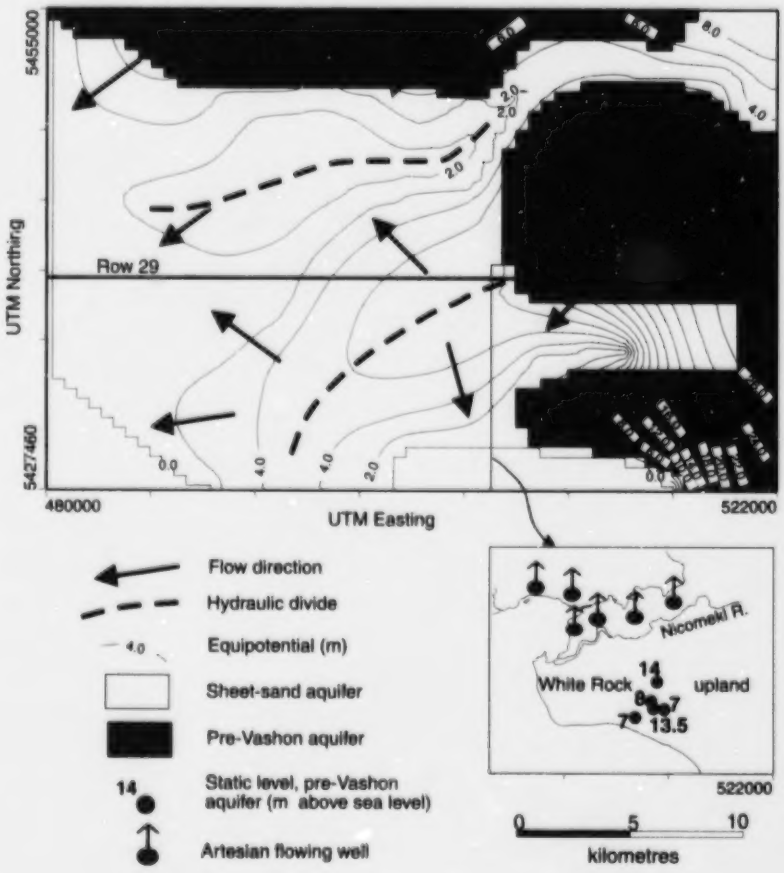

Figure 7. *Predicted potentiometric surface for layer 3 (sheet-sand aquifer;* from *Ricketts (1998)). Inset map shows calibration wells in the White Rock upland area.*

with observed static levels from wells in the White Rock area (inset in Fig. 7; Halstead, 1986; Ricketts and Makepeace, 2000).

Simulated hydraulic gradients in the deeper, confined Pleistocene aquifers (e.g. the aquifer at 280–300 m below sea level in layer 11) are lower than in layer 3, and the local flow systems also appear to have been dampened at these depths in the model. Recharge to the deeper, confined aquifers is probably derived by vertical leakage from glaciomarine clay, silt, and diamictons. Recharge to the deeper Pleistocene aquifers from Tertiary bedrock may also be significant, because the hydraulic conductivity of coarse-grained Tertiary rock is two or three orders of magnitude greater than that of the fine-grained marine and glaciogenic deposits. Furthermore, fluid pressures in fresh water from drill-stem tests at a depth of 930 m in Tertiary sandstone (south of Langley) are about 1000 kPa greater than normal hydrostatic pressures (Jim Britton, Dynamic Oil, pers. comm., 1996), indicating an upward component of flow (for a hydrostatic gradient of 9.5–10 kPa/m).

The model results indicate that groundwater flow in the Fraser delta has a strong upward component beneath the outer part of the delta plain and tidal flats. This is consistent with observations in deep boreholes of artesian pressures in the fine-grained delta slope and prodelta deposits (Christian et al., 1995).

Discussion

Fresh groundwater flow has been documented beneath continental shelves (common in coastal plain and delta successions) and carbonate platforms. Therefore, given sufficient hydraulic potential, either submarine discharge or seepage of fresh water would be expected from morphological features such as a shelf-slope break, delta front, or fault or slump scarp. Some good examples of submarine groundwater flow and seepage have been documented on the Atlantic coast of North America. Freshwater artesian-flow conditions were encountered during drilling through carbonate platform rocks (Floridan aquifer) up to 120 km from the Florida coast and 130 m below the sea floor (Manheim, 1967). Groundwater, derived from the Atlantic uplands, flows to the Atlantic coast through an eastward-thickening, Cretaceous to Holocene aquifer complex, with seepage from local and regional flow systems (e.g. Harsh and Laczniak, 1990; Leahy and Martin, 1993; Richardson, 1994). The extent of this kind of subsea flow depends primarily on aquifer dimensions onshore and offshore, the degree of hydraulic continuity, and, in particular, elevation and topographic relief of the aquifer recharge area. If the topographic drive is insufficient, the seaward flow of groundwater will be counteracted by landward migration of a saline wedge.

In the Fraser River delta, the limited amount of groundwater and borehole data available indicates that seaward flow is possible in both shallow and deep aquifers, although this flow takes place above a saline wedge in the sheet-sand aquifer. Modelled flow beneath the delta is made up of local flow systems originating on the delta itself, and intermediate flow systems for which the driving force is elevated topography in the Fraser lowland. Artesian flow conditions encountered in delta sediments adjacent to the Surrey upland are successfully reproduced in the three-dimensional simulations.

There has been no direct observation of fresh (or brackish) water seepage at the sediment-water interface on the delta front; however, the model does present conclusions that can be tested. Groundwater-flow modelling of the Fraser River delta demonstrates the possibility of submarine freshwater seepage at the delta front. Submarine seepage occurs independently of other marine and submarine processes, such as seismic activity, shear stress generated by storm waves and currents, or clay leaching, but may act in concert with them. Seepage has the effect of increasing sediment buoyancy, thereby reducing its shear strength. Failure will occur if buoyancy exceeds the frictional forces that are active during sediment accumulation. Repeated failure of the delta-front crest at the Sand Heads sea valley (McKenna et al., 1992) may represent the situation where groundwater seepage has operated in tandem with rapid sediment loading.

The three-dimensional model indicates that most of the groundwater flowing to the delta front is derived from surface recharge (precipitation). Although recharge itself is distinctly seasonal, the variations in flux are likely attenuated at depth in the sheet-sand aquifer. Therefore, submarine seepage is probably quasi-continuous, unlike many of the other processes that can generate failure on the delta front.

Maximum simulated flow velocities for the sheet-sand aquifer in layers 3 and 4 are 1.4 and 1.1 m/d, respectively. Average flow velocities will be lower than these simulated values, so groundwater residence times calculated from them will be minimum times; for example, groundwater will take a minimum of about 20 years to travel 10 km. In comparison, residence times for groundwater in the deeper aquifers are about two orders of magnitude greater; however, even these rates are much higher than flow rates in the prodelta and slope aquitards, which range from 0.0001–0.001 m/d. Thus, despite the occurrence of artesian pore pressures in these fine-grained sediments, the fluid-flow rates, and therefore the clay-leaching processes suggested by Christian et al. (1995), would be extremely slow.

Electrical-conductivity profiles across the delta plain indicate mixing of seaward-flowing groundwater and the saline wedge, resulting in a highly irregular saline migration front (Hunter et al., 1994). Groundwater flow toward the delta front appears to be focused into zones or plumes of fresh water that mix with the saline groundwater (*see* Ricketts, 1998, Fig. 11). Repeated failure of the delta front at Sand Heads (Fig. 1, main channel; Luternauer and Finn (1983)), may result from groundwater flow and seepage focused beneath and adjacent to the main channel of the Fraser River.

BROOKSWOOD AQUIFER

Langley, with a population in 1991 of 83 000, depends heavily on groundwater. The Brookswood aquifer, south of the Nicomekl–Serpentine valley, is the principal source of shallow groundwater for domestic, agriculture, forestry, and

light industry users. With more than 500 pumping wells in an area of about 38 km^2, the Brookswood is one of the most utilized unconfined aquifers in the Fraser lowland, second only to the Abbotsford–Sumas aquifer. In their assessment of 'aquifer risk', Kreye and Wei (1994) classified the Brookswood aquifer as type 1A, the category for highest demand (relative to productivity) and highest vulnerability (to contamination). Indeed, it has been known for some time that Brookswood groundwater contains elevated concentrations of nitrate, derived primarily from agricultural uses of manures. Recent studies of observation wells by the British Columbia ministries of Environment and Health showed median and mean nitrate-nitrogen levels of about 1.0 and 10.0 mg/L, respectively, with one well registering 72.7 mg/L (Carmichael et al., 1995). Twenty-five per cent of studied wells in the Brookswood aquifer contained nitrate-nitrogen greater than 10.0 mg/L, the maximum concentration permitted by the guidelines for Canadian drinking water (McNeely et al., 1979; Canadian Council of Resource and Environment Ministers, 1987).

How long will contaminants like nitrates or pesticides reside in the groundwater system? How will they be dispersed? Where will they end up? Remediation of groundwater contamination, to be cost effective, requires knowledge of the geological conditions in which groundwater occurs, which in turn will provide answers to these questions. In this project, geological studies have been combined with geophysical surveys and groundwater modelling to 1) examine the efficacy of different techniques for unravelling aquifer-aquitard architecture, and 2) develop preliminary models of groundwater flow.

Geomorphology and aquifer recharge

The Brookswood proglacial delta rises abruptly above the Nicomekl River flood plain, to about 30 m above sea level at its northern limit and more than 65 m at its southern margin (Fig. 8). Its northern edge is a steep face that probably mimics the depositional face of the glaciofluvial delta that prograded into the sea between 12 000 and 11 000 BP. The southern and eastern limits of the aquifer pinch out against clay, silt, and till aquitards (Fort Langley and Capilano formations). The aquifer surface has little relief, except near the margins where it is incised by streams. Hummocky ground near the eastern margin, corresponding to unit Sd of Armstrong and Hicock (1980a, b), is underlain by ice-contact deposits.

Two streams figure prominently on the Brookswood aquifer: Anderson Creek, which drains into the Nicomekl River, and the Campbell River, which meanders in the opposite direction to Semiahmoo Bay. The upstream portion of the Campbell River is incised into clay-till uplands. Both streams recharge the aquifer during the wet winter months, but stream-water supply during the summer relies mostly on the local water table. Observations along their stream beds indicate good hydraulic connection with the aquifer. This is illustrated in observation wells near Anderson Creek, where rising water-table levels correspond to the period of peak stream discharge from November to April, with maximum levels in March and April (Halstead, 1978).

Some reaches become dry during the summer months (Fig. 9a). Anderson Creek, from about 24th Avenue to north of its intersection with 200th Street, was a dry gravel bed in August and September 1995. During this period, the Campbell River was also dry north of 24th Avenue and between 200th and 204th streets. Surface flow in the Campbell River resumed just west of 200th Street, where the stream bed intersected the (summer) water table. Groundwater, derived from trenches in Stoke's gravel pit, also flows southeast into the Campbell River.

Many of the gravel pits in the Brookswood aquifer are no longer used. Most were excavated to the local water table and several have since been developed into small residential lakes, surrounded by houses. Lake levels fluctuate in concert with local water tables, responding to seasonal changes in recharge (Fig. 9b).

Annual precipitation over most of the aquifer averages 1200 mm, compared to 1450 mm at Langley and 900–1200 mm over the Fraser River delta. The Brookswood aquifer is recharged primarily by direct precipitation (about 55%) and infiltration from streams (about 19%, but seasonally dependent; estimates from Dakin (1994)). Some recharge is probably derived from surface runoff from clay uplands bordering the western and southeastern aquifer margins (21%). Total recharge is approximately 13 x 10^6 m^3/a (Dakin, 1994). Hydrographs from the Brookswood aquifer show a close correspondence between winter precipitation (also stream discharge) and high static levels in observation wells (Fig. 10). Water tables reach their nadir in October and November.

Hydrostratigraphy and sedimentology

The Brookswood and Abbotsford–Sumas aquifers are the largest unconfined aquifers in the Fraser lowland. The Abbotsford–Sumas is the larger of these, covering an area of about 200 km^2 (about 100 km^2 in British Columbia and 100 km^2 in Washington). The Brookswood covers about 50 km^2 in total, but the southeastern segment, composed of flowtill and other ice-contact deposits, is little more than a veneer (<10 m thick); therefore, the area of the main aquifer body is 38–40 km^2 (Fig. 11). The Brookswood aquifer, like the Abbotsford–Sumas, occupies a stratigraphic position within the Sumas Drift (Armstrong, 1981), which was deposited during a brief glacial readvance near the end of the Fraser Glaciation, about 11 000 BP. Most of the aquifer consists of a complex amalgamation of fluvial, delta, and fan-delta deposits, and subordinate ice-contact deposits, corresponding to hydrostratigraphic unit C of Halstead (1986). The proglacial delta complex prograded west and northwest from a prominent meltwater river, the remnants of which extend eastward from the southern edge of the aquifer. The aquifer thins, onlaps, and partly interfingers with fine-grained Fort Langley and Capilano formation deposits along its southern margin. The southwestern margin also overlaps Capilano deposits along an east-trending topographic high that extends from White Rock to Hazelmere.

Aquifer delineation using geophysics

Geophysical surveys have also served to delineate the aquifer hydrostratigraphy (Fig. 11). Combinations of various methods, such as ground-penetrating radar (GPR), electromagnetic (EM), high-resolution seismic reflection, and gravity, have been used at some locations. The northern and western aquifer margins, also referred to as the seepage face, represent an abrupt aquifer boundary. Electromagnetic surveys across this boundary (28th and 40th avenues) have successfully outlined the main aquifer body (sand and gravel), as well as a sandy layer several metres thick that extends beyond the seepage face (Fig. 12; Best and Todd, 2000; Roberts et al., 2000). The aquifer here overlies a low-resistivity layer (Fort Langley Formation). Ground-penetrating radar profiling across the same margin (40th Avenue; Roberts et al. (2000)) shows the sand beyond the seepage face to be about 5 m thick and dominated by horizontal or slightly inclined reflections; the sand facies may be the product of erosion from the aquifer, or bottomset beds associated with actual delta growth. A detailed gravity survey at the same location (5 m spacings) shows the corresponding sediment density differences at the aquifer margin, wherein the gravity anomaly can be resolved to within 0.5 mGal (D. Seemann, pers. comm., 1996).

Ground-penetrating radar profiles along the contact where Brookswood deposits overlap the White Rock–Hazelmere high (e.g. 20th Avenue) clearly illustrate the onlap geometry (Roberts et al., 2000). Electromagnetic profiles at the same site show a high-resistivity aquifer layer overlying low-resistivity Fort Langley deposits and pinching out against less conductive Vashon Drift (Best and Todd, 2000).

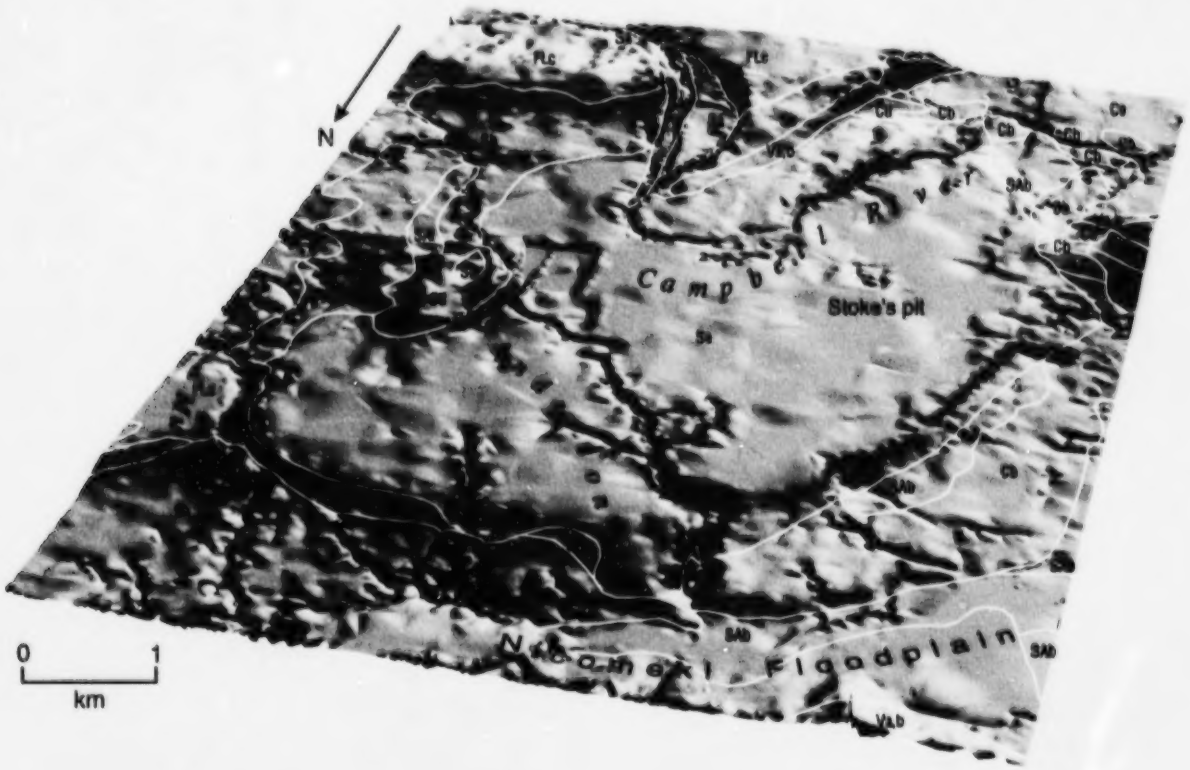

Figure 8. *Geomorphic expression of the Brookswood aquifer and the bordering uplands and Nicomekl River floodplain, constructed using an ARC/INFO® triangulated irregular network (TIN) from a Terrain Resource Inventory Mapping (TRIM) digital elevation model (DEM). Surficial geology units* (from *Armstrong and Hicock, 1980a, b*)*: SA, postglacial Salish sediments (subunits b and e, lowland peat; subunit i, mountain-stream marine-deltaic medium to coarse gravel; subunit k, lowland-stream channel-fill sand to gravel); S, Pleistocene Sumas Drift (subunit a, outwash sand and gravel; subunits b and d, ice-contact gravel and sand; subunit e, raised proglacial deltaic gravel and sand); FLc, Pleistocene Fort Langley Formation (glaciomarine stony clayey silt to silty sand); C, Pleistocene Capilano sediments (subunit b, raised-beach medium to coarse sand; subunit d, marine and glaciomarine stony to stoneless silt loam to clay loam; subunit e, mainly marine silt loam to clay loam); V, Pleistocene Vashon Drift (subunit a, lodgment till and minor flow till; subunit b, glaciofluvial sandy gravel and gravelly sand outwash and ice-contact deposits).*

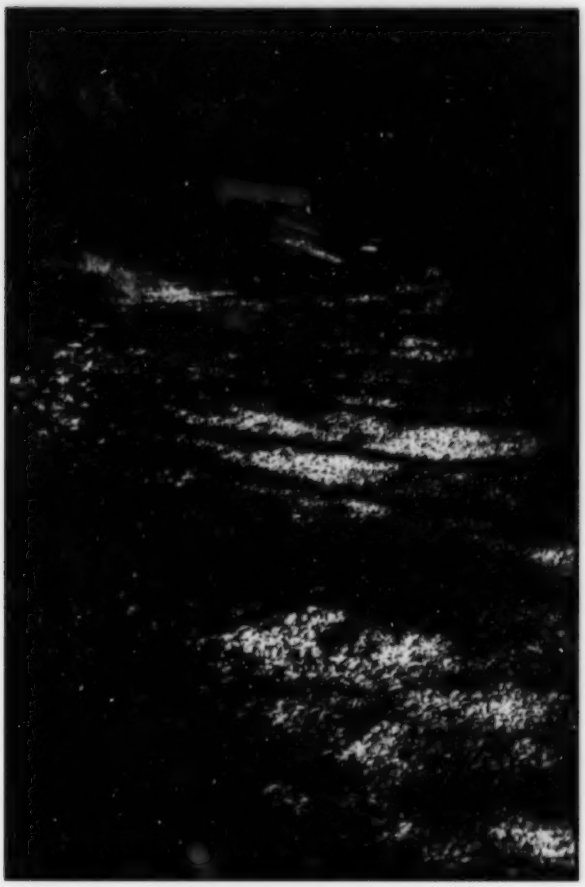

Figure 9. a) *Dry gravel and sand river bed on a reach of Anderson Creek, during the summer months when the local water table dropped below surface level. GSC 1999-062A* ***b)*** *Old gravel pit on 24th Avenue and 200th Street, excavated to expose the water table and used as a recreational lake; seasonally high water-table levels are preserved as raised shorelines. GSC 1999-062B*

The EM data also show that Brookswood deposits at this location are more conductive than is common for the aquifer, indicating a compositional change in the sediments.

The Stoke's municipal gravel pit (Fig. 11) also affords an ideal location for testing different geophysical methods (Fig. 13). Ground-penetrating radar signal penetration here is 20–25 m, thus complementing the seismic-reflection method's penetration depth of about 40 m to more than 500 m; the upper 40 m of most high-resolution seismic profiles in the Fraser lowland are not resolved because of acoustic noise (Rea et al., 1994a; Pullan et al., 1995). The GPR image also records the water table (at a depth of about 3 m) crosscutting large, dipping foreset strata. Electromagnetic results at the same location indicate a sandy layer (high resistivity) to a depth of 40–50 m and a change to significantly lower resistivity between 120 and 150 m in depth (Best et al., 1995; Best and Todd, 2000). The latter corresponds to a stratigraphic onlap surface, or unconformity, at about the same depth as in the seismic record (Fig. 13). At Stoke's pit, therefore, Brookswood aquifer geometry can be reconstructed in two dimensions. The topmost, high-resistivity layer in the EM profile demonstrates that the base of the aquifer, approximated here by the base of the sandy layer, has more than 10 m of relief over the profile length.

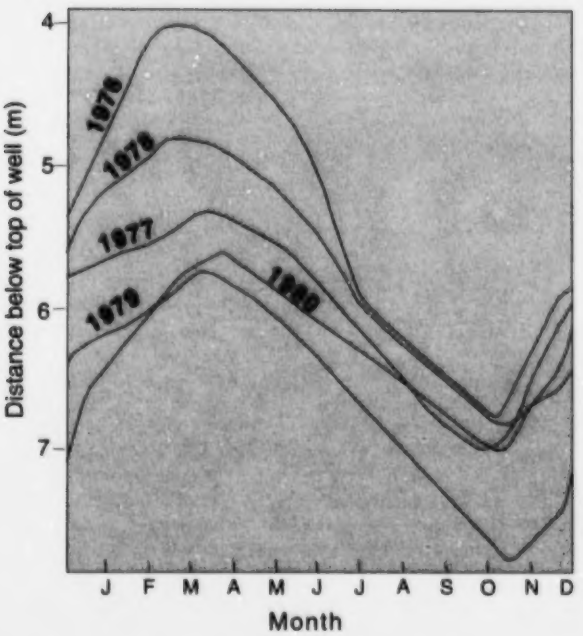

Figure 10.

Hydrographs from an observation well in the Brookswood aquifer, showing seasonal variation in static levels.

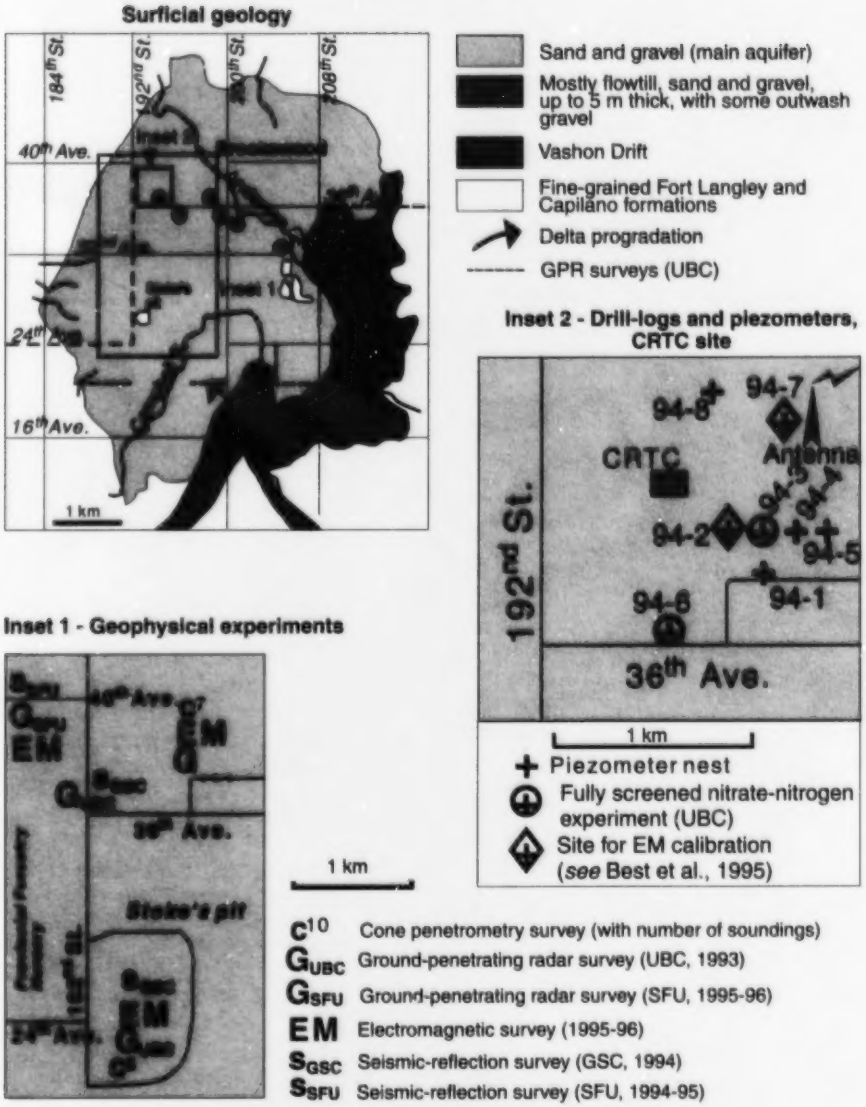

Figure 11. *Surficial geology of the Brookswood aquifer* (modified from *Armstrong and Hicock, 1980a, b*), *and locations of geophysical surveys conducted over the aquifer. Note that the University of British Columbia (UBC) ground-penetrating radar (GPR) survey lines (Rea et al., 1994b; Rea and Knight, 2000) are shown on the surficial geology map. Observation wells are identified by circled numbers and are listed in Table 2; N denotes the three wells of the Provincial Forestry Nursery. Other abbreviations used: C, cone penetrometry; EM, electromagnetic; GPR, G, ground-penetrating radar; GSC, Geological Survey of Canada; S, seismic reflection; SFU, Simon Fraser University.*

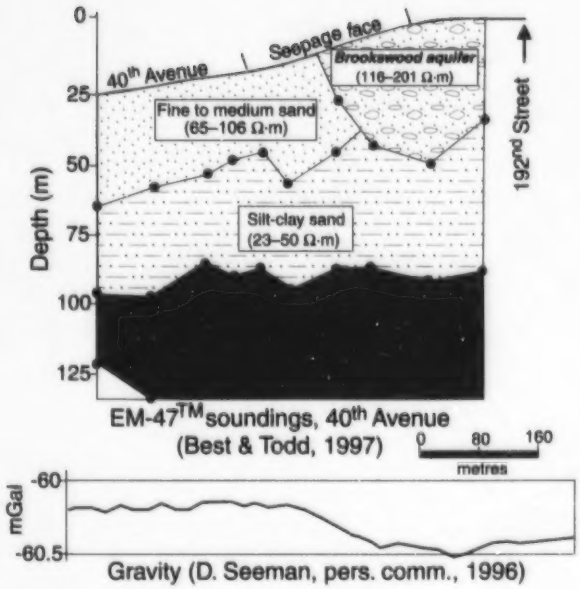

Figure 12. *Electromagnetic and gravity profiles across the northwest (seepage) margin of the Brookswood aquifer, along 40th Avenue (see Fig. 11 for location;* modified from *Best and Todd (2000), D. Seemann (pers. comm., 1996)).*

Combined GPR (Rea, 1996) and EM (Best and Todd, 2000) surveys were also undertaken near the southeastern pinch-out of the aquifer. These experiments further illustrate the value of using different geophysical methods to unravel stratigraphic and hydrostratigraphic problems (Fig. 14). Initial GPR surveys indicated a possible sand pinch-out against a near-surface clay layer (left side of profile). The total thickness of both sand and clay layers could not be determined. Subsequent EM surveys over the same location showed that the high-resistivity sandy layer in fact continues to a depth of 30 m, and that the GPR signal is attenuated by a thin clay layer overlying the sand.

Sedimentology

Common sedimentological features in the Sumas deposits are fan deltas (several metres thick), characterized by large-scale sand and gravel foreset beds that dip 20–30°, and trough-crossbedded topset beds (Fig. 15a). Some foresets are draped by mud veneers. Large foresets of sand and gravel, extending more than 200 m laterally in the Brookswood area, have also been identified in the subsurface by ground-penetrating radar (Rea et al., 1994a, b; Rea and Knight, 2000). Soft-sediment deformation is present locally (Fig. 15b) but is less common than in the Abbotsford–Sumas aquifer, where flowtill deposits, dewatering structures (overturned and folded bedding), and small faults (possibly generated during earthquakes) occur in the glaciofluvial facies. Fluvial channels are also common and are filled with coarse gravel or mud and silt, the latter representing abandoned channel fills. Braided, glacial-outwash stream deposits contain multiple sets of planar-tabular crossbedded gravel and sand, representing channel bars (Fig. 16a, b).

At a few localities, shallow-dipping, sand-mud foreset couplets contain lenticular and flaser ripple bedding (e.g. in Stoke's pit, and a now-abandoned gravel pit immediately north of the CRTC site on 192nd Street; Fig. 11, 17). This association of structures is similar to some modern estuary-channel–point-bar facies, hinting that weak tidal currents, possibly in an estuarine environment, were active in some parts of the Brookswood delta complex (Ricketts and Jackson, 1994).

Ground-penetrating radar facies

Facies identified using GPR (radar facies) contain the fundamental depositional types noted above, except that 1) radar facies boundaries, which depend primarily on contrasts in dielectric constant, commonly differ from those of sedimentary facies; and 2) the geometry and internal organization of reflections in a radar facies may resemble more than one kind of sedimentary facies (Rea, 1996; Rea and Knight, 2000). For example, radar facies units characterized by horizontal reflections may be either delta-topset or crossbedded sheetflood units of fluvial origin, the reflections in this case corresponding to approximately horizontal surfaces that bound sets of trough and planar crossbeds. Channel-like radar facies generally have concave upward surfaces and horizontal or dipping internal reflections that intersect part of the channel margin. Units containing large-scale dipping reflections, which can be traced several tens of metres in some profiles, are good candidates for fan-delta accretionary foreset beds (Fig. 13).

Hydrological database

Water wells and boreholes, of which there are about 500 in the Brookswood aquifer, provide data on hydrostratigraphy, water-table elevation, well yields, and, in a few cases, hydraulic properties. Mapping of the Brookswood aquifer using a GIS (ARC/INFO®) is described in detail in Makepeace and Ricketts (2000). The subsurface extent of the aquifer has been determined at different elevations, the two examples illustrated in Figure 18 representing 'slices' at 20 and 40 m above sea level (*from* Makepeace and Ricketts, 2000). Maps and stratigraphic cross-sections generated during this exercise were used to determine model grid-size and layer geometry.

Well static levels were used to calibrate the models. It is assumed that the static levels approximate the regional water table; however, as a cautionary note, it is possible that levels in some wells were measured in areas of significant drawdown by neighbouring wells. Wells particularly prone to this effect would be those located near high-capacity community and irrigation wells.

Like many parts of the Fraser lowland and delta, there are very few published estimates of hydraulic conductivity for the Brookswood aquifer. Transmissivity values, derivedfrom

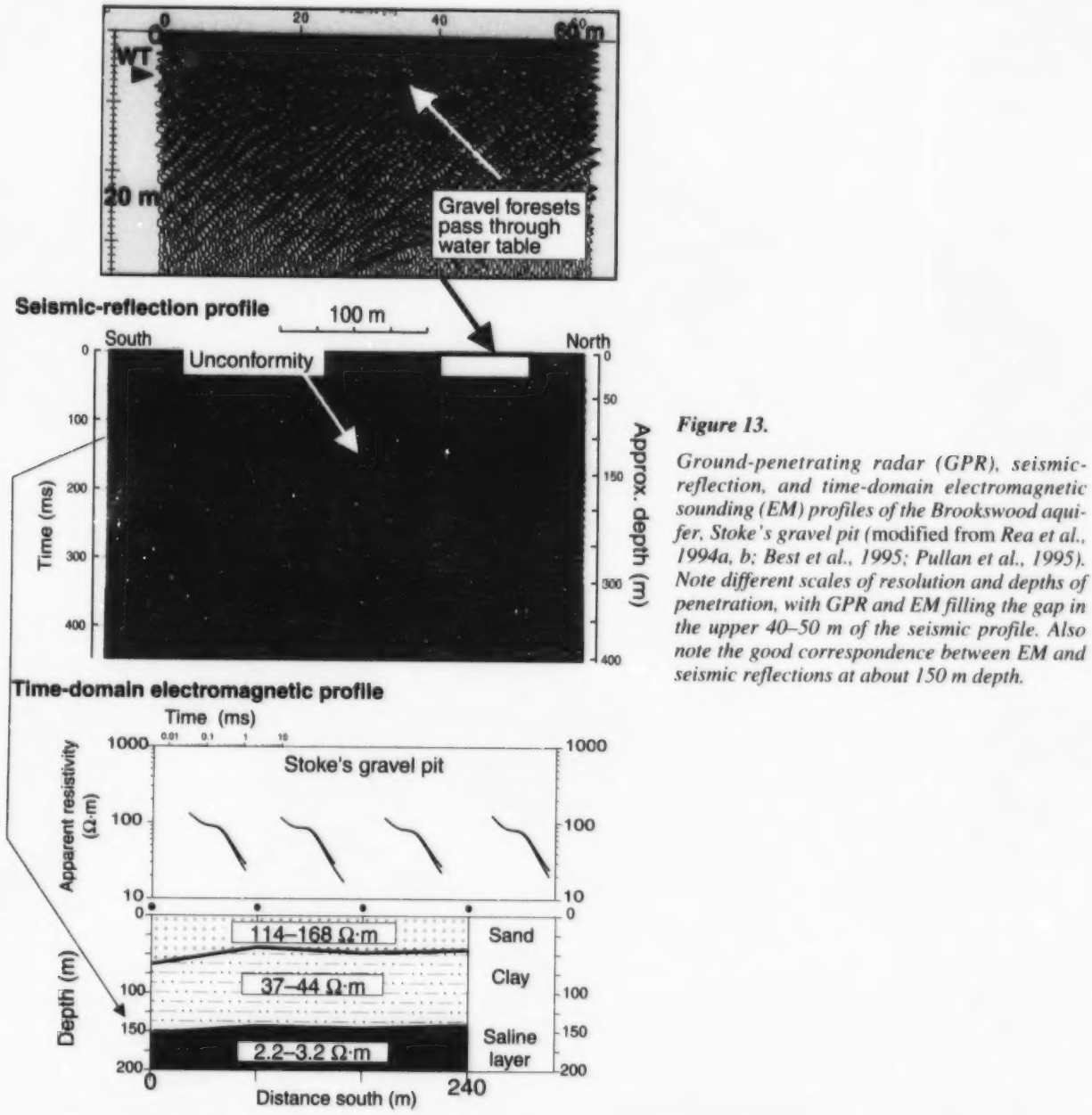

Figure 13.

Ground-penetrating radar (GPR), seismic-reflection, and time-domain electromagnetic sounding (EM) profiles of the Brookswood aquifer, Stoke's gravel pit (modified from *Rea et al., 1994a, b; Best et al., 1995; Pullan et al., 1995*). *Note different scales of resolution and depths of penetration, with GPR and EM filling the gap in the upper 40–50 m of the seismic profile. Also note the good correspondence between EM and seismic reflections at about 150 m depth.*

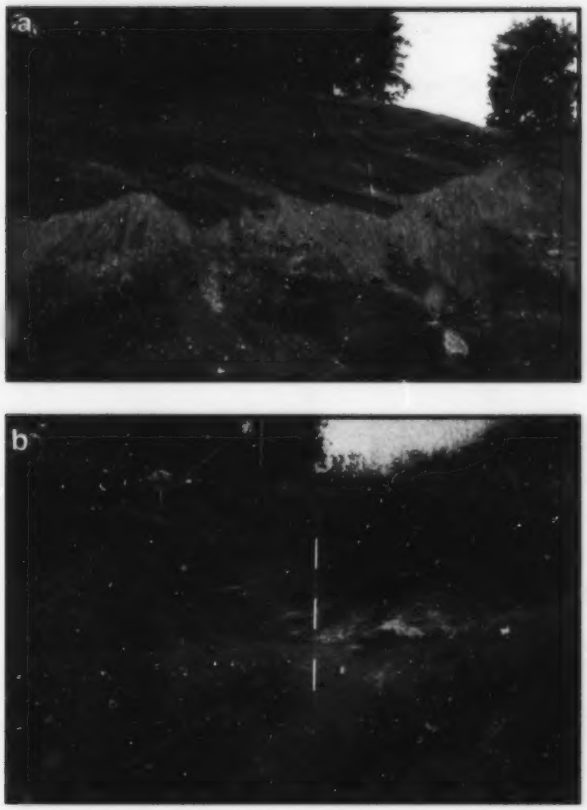

Figure 15. a) *Large fan-delta–like accretionary foreset beds of gravelly sand exposed in an abandoned gravel pit on 16th Avenue, just east of the Campbell River. There is a clear demarcation between the foreset and topset layers, the latter consisting of trough crossbeds. Measuring pole marked in feet. GSC 1999-062C* ***b)*** *Deformed glaciofluvial-delta deposits (same location as Fig. 15a). Folding may have developed beneath the ice (i.e. as ice-contact deposits, although diamictons were not seen at this locality), through gravitational slumping (the folds are down-dip of the fan delta), or through seismically triggered dewatering (similar structures are present in the Abbotsford–Sumas aquifer). Measuring pole marked in feet. GSC 1999-062D*

Figure 14.

Electromagnetic (EM; Best and Todd (2000)) and ground-penetrating radar (GPR; Rea (1996)) surveys near the south-east pinch-out margin of the Brookswood aquifer (208th St. and 20th Ave.) illustrate the value of combining different geophysical methods to solve hydrostratigraphic problems. The GPR data indicate a possible sand pinch-out against a near-surface clay layer (left side of profile). However, the EM survey shows that the high-resistivity sandy layer in fact continues to 30 m depth, and that the GPR signal is attenuated by a thin clay layer overlying the sand. Note the vertical scale difference between the EM and GPR profiles.

pumping tests, are available for production wells in the Municipality of Langley, located just south of Brookswood, and the Provincial Forestry Nursery (Table 2; Fig. 11). Transmissivity is a measure of the ability of an aquifer to permit lateral flow, and is the product of hydraulic conductivity and aquifer thickness; in the case of an unconfined aquifer, aquifer thickness would be the saturated thickness (Freeze and Cherry, 1979; Belitz and Bredehoeft, 1988). Hydraulic conductivities for the Brookswood wells range from 0.004 to 0.2 cm/s, and average 0.07 cm/s (Halstead, 1986). These are average values over the depth of each well.

Hydraulic conductivity (K) can also be estimated using sediment grain-size distribution, employing the empirical expression $K = A (d_{10})^2$, derived by Hazen (*see* Freeze and Cherry, 1979). From cumulative grain-size distribution curves of medium- to fine-grained sand, the particle diameter (d_{10}) is read at the point where 10% (by weight) of the sample is finer and 90% is coarser; A is a constant. The method was used on 14 samples from three boreholes at the CRTC property (Fig. 19). Calculated hydraulic conductivities range from

Figure 16. a) *Braided glaciofluvial deposits on the east-facing wall of Stoke's gravel pit. Large planar crossbed sets and subhorizontal bedding accumulated as transverse bars. Field notebook (circled) indicates scale. GSC 1999-062E* ***b)*** *Detail of braided, transverse-bar crossbedding, Stoke's gravel pit. Circled cobble is 10 cm across. GSC 1999-062F*

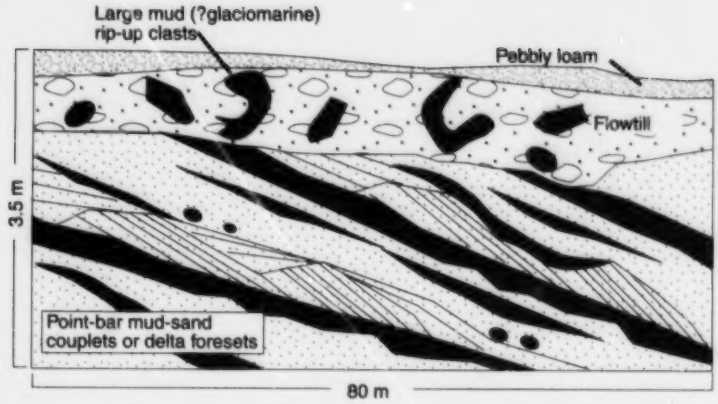

Figure 17.

Field sketch of large sand (crossbedded)-mud foreset couplets that are possible candidates for estuarine point bars, exposed in abandoned gravel pit north of CRTC site, east of 192nd Street (from *Ricketts and Jackson, 1994*).

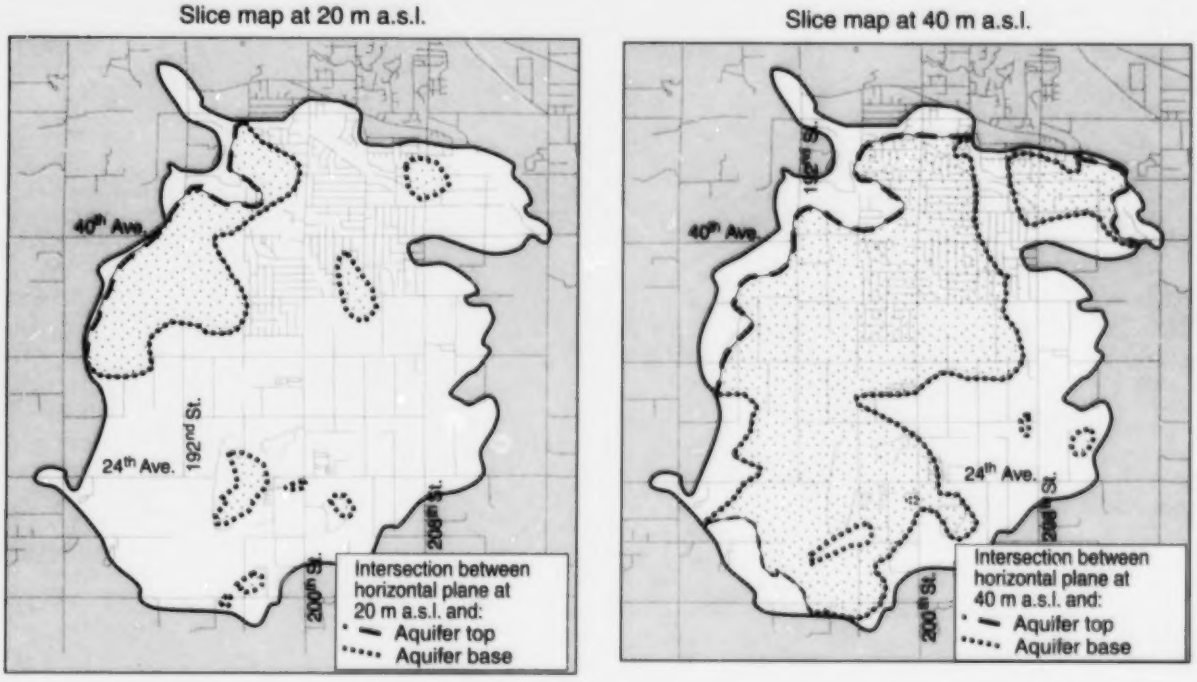

Figure 18. *Sample 'slice' maps of the subsurface extent (stippled areas) of the Brookswood aquifer at 20 and 40 m above sea level. Note that the aquifer outline is based entirely on evidence from water wells in the map area, rather than the surficial geology outline mapped by Armstrong and Hicock (1980a, b). Aquifer mapping is discussed in Makepeace and Ricketts (2000).*

Table 2. Hydraulic conductivities calculated from transmissivity data in Halstead (1986). Well locations shown on Figure 11.

Observation well	Depth (m)	Static level (m)	Average transmissivity (m^2/s)	Hydraulic conductivity (cm/s)	Yield (L/s)	Year
B.C. Forestry Nursery	28	5.5	0.002	0.009	20	-
B.C. Forestry Nursery	28.4	5.4	0.045	0.196	38	1980
B.C. Forestry Nursery	43.9	4.3	0.038	0.091	38	1980
Sully well 2	20	2	0.036	0.2	38	1960
Langley Municipality well 5	23.7	2	0.007	0.032	10	1971
Langley Municipality well 4	27	-	0.004	0.015	16	1973
Langley Municipality well 8	35.4	4.5	0.004	0.013	30	1979
Langley Municipality well 7	57.9	5.3	0.002	0.004	30	1974

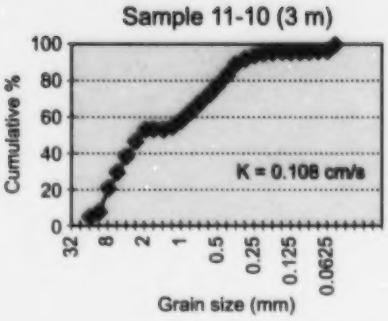

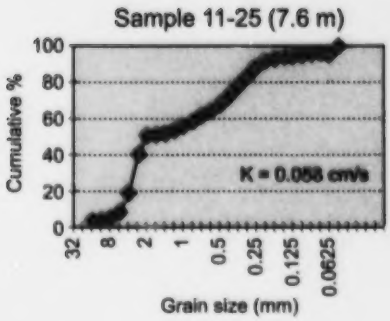

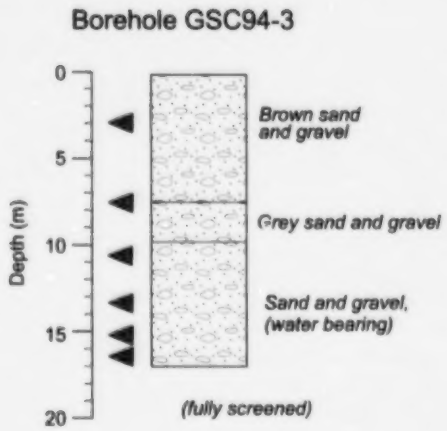

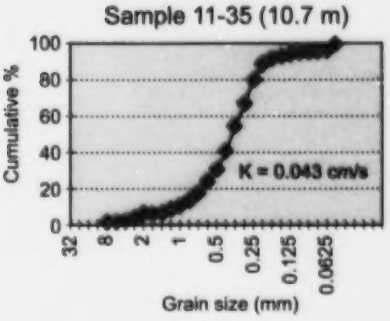

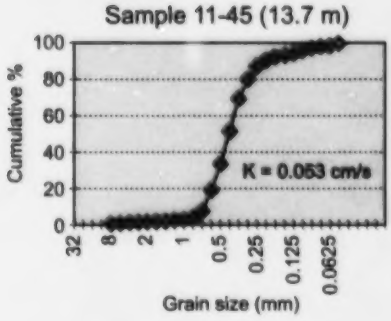

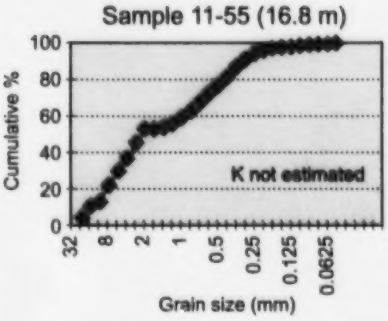

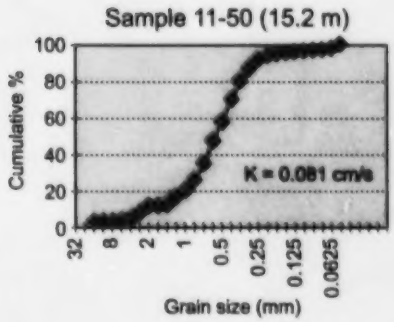

Figure 19a.

Figure 19. *Grain-size distributions and calculated hydraulic conductivities for selected samples from three boreholes on the CRTC property (locations shown on Fig. 11):* ***a)*** *GSC94-3,* ***b)*** *GSC94-6,* ***c)*** *GSC94-7.*

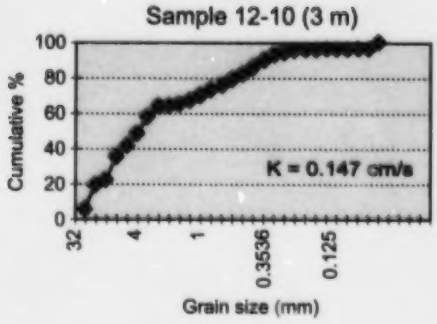
Sample 12-10 (3 m)
Cumulative %
100
80
60
40
20
0
K = 0.147 cm/s
32
4
1
0.3536
0.125
Grain size (mm)

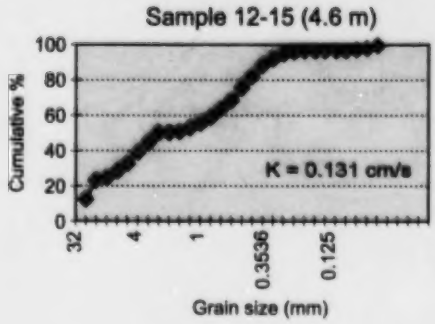
Sample 12-15 (4.6 m)
Cumulative %
100
80
60
40
20
0
K = 0.131 cm/s
32
4
1
0.3536
0.125
Grain size (mm)

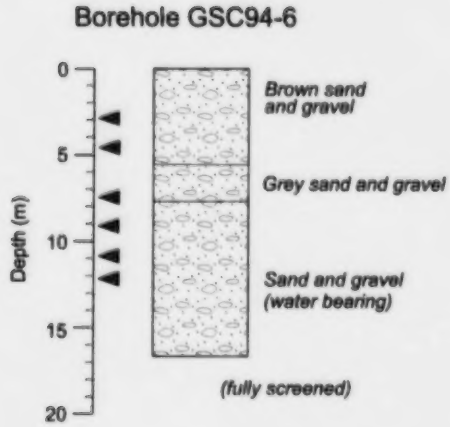
Borehole GSC94-6
Depth (m)
0
5
10
15
20
Brown sand and gravel
Grey sand and gravel
Sand and gravel (water bearing)
(fully screened)

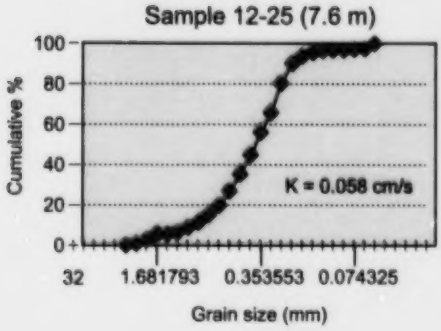
Sample 12-25 (7.6 m)
Cumulative %
100
80
60
40
20
0
K = 0.058 cm/s
32
1.681793
0.353553
0.074325
Grain size (mm)

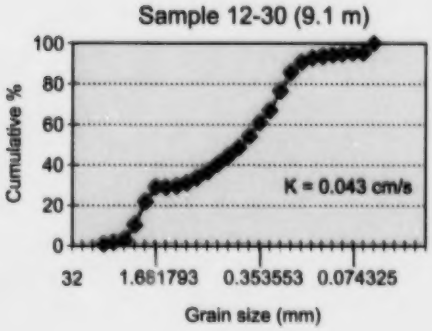
Sample 12-30 (9.1 m)
Cumulative %
100
80
60
40
20
0
K = 0.043 cm/s
32
1.681793
0.353553
0.074325
Grain size (mm)

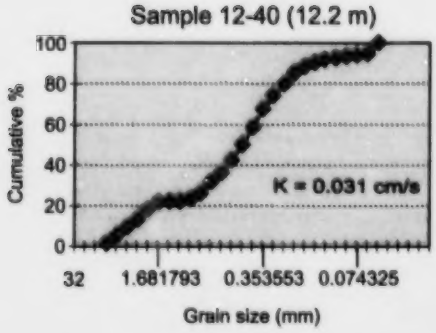
Sample 12-40 (12.2 m)
Cumulative %
100
80
60
40
20
0
K = 0.031 cm/s
32
1.681793
0.353553
0.074325
Grain size (mm)

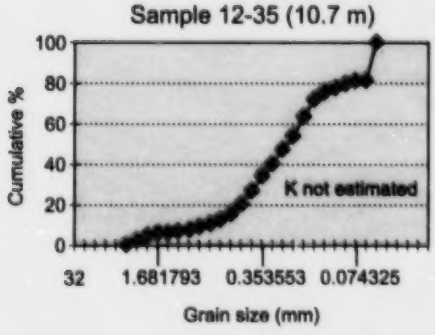
Sample 12-35 (10.7 m)
Cumulative %
100
80
60
40
20
0
K not estimated
32
1.681793
0.353553
0.074325
Grain size (mm)

Figure 19b.

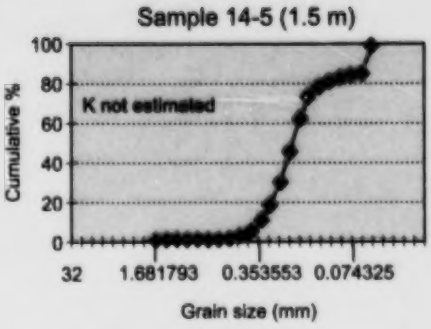
Sample 14-5 (1.5 m)
Cumulative %
K not estimated
100
80
60
40
20
0
32
1.681793
0.353553
0.074325
Grain size (mm)

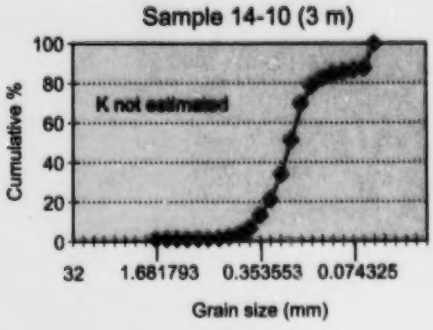
Sample 14-10 (3 m)
Cumulative %
K not estimated
100
80
60
40
20
0
32
1.681793
0.353553
0.074325
Grain size (mm)

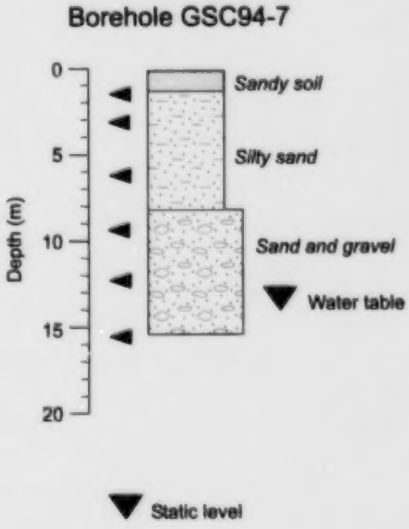
Borehole GSC94-7
Depth (m)
0
5
10
15
20
Sandy soil
Silty sand
Sand and gravel
Water table
Static level

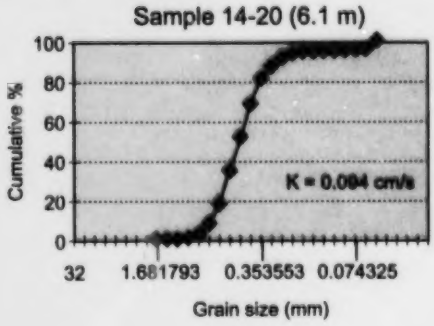
Sample 14-20 (6.1 m)
Cumulative %
K = 0.094 cm/s
100
80
60
40
20
0
32
1.681793
0.353553
0.074325
Grain size (mm)

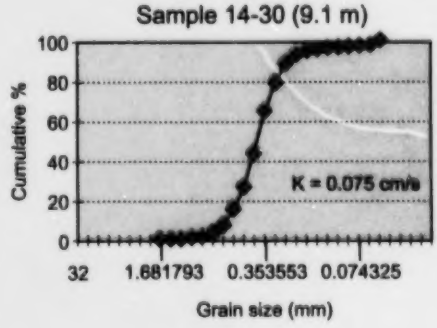
Sample 14-30 (9.1 m)
Cumulative %
K = 0.075 cm/s
100
80
60
40
20
0
32
1.681793
0.353553
0.074325
Grain size (mm)

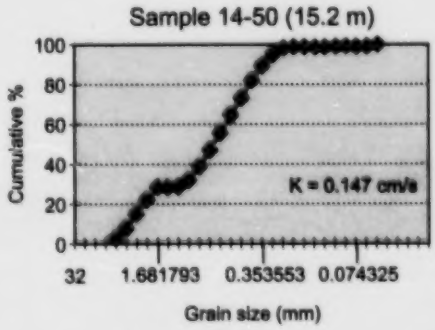
Sample 14-50 (15.2 m)
Cumulative %
K = 0.147 cm/s
100
80
60
40
20
0
32
1.681793
0.353553
0.074325
Grain size (mm)

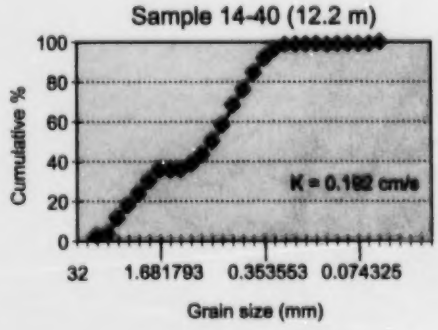
Sample 14-40 (12.2 m)
Cumulative %
K = 0.182 cm/s
100
80
60
40
20
0
32
1.681793
0.353553
0.074325
Grain size (mm)

Figure 19c.

Table 3. Model parameters for the Brookswood aquifer.

Model parameter	Values for Brookswood aquifer model
Elevation	70 m above sea level to 20 m below sea level
Grid size	50 rows by 50 columns, equally spaced
Number of layers	4
Cell faces	Approximately 170 m wide
Model boundaries	Northern boundary coincides with the Nicomekl River flood plain; remaining boundaries approximate the limits of the aquifer to the south, east, and west
Heads	Constant heads applied along two main reaches of Anderson Creek: from 62 to 55 m above sea level in the southern half of the aquifer, and from 54 to 13 m above sea level in the north (where the creek enters the Nicomekl River flood plain); constant heads applied to the Campbell River in two parts: from 54 m at the upstream intersection with the aquifer, decreasing regularly to 50 m (at row 27, column 24), and from 49 to 24 m at the downstream intersection with the aquifer
Recharge	Total recharge over the aquifer was set at 400 mm/a, which represents about a third of the total precipitation
Drains	Several drains were added along the northwestern and northern aquifer margins, to simulate natural seepage along the exposed aquifer face; conductance is set at 100 m^2/d, a relatively high figure compared with drains in the Fraser River delta models, but this value is intended to represent seepage along the entire margin and not just the drains themselves
Water withdrawal	Water withdrawal from a large number of privately owned water wells, few municipal wells; discharge is highly variable and not incorporated into the model

1.92×10^{-1} cm/s, for the coarsest sample, to 3.1×10^{-2} cm/s, and average 9.0×10^{-2} cm/s. The values compare favourably with those calculated from pumping tests (Table 2). The numerical differences among samples in each borehole further indicate considerable vertical anisotropy, despite the relatively coarse nature of the aquifer sediments. A hydraulic conductivity of 6.0×10^{-2} cm/s was assumed for most of the Brookswood aquifer in the models. More heterogeneous ice-contact deposits in the southeast corner of the aquifer were assigned a value of 5.0×10^{-3} cm/s; the fine-grained Fort Langley and Capilano formations were assigned a value of 10^{-5} cm/s.

Flow modelling

Model parameters

Brookswood aquifer simulations were undertaken using three- and two-dimensional models. The three-dimensional models provide a picture of groundwater flow across the entire aquifer. Two-dimensional simulations were done on a short transect through Stoke's gravel pit, to demonstrate the efficacy of ground-penetrating radar data in resolving local groundwater-flow problems. Model parameters that apply to the three-dimensional simulations are summarized in Table 3. Details on the model parameters can be found in Ricketts (1998).

Aquifer hydrostratigraphy is shown in Figures 20 and 21. In layer 1, the region beyond the aquifer seepage face is designated no flow (groundwater neither moves into nor out of this region).

Model calibration

Unlike the Fraser delta, there is a wealth of water-well data on the Brookswood aquifer that can be used to calibrate simulated potentiometric surfaces. Water-table maps were constructed by taking static levels in wells for specific time periods, the dry summer season (July–September) and winter recharge (January), from drill records submitted to the British Columbia Ministry of Environment between 1960 and 1985 (Fig. 22). This was done in order to compare seasonal variations in static level, which can be high as 4 m in individual wells (Fig. 10). The maps were compared to the simulated potentiometric surface; values of aquifer recharge and the number of drains (that simulate groundwater discharge at the exposed face of the aquifer) were adjusted to achieve a reasonable fit.

Water-table elevations are also available in the observation wells listed in Table 2 and Figure 11. Additional piezometer readings were taken in boreholes at the CRTC property (Fig. 11; Table 4). Water-level readings were taken in late June and therefore correspond to the 'summer' map in Figure 22. The average horizontal hydraulic gradient for this site is 7.2 m/km. Gradient steepness here is partially due to proximity to the exposed northwest margin of the aquifer. From the water-table maps, the regional gradient in a northwest direction across the entire aquifer is 4.6 m/km.

Piezometer nests at the CRTC site show slight differences in static level, although these are no more than 2–3 cm in most boreholes and probably within the range of measurement error (Table 4). Borehole 94-5 piezometers show a vertical water table difference of 10 cm over a depth range of 7.8 m, suggesting a possible vertical gradient of 1.3 cm/m.

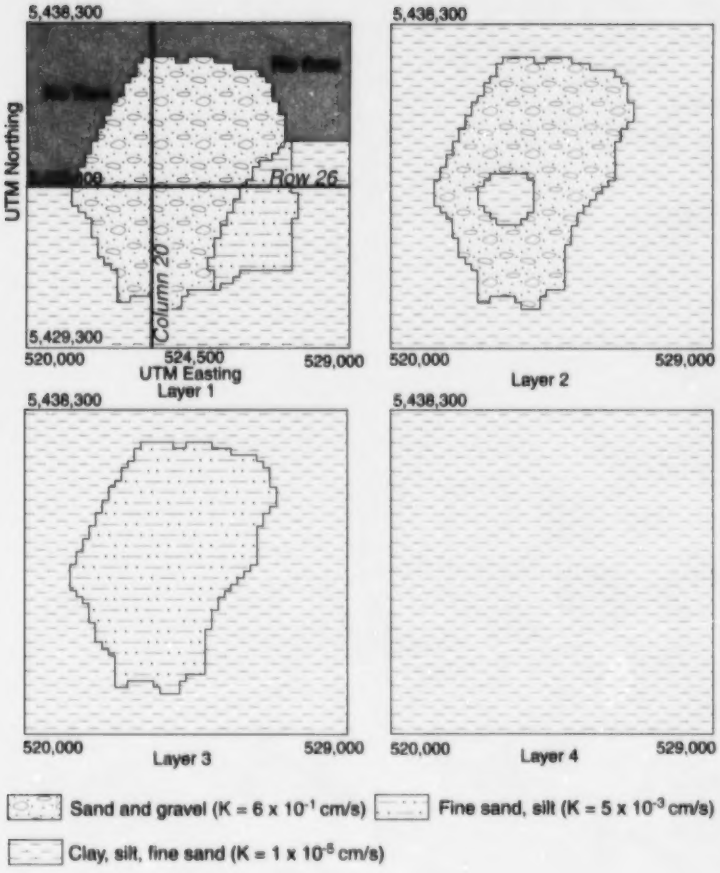

Figure 20.

Aquifer properties, by layer, in the three-dimensional Brookswood model. The aquifer and bounding units have been simplified to three basic sediment types. Grid references are in UTM co-ordinates. Locations of the cross-sections in Figure 21 are shown on layer 1.

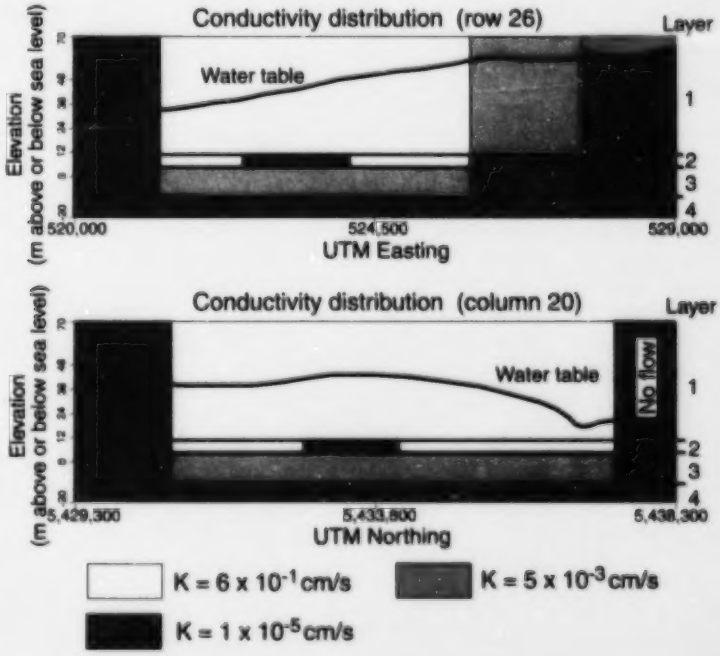

Figure 21.

Cross-sections through the Brookswood model, illustrating the three-dimensional distribution of conductivity. Locations of the sections are shown on Figure 20. The simulated water table is also shown for reference.

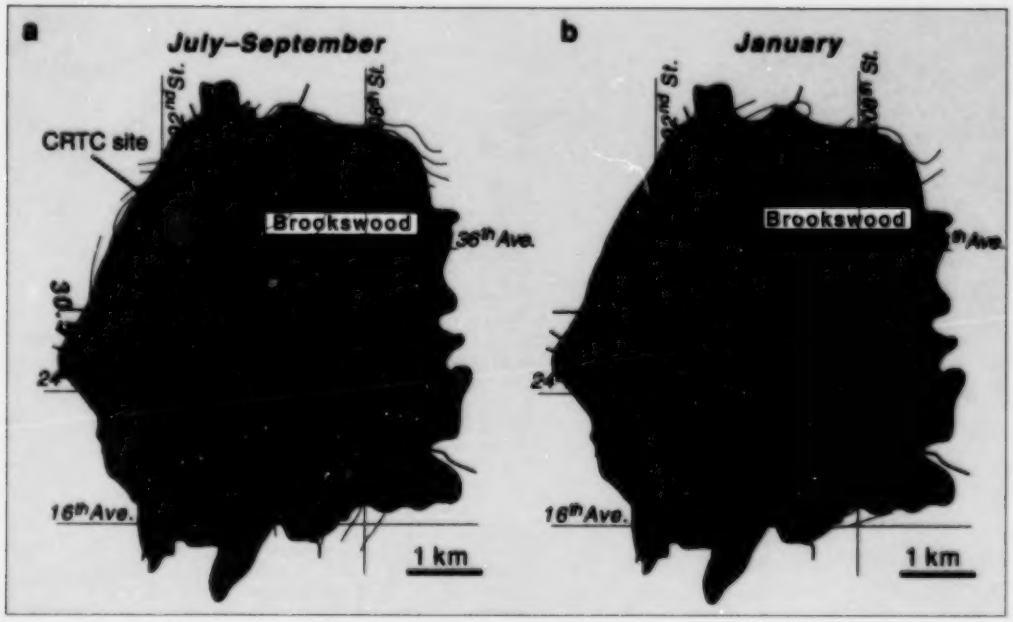

Figure 22. *Water table maps constructed for two time periods, corresponding to* ***a)*** *the summer dry season (July–September), and* ***b)*** *winter recharge (January). Static levels were taken from records of wells drilled between 1960 and 1985. Contours to the nearest 0.5 m* (modified from *Ricketts and Liebscher, 1994*).

Table 4. Borehole data from test drilling at the CRTC site.

Hole no.	P1	P2	P3	SL1	SL2	SL3	Standpipe	Bottom temperature (°C)
94-1	17.62	10.46	7.49	7.13	7.12	7.13	1.09	10.2
94-2	17.83	11.27	8.6	7.67	7.7	7.71	1.01	9.8
94-3[1]	16.76	-	-		-	-		
94-4	16.27	9.6	7.86	7.6	7.62	7.64	0.87	10.1
94-5	15.41	10.37	7.6	7.56	7.54	7.46	0.89	10
94-6[1]	16.76							
94-7	15.11	12.6	9.73	13.91	-	-	0.88	10.2
94-8	15.15	12.52	10.88	13.13		-	0.91	10.2

[1] One fully screened piezometer installed.
P1, **P2**, etc. refer to piezometers installed in each borehole.
SL1, **SL2**, etc. refer to static water levels in the corresponding piezometers.
All depths in metres relative to ground level, recalculated by subtracting the height of the standpipe or piezometer above ground.
Temperature measured at bottom of borehole, June 22, 1994.

Results of three-dimensional simulations

Simulated groundwater potentials for the Brookswood aquifer have a relatively simple pattern (Fig. 23), and compare favourably with the water-table maps reconstructed from measured static levels (Fig. 22). In both sets of maps, inferred groundwater flow is quasi-radial, from west to north. The local southeasterly flow observed in the Stoke's gravel pit area is also reasonably well simulated. Only in the southeast sector, where the aquifer consists of thin ice-contact deposits, are the equipotential contours skewed compared to the calibration maps. In the model, the high degree of heterogeneity of these deposits, relative to the main part of the aquifer, was represented by applying an hydraulic conductivity one order of magnitude lower (5×10^{-3} cm/s) than that of the main aquifer (6×10^{-2} cm/s). This artifact may account for some of the difference in simulated equipotential, but of greater influence is the juxtaposition of opposing constant heads in Anderson Creek and the Campbell River. Constant heads are invariant, and two cells with heads set (for example) at 54 m in separate water bodies will force the 54 m equipotential contour to pass through both cells. Although these constant heads could be

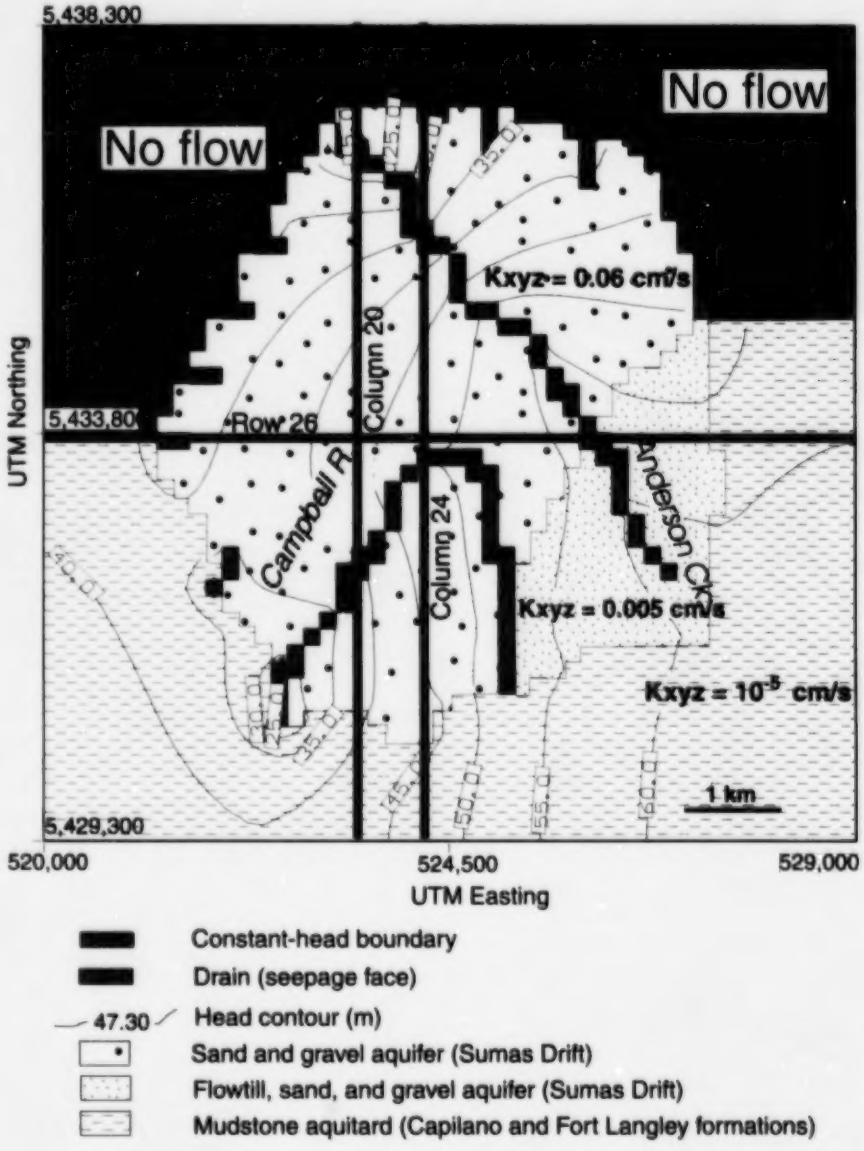

Figure 23. *Equipotential contours, aquifer map outline, and hydraulic conductivities for layer 1 of the Brookswood aquifer three-dimensional simulation. Contour interval is 5 m.*

removed from the model, some constant-head cells must be retained to define the upper limit of the water table in this part of the aquifer.

Seepage at the exposed aquifer margin takes place as diffuse flow or as springs near the base of the escarpment. Groundwater budget calculations in the simulation indicate that about 15% of total discharge occurs via the drains. This is somewhat greater than the seepage face discharge of 0.6×10^6 m^3/a, or 6% of the total discharge, estimated by Dakin (1994).

An hydraulic divide, extending west from the northern limit of the Campbell River and coinciding approximately with row 26 in Figure 23, separates west-southwest flow from northwest flow (Fig. 24). Simulated horizontal hydraulic gradients north of the divide are approximately 6 m/km (along column 24 in Fig. 24) and 7 m/km in a northwest direction, comparing favourably with measured gradients in the same part of the aquifer.

Much of the local complexity in the measured values of groundwater equipotential is not accounted for in the simulated water table. Variations in static levels probably result

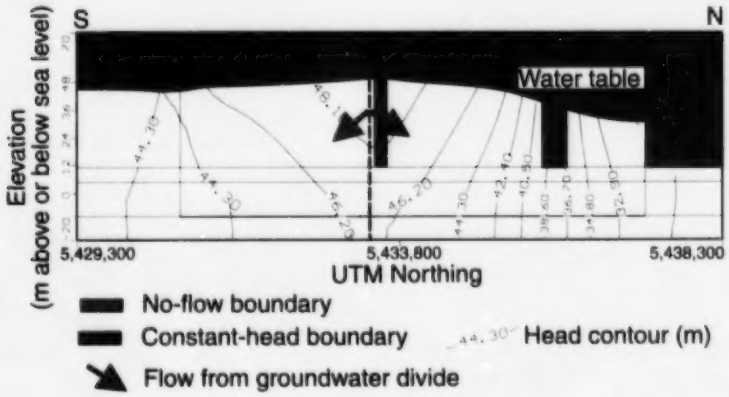

Figure 24.

Equipotential profile for column 24 in the Brookswood aquifer three-dimensional simulation. Contour interval is 1.9 m.

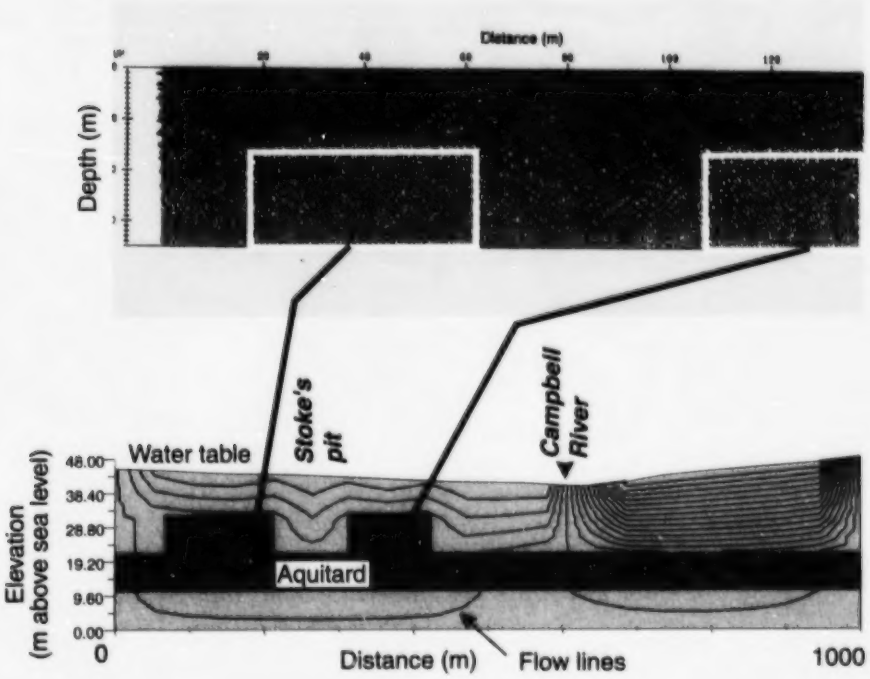

Figure 25. *Two-dimensional simulation of streamflow in the Stoke's pit–Campbell River profile, based on the first interpretation of the ground-penetrating radar data. Vertical exaggeration is 5x.*

from local topographic differences, adjustment of the local water table during drilling, and the effects of groundwater withdrawal in neighbouring wells.

Results of two-dimensional simulations

Two-dimensional simulations of stream flow and equipotential were performed on a short east-west transect through Stoke's gravel pit and the Campbell River (Fig. 11). The models incorporate hydrostratigraphic data from a ground-penetrating radar (GPR) profile through part of Stoke's pit, and compare the effects on groundwater flow of two different interpretations of the radar images.

In the first simulation, the grid (20 columns, 10 rows) contained three constant-head cells, representing the water table at the east end of the profile, the Campbell River, and Stoke's pit (Fig. 25). Three layers represented the unconfined aquifer ($K = 51.84$ m/d, equivalent to 6×10^{-2} cm/s used in the three-dimensional models), a middle aquitard (Capilano Formation, $K = 0.09$ m/d), and a thin, confined sand aquifer ($K = 51.84$ m/d). The GPR profile was interpreted as a contiguous sand-gravel body with dipping foresets, overlying and interfingering with clay. Contact between the two layers is undulating, with vertical relief of 5–8 m. This geometry was represented in the model as two rectangular clay bodies, overlying the aquitard and intercalated with the sand and gravel.

Groundwater flows from both east and west into the Campbell River (Fig. 25). Streamflow contours have simple geometry, but are deflected around the clay bodies; flowlines dip between the clay bodies. Flow generated farthest west of the clay is deflected below the aquifer layer to create a larger flow system.

For the second simulation, the clay bodies were replaced by a dipping clay layer, below which was sand and gravel contiguous with the main part of the aquifer (Fig. 26). In this interpretation, Rea (1996) noted that the clay layer would attenuate the radar signal to give the appearance of a more continuous clay body. The dipping layer has been added to the model; four grid columns were also added to improve resolution around the layer. The boundary conditions remained the same.

Simulated flow in the immediate vicinity of Stoke's pit is complicated by the dipping layer. Eastward flow near the top of the aquifer is forced over the top of the layer; flow deeper in the aquifer extends through the aquitard to the confined aquifer. Flow beyond the limits of Stoke's Pit is similar to that in the first simulation.

Flow velocities are similar in both two-dimensional models, despite significant differences in the vicinity of Stoke's pit. Maximum velocities near the Campbell River are about 4.2 m/d in the main aquifer. Flow around the clay bodies averages 1–2 m/d. Note that these values assume isotropic and homogenous conditions in each hydrostratigraphic unit, and therefore are probably maxima. Within the clay itself,

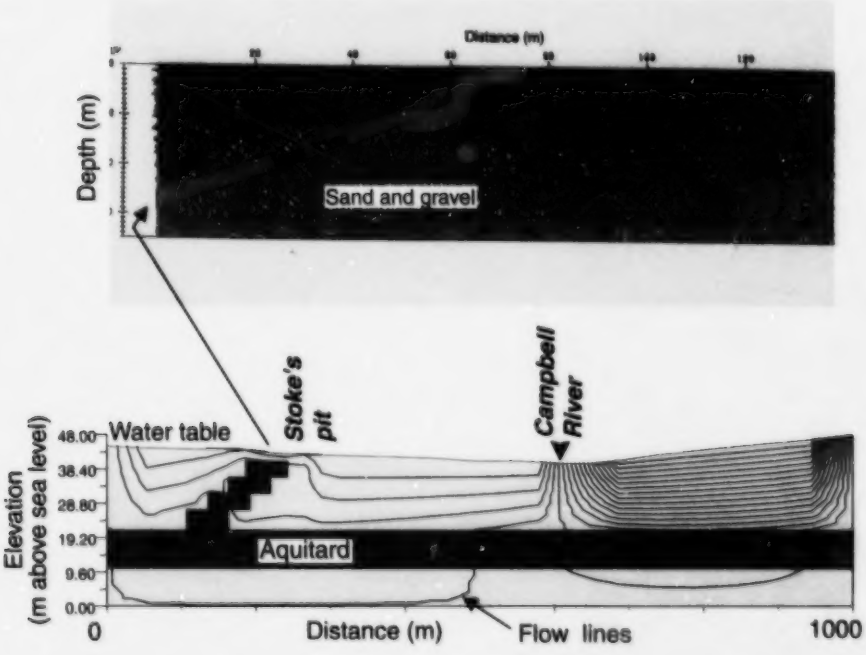

Figure 26. *Two-dimensional simulation of streamflow in the Stoke's pit–Campbell River profile, based on the second interpretation of the ground-penetrating radar data. Vertical exaggeration is 5x.*

velocities are lowest, ranging from 4×10^{-3} to 4×10^{-4} m/d. For example, vertical leakage through a metre-thick clay layer could take up to 2500 days. This rate is several orders of magnitude less than flow rates in the main aquifer and, from a regional perspective, will have little influence on total aquifer recharge and discharge; however, local barriers like this could have a significant effect on local travel times and dispersion of contaminants: the barriers could delay travel of a contaminant downgradient of its source (because of increased travel paths) and, in some cases, could redirect contaminant flow from expected paths.

CONCLUSIONS

Three- and two-dimensional numerical simulations of groundwater flow have been made for the Fraser River delta and the unconfined Brookswood aquifer. The three-dimensional analyses were undertaken to determine regional flow patterns and to assess major controls on flow. The two-dimensional analyses examined the effects of anisotropy and heterogeneity in the Brookswood aquifer. There is very little data with which to calibrate the Fraser River delta model, but ample water-well data existed for the Brookswood aquifer.

Shallow groundwater beneath the Fraser River delta (mostly in the delta topset unit, referred to as the sheet-sand aquifer) is recharged by a combination of precipitation and topography-driven flow from the adjacent uplands. Simulated hydraulic gradients at the water table are shallow (0.1–0.25 m/km). Groundwater in the delta may also originate as flow from deeper Pleistocene aquifers.

Flow velocities increase toward the delta front. Maximum velocities are 1.1 to 1.4 m/d in the three-dimensional sheet-sand aquifer model. This means that groundwater beneath the delta could take between 1000 and 5000 days to travel 1 km, depending on lithological variations within the aquifer.

An important inference from the Fraser River delta models is the possibility of groundwater flow to the delta front and subsequent submarine seepage. This is supported by electrical conductivity data, which show mixing of seawater and fresh water as far west as the low-tide limit on the delta plain; however, seaward flow of groundwater apparently does not occur as a simple migrating front, but rather as zones. The controls on these zones are not known, but presumably include factors such as the location of old distributary channels and local variations in hydraulic head. Zones of submarine seepage could raise pore pressures, thereby decreasing sediment shear strength and increasing the susceptibility of the delta front to failure (Ricketts, 1998).

The Brookswood unconfined aquifer is underlain by predominantly fine-grained glaciomarine deposits (aquitard). Recharge is by a combination of direct precipitation, infiltration from the Campbell River and Anderson Creek (winter only), and some runoff from clay uplands south of the aquifer. Simulated groundwater flow is quasi-radial, predominantly to the north and west. Reverse flow to the southeast, observed from Stoke's pit to the Campbell River, was also simulated. An east-west hydraulic divide crosses the aquifer, just north of the Campbell River. Simulated hydraulic gradients north of the divide are approximately 6 to 7 m/km and compare favourably with gradients estimated from water-well static levels. The magnitude of the gradients reflects regional topography and the presence of a steep seepage face along the northern and western margins of the aquifer; the seepage face approximates the front of the old proglacial (Sumas) delta. According to the simulation, about 15% of total discharge occurs at the aquifer seepage face; this compares with about 6% estimated by Dakin (1994).

Two-dimensional simulations of stream flow were performed on a short transect through Stoke's pit and the Campbell River, in order to compare two different interpretations of a ground-penetrating radar profile along the same transect (*from* Rea and Knight, 2000). Regional flow in the two-dimensional models is toward the Campbell River; however, there are significant differences in flow patterns, depending on the geometry of the clay body that interfingers with the aquifer.

ACKNOWLEDGMENTS

I owe a debt of gratitude to those who have gently nudged me through the mysteries, vagaries and foibles of groundwater modelling, in particular to Hugh Liebscher (Environment Canada) for introducing me to Fraser lowland groundwater and Tony Sperling (Sperling Hansen Associates) for guidance in aspects of modelling. Dirk Tempelman-Kluit, former director of the GSC Vancouver office, provided encouragement and assistance throughout the project. The paper has benefited greatly from the comments and criticisms of Roger Beckie and Laurie Welch (University of British Columbia). And lastly, I wish to thank Bev Vanlier for shepherding this paper, and indeed the entire bulletin, through the GSC mill.

REFERENCES

Ages, A.B. and Woollard, A.L.
1994: The salinity intrusion in the Fraser River: observations of salinities, temperatures and currents by time-series and hovercraft coverage, 1985, 1986, 1987; Fisheries and Oceans Canada, Canadian Data Report of Hydrography and Ocean Sciences, no. 126, 166 p.

Armstrong, J.E.
1981: Post-Vashon Wisconsin glaciation, Fraser Lowland, British Columbia; Geological Survey of Canada, Bulletin 322, 34 p.
1984: Environmental and engineering applications of the surficial geology of the Fraser Lowland, British Columbia; Geological Survey of Canada, Paper 83-23, 54 p.

Armstrong, J.E. and Hicock, S.R.
1980a: Surficial geology, New Westminster, British Columbia; Geological Survey of Canada, Map 1484A, scale 1:50 000.
1980b: Surficial geology, Vancouver, British Columbia; Geological Survey of Canada, Map 1486A, scale 1:50 000.

Bazett, D.J. and McCammon, N.R.
1986: Foundations of the Annacis cable-stayed bridge; Canadian Geotechnical Journal, v. 23, p. 458–471.

Bellitz, K. and Bredehoeft, J.D.
1988: Hydrodynamics of Denver Basin: explanation of subnormal fluid pressures; American Association of Petroleum Geologists Bulletin, v. 72, p. 1334–1359.

Best, M.E. and Todd, B.J.
2000: Electromagnetic mapping of groundwater aquifers in the Fraser lowland; *in* Mapping, Geophysics, and Groundwater Modelling in Aquifer Delineation, Fraser Lowland and Delta, British Columbia, (ed.) B.D. Ricketts; Geological Survey of Canada, Bulletin 552.

Best, M.E., Todd, B.J., and O'Leary, D.O.
1995: Groundwater mapping using time-domain electromagnetics: examples from the Fraser Valley, British Columbia; *in* Current Research 1995-A; Geological Survey of Canada, p. 19–27.

Bredehoeft, J.D., Back, W., and Hanshaw, B.B.
1982: Regional ground-water flow concepts in the United States: historical perspective; *in* Recent Trends in Hydrogeology, (ed.) T.N. Narasimhan; Geological Society of America, Special Paper 189, p. 297–316.

Britton, J.R., Harris, J.B., Hunter, J.A., and Luternauer, J.L.
1995: The bedrock surface beneath the Fraser River delta from seismic measurements; *in* Current Research 1995-E; Geological Survey of Canada, p. 83–89.

Canadian Council of Resource and Environment Ministers (CCREM)
1987: Canadian Water Quality Guidelines; CCREM Task Force on Water Quality Guidelines, Environment Canada, Ottawa, Ontario.

Carmichael, V., Wei, M., and Ringham, L.
1995: Fraser Valley groundwater monitoring program, final report; B.C. Ministry of Health and B.C. Ministry of Environment, Lands and Parks.

Christian, H.A., Barrie, J.V., MacDonald, R., Monahan, P.A., Hunter, J.A., and Luternauer, J.L.
1995: Slope instability on Roberts Bank, Fraser River delta, Vancouver, British Columbia; *in* Preprint Volume 2, Canadian Geotechnical Conference, Vancouver, B.C., September 25–27, 1995; Canadian Geotechnical Society, p. 937–946.

Clague, J.J.
1977: Quadra Sand: a study of the Late Pleistocene geology and geomorphic history of coastal southwest British Columbia; Geological Survey of Canada, Paper 77-17, 24 p.

Clague, J.J., Luternauer, J.L., Pullan, S.E., and Hunter, J.A.
1991: Postglacial deltaic sediments, southern Fraser River delta, southern British Columbia; Canadian Journal of Earth Sciences, v. 28, p. 1386–1393.

Dakin, A.
1994: Coastal basins, lowlands and plains; *in* Chapter 9 of Groundwater Resources of British Columbia, (ed.) J. Atwater, L.V. Brandon, W.L. Brown, R.A. Dakin, H.D. Foster, J.C. Foweraker, R.A. Freeze, E.C. Halstead, H.G. Harris, W.S. Hodge, A.T. Holmes, B. Ingimundson, D. Johanson, A.P. Kohut, H. Liebscher, E. Livingston, H.W. Nasmith, M.L. Parsons, O. Quinn, K. Ronneseth, J.L. Smith, D.F. Van Dine, M. Wei, and M. Zubel; Environment Canada, p. 9.1–9.30.

Dallimore, S.R., Edwardson, K.A., Hunter, J.A., Clague, J.J., and Luternauer, J.L.
1995: Composite geotechnical logs for two deep boreholes in the Fraser River delta, British Columbia; Geological Survey of Canada, Open File 3018.

Dunn, D. and Ricketts, B.D.
1994: Surficial geology of Fraser Lowlands digitized from GSC Maps 1484A, 1485A, 1486A and 1487A (NTS 92G/1, /2, /3, /6, /7, and 92H/4); Geological Survey of Canada, Open File 2894 (3.5-inch diskette).

Freeze, A. and Cherry, J.
1979: Groundwater; Prentice-Hall, New Jersey, 604 p.

Halstead, E.C.
1978: Nicomekl–Serpentine basin study, British Columbia; Fisheries and Environment Canada, Scientific Series no. 94, 36 p.
1986: Ground water supply – Fraser Lowland, British Columbia; Environment Canada, Inland Waters Directorate, National Hydrology Research Institute Paper no. 26, Scientific Series no. 145, 80 p.

Hamilton, T.S. and Ricketts, B.D.
1994: Contour map of bedrock surface, Georgia Strait and Lower Mainland region; *in* Geology and Geological Hazards of the Vancouver Region, Southwestern British Columbia, (ed.) J.W.H. Monger; Geological Survey of Canada, Bulletin 481, p. 193–196.

Harris, J.B., Hunter, J.A., Luternauer, J.L., and Finn, W.D.L.
1995: Site amplification modelling of the Fraser River Delta, British Columbia; *in* Preprint Volume 2, Canadian Geotechnical Conference, Vancouver, British Columbia, September 25–27, 1995; Canadian Geotechnical Society, p. 947–954.

Harsh, J.F. and Laczniak, R.J.
1990: Conceptualization and analysis of ground-water flow system in the coastal plain of Virginia and adjacent parts of Maryland and North Carolina; United States Geological Survey, Professional Paper 1404-7, 100 p.

Hart, B.S., Prior, D.B., Barrie, J.V., Currie, R.G., and Luternauer, J.L.
1992: A river mouth submarine channel and failure complex, Fraser Delta, Canada; Sedimentary Geology, v. 81, p. 73–87.

Hunter, J.A., Luternauer, J.L., Roberts, M.C., Monahan, P.A., and Douma, M.
1994: Borehole geophysical logs, Fraser River delta (92G), British Columbia; Geological Survey of Canada, Open File 841, 30 p.

Joi, H.M. and Roberts, M.C.
1988: The seismic facies of a delta onlapping an offshore island: Fraser River delta, British Columbia; *in* Sequences, Stratigraphy, Sedimentology: Surface and Subsurface, (ed.) D.P. James and D.A. Leckie; Canadian Society of Petroleum Geologists, Memoir 15, p. 137–142.

Kreye, R. and Wei, M.
1994: A proposed aquifer classification system for groundwater management in British Columbia; British Columbia Ministry of Environment, Lands and Parks, Hydrology Branch, Groundwater Section, 68 p.

Leahy, P.P. and Martin, M.
1993: Geohydrology and simulation of groundwater flow in the northern Atlantic coastal plain aquifer system; United States Geological Survey, Professional Paper 1404-K, 81 p.

Luternauer, J.L. and Finn, W.D.L.
1983: Stability of the Fraser River delta front; Canadian Geotechnical Journal, v. 20, p. 603–616.

Luternauer, J.L. and Hunter, J.A.
1996: Mapping Pleistocene deposits beneath the Fraser River delta: preliminary geological and geophysical results; *in* Current Research 1996-E; Geological Survey of Canada, p. 41–48.

Luternauer, J.L., Barrie, J.V., Christian, H.A., Clague, J.J., Evoy, R.W., Hart, B.S., Hunter, J.A., Killeen, P.G., Kostaschuk, R.A., Mathewes, R.W., Monahan, P.A., Moslow, T.F., Mwenifumbo, C.J., Olynyk, H.W., Patterson, R.T., Pullan, S.E., Roberts, M.C., Robertson, P.K., Tarbotton, M.R., and Woeller, D.J.
1994: Fraser River delta: geology, geohazards and human impact; *in* Geology and Geological Hazards of the Vancouver Region, Southwestern British Columbia, (ed.) J.W.H. Monger; Geological Survey of Canada, Bulletin 481, p. 197–220.

Makepeace, A.J. and Ricketts, B.D.
2000: Aquifer mapping and database development using a geographic information system, Fraser lowland; *in* Mapping, Geophysics, and Groundwater Modelling in Aquifer Delineation, Fraser Lowland and Delta, British Columbia, (ed.) B.D. Ricketts; Geological Survey of Canada, Bulletin 552.

Manheim, F.T.
1967: Evidence for submarine discharge of water on the Atlantic continental slope of the southern United States, and suggestions for further research; New York Academy of Sciences, Transactions, ser. 2, v. 29, p. 839–853.

McKenna, G.T., Luternauer, J.L., and Kostaschuk, R.A.
1992: Large-scale mass-wasting events on the Fraser River delta front near Sand Heads, British Columbia; Canadian Geotechnical Journal, v. 29, p. 151–156.

McNeely, R.N., Neimanis, V.P., and Dwyer, L.
1979: Water quality sourcebook, a guide to water quality parameters; Environment Canada, Inland Waters Directorate, Water Quality Branch, Ottawa.

Monahan, P.A., Luternauer, J.L., and Barrie, J.V.
1993: A delta plain sheet sand in the Fraser River delta, British Columbia, Canada; Quaternary International, v. 20, p. 27–38.

Mustard, P.S. and Rouse, G.E.
1994: Stratigraphy and evolution of Tertiary Georgia Basin and subjacent Upper Cretaceous sedimentary rocks, southwestern British Columbia and northwestern Washington State; *in* Geology and Geological Hazards of the Vancouver Region, Southwestern British Columbia, (ed.) J.W.H. Monger; Geological Survey of Canada, Bulletin 481, p. 97–169.

Pullan, S.E., Good, R.L., and Ricketts, B.D.
1995: Preliminary results from a shallow seismic reflection survey, Lower Fraser Valley hydrogeology project, British Columbia; *in* Current Research 1995-A; Geological Survey of Canada, p. 11–18.

Pullan, S.E., Jol, H.M., Gagne, R.M., and Hunter, J.A.
1989: Compilation of high resolution 'optimum offset' shallow seismic reflection profiles from the southern Fraser River delta, British Columbia; Geological Survey of Canada, Open File 1992, 8 p.

Rea, J.M.A.
1996: Ground penetrating radar applications in aquifer characterization; Ph.D. thesis, Department of Earth and Ocean Sciences, University of British Columbia, Vancouver, British Columbia, 84 p.

Rea, J.M.A. and Knight, R.J.
2000: Characterization of the Brookswood aquifer using ground-penetrating radar; *in* Mapping, Geophysics, and Groundwater Modelling in Aquifer Delineation, Fraser Lowland and Delta, British Columbia, (ed.) B.D. Ricketts; Geological Survey of Canada, Bulletin 552.

Rea, J.M.A., Knight, R.J., and Ricketts, B.D.
1994a: Ground-penetrating radar survey of the Brookswood aquifer, Fraser Valley, British Columbia; *in* Current Research 1994-A; Geological Survey of Canada, p. 211–216.
1994b: Ground penetrating radar, Brookswood aquifer, Lower Fraser Valley, British Columbia; Geological Survey of Canada, Open File 2821, 13 p.

Richardson, D.L.
1994: Hydrology and analysis of the ground-water flow system of the eastern shore, Virginia; United States Geological Survey, Water-Supply Paper 2401.

Ricketts, B.D. (cont.)
1995: Progress report and field activities of the Fraser Valley hydrogeology project, British Columbia; *in* Current Research 1995-A; Geological Survey of Canada, p. 1–5.

Ricketts, B.D.
1998: Groundwater flow beneath Fraser River delta, British Columbia: a preliminary model; *in* The Fraser River Delta: Recent Geological, Geophysical, Geotechnical, and Geochemical Research, (ed.) J.J. Clague, J.L. Luternauer, and D.C. Mosher; Geological Survey of Canada, Bulletin 525, p. 241–256.

Ricketts, B.D. and Dunn, D.
1995: The groundwater database, Fraser Valley, British Columbia; *in* Current Research 1995-A; Geological Survey of Canada, p. 7–10.

Ricketts, B.D. and Jackson, L.E., Jr.
1994: An overview of the Vancouver–Fraser Valley hydrogeology project, southern British Columbia; *in* Current Research 1994-A; Geological Survey of Canada, p. 201–206.

Ricketts, B.D. and Liebscher, H.
1994: The geological framework of groundwater in the Greater Vancouver area; *in* Geology and Geological Hazards of the Vancouver Region, Southwestern British Columbia, (ed.) J.W.H. Monger; Geological Survey of Canada, Bulletin 481, p. 287–298.

Ricketts, B.D. and Makepeace, A.J. (ed.)
2000: Aquifer delineation, Fraser lowland and delta, British Columbia: mapping, geophysics and groundwater modelling; Geological Survey of Canada, Open File D3828.

Roberts, M.C., Vanderburgh, S., and Jol, H.
2000: Radar facies and geomorphology of the seepage face of the Brookswood aquifer, Fraser lowland; *in* Mapping, Geophysics, and Groundwater Modelling in Aquifer Delineation, Fraser Lowland and Delta, British Columbia, (ed.) B.D. Ricketts; Geological Survey of Canada, Bulletin 552.

Toth, J.
1963: A theoretical analysis of groundwater flow in small drainage basins; Journal of Geophysical Research, v. 68, p. 4795–4812.

Woodsworth, G.J. and Ricketts, B.D.
1994: A digital database for Fraser Valley groundwater data; *in* Current Research 1994-A; Geological Survey of Canada, p. 207–210.

AUTHOR INDEX

MAPS NOT FILMED

CARTES NON REPRODUITES

micromedia
a division of IHS Canada

20 Victoria Street
Toronto, Ontario M5C 2N8
Tel.: (416) 362-5211
Toll Free: 1-800-387-2689
Fax: (416) 362-6161
Email: info@micromedia.on.ca